DEVELOPMENT OF A MODEL UPDATING TECHNIQUE FOR NONLINEAR SYSTEMS

A THESIS SUBMITTED TO
THE GRADUATE SCHOOL OF NATURAL AND APPLIED SCIENCES
OF
MIDDLE EAST TECHNICAL UNIVERSITY

BY

GÜVENÇ CANBALOĞLU

IN PARTIAL FULFILLMENT OF THE REQUIREMENTS
FOR
THE DEGREE OF DOCTOR OF PHILOSOPHY
IN
MECHANICAL ENGINEERING

SEPTEMBER 2015

Approval of the thesis:

DEVELOPMENT OF A MODEL UPDATING TECHNIQUE FOR NONLINEAR SYSTEMS

submitted by **GÜVENÇ CANBALOĞLU** in partial fulfillment of the requirements for the degree of **Doctor of Philosophy in Mechanical Engineering Department, Middle East Technical University by,**

Prof. Dr. Gülbin Dural Ünver
Dean, Graduate School of **Natural and Applied Sciences** _____

Prof. Dr. Tuna Balkan
Head of Department, **Mechanical Engineering** _____

Prof. Dr. H. Nevzat Özgüven
Supervisor, **Mechanical Engineering Dept., METU** _____

Examining Committee Members:

Assoc. Prof. Dr. Ender Ciğeroğlu
Mechanical Engineering Dept., METU _____

Prof. Dr. H. Nevzat Özgüven
Mechanical Engineering Dept., METU _____

Prof. Dr. Yavuz Yaman
Aerospace Engineering Dept., METU _____

Prof. Dr. Özgür Anıl
Civil Engineering Dept., Gazi University _____

Assist. Prof. Dr. Mehmet Bülent Özer
Mechanical Engineering Dept., TOBB ETU _____

Date: 04.09.2015

I hereby declare that all information in this document has been obtained and presented in accordance with academic rules and ethical conduct. I also declare that, as required by these rules and conduct, I have full cited and referenced all material and results that are not original to this work.

Name, Last name : Güvenç CANBALOĞLU

Signature :

ABSTRACT

DEVELOPMENT OF A MODEL UPDATING TECHNIQUE FOR NONLINEAR SYSTEMS

Canbaloğlu, Güvenç
Ph.D., Department of Mechanical Engineering
Supervisor: Prof. Dr. H. Nevzat Özgüven
September 2015, 264 pages

In structural dynamics, obtaining an accurate numerical model is very crucial. However there are usually discrepancies between calculated dynamic behavior from numerical models and the ones obtained experimentally, and therefore it will be necessary to update the numerical models. In real life applications, structures usually have nonlinearity, and for nonlinear structures, in order to update the numerical model, firstly nonlinearity in the structure can be identified, and then updating procedure may be applied to the linear part of the model. Application of such an approach may not be straightforward, especially for nonlinear systems having multiple nonlinearities including friction type of nonlinearity.

In this thesis, a new model updating technique for nonlinear structures that have multiple nonlinearities including friction type of nonlinearity is developed. The method identifies multiple nonlinearities in the structure and simultaneously extracts the FRFs of the underlying linear system. The accuracy of the method developed is first verified by using nonlinear lumped SDOF and MDOF systems, as well as with nonlinear structure using simulated experimental data. Then, as experimental studies,

method developed is applied to a real test system and finally to an engineering system (nonlinear gun barrel of a battle tank). It is shown that, the method developed can be successfully applied both to a test system and to a complex engineering problem for obtaining an accurate nonlinear model. In conclusion, the validation and application of the model updating method developed for nonlinear structures are demonstrated successfully with both simulated case studies and experimental real life applications.

Keywords: Nonlinear Model Updating, Nonlinear Identification, Nonlinear Systems, Numerical Model

ÖZ

DOĞRUSAL OLMAYAN YAPILAR İÇİN MODEL GÜNCELLEME YÖNTEMİ GELİŞTİRİLMESİ

Canbaloğlu, Güvenç
Doktora, Makina Mühendisliği Bölümü
Tez Yöneticisi: Prof. Dr. H. Nevzat Özgüven
Eylül 2015, 264 sayfa

Yapısal dinamikte, doğru bir sayısal model elde etmek oldukça önemlidir. Ancak sayısal modellerden hesaplanan dinamik davranışlarla deneyden elde edilmiş sonuçlar arasında her zaman farklılıklar mevcuttur, bu yüzden sayısal modellerin güncellenmesi gerekmektedir. Gerçek hayat uygulamalarında, yapılar çoğunlukla doğrusal olmayan özelliklere sahiptir ve doğrusal olmayan yapılar için, sayısal modelleri güncelleyebilmek için ilk önce yapıdaki doğrusal olmayan özellikler belirlenebilir, daha sonra da güncelleme prosedürü modelin doğrusal olan kısmına uygulanabilir. Bu yaklaşımın uygulaması, özellikle sürtünme tipi doğrusal olmayan özellik içeren çoklu doğrusal olmayan özelliklere sahip sistemlerde çok basit olmayabilir.

Bu tezde, sürtünme tipi doğrusal olmayan özellik içeren çoklu doğrusal olmayan özelliklere sahip doğrusal olmayan yapılar için yeni bir model güncelleme yöntemi geliştirilmiştir. Yöntem, yapıdaki doğrusal olmayan özellikleri belirleyip aynı zamanda yapının doğrusal kısmının frekans tepki fonksiyonlarını da çıkarmaktadır. Geliştirilen yöntemin doğruluğu ilk olarak, gerçek olmayan deneysel veri kullanan

doğrusal olmayan tek ve çok serbestlik derecesine sahip sistemlerle aynı zamanda da doğrusal olmayan bir yapıyla gösterilmiştir. Deneysel çalışma olarak, geliştirilen yöntem önce gerçek bir test sistemine son olarak da bir mühendislik sistemine (savaş tankı namlusu) uygulanmıştır. Geliştirilen yöntemin, bir test sistemine ve karmaşık bir mühendislik sistemine, doğru bir doğrusal olmayan model elde etmek için başarıyla uygulanabildiği gösterilmiştir. Sonuç olarak, doğrusal olmayan yapılar için geliştirilmiş olan model güncelleme yönteminin doğrulaması ve uygulaması hem sayısal çalışmalarla hem de deneysel gerçek hayat uygulamalarıyla başarıyla gösterilmiştir.

Anahtar Kelimeler: Doğrusal Olmayan Model Güncelleme, Doğrusal Olmayan Eleman Tanımlama, Doğrusal Olmayan Modeller, Sayısal Model

To My Family

ACKNOWLEDGEMENTS

I would like to express my sincere appreciation to my supervisor, Prof. Dr. H. Nevzat Özgüven for his boundless help, excellent supervision and leading guidance from beginning to end of thesis work.

The author also would like to thank Prof. Dr. Yavuz Yaman and Assoc. Prof. Dr. Ender Ciğeroğlu for their guidance as members of thesis progress committee.

I would like to express my special thanks to Arif Cem Gözükara for his continuous moral support throughout this work.

I want to thank my colleagues Taner Kalaycıoğlu, Özlem Demirkan, Salih Alan, Dr. Murat Aykan and Mustafa Ocak for their technical support and helpful advice.

Also I would like to thank my managers Dr. Ali Mürteza Çolakoğlu, Dr. İhsan Özsoy, Sabri Çetin, Hikmet Balcı and Enis Naci Özkan for giving me the opportunity to use the computational and testing capabilities in ASELSAN.

Also I would like to thank the Scientific and Technological Research Council of Turkey (TÜBİTAK) for giving me the financial support throughout this work.

TABLE OF CONTENTS

LIST OF TABLES

TABLES

LIST OF FIGURES

FIGURES

LIST OF SYMBOLS

$[C]$	Viscous damping matrix
$[D]$	Structural damping matrix
F_{ext}	External forcing
$\{f_{ext}(t)\}$	External forcing vector
$[H]$	Receptance matrix
$[I]$	Identity matrix
i	Unit imaginary number
$[K]$	Stiffness matrix
k^*	Cubic stiffness
k_f	Frictional stiffness
k	Stiffness
$[M]$	Mass matrix
m	Mass
$\{N(x,\dot{x},t)\}$	Nonlinear internal force vector
$\{p\}$	Parameter vector
$\{r\}$	Response vector
$[S]$	Sensitivity matrix
t	Time
$\{X\}$	Complex amplitude displacement vector
x	Displacement
$\{x(t)\}$	Displacement vector

$\{\dot{x}(t)\}$	Velocity vector
$\{\ddot{x}(t)\}$	Acceleration vector
$[\Delta]$	Nonlinearity matrix
γ	Loss factor
μ	Friction coefficient
ν	Describing function representation of the nonlinearity
θ	Generic angle
ω	Frequency
ψ	Phase angle

Subscripts

a	Nonlinear coordinate
b	Linear coordinates
f	Friction
HF	High forcing
r, j	Coordinate

Superscripts

H	Complex conjugate transpose
L	Linear
m	Harmonic number
NL	Nonlinear

Abbreviations

AFMM	Amplitude and frequency modulation
DDF	Direct nonlinearity by describing functions

EMD	Empirical mode decomposition
FE	Finite element
FRAC	Frequency response assurance criteria
FRF	Frequency response function
HHT	Hilbert–Huang transform
MCI	Miscorrelation index
MDOF	Multi degree of freedom
NSI	Nonlinear subspace identification
PRD	Pseudo receptance difference
SDOF	Single degree of freedom
SHMC	Shadow Hybrid Monte Carlo

CHAPTER 1

INTRODUCTION

1.1 Structural Model Updating

Structural modeling is one of the key steps in the design stage of a system. There is always iteration in the design stage, therefore it is important to have accurate structural model of the system so that predictions can be made for different design alternatives before any production. Finite element (FE) method is the most common numerical method used for predicting and simulating the dynamic response of engineering structures. Once the design is completed, the prototype can be experimentally investigated. However, due to the cost of making experiment at all possible forcing conditions, it is a common practice to verify the mathematical model used in design stage by comparing the simulated responses with experimentally measured ones. However, there are always discrepancies between the dynamic behavior of the structures obtained by the test and simulation due to the assumptions used in FE model. FE analysis may yield inaccuracies, mainly due to the modelling errors. If the modal analysis results are considered, the aim is to obtain either the frequency response functions (FRFs) or the modal properties (natural frequency, modeshapes, modal damping) of the structure. However, the results obtained by the FE analysis may have similarities with the experimental results up to a certain limit. Therefore, the FE models have to be updated by using the experimental test data. With the comparison and correlation of experimental and simulation results, numerical changes are applied to original system matrices or to updating parameters selected in the FE model, so that the FE analysis results match better with the experimental results.

Most of the structures in engineering problems have nonlinear behaviors therefore this makes accurate structural modelling much more difficult. It is more complex to deal with nonlinear structure both experimentally and analytically. In order to have accurate analytical model of nonlinear structures, experimental system identification plays a key role. In order to apply model updating techniques developed for linear systems to nonlinear structures and to correct linear system matrices, linear dynamic behaviors of the structure have to be experimentally obtained which may require identification of nonlinearity first. However, for systems having complex nonlinearities including friction type of nonlinearity, obtaining linear dynamic behavior and also identifying nonlinearity simultaneously is not a straight forward task. Yet, if the linear dynamic behavior can be extracted, then by applying linear model updating techniques, FE models can be corrected. Thus using these linear FE models and identified nonlinearities, updated nonlinear models of the structure can be constructed.

1.2 Literature Survey

In the literature there are various model updating techniques proposed, in order to have more accurate mathematical models. However most of these methods can be applicable only to linear systems. Dascotte and Vanhonacker [1] developed a computer code in order to update the FE models automatically. Sensitivity of natural frequencies was used in the updating method and iterative solution method was employed. Nalitolela et al. [2] presented a model updating technique which is capable of solving the problems arising from incomplete modes and unmeasured degrees of freedom. Roy et al. [3] studied an updating method which is based on direct energy approach. Modal expansion was applied to experimental modes and those expanded modes were used to correlate the kinetic and strain energies of the FE model to the experimental results. Brughmans et al. [4] used sensitivity based model updating method, and tuned FE model of an aircraft by using the ground vibration test results of the aircraft. Link and Zhang [5] investigated the effect of

using different residual error vectors on the performance of the updating method. This study was demonstrated on a real test structure. Ibrahim et al. [6] used direct updating method for the model updating of FE models. In the updating procedure, there was no modal identification and mode pairing; only input and output measurements were used. Aiad et al. [7] studied direct model updating approach and mass and stiffness matrices were updated globally based on the modeshapes and natural frequencies obtained experimentally. Jung and Ewins [8] used inverse eigensensitivity method for model updating and investigated the effect of measurement noise on the method by studying different noise levels. In order to investigate the potential errors causing the discrepancies between analytical and experimental normal modes, Miccoli and Agostoni [9] used the sensitivity based model updating for correlating the experimental and analytical models of a plate with stiffeners at its edges. Dascotte et al. [10] studied a sensitivity based model updating method. The stability problem encountered during the solution was solved by using different scaling factors for sensitivity matrix. Imregun et al. [11] presented a model updating method which is based on FRF data. The proposed method was investigated under different conditions such as incompleteness of the experimental data, noisy experimental measurements or excitation direction used in the experiments. Then in a later study this FRF based model updating method was applied to a plate-beam like structure by Imregun et al. [12]. Hemez [13] presented sensitivity based updating method in order to correlate the damped analytical and experimental structures. Lenoir et al. [14] proposed a model updating technique which uses experimental forced responses. Mottershead et al. [15] updated FE model of an aluminum space frame by using various updating parameter sets and the results were compared and investigated for each of different updating parameter sets. In a later work, a new method was developed for structural model updating and identification of joint stiffness by Li [16]. Modak et al. [17] presented a constrained optimization based model updating method and studied the updating of a FE model of a structure using experimental modal data and its use for the prediction of the effects of structural modifications. Kim and Park [18] proposed a multi objective optimization technique

for the FE model updating in order to improve the parameter selection in the updating procedure. Cottin and Reetz [19] investigated the effect of number of natural frequencies and accuracy of measurement to obtain reliable model parameter estimation for a given set of model parameters for the dynamic model updating. Lin [20] used and further developed a FRF based model updating method to identify damping matrices of structural systems, as well as mass and stiffness matrices for proportionally and non-proportionally damped structures. Carvalho et al. [21] proposed a new method which is capable of handling the difficulty of the incomplete measured data for the updating of FE matrix in an undamped model. Arora et al. [22] studied on the updating of the FE model using the FRF data with damping identification using complex modal data. Firstly, FRF based model updating technique was employed to update the mass and stiffness matrices, then the damping was identified by using updated mass and stiffness matrices. In their later study, Arora et al. [23] made a detailed comparison of two approaches of obtaining damped FE model updating methods with the objective that the FRFs obtained from damped updated FE models is able to predict the measured FRFs accurately. Kozak et al. [24] presented a new model updating method based on minimization of an index called Miscorrelation Index (MCI). This index mainly localizes the coordinates in FE model that has errors. The proposed model updating method was demonstrated on simulated and real test cases. Tarazaga et al. [25] presented the modified Quadratic Compression Method in order to update the mass and stiffness matrices of a model. Adhikari and Friswell [26] proposed an approach to take account the distributed nature of the parameters to be updated by expressing the parameters as spatially correlated random fields. In the approach, those fields were expanded in a spectral decomposition which is Karhunen-Loève expansion. In a more recent study, Zapico-Valle et al. [27] presented an updating method for FE models by minimizing an error function defined in the time domain using an adaptive sampling algorithm for the parameters to be updated. Mottershead et al. [28] presented a basic introduction to the most important procedures of computational model updating based on the sensitivity approach, including tutorial examples and gave a detail literature survey.

Yuen [29] studied on the model updating for mechanical or structural systems in case of incomplete modal measurements and applied the approach to a 1600 degrees of freedom spring mass system to demonstrate the efficiency of the proposed approach for large structure. Then in a very recent study, Sipple and Sanayei [30] proposed a FRF based FE model updating method to make parameter estimation of the University of Central Florida Grid Benchmark Structure and demonstrated the usefulness of the presented approach. Very recently, Boulkaibet et al. [31] studied the use of the Shadow Hybrid Monte Carlo (SHMC) in model updating of structures. They investigated the efficiency and accuracy of the SHMC method by applying the method to two real structures.

In engineering problems there are usually nonlinearities in structures; therefore it is vital to have model updating methods for nonlinear structures as well. In literature there are different studies performed to update directly the nonlinear model of a structure. Hasselman et al. [32] presented Principal Components Analysis for model correlation and updating of nonlinear structures. In the Principal Components Analysis mainly singular value decomposition of response time histories is performed. Principal Components Analysis was also used by Anderson et al. [33] for the correlation of experimental and numerical results and for the updating of model parameters of a nonlinear FE model using crash test data. In a later study, the minimization of the parameter correlation in the model updating of nonlinear structures was studied by Anderson and Hasselman [34]. Burton et al. [35] correlated time responses of a nonlinear structural model with the experimental data and investigated the efficiency of model reduction for the model validation. Lenaerts et al. [36] studied the use of the proper orthogonal modes of displacements for the identification of parameters of nonlinear dynamical structures with an optimization procedure based on the difference between the experimental and simulated proper orthogonal modes. Hemez and Doebling [37] emphasized the need of validating numerical models based on time domain data for nonlinear, transient, structural dynamics by using various numerical and experimental test cases in their study. In a

later study, Meyer and Link [38] proposed a method for the identification of local nonlinear stiffness and damping parameters and updated the selected linear and nonlinear parameters of an initial model by minimizing the differences between analytical and experimental responses. In a more recent work, Isasa et al. [39] presented an approach which is based on multi-harmonic balance method and extended constitutive relation error for the updating of nonlinear models.

For nonlinear structures, it is possible to employ the model updating techniques developed for the linear systems, provided that the dynamic characteristics of the linear part of the structure are extracted, which may require identification of nonlinearity in the system first. However, for systems having complex nonlinearities including friction type of nonlinearity, extraction of linear dynamic characteristics and at the same time identifying nonlinearity is not a straight forward task. In early 1980's Masri et al. [40] used the restoring force surface method for the identification of nonlinearity in the nonlinear MDOF systems. Crawley et al. [41, 42] proposed a force state mapping method which is very similar to restoring force surface method for the identification of nonlinear elements in structures and joints. Yasuda et al. [43] proposed a new method for identifying nonlinear MDOF systems based on harmonic balance principle for determining the unknown coefficients of the polynomials which represent the nonlinearity in the system. In early 1990's Benhafsi et al. [44] used describing function method to parametrically identify the nonlinearities in structures. Rice [45] presented an approach for nonlinear identification by using an equivalent linearization approach for the analysis of weakly nonlinear structures. In the middle of 1990's, Soize [46] studied the identification of a SDOF nonlinear system driven by a broad-band or a colored Gaussian noise by employing a stochastic linearization approach with random parameters which approximate the power spectral density function. Thouverez and Jezequel [47] studied the identification of localized nonlinearity in structures by using an approach which is based on the Volterra kernels. Richards and Singh [48] proposed a spectral method which is based on a reverse path formulation for the identification MDOF nonlinear systems. They made

some modifications on reverse path formulation in order to use it for MDOF nonlinear systems. In a later work, Kerschen et al. [49] investigated the performance of the restoring force surface method for the identification of nonlinear systems by studying the vibrations of a fixed-free beam with two different kinds of nonlinearity. Özer et al. [50] proposed a method for localization of nonlinearity and parametric identification of the nonlinearity. Then in a later study, Özer et al. [51] extended their previous study and used describing functions and Sherman-Morrison method to identify the nonlinearity in structures. Kerschen et al. [52] used restoring force surface method to identify the nonlinearities in a system consists of a wire rope isolator maintained between a base and load mass. In a later study Bellizzi and Defilippi [53] presented a technique to identify the parameters involved in the nonlinear terms of randomly excited mechanical systems. Thothadri et al. [54] extended the nonlinear system identification method which is based on harmonic balance to MDOF systems and employed the method to both theoretical and experimental systems. Muravyov and Rizzi [55] proposed a method for determining the nonlinear modal stiffness coefficients for a FE model. Kerschen et al. [56] studied conditioned reverse path method to identify the dynamic characteristics of a continuous nonlinear system consisting of an experimental cantilever beam with a geometrical nonlinearity. Haroon et al. [57] proposed a technique for the identification of nonlinear mechanical systems without using an input measurement data. They combined time and frequency domain techniques to identify a nonlinear system. In a later study, Kerschen et al. [58] presented a very detailed literature survey in which more than 400 papers were cited for nonlinear system identification. Spottswood and Allemang [59] proposed a method for obtaining nonlinear modal models and identifying nonlinear parameters. They demonstrated the application of the approach on a fixed-fixed beam test structure. Pai and Palazotto [60] presented an amplitude and frequency modulation method (AFMM) based on empirical mode decomposition (EMD) and Hilbert–Huang transform (HHT), and developed a perturbation analysis for the identification of nonlinearities and system parameters by analyzing transient and steady-state responses. Marchesiello and Garibaldi [61]

used nonlinear subspace identification (NSI) method for the identification of clearance type of nonlinearity by applying the method to an experimental problem. Xueqi et al. [62] presented an approach which is based on direct parameter estimation and Legendre series approximation in order to identify parameters for a nonlinear system with symmetrical piecewise linear restoring forces. Worden et al. [63] applied various time and frequency based nonlinear identification methods to a damper of an automobile. Carrella and Ewins [64] proposed a method which is based on measuring different amplitudes of vibration response for identifying and quantifying nonlinearities in structures. In a more recent study by Arslan et al. [65], two different methods which are capable of identifying nonlinearities in structures were introduced and applied on a nonlinear test system. They used low forcing level excitations in the experiments in order to obtain the linear FRFs of the structure. Jalali et al. [66] applied the describing function inversion method to a clamped beam in order to identify the nonlinearities in the structure. In a recent study, Aykan and Özgüven [67] proposed a method based on describing function inversion for detection, localization, characterization and parametric identification of nonlinear elements by using incomplete experimental data. By using describing function inversion, identification of the restoring force of multiple nonlinearities which exist at the same location was performed. Very recently, Eriten et al. [68] presented nonlinear system identification (NSI) approach in which experimental measurements are combined with slow-flow dynamic analysis and empirical mode decomposition. Then the method reconstructs the dynamics through reduced-order models for investigating effects of frictional connections in bolted structures.

When multiple nonlinearities exist in a structure together with friction type of nonlinearity, it will not be possible to accurately measure the linear FRFs at low levels of force excitation, and furthermore it will be more difficult to identify nonlinearity in the system. Aykan and Özgüven [69] presented an approach (later called as Direct Nonlinearity by Describing Functions (DDF) method) for the nonlinear identification by using nonlinear FRF measurements, and using

nonlinearity matrix they demonstrated that FRFs measured at low forcing levels may deviate from the linear FRFs of the structures. The most recent publications in this area include the papers written from this present thesis study: A new method named Pseudo Receptance Difference Method (PRD) for obtaining linear FRFs in order to update linear model parameters of a nonlinear structure having multiple nonlinearities including friction type of nonlinearity is presented in references [70] and [71]. Very recently, the proposed method is experimentally validated by applying the approach to a real nonlinear T-beam test structure [72].

1.3 Motivation

ASELSAN Inc. is the largest research and development defence industry company in Turkey. Main mission of ASELSAN Inc. is to design, manufacture and integrate military products by using its own research and development capabilities. One of the critical research areas of ASELSAN Inc. is to design stabilized weapons, turret or targeting systems and to integrate these systems to different platforms such as helicopters, aircrafts and battle tanks. Since integration of these systems may change the dynamic characteristics of the platforms, and also since the systems have various moving components which make the dynamic modelling very complex, integrations of such systems to these platforms are very challenging. Examples of such integration projects are shown in Figure 1.1 and Figure 1.2.

Figure 1.1 Integration of a targeting system to an aircraft

Figure 1.2 Integration of a turret system to a helicopter

It is very important to understand the dynamic behavior of the platforms in order to increase the overall performance of the systems integrated to platforms. An example of that is to increase the shooting performance of a battle tank (Figure 1.3) with integration of tank fire control system.

Figure 1.3 Integration of a tank fire control system to a battle tank

The common problem encountered in such type of integration projects is to model the structural behaviors of the platforms or systems accurately. This modelling is commonly performed by using FE methods. However in all these types of integration projects there are nonlinear behaviors due to joints or moving components in the system or due to joints and driving systems on the platforms. Therefore the ultimate purpose is to have a mathematical model that simulates the nonlinear dynamic behavior of the system or the platform accurately. Since there are always discrepancies between predictions of the dynamic models and experimentally measured values, these models have to be updated. Although linear dynamic characteristics of systems can be obtained by using low excitation levels, sometimes this approach may not give accurate results. This happens when the excitation forcing is not low enough, or if there are multiple nonlinearities including friction type of nonlinearity in the system. Then linear dynamics of the system cannot be accurately obtained. Therefore in order to construct an accurate nonlinear model, nonlinearity in the system has to be identified and also the linear dynamics of the system has to be extracted. Then nonlinear model of the system can be obtained by model updating of the linear model first and then by combining the updated model with the identified nonlinearity.

These engineering problems are the main motivation of this thesis.

1.4 Outline of the Thesis

The outline of this thesis is given below:

In Chapter 2, the theory of model updating approach proposed for nonlinear structures is given. The theory of the proposed model updating approach for nonlinear structures which is capable of identifying the nonlinearities and extracting the linear FRFs simultaneously, is presented by explaining the identification of

nonlinearities and obtaining of linear FRFs. Then the theory of model updating of linear FE models by inverse eigensensitivity method is given.

In Chapter 3, the verification of the PRD method is demonstrated through some case studies (nonlinear lumped SDOF, MDOF systems and a nonlinear structure). In the first case study, by using nonlinear FRF measurements (with and without polluted data), nonlinearities are identified and the linear FRFs are obtained for a nonlinear SDOF system. In the second case study, application of PRD method to a nonlinear MDOF system that has multiple nonlinearities including friction is demonstrated. In the third case study, a nonlinear simulated experimental structure (T-beam with cubic stiffness and dry friction nonlinearities) is used to verify the PRD method. In the fourth case study, the effect of the excitation frequency at which measurements are made, on the accuracy of the proposed method is investigated by using the T-beam structure used in the third case study. As a final case study, in order to compare the proposed PRD method with DDF method, nonlinear parameter value is calculated for a SDOF system with cubic stiffness nonlinearity, and the results found by these two methods are compared.

In Chapter 4, the proposed model updating approach is applied to a real T-beam test system to illustrate the verification of the method on a real nonlinear system. In the first section, by applying PRD method, both linear FRFs and the nonlinearities in the system are obtained from experimentally measured nonlinear FRFs. The linear FE model of the system which is modelled in ANSYS is updated for the first mode of the structure by employing the inverse eigensensitivity method and also by using the linear FRFs obtained through PRD method. By using the identified nonlinearity and the updated linear FE model, updated nonlinear model of the T-beam is obtained. Predicted nonlinear FRFs of the system are compared with the measured FRFs at different forcing levels in order to illustrate the accuracy of the updated nonlinear model of the system. In the second section of this chapter, linear FRFs are obtained from experimentally measured nonlinear FRFs for the first, second and third global

mode of the test system by using PRD method. Then the linear FE model of the test system is updated for the first three global modes of the structure by using the extracted linear FRFs employing first the PRD method and then using ANSYS Design Exploration Optimization. Combining updated linear FE models with the identified nonlinearity, updated nonlinear models of the test structure are constructed. Finally, in order to demonstrate the accuracy of the updated nonlinear models of the system, predicted and measured FRFs of the test structure are compared at different forcing levels.

In Chapter 5, application of PRD method to real engineering problem is given. Detailed structural model of a nonlinear gun barrel of a battle tank at the fundamental frequency is studied and model updating of the nonlinear gun barrel is performed by using the proposed model updating approach. First, using the PRD method, both linear FRFs and the nonlinearities in the system are obtained from experimentally measured nonlinear FRFs. Furthermore, in order to compare the results obtained by using the PRD method, both linear FRFs and the nonlinearities in the system are also calculated by using the DDF method. Linear FE model of the gun barrel built in ANSYS is updated by using the linear FRFs obtained through the PRD method. Combining updated linear FE model of the gun barrel with the identified nonlinearity, updated nonlinear model of the gun barrel is constructed. Finally, predicted and measured FRFs of the gun barrel are compared at different forcing levels in order to demonstrate the accuracy of the updated nonlinear model of the system. To sum up, using this real engineering problem, the performance of the proposed method on real engineering problem is examined and it is shown that, the method can be applied to a real engineering problem successfully.

In Chapter 6 brief summary and conclusions is given.

CHAPTER 2

THEORY

2.1 Introduction

In this chapter, mainly the theory of model updating approach proposed for nonlinear structures is presented. Firstly, modelling of nonlinearities is briefly described in Section 2.2. After the brief explanation of modelling nonlinearities, calculation of nonlinear response by using describing function method is presented in Section 2.3. In Section 2.4, theory of the proposed model updating approach for nonlinear structures is given by explaining the nonlinear identification, obtaining linear FRFs and model updating of linear FE models by inverse eigensensitivity method.

2.2 Modeling Nonlinearities

For a nonlinear MDOF system, the equation of motion can be written as

$$[M]\{\ddot{x}(t)\}+[C]\{\dot{x}(t)\}+i[D]\{x(t)\}+[K]\{x(t)\}+\{N(x,\dot{x},t)\}=\{f_{ext}(t)\} \tag{2.1}$$

where $[M]$, $[C]$, $[D]$, $[K]$ represent mass, viscous damping, structural damping and stiffness matrices of the system, respectively. $\{x(t)\}$, $\{f_{ext}(t)\}$ stand for displacement response and external forcing vector, respectively, i and dot are the imaginary number and derivation with respect to time, respectively. All the nonlinear internal forces are represented by $\{N(x,\dot{x},t)\}$ vector which depends on displacement and velocity. If we consider the r^{th} element of the nonlinear internal forcing vector

$\{N(x,\dot{x},t)\}$ and show that element as N_r, for a "n" degrees of freedom system, we can define N_r as

$$N_r = \sum_{j=1}^{n} n_{rj} \qquad r = 1, 2, ..., n \tag{2.2}$$

In Equation (2.2), if $r \neq j$, n_{rj} represents the nonlinear internal force between the coordinates r and j, and if $r=j$, n_{rj} stands for the nonlinear internal force between ground and the coordinate r. Let us define intercoordinate displacement between the coordinates r and j as

$$x_{rj} = x_r - x_j \qquad for \;\; r \neq j \tag{2.3}$$

$$x_{rj} = x_r \qquad for \;\; r = j \tag{2.4}$$

Note that n_{rj} can be any function of displacement and velocity, therefore we can represent it with the following equation.

$$n_{rj} = n_{rj}(x_{rj}, \dot{x}_{rj}) \tag{2.5}$$

If we consider the external forcing vector $\{f_{ext}(t)\}$, we can express it in complex vector form as

$$\{f_{ext}(t)\} = \{F_{ext}\} e^{i\omega t} \tag{2.6}$$

Let us define the product of angular frequency ω and time t as generic angle θ and rewrite the Equation (2.6) as

$$\{f_{ext}(t)\} = \{F_{ext}\} e^{i\theta} \tag{2.7}$$

In Equation (2.7), $\{F_{ext}\}$ is the external forcing amplitude vector. When a nonlinear system is excited with a harmonic force, the response is not composed of terms with only input forcing frequency, but composed of terms with also harmonics of that frequency. Therefore, the response is periodic and this response can be defined by Fourier series representation as

$$\{x(t)\} = \sum_{m=0}^{\infty} \{X\}_m e^{im\theta} \tag{2.8}$$

In Equation (2.8), m is the degree of harmonic order and $\{X\}_m$ represents the complex amplitude displacement response of the m^{th} harmonic. If we consider the complex amplitude displacement response attached to coordinate r, for the m^{th} harmonic we can define it as

$$\left(X_r\right)_m = \left(\left|X_r\right| \angle \psi_r\right)_m = \left|X_r\right|_m e^{i(\psi r)m} \tag{2.9}$$

Equation (2.9) is the magnitude and the phase notation form of the complex displacement response. In Equation (2.9) $\left|X_r\right|_m$ and $\left(\psi_r\right)_m$ is the magnitude and phase of the complex amplitude displacement response. If we consider the Fourier series representation of the response given in Equation (2.8) it has infinite terms which are practically not possible to calculate; therefore truncation has to be applied to the formulation by just considering the first p harmonics. Then the response can expressed approximately as

$$\{x(t)\} \approx \sum_{m=0}^{p} \{x(t)\}_m = \sum_{m=0}^{p} \{X\}_m e^{im\theta} \tag{2.10}$$

Since Fourier series representations are obtained for the responses, then we can extend these formulation for the relative displacement responses (i.e. intercoordinate displacement response) between arbitrary coordinates. Let us define relative displacement response between coordinates *r* and *j* as

$$x_{rj}(t) = x_r(t) - x_j(t) \tag{2.11}$$

Fourier series representation of $x_{rj}(t)$ can be written as

$$x_{rj}(t) = \sum_{m=0}^{\infty} x_{rj}(t)_m = \sum_{m=0}^{\infty} \left(X_{rj}\right)_m e^{im\theta} \tag{2.12}$$

In Equation (2.12), $\left(X_{rj}\right)_m$ is given by

$$\left(X_{rj}\right)_m = \left(X_r\right)_m - \left(X_j\right)_m \qquad for\ r \neq j \tag{2.13}$$

If we consider the complex relative displacement response $\left(X_{rj}\right)_m$ for the m^{th} harmonic, we can express it as

$$\left(X_{rj}\right)_m = \left(\left|X_{rj}\right| \angle \psi_{rj}\right)_m = \left|\left(X_{rj}\right)_m\right| e^{i(\psi_{rj})m} \tag{2.14}$$

Equation (2.14) is the magnitude and the phase notation form of the complex relative amplitude displacement response between coordinates *r* and *j*. In Equation (2.14),

$\left|\left(X_{rj}\right)_m\right|$ and $\left(\psi_{rj}\right)_m$ is the magnitude and phase of the complex amplitude relative displacement response. Similarly performing truncation for the Fourier series representation and considering only the first p harmonics, approximate relative response can be written as

$$x_{rj}(t) \approx \sum_{m=0}^{p} x_{rj}(t)_m = \sum_{m=0}^{p} \left(X_{rj}\right)_m e^{im\theta} \tag{2.15}$$

2.3 Calculation of Nonlinear Response by Using Describing Function Method

In this section, brief theory of the nonlinear response calculation by using describing function method [73] will be given. Let us consider n_{rj} (the nonlinear internal force between the coordinates *r* and *j*) which is defined by the Equation (2.5). Assuming that for simplicity n_{rj} is dependent only on displacement, Fourier series representation of this force can be written as

$$n_{rj} = n_{rj}(x_{rj}) = \sum_{m=0}^{\infty} \left(n_{rj}(x_{rj})\right)_m e^{im\theta} \tag{2.16}$$

$\left(n_{rj}(x_{rj})\right)_m$ terms can be obtained by Fourier integrals and they are given as

$$\left(n_{rj}(x_{rj})\right) = \frac{1}{2\pi}\int_0^{2\pi} n_{rj}(x_{rj})d\theta \qquad for\ m = 0 \tag{2.17}$$

$$\left(n_{rj}(x_{rj})\right) = \frac{i}{\pi}\int_0^{2\pi} n_{rj}(x_{rj})e^{-im\theta}d\theta \qquad for\ m \neq 0 \tag{2.18}$$

If nonlinear element is odd, then $\left(n_{rj}(x_{rj})\right)$ in Equation (2.17) will be zero. When, only single harmonic response is assumed, Equation (2.16) will simplify to the following form

$$n_{rj}(x_{rj}) = \left(\frac{i}{\pi} \int_0^{2\pi} n_{rj}(x_{rj}) e^{-i\theta} d\theta \right) e^{i\theta} \tag{2.19}$$

$n_{rj}(x_{rj})$ can also defined by using describing function v_{rj}. The v_{rj} is actually the equivalent linear complex stiffness of $n_{rj}(x_{rj})$ for harmonic x_{rj}. Also, v_{rj} is a function of the absolute value of complex amplitude displacement response, and by using those definitions we can write the nonlinear internal forces as

$$n_{rj}(x_{rj}) = v_{rj}\left(\left|X_{rj}\right|\right) X_{rj} e^{i\theta} \tag{2.20}$$

If the nonlinear force representations in Equation (2.19) and (2.20) are compared, we can easily write the following equation.

$$v_{rj} = \frac{i}{\pi \left|X_{rj}\right|} \int_0^{2\pi} n_{rj}(x_{rj}) e^{-i\theta} d\theta \tag{2.21}$$

Budak and Özgüven [74] express the nonlinear forcing vector in a nonlinear structure as a matrix multiplication form for harmonically excited nonlinear systems and this form of nonlinear forces were employed in response calculation of nonlinear systems in different studies [75,76]. The internal nonlinear forces are defined as

$$\{N(x,\dot{x})\} = [\Delta(x,\dot{x})]\{X\} e^{i\omega t} \tag{2.22}$$

$\left[\Delta(x,\dot{x})\right]$ is the "nonlinearity matrix" which was first presented by Budak and Özgüven [74] for certain types of nonlinearities. Then Tanrıkulu et al. [77] used nonlinearity matrix and define it for any type of nonlinearity by using describing functions.

The elements of $\left[\Delta(x,\dot{x})\right]$ are defined with the following equations [77]:

$$\Delta_{rr} = \nu_{rr} + \sum_{\substack{j=1 \\ j\neq r}}^{n} \nu_{rj} \qquad r = 1, 2, ..., n \tag{2.23}$$

$$\Delta_{rj} = -\nu_{rj}, \qquad r \neq j, \qquad r = 1, 2, ..., n \tag{2.24}$$

If we consider the nonlinear MDOF system which was defined by Equation (2.1), we can express FRF matrix (in the form of receptances) of the linear part of this nonlinear system as

$$\left[H^{L}\right] = \left[-\omega^2\left[M\right] + i\omega\left[C\right] + i\left[D\right] + \left[K\right]\right]^{-1} \tag{2.25}$$

Similarly by using the nonlinearity matrix we can write the nonlinear FRF matrix (in the form of receptances) of the same nonlinear system as

$$\left[H^{NL}\right] = \left[-\omega^2\left[M\right] + i\omega\left[C\right] + i\left[D\right] + \left[K\right] + \left[\Delta\right]\right]^{-1} \tag{2.26}$$

Note that, In Equation (2.26), nonlinear FRF matrix $\left[H^{NL}\right]$ is response dependent. Then by using the definition of receptance we can find the response of the system. It is given by the following equation.

$$\left\{X\right\} = \left[H^{NL}\right]\left\{F_{ext}\right\} \tag{2.27}$$

Since nonlinear FRF matrix $\left[H^{NL}\right]$ is response dependent, in order to solve Equation (2.27), iteration has to be made. Performing iterations, the nonlinear response of the system can be calculated. As a starting initial guess, linear response of the nonlinear system can be used. By using the linear responses, initial nonlinearity matrix can be obtained. Then by using Equation (2.27), the new responses can be estimated. This iteration goes on until certain error criterion is satisfied. In this thesis, in order to solve Equation (2.27), fixed point iteration method is used. The iteration step is given by the following equation.

$$\{X\}_{i+1} = \left[H^{NL}\left(\{X\}_i\right)\right]\{F_{ext}\} \tag{2.28}$$

Iterations are repeated until the relative error given below drops below a certain value.

$$e = \max\left(\left|\frac{X^n{}_{i+1} - X^n{}_i}{X^n{}_i}\right|\right), \qquad n = 1, 2, ..., N \tag{2.29}$$

where N is the number of degrees of freedom.

In order to avoid divergence or to obtain faster convergence, relaxation is applied to the fixed point iteration:

$$\left\{X^*\right\}_{i+1} = (\lambda)\{X\}_{i+1} + (1-\lambda)\{X\}_i, \qquad 0 < \lambda < 1 \tag{2.30}$$

where λ is the weighting factor.

In this thesis, single harmonic describing functions of nonlinearities are used. The single harmonic describing functions of different nonlinearities can be found in [73].

For the nonlinearity types that are used in Chapter 3, single harmonic describing function representations are given below [78].

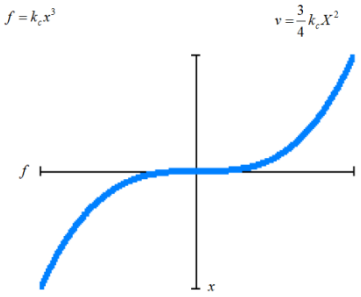

Figure 2.1 Single harmonic describing function of cubic stiffness

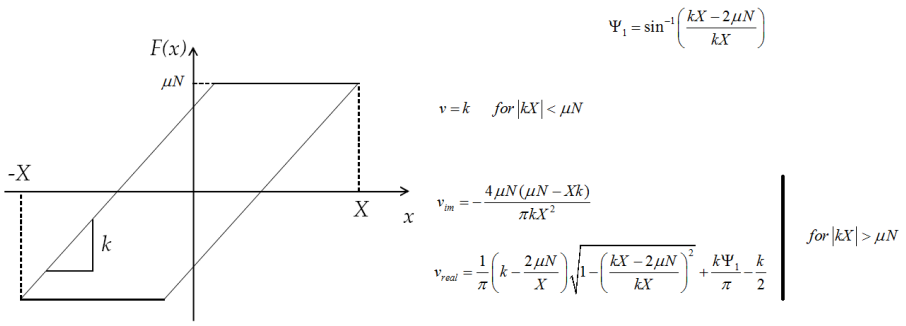

Figure 2.2 Single harmonic describing function of dry friction model

2.4 Model Updating of Nonlinear System

In this section theory that is used for model updating approach for nonlinear structures is explained. Firstly theory of the proposed Pseudo Receptance Difference

(PRD) method is given for nonlinear identification and obtaining nonlinearities [70]. Then in the next section, theory of DDF method [79] that is proposed by Aykan and Özgüven is presented. Then as the final part in this section, model updating of linear FE models by using inverse eigensensitivity method is explained.

2.4.1 Nonlinear Identification and Obtaining Linear FRFs by PRD Method

In this section the theory of the PRD method developed will be given. PRD method developed is based on the main theory given in [50, 74, 77]. Let us consider the FRF matrix of the linear part of the nonlinear system given by Equation (2.25) and the response level dependent nonlinear FRF matrix given by Equation (2.26). If we take the inverses of $\left[H^{NL}\right]$ and $\left[H^{L}\right]$ matrices, we can write the following equations:

$$\left[H^{L}\right]^{-1}=\left[-\omega^{2}\left[M\right]+i\omega\left[C\right]+i\left[D\right]+\left[K\right]\right] \tag{2.31}$$

$$\left[H^{NL}\right]^{-1}=\left[-\omega^{2}\left[M\right]+i\omega\left[C\right]+i\left[D\right]+\left[K\right]+\left[\Delta\right]\right] \tag{2.32}$$

Subtracting Equation (2.31) from Equation (2.32), the equation given below is obtained.

$$\left[\Delta\right]=\left[H^{NL}\right]^{-1}-\left[H^{L}\right]^{-1} \tag{2.33}$$

Let us consider a nonlinear MDOF system that has multiple nonlinearities including friction type of nonlinearity, then it is possible to partition the nonlinearity matrix $\left[\Delta\right]$ as

$$\left[\Delta\right]=\left[\Delta_{f}\right]+\left[\Delta_{HF}\right] \tag{2.34}$$

In Equation (2.34), $[\Delta_{HF}]$ represents the nonlinearity matrix due to nonlinearities which act dominantly at high forcing levels of excitation and $[\Delta_f]$ represents nonlinearity matrix due to friction type of nonlinearity.

Substituting Equation (2.34) into Equation (2.33) gives the following equation.

$$[\Delta_f]+[\Delta_{HF}]=[H^{NL}]^{-1}-[H^L]^{-1} \tag{2.35}$$

Depending on the level of the excitation force, $[\Delta_f]$ and $[\Delta_{HF}]$ matrices will have negligible terms. For low forcing levels, $[\Delta_f]$ will have larger terms compared to those of $[\Delta_{HF}]$. Therefore at low forcing levels, Equation (2.35) can approximately be written as

$$[\Delta_f]\cong[H^{NL}]^{-1}-[H^L]^{-1} \tag{2.36}$$

On the other hand, when the structure is excited at high forcing levels, $[\Delta_{HF}]$ will be dominant and the terms of $[\Delta_f]$ will be negligible. Then at high forcing levels Equation (2.35) can approximately be written as

$$[\Delta_{HF}]\cong[H^{NL}]^{-1}-[H^L]^{-1} \tag{2.37}$$

If Equation (2.36) is used once and Equation (2.37) is used several times for FRFs measured at the same frequency but at different forcing levels, nonlinearities in the system can be identified and the linear FRFs of the structure can be extracted.

Firstly, let us excite the system once at low forcing level, by using Equation (2.36), the following equation can be written.

$$\left[\Delta_f\right]_1 = \left[H^{NL}\right]_1^{-1} - \left[H^{L}\right]_1^{-1} \tag{2.38}$$

Then let the system be excited (*n-1*) times at different high forcing levels. Using Equation (2.37), the following set of equations can be obtained.

$$\left[\Delta_{HF}\right]_2 = \left[H^{NL}\right]_2^{-1} - \left[H^{L}\right]_2^{-1} \tag{2.39}$$

$$\left[\Delta_{HF}\right]_3 = \left[H^{NL}\right]_3^{-1} - \left[H^{L}\right]_3^{-1} \tag{2.40}$$

$$\left[\Delta_{HF}\right]_4 = \left[H^{NL}\right]_4^{-1} - \left[H^{L}\right]_4^{-1} \tag{2.41}$$

$$\vdots$$

$$\left[\Delta_{HF}\right]_n = \left[H^{NL}\right]_n^{-1} - \left[H^{L}\right]_n^{-1} \tag{2.42}$$

Equations from (2.39) to (2.42) can be written in a more compact form as

$$\left[\Delta_{HF}\right]_i = \left[H^{NL}\right]_i^{-1} - \left[H^{L}\right]_i^{-1} \qquad i = 2,3,...,n \tag{2.43}$$

Subtracting Equation (2.38) from each of the equations given in Equation (2.43), a new set of equations is obtained and it is given below.

$$\left[\Delta_{HF}\right]_{i+1} - \left[\Delta_f\right]_1 = \left[H^{NL}\right]_{i+1}^{-1} - \left[H^{NL}\right]_1^{-1} \qquad i = 1,2,...,(n-1) \tag{2.44}$$

In Equation (2.44), subscript 1 indicates low level of force excitation case, subscripts 2, 3, … n indicate high level of force excitation cases. Since the linear FRF matrix does not depend on the force excitation level and it is always constant for different force excitation levels, as can be seen above, these terms drop out and they do not exist in Equation (2.44).

Considering the set of equations given in Equation (2.44), at the left hand sides of the equations, both zero and nonzero elements exist. These nonzero elements are related to nonlinear coordinates (coordinates to which nonlinear elements are attached) and they can be represented by polynomial functions of response amplitudes with unknown coefficients. These polynomial functions are the describing functions of the corresponding nonlinearities in the structure. Since there are always more data points than the number of unknown coefficients, in order to obtain the unknown coefficients, least square fit can be applied. Performing polynomial fit for (*n-1*) data points in a least square sense, the equation of the corresponding regression curve can be obtained, to calculate unknown coefficients. If the nonlinearity in the structure is more complex, polynomial fit may be insufficient; therefore it may be more proper to use nonlinear fit. By comparing the terms of the regression equation with the corresponding describing functions, identification of the nonlinearity can be performed parametrically. Once the nonlinearities in the structure are identified, then linear FRFs can easily be obtained by employing the equation given below:

$$\left[H^{L}\right]_1 = \left[\left[H^{NL}\right]_1^{-1} - \left[\Delta_f\right]_1\right]^{-1} \tag{2.45}$$

From Equation (2.45) it can be observed that full matrix inversions have to be made in order to obtain the linear FRF of the structure. This is the main drawback of the above equation. However, for most of the nonlinear structures, nonlinear elements in the structure are localized therefore the nonlinearity matrix can be partitioned as

$$\left[\Delta\right]=\begin{bmatrix}\left[\Delta_{aa}\right] & \left[0\right]\\ \left[0\right] & \left[0\right]\end{bmatrix} \tag{2.46}$$

where subscript *a* stands for the coordinates where nonlinear elements are attached to ("nonlinear coordinates" in short). Pre-multiplication of all the terms in Equation (2.33) by $\left[H^{L}\right]$ and post- multiplication by $\left[H^{NL}\right]$ yields the following equation.

$$\left[H^{L}\right]\left[\Delta\right]\left[H^{NL}\right]=\left[H^{L}\right]\left[H^{NL}\right]^{-1}\left[H^{NL}\right]-\left[H^{L}\right]\left[H^{L}\right]^{-1}\left[H^{NL}\right] \tag{2.47}$$

Performing some simplifications, Equation (2.47) reduces to

$$\left[H^{L}\right]\left[\Delta\right]\left[H^{NL}\right]=\left[H^{L}\right]\left[I\right]-\left[I\right]\left[H^{NL}\right] \tag{2.48}$$

Substituting the nonlinearity matrix given in Equation (2.46) into Equation (2.48), the following equation is obtained:

$$\begin{bmatrix}\left[H^{L}{}_{aa}\right] & \left[H^{L}{}_{ab}\right]\\ \left[H^{L}{}_{ba}\right] & \left[H^{L}{}_{bb}\right]\end{bmatrix}\begin{bmatrix}\left[\Delta_{aa}\right] & \left[0\right]\\ \left[0\right] & \left[0\right]\end{bmatrix}\begin{bmatrix}\left[H^{NL}{}_{aa}\right] & \left[H^{NL}{}_{ab}\right]\\ \left[H^{NL}{}_{ba}\right] & \left[H^{NL}{}_{bb}\right]\end{bmatrix}=\ldots$$
$$\ldots\begin{bmatrix}\left[H^{L}{}_{aa}\right] & \left[H^{L}{}_{ab}\right]\\ \left[H^{L}{}_{ba}\right] & \left[H^{L}{}_{bb}\right]\end{bmatrix}-\begin{bmatrix}\left[H^{NL}{}_{aa}\right] & \left[H^{NL}{}_{ab}\right]\\ \left[H^{NL}{}_{ba}\right] & \left[H^{NL}{}_{bb}\right]\end{bmatrix} \tag{2.49}$$

Subscript *b* in Equation (2.49) stands for linear coordinates. Making matrix multiplication for the left hand side of the equation and considering the first submatrix of the resultant matrix, the following equation can be written:

$$\left[H^{L}{}_{aa}\right]\left[\Delta_{aa}\right]\left[H^{NL}{}_{aa}\right]=\left[H^{L}{}_{aa}\right]-\left[H^{NL}{}_{aa}\right] \tag{2.50}$$

Pre-multiplication of all terms in Equation (2.50) with $\left[H^{L}{}_{aa}\right]^{-1}$ and post-multiplication with $\left[H^{NL}{}_{aa}\right]^{-1}$ yields

$$\begin{aligned}&\left[H^{L}{}_{aa}\right]^{-1}\left[H^{L}{}_{aa}\right]\left[\Delta_{aa}\right]\left[H^{NL}{}_{aa}\right]\left[H^{NL}{}_{aa}\right]^{-1}=...\\&...\left[H^{L}{}_{aa}\right]^{-1}\left[H^{L}{}_{aa}\right]\left[H^{NL}{}_{aa}\right]^{-1}-\left[H^{L}{}_{aa}\right]^{-1}\left[H^{NL}{}_{aa}\right]\left[H^{NL}{}_{aa}\right]^{-1}\end{aligned} \tag{2.51}$$

Performing some simplifications, Equation (2.51) reduces to

$$\left[\Delta_{aa}\right]=\left[H^{NL}{}_{aa}\right]^{-1}-\left[H^{L}{}_{aa}\right]^{-1} \tag{2.52}$$

When the resulting equation given above is compared to Equation (2.33), it is observed that they are similar equations. Therefore proposed approach for nonlinear identification and linear FRF calculation can be applied to Equation (2.52). Then the linear FRF matrix for the nonlinear coordinates can be written as

$$\left[H^{L}{}_{aa}\right]_{1}=\left[\left[H^{NL}{}_{aa}\right]_{1}^{-1}-\left[\Delta_{f\,aa}\right]_{1}\right]^{-1} \tag{2.53}$$

As can be seen from Equation (2.53), considerable reduction in computational effort will be achieved for the structures that have localized nonlinearities.

Once the linear FRFs are obtained by using Equation (2.53), then these linear FRFs can be used for the model updating of a FE model. In several model updating methods, measuring FRFs at limited number of coordinates is enough. Therefore, having FRF of even a single coordinate may be sufficient for applying model updating method. However, if FRFs of the linear coordinates are also necessary to employ the model updating method, then the other 3 matrix equations obtained from

Equation (2.49) have to be solved. Then it would be necessary to measure the nonlinear responses at required linear coordinates as well.

When multiple measurement points are used on a structure, then all the elements of the nonlinear FRF matrix need to be obtained, which may be difficult in practice. For structures having localized nonlinearities, which can be modelled as nonlinear elements connected to a single coordinate, the measurement at this single coordinate can be considered, which reduces Equation (2.44) to a very simple algebraic equation:

$$\Delta_{HF_{i+1}} - \Delta_{f_1} = \frac{1}{H^{NL}_{i+1}} - \frac{1}{H^{NL}_{1}} \qquad i = 1,2,...,(n-1) \tag{2.54}$$

Since all the matrix inversions vanish and are reduced to inversions of scalar values, it is much simpler to calculate the right hand side of Equation (2.54) for all *i* values by using experimental measurements. Similarly, for the calculation of linear FRFs of the system, it is possible to write the following equation:

$$\frac{1}{H^{L}_{1}} = \frac{1}{H^{NL}_{1}} - \Delta_{f_1} \tag{2.55}$$

All of the above equations are valid at any frequency. However for an arbitrary excitation frequency, the difference between the linear and nonlinear FRFs may be very small, so that this may make the identification of nonlinearity very difficult. Therefore nonlinear identification can be performed most accurately at frequencies where system response is mostly affected from the existence of nonlinearity.

2.4.2 Nonlinear Identification and Obtaining Linear FRFs by DDF Method

DDF method [79] is based on the same equation given by Equation (2.33). The method is capable of both identifying nonlinearity and obtaining linear FRFs of a nonlinear structure that has multiple nonlinearities. Considering two different force excitation levels F_1 and F_2, Equation (2.33) can be written as

$$\left[\Delta\right]_1 = \left[H^{NL}\right]_1^{-1} - \left[H^{L}\right]_1^{-1} \quad for\ F = F_1 \tag{2.56}$$

$$\left[\Delta\right]_2 = \left[H^{NL}\right]_2^{-1} - \left[H^{L}\right]_2^{-1} \quad for\ F = F_2 \tag{2.57}$$

Noting that $\left[H^{L}\right]$ is not dependent on the force level, subtracting Equation (2.56) from Equation (2.57), the following equation can be obtained.

$$\left[\Delta\right]_2 - \left[\Delta\right]_1 = \left[H^{NL}\right]_2^{-1} - \left[H^{NL}\right]_1^{-1} \tag{2.58}$$

As seen from Equation (2.58), linear FRF matrix $\left[H^{L}\right]$ cancels out in the resulting equation. For structures having localized nonlinearities, which can be modelled as nonlinear elements connected to a single coordinate, the measurement at this single coordinate can be considered, which reduces Equation (2.58) to a very simple algebraic equation:

$$\Delta_2 - \Delta_1 = \frac{1}{H^{NL}_2} - \frac{1}{H^{NL}_1} \tag{2.59}$$

As seen from Equation (2.59), the terms on the right hand side of Equation (2.59) can be experimentally measured. Assuming that nonlinearity matrix is dependent on

displacements only, if a polynomial function is assumed for the nonlinearity matrix, then it can be expressed as

$$\Delta(x) = \sum_{i=1}^{\infty} c_i x^i \tag{2.60}$$

In order to solve Equation (2.59), number of equations must be at least as many as the order of the polynomial. Since Equation (2.59) is valid at any frequency, the necessary number of equations can be obtained by using nonlinear FRF measurements at different frequencies. Generally the number of equations is much more than the number of unknowns (coefficients of the polynomial function). Then, least square fit for the polynomial coefficients can be applied.

Considering an i^{th} order polynomial for nonlinearity matrix, and substituting Equation (2.60) into Equation (2.59) yields the following equation

$$(c_1 x_2 + c_2 x_2^2 + \ldots + c_i x_2^i) - (c_1 x_1 + c_2 x_1^2 + \ldots + c_i x_1^i) = \frac{1}{H^{NL}{}_2} - \frac{1}{H^{NL}{}_1} \tag{2.61}$$

which can also be written in compact form as

$$\begin{bmatrix} x_2 - x_1 & x_2^2 - x_1^2 & \ldots & x_2^i - x_1^i \end{bmatrix} \begin{bmatrix} c_1 \\ c_2 \\ \vdots \\ c_i \end{bmatrix} = \frac{1}{H^{NL}{}_2} - \frac{1}{H^{NL}{}_1} \tag{2.62}$$

Since the above equation is valid for any frequency, measuring nonlinear FRFs at "*n*" different frequencies (*n > i)*, the following set of equations can be written

$$\begin{bmatrix} x_2(\omega_1)-x_1(\omega_1) & x_2^2(\omega_1)-x_1^2(\omega_1) & \dots & x_2^i(\omega_1)-x_1^i(\omega_1) \\ x_2(\omega_2)-x_1(\omega_2) & x_2^2(\omega_2)-x_1^2(\omega_2) & \dots & x_2^i(\omega_2)-x_1^i(\omega_2) \\ \vdots & \vdots & \vdots & \vdots \\ x_2(\omega_n)-x_1(\omega_n) & x_2^2(\omega_n)-x_1^2(\omega_n) & \cdots & x_2^i(\omega_n)-x_1^i(\omega_n) \end{bmatrix} \begin{bmatrix} c_1 \\ c_2 \\ \vdots \\ c_i \end{bmatrix} = \dots$$

$$\dots \begin{bmatrix} \frac{1}{H^{NL}{}_2(\omega_1)} - \frac{1}{H^{NL}{}_1(\omega_1)} \\ \frac{1}{H^{NL}{}_2(\omega_2)} - \frac{1}{H^{NL}{}_1(\omega_2)} \\ \vdots \\ \frac{1}{H^{NL}{}_2(\omega_n)} - \frac{1}{H^{NL}{}_1(\omega_n)} \end{bmatrix} \tag{2.63}$$

Equation (2.63) can be solved by using pseudo inversion in order to obtain the polynomial coefficients. Once the nonlinearities are identified, then by using either of Equation (2.56) or (2.57), the linear FRFs of the system can be calculated.

2.4.3 Model Updating of Linear FE Models-Inverse Eigensensitivity Method

Since the FRFs of the underlying linear part of a nonlinear structure can be calculated by using either of the methods given in last two sections, then any model updating approach developed for a linear system can be employed for the model updating of the structure. One of the common methods used for model updating is the inverse eigensensitivity method [80]. The most advantageous aspect of this method is that there is no need to apply a model reduction /expansion method. Only the information at the measured coordinates and natural frequencies are necessary for the application of the method.

Inverse eigensensitivity method is based on the following equation:

$$\{\Delta r\} = [S]\{\Delta p\} \tag{2.64}$$

where $\{\Delta r\}$ is the residual vector between the reference and actual responses, $\{\Delta p\}$ is the change that needs to be done in parameter vector, and $[S]$ is the sensitivity matrix.

If we consider the modal analysis context, we can redefine each term in Equation (2.64). In Equation (2.64), $\{r\}$ consists of modeshapes and natural frequencies, $\{p\}$ consists of geometrical dimensions or material properties used in the mathematical or FE model, and $[S]$ is the modal sensitivity matrix. Sensitivity matrix $[S]$ in Equation (2.64) can be expressed as

$$[S] = \begin{bmatrix} S_{r_1}{}^{p_1} & \cdots & S_{r_1}{}^{p_m} \\ \vdots & \ddots & \vdots \\ S_{r_n}{}^{p_1} & \cdots & S_{r_n}{}^{p_m} \end{bmatrix} \tag{2.65}$$

In Equation (2.65), $S_{r_n}{}^{p_m}$ represents the sensitivity of the n^{th} modal parameter to the m^{th} updating parameter. It can also be defined mathematically as the partial derivative of the n^{th} modal parameter to the m^{th} updating parameter and it is given by the following equation:

$$S_{r_n}{}^{p_m} = \frac{\partial r_n}{\partial p_m} \tag{2.66}$$

In order to calculate the sensitivities for simple structures, modal parameters can be formulated as the functions of updating parameters and by using these functions the sensitivities can be obtained performing simple differentiation. However it is not straightforward to calculate the sensitivities for complex structures, therefore it is necessary to use numerical differentiation.

Once $[S]$ matrix and $\{\Delta r\}$ vector are calculated, then $\{\Delta p\}$ vector can be obtained by using Equation (2.67):

$$\{\Delta p\} = [S]^{-1}\{\Delta r\} \tag{2.67}$$

Usually, the number of unknowns is less than the number of equations, therefore in order to solve Equation (2.64) for $\{\Delta p\}$, least square solution should be applied. Furthermore, since the relation between the modal parameters and updating parameters are generally nonlinear, iteration has to be performed in order to calculate the updating parameters.

CHAPTER 3

CASE STUDIES WITH SIMULATED EXPERIMENTAL DATA-APPLICATION OF MODEL UPDATING APPROACH TO NONLINEAR SYSTEMS

In this chapter, applications of the PRD method to nonlinear lumped SDOF and MDOF systems, and a nonlinear structure are demonstrated. In the first case study nonlinearities are identified and the linear frequency response function is calculated for a nonlinear SDOF system, by using nonlinear FRF measurements. Firstly, pure theoretical data is used in the analysis and then polluted data is used in the analysis in order to simulate the experimental measurements more realistically. In the second case study, PRD method is applied to a nonlinear MDOF system. The system has multiple nonlinearities including friction. In this case study, simulated experimental data is used in the analysis. As a third case study, PRD method is applied to a nonlinear structure where the simulated experimental results are obtained from the FE model of the structure. The nonlinear structure is a T-beam which has cubic stiffness and dry friction nonlinearities. In order to simulate the experimental measurements, again polluted data is used in the analysis. Identification of nonlinearities and calculation of linear FRFs of the system are presented by using the approach proposed. In obtaining all simulated experimental data, harmonic balance approach is used. In the fourth case study, the effect of the excitation frequency at which measurements are made, on the accuracy of the proposed method is investigated. The nonlinear T-beam used in the third case study is employed. Applying the PRD method, the values of the nonlinear parameters are calculated by using the simulated experimental FRF values obtained at a different excitation frequency each time. Then these nonlinear parameter values are compared with each

other. In the first four case studies, cubic stiffness and only stiffness part of the frictional nonlinearity are identified, since in the experimental studies given Chapter 4 and Chapter 5, all the nonlinearities including friction are identified in terms of describing functions. As a final case study, in order to compare the proposed PRD method with DDF method, the value of the nonlinear parameter is calculated for a SDOF system with cubic stiffness nonlinearity. Identified nonlinear parameter values are compared to each other.

3.1 Application of PRD Method to a SDOF Lumped System

In this case study, nonlinear SDOF system with cubic stiffness and dry friction nonlinearities is used. Firstly, pure theoretical data is used in the analysis and nonlinearities are identified by using the PRD method. As a next study in this section the same nonlinear SDOF system is analyzed by using a polluted data.

3.1.1 Application of PRD Method without Polluted Data

The nonlinear SDOF system used in this case study has cubic stiffness and dry friction nonlinearities. The dry friction model and nonlinear SDOF system studied are given in Figure 3.1.

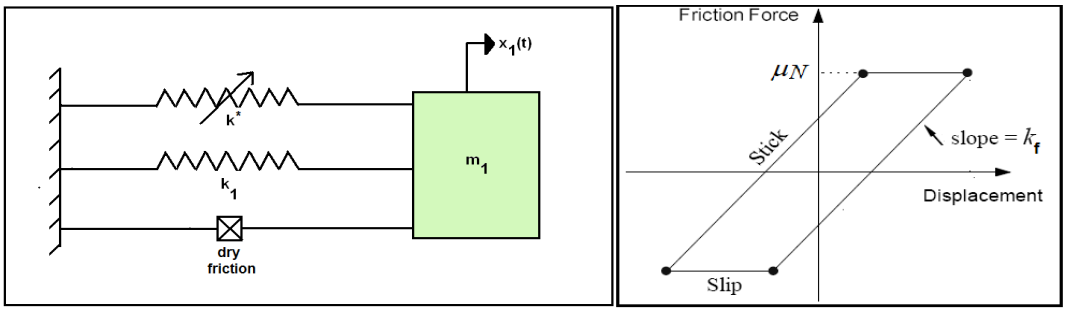

(a) (b)

Figure 3.1 (a) SDOF nonlinear system (b) Dry friction model

The parameters of these nonlinear elements and the properties of the system are given as follows:

$$m_1 = 0.1\,kg,\ \ k_1 = 2x10^6\ N/m\ \ and\ \ \gamma\,(loss\ \ factor) = 0.01$$

$$k^* = 1x10^{10}\ N/m^3$$

$$\mu = 0.1,\ \ Normal\ Force = 10\ N\ \ \ and\ \ \ k_f = 3x10^5\ N/m$$

Firstly, low amplitude harmonic force (F=0.01N) is used to excite the system. At this forcing level, response of the system and the linear frequency response of the system obtained disregarding both friction and cubic stiffness nonlinearity are compared to each other. This comparison is given in Figure 3.2.

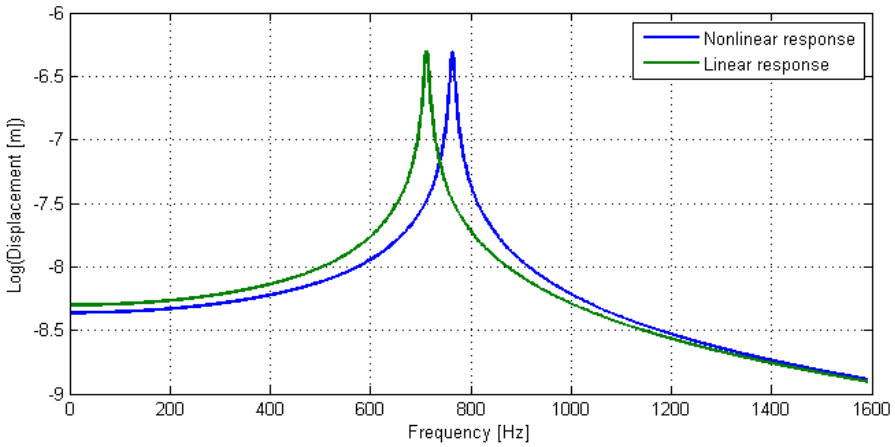

Figure 3.2 Harmonic response of the system for F=0.01N

It is observed from Figure 3.2 that, friction is the only nonlinear effect, because at low forcing level, response amplitudes are low and nonlinear internal forces due to cubic stiffness are negligible. It is clearly seen from Figure 3.2 that, there is a shift in

the resonance frequency due to the stiffness component of frictional nonlinearity. Afterwards, by increasing the amplitude of the harmonic excitation force 30N at a time, between 100N and 400N, the responses of the system are calculated for 11 different higher excitation forcing cases. In Figure 3.3, nonlinear harmonic responses are shown for only the forcing levels of F=130N and F=280N.

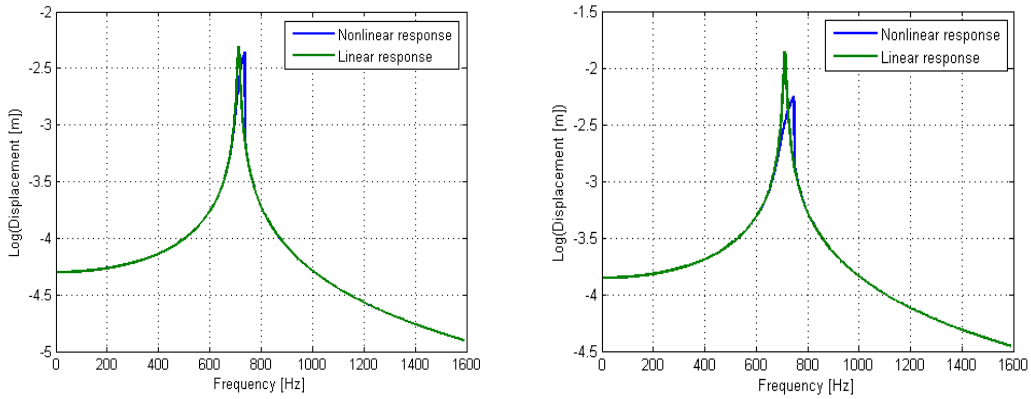

(a) (b)

Figure 3.3 Harmonic response of the system for (a) F = 130N, (b) F = 280N

Since nonlinear forces due to friction is negligible at high forcing levels, as observed from the Figure 3.3, only nonlinear forces due to cubic stiffness will be effective, and this will cause a jump around resonance in the frequency response of the system which is a typical response characteristic of a vibratory system with cubic stiffness. PRD method is applied by using low forcing level excitation and 11 different FRFs obtained at the excitation frequency of 710 Hz.

The equation of the regression curve is obtained by employing “polyfit” function of MATLAB. Since equation of the regression equation is directly related with the corresponding describing functions, by comparing the terms of the regression equation with those of the corresponding describing functions, the values of the

nonlinear parameters are calculated. The regression curve obtained is shown in Figure 3.4.

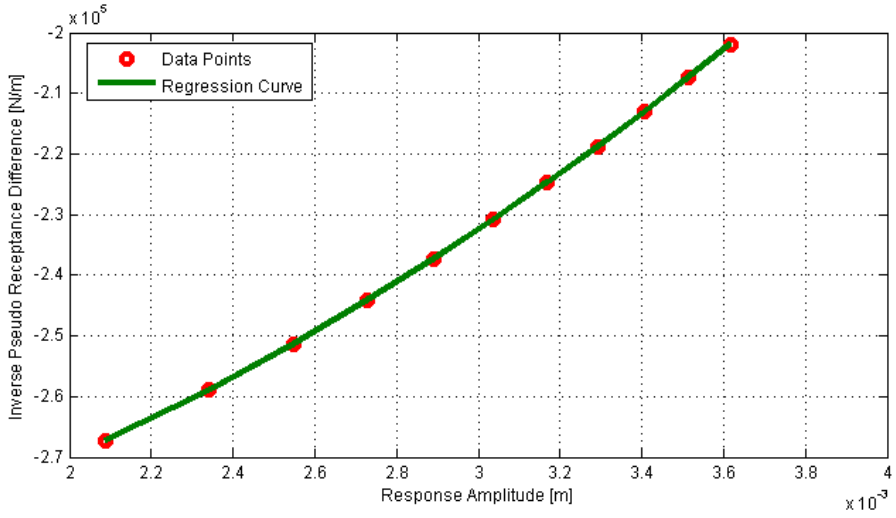

Figure 3.4 Polynomial regression curve for the available data points

The estimated values of the nonlinear parameters are as follows:

$$k^* = 9.9x\,10^9\ N/m^3 \quad and \quad k_f = 3x\,10^5\ N/m$$

It can be seen that there is a perfect match between the estimated and the actual values of the nonlinear parameters.

Estimated and actual linear frequency responses are also compared in Figure 3.5. As expected, estimated linear frequency response matches perfectly with the actual linear frequency responses of the system.

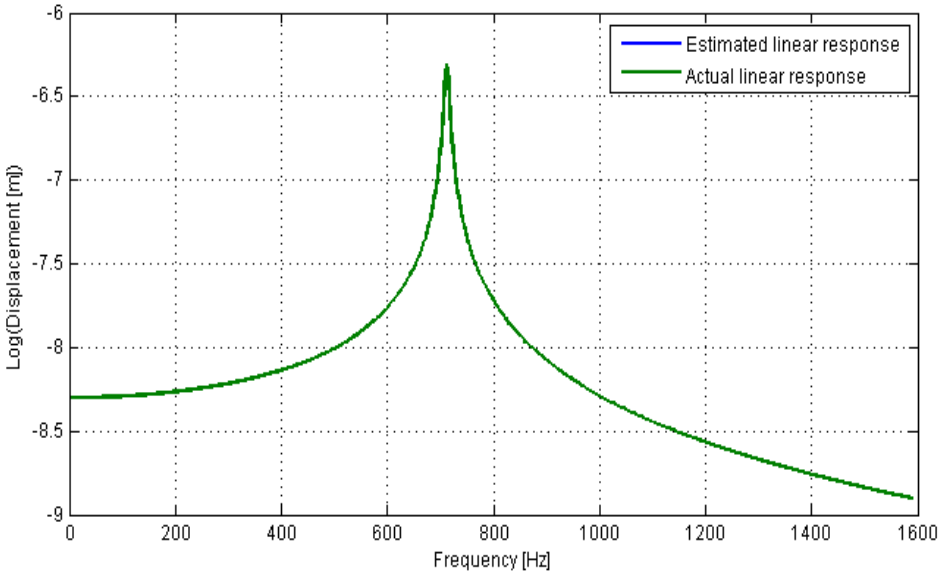

Figure 3.5 Comparison of the estimated and actual linear frequency responses of the system

3.1.2 Application of PRD Method with Polluted Data

In this case study, the same nonlinear SDOF system used in previous case study is analyzed. In order to simulate the experimental data, theoretical data is polluted with 5% noise that has normal distribution. The standard deviation used in the noise is 5% of the amplitude of the original response. The system is excited with a low forcing amplitude and then with 11 different high forcing amplitudes. In Figure 3.6, the response of the system at low excitation force (F=0.01N) and the linear frequency response of the system obtained disregarding both friction and cubic stiffness nonlinearity are compared to each other. The frequency responses of the system for F=130N and F=280N are also shown in Figure 3.7.

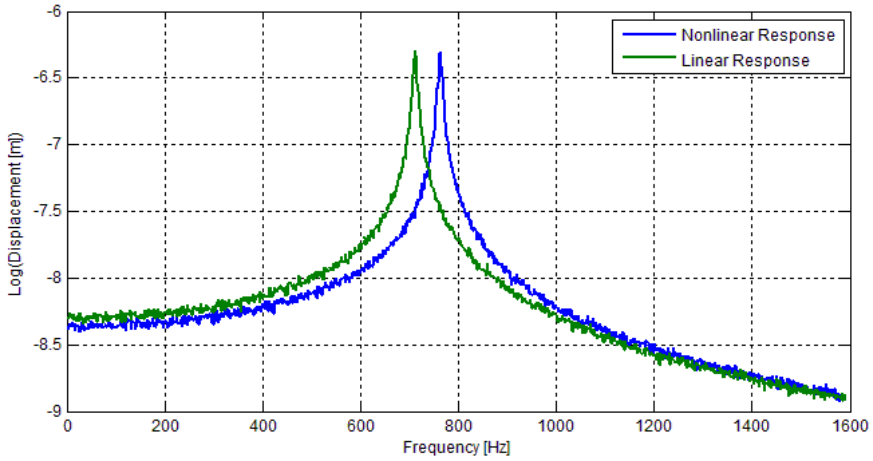

Figure 3.6 Frequency response of the system for F=0.01N with 5% noise

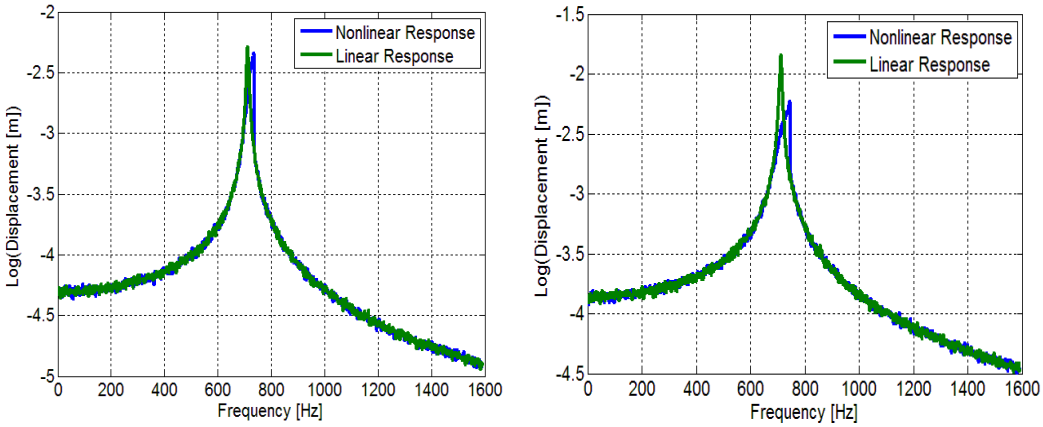

Figure 3.7 Frequency response of the system with 5% noise for
(a) F = 130N (b) F = 280N

At the excitation frequency of 710 Hz, the polynomial regression curve is obtained for 11 different data points as shown in Figure 3.8.

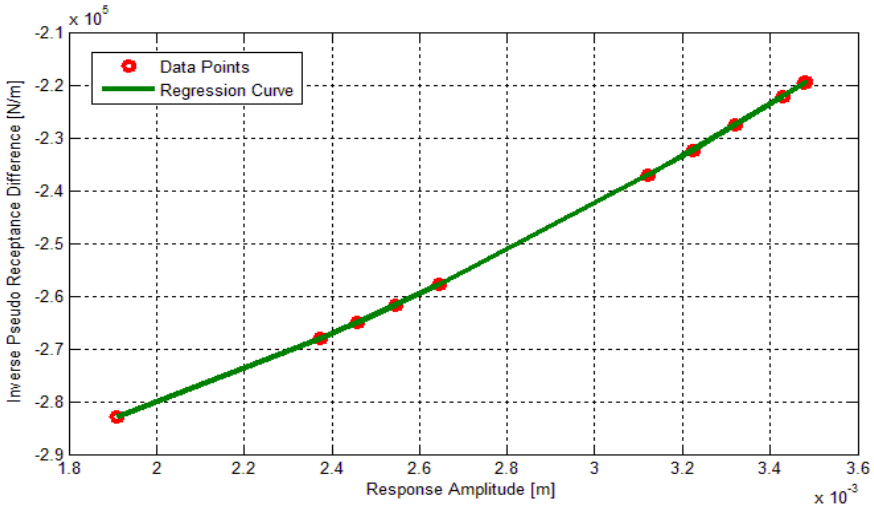

Figure 3.8 Polynomial regression curve for the available data points

Identified nonlinear parameters and comparison of these values with the actual ones are given in Table 3.1.

Table 3.1 Comparison of nonlinear parameters

Nonlinear Parameters	**Estimated**	**Actual**	**Error (%)**
k^* (N/m^3)	9.9×10^9	1×10^{10}	-1.0
k_f (N/m)	3.1×10^5	3×10^5	3.3

It is observed from Table 3.1 that, the estimated nonlinear parameters are slightly different from the actual nonlinear parameters due to using polluted data.

The linear frequency response calculated by using PRD method is compared with the actual one in Figure 3.9. As observed from Figure 3.9 there is a perfect agreement between the calculated linear frequency response and the actual one.

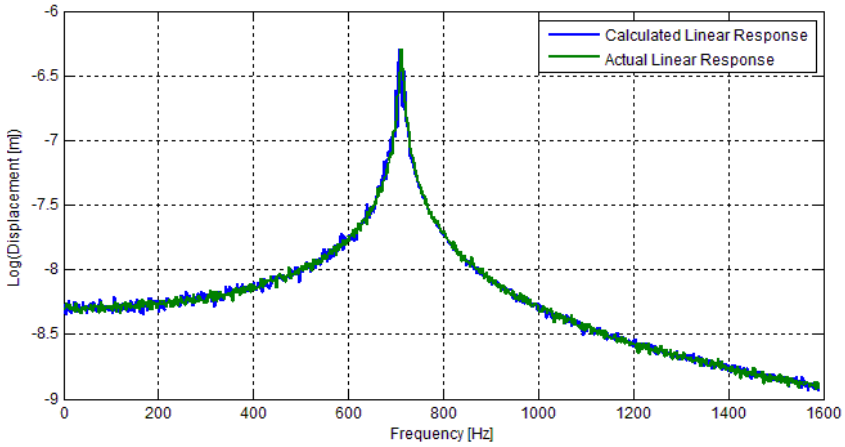

Figure 3.9 Comparison of the calculated and actual linear frequency responses of the system

3.2 Application of PRD Method to a MDOF Lumped System

In this case study, PRD method is applied to a nonlinear 2 DOF system (Figure 3.10) that has cubic stiffness and dry friction nonlinearities. Polluted data is used in the analysis of the system. The same dry friction model given in previous case study is used here as well.

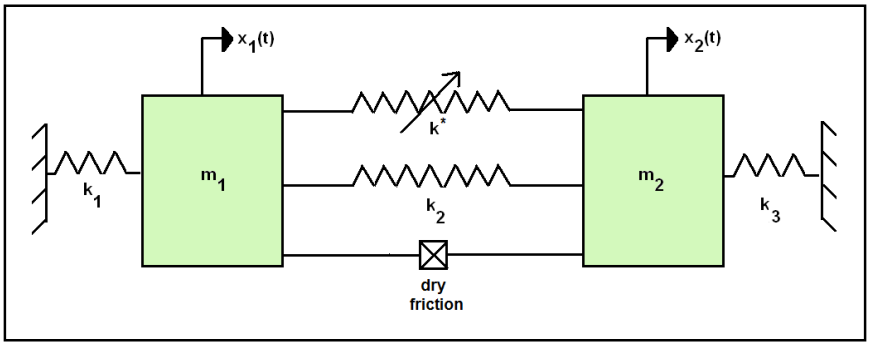

Figure 3.10 2 DOF nonlinear system used in the case study

The nonlinear responses of the system are calculated by using the harmonic balance method. Nonlinear parameter values used in the case study and linear system properties are given as follows:

$$m_1 = 0.1\,kg,\ m_2 = 0.5\,kg\ ,\ \ k_1 = k_2 = k_3 = 1x10^6\ N/m\ \ and\ \ \gamma\,(loss\ \ factor) = 0.005$$

$$\mu = 0.1,\ Normal\ Force = 10\ N\ \ and\ \ k_f = 8x10^4\ N/m$$

$$k^* = 1x10^{10}\ N/m^3$$

In order to simulate the experimental data, theoretical FRF data obtained from harmonic balance analysis of the system is polluted with 5% noise that has normal distribution. The standard deviation used in the noise is 5% of the amplitude of the original response. The system is excited with a low forcing amplitude and then with 11 different high forcing amplitudes. The frequency responses of the system at forcing levels of F_1=0.01N and F_1=100N are shown in Figure 3.11 and Figure 3.12, respectively together with the linear frequency response of the system obtained disregarding both friction and cubic stiffness nonlinearity.

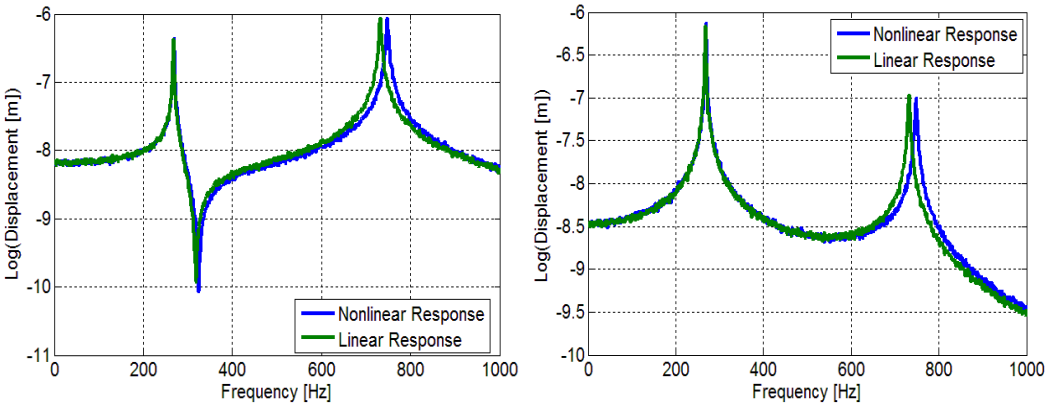

Figure 3.11 Frequency responses of the system with 5% noise for F_1=0.01N (a) 1st coordinate, (b) 2nd coordinate

As can be observed from Figure 3.11, for low forcing amplitudes, friction is the only nonlinear effect, which causes a shift in the resonance frequency due to the stiffness component of the frictional nonlinearity. The frictional nonlinearity is much more effective in the 2nd mode.

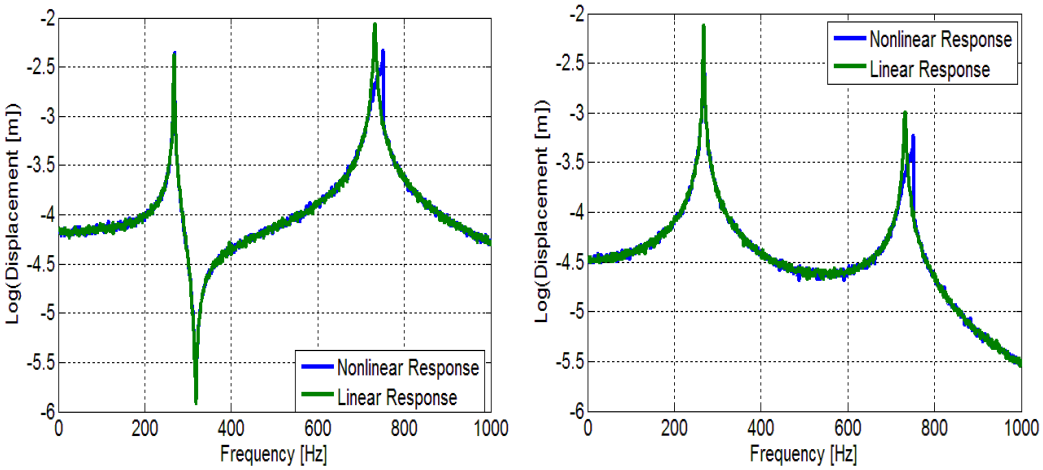

Figure 3.12 Frequency responses of the system with 5% noise for F_1=100N (a) 1st coordinate, (b) 2nd coordinate

As can be seen in Figure 3.12, since nonlinear forces due to friction is negligible at high forcing levels, the nonlinearity due to cubic stiffness is the only nonlinear effect and it changes the response of the system around 2nd resonance considerably by causing a jump. It is observed that, existence of the stiffness nonlinearity does not considerably affect the 1st mode of the system, as in the low forcing level case. By applying PRD method, the nonlinear parameters are calculated and they are given in Table 3.2. The corresponding regression curve is also shown in Figure 3.13.

Table 3.2 Comparison of nonlinear parameters

Nonlinear Parameters	Estimated	Actual	Error (%)
k^* (N/m^3)	9.9×10^9	1×10^{10}	-1.0
k_f (N/m)	8.03×10^4	8×10^4	0.4

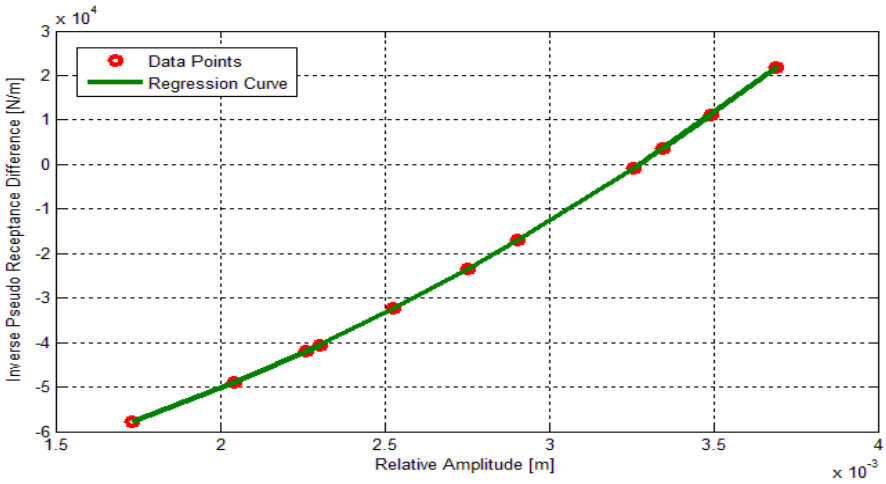

Figure 3.13 Polynomial regression curve for the available data points

It is seen from Table 3.2 that, there is a perfect match between the estimated and actual nonlinear parameters.

As mentioned in the theory chapter, excitation frequency is a free parameter in PRD method (i.e., derived equations are valid for any excitation frequency and for any forcing level), the effect of the excitation frequency used in the experiments on the performance of PRD method needs to be investigated. This investigation will be given in Section 3.4.

3.3 Application of PRD Method to a Nonlinear Structure

In the third case study, application of the PRD method to a nonlinear structure is given. The nonlinear structure used in this case study is a T-beam that has cubic stiffness and dry friction nonlinearities. In order to simulate the nonlinear response of the system, first FE model of the linear part of the T-beam is constructed in ANSYS, and linear FRFs are obtained by performing modal analysis in ANSYS. Then using the nonlinear parameters for cubic stiffness and dry friction and calculated linear FRFs, nonlinear responses are obtained by employing the harmonic balance method. Afterwards, in order to have more realistic simulated experimental measurements, the calculated FRFs are polluted by addition of noise to the FRFs. Finally, the nonlinearities in the system are identified and linear FRFs of the test system are obtained by using the simulated experimental data and applying the PRD method. In Figure 3.14 dry friction model and nonlinear T-beam used in the case study are shown.

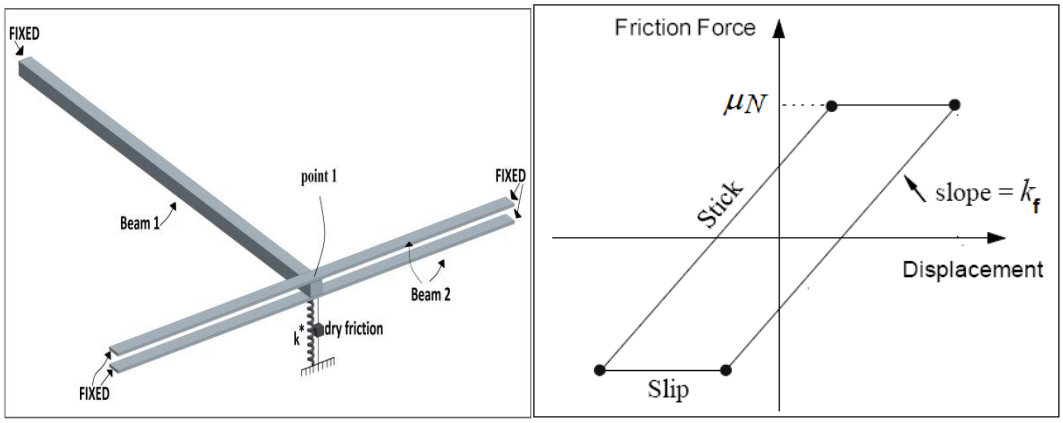

(a) (b)

Figure 3.14 (a) Nonlinear T-beam test system, (b) Dry friction model

As seen from Figure 3.14, T-beam is composed of a cantilever beam with its free end is maintained between two thin identical beams. All the end conditions of the beams are fixed. Geometric and material properties of these beams are given Table 3.3

Table 3.3 Geometric and material properties of the T-beam

	Height (mm)	**Length (mm)**	**Width (mm)**	**Modulus of Elasticity (E) (GPa)**	**Poisson's Ratio (ν)**	**Density (ρ) (kg/m^3)**
Beam1	8	430	12	210	0.3	7850
Beam2	1.5	400	13	210	0.3	7850

The nonlinear parameter values and loss factor for the system are given below:

$\mu = 0.01,\ Normal\ Force = 50\ N,\ k_f = 3x10^4\ N/m \quad and \quad k^* = 3x10^9\ N/m^3$

$\gamma\ (loss\ factor) = 0.02$

In order to calculate the linear FRFs of the T-beam, ANSYS is used. The mesh used in the FE model is given Figure 3.15. The FE model has 152 elements (SOLID 186) and 1331 nodes.

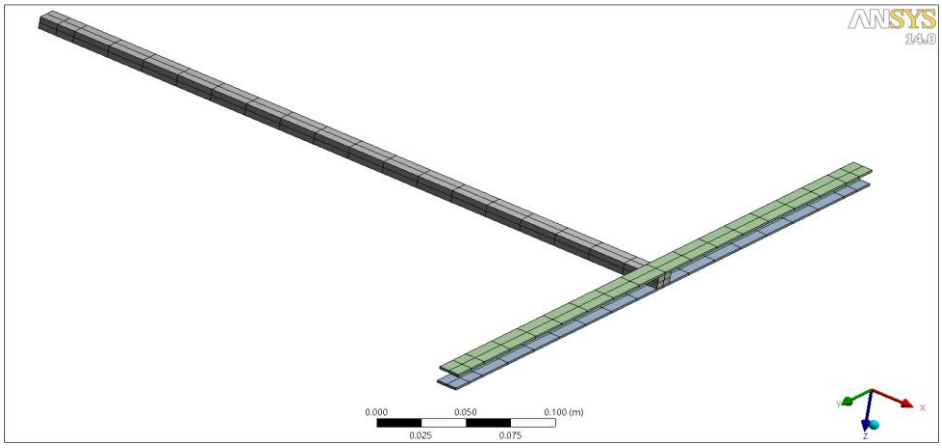

Figure 3.15 FE mesh used in ANSYS

By performing modal analysis in ANSYS, the linear driving point FRFs of the structure at the tip of the beam 1 (point 1 in Figure 3.14) in Z (transverse) direction are obtained. By using the nonlinear parameters and the calculated linear FRFs, the nonlinear driving point FRFs at the tip of beam 1 are calculated by employing the harmonic balance method. The nonlinear responses are obtained for various forcing levels. In order to simulate experimental measurements, calculated FRF values are polluted with 5% noise which has normal distribution. The standard deviation of the noise is 5% of the amplitude of the original response. Firstly, low amplitude harmonic force (F_1=0.01N) is used to excite the system. At this forcing level, frequency response of the system is compared with the linear frequency response of the system obtained disregarding both friction and cubic stiffness nonlinearity. These FRFs are given in Figure 3.16.

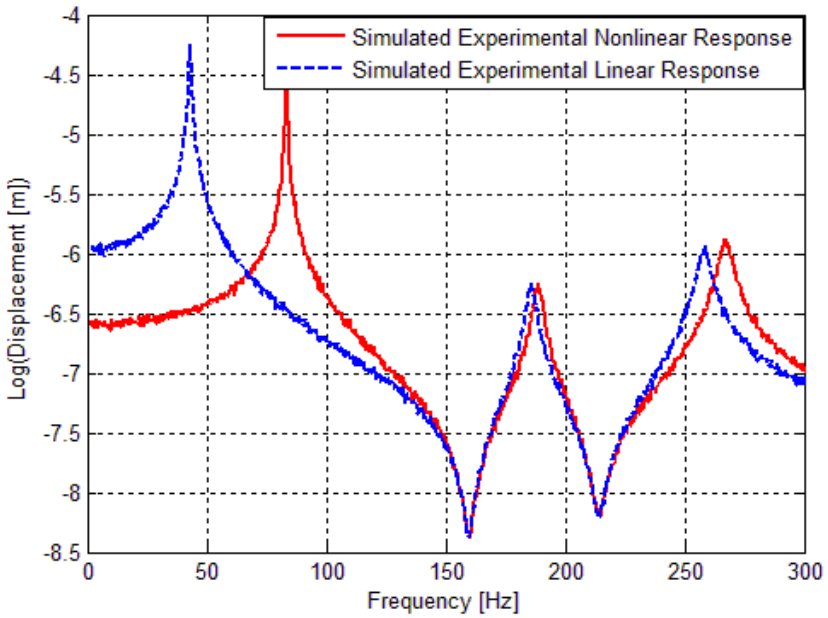

Figure 3.16 Frequency response of the system at F_1=0.01 N with 5% noise

As can be seen in Figure 3.16, for low forcing amplitudes, friction is the only nonlinear effect, which causes a shift in the resonance frequency due to the stiffness component of the frictional nonlinearity. Afterwards, by increasing the amplitude of the harmonic excitation force 5N at a time between 10N and 50N, the responses of the system are calculated for 9 different higher excitation forcing cases. The nonlinear harmonic responses at only the forcing levels of F_1=25N and F_1=50N are shown in Figure 3.17 and Figure 3.18, respectively.

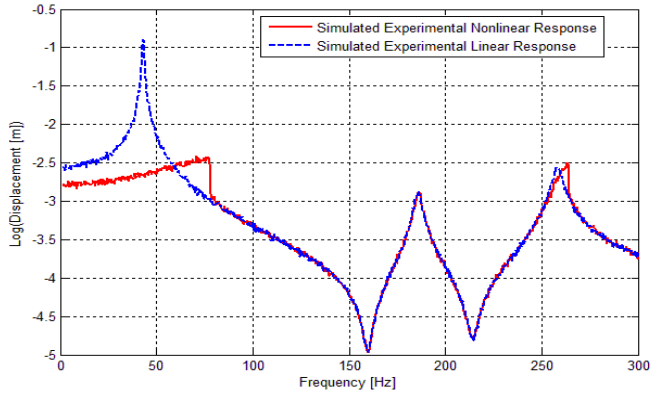

Figure 3.17 Frequency responses of the test system for F_1 = 25N

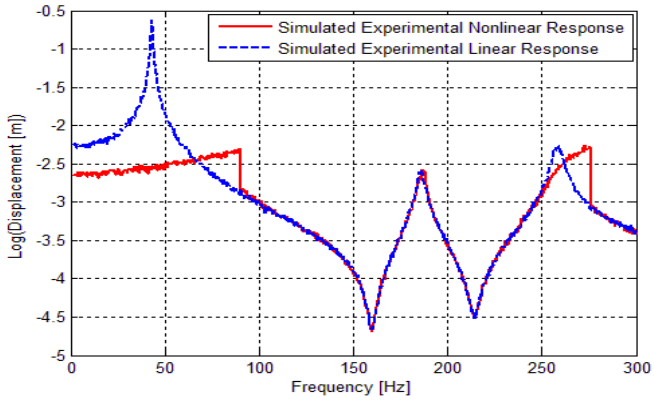

Figure 3.18 Frequency responses of the test system for F_1 = 50N

As can be seen in Figure 3.17 and Figure 3.18, since the nonlinear forces due to friction are negligible compared to other forces at high forcing levels, the nonlinearity due to cubic stiffness is the only nonlinear effect, and it changes the response of the system around 1st and 3rd resonances considerably by causing a jump. It is observed that existence of the stiffness nonlinearity affects the 2nd mode of the system slightly due to the relatively small deflection of the point where cubic stiffness is attached.

By using the FRFs obtained for low and several high forcing levels, at the excitation frequency of 42 Hz, the equation of the regression curve is obtained. By comparing the terms of the regression equation with the corresponding describing functions, frictional stiffness and cubic stiffness parameters are identified. The corresponding regression curve is also shown in Figure 3.19.

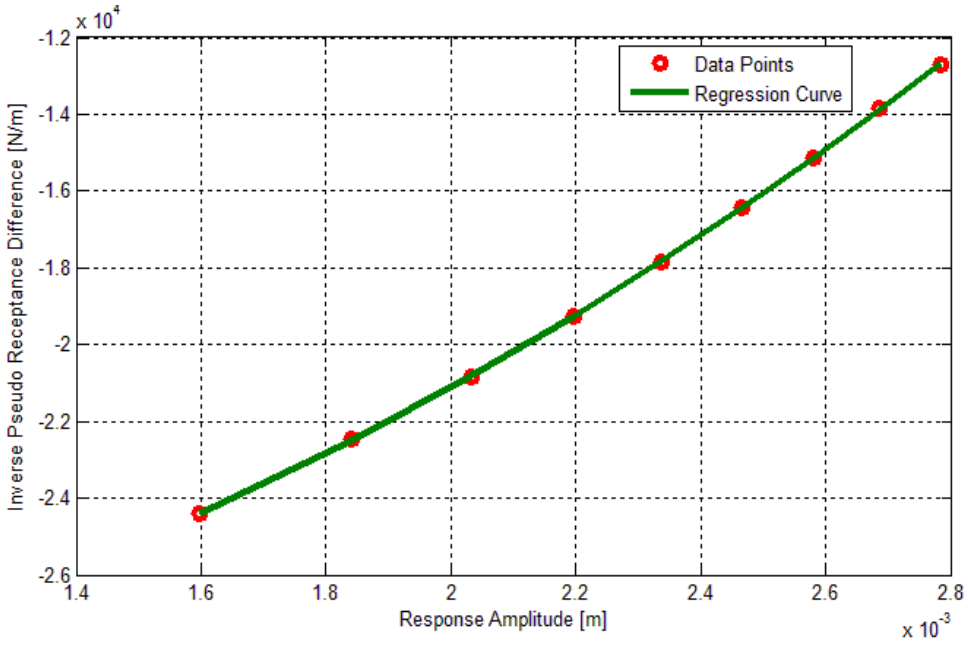

Figure 3.19 Polynomial regression curve fitted to data points

The estimated nonlinear parameters are compared with the actual ones in Table 3.4.

Table 3.4 Comparison of nonlinear parameters

Nonlinear Parameters	Estimated	Actual	Error (%)
k^* (N/m^3)	3.04×10^9	3×10^9	1.3
k_f (N/m)	2.99×10^4	3×10^4	-0.3

It is observed from Table 3.4 that there is a very small discrepancy between the estimated and actual nonlinear parameter values. This difference is mainly due to polluting the theoretical FRFs to simulate actual experiments and thus to have more realistic values that should be expected in real applications.

Once the nonlinear parameters are identified, by applying PRD method, linear frequency response of the system is calculated. The calculated linear frequency response is compared with the actual linear frequency response of the system in Figure 3.20. As can be seen from Figure 3.20, there is perfect agreement between the calculated and actual linear frequency responses.

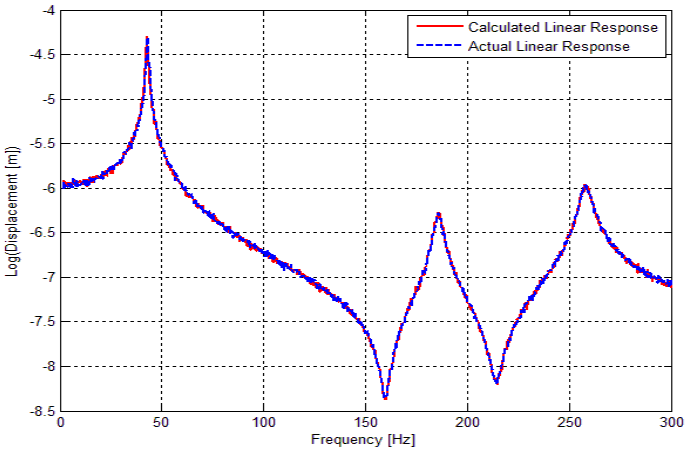

Figure 3.20 Comparison of the calculated and actual linear frequency response of the system

3.4 Effect of Excitation Frequency Used on the Performance of PRD Method

In this case study, in order to see the effect of choosing different frequencies of excitation in the application of the PRD method, on the performance of the method, the simulated test results obtained at various different frequencies are analyzed. The system used in this test is the nonlinear T-beam used in Section 3.3. By using the simulated test results obtained at different frequencies, nonlinearities in the system are identified. The identified nonlinear parameters by using different excitation frequencies are compared with each other, as well as with the actual values. The comparison is given in Table 3.5.

Table 3.5 Comparison of nonlinear parameters identified by using different excitation frequencies (Actual values: $k^* = 3.0 \times 10^9$ N/m^3, $k_f = 3.0 \times 10^4$ N/m)

Excitation Frequency (Hz)	**Estimated k^* (N/m^3)**	**Error in k^* (%)**	**Estimated k_f (N/m)**	**Error in k_f (%)**
36.0	2.96×10^9	-1.33	3.02×10^4	0.67
37.0	3.07×10^9	2.33	2.99×10^4	-0.33
38.0	3.12×10^9	4.00	2.96×10^4	-1.33
39.0	2.89×10^9	-3.67	3.04×10^4	1.33
40.0	2.98×10^9	-0.67	3.01×10^4	0.33
41.0	2.97×10^9	-1.00	3.01×10^4	0.33
42.0	3.03×10^9	1.00	2.99×10^4	-0.33
43.0	3.01×10^9	0.33	3.01×10^4	0.33
44.0	3.01×10^9	0.33	3.01×10^4	0.33
45.0	3.02×10^9	0.67	3.01×10^4	0.33
46.0	3.05×10^9	1.67	2.98×10^4	-0.66
47.0	2.91×10^9	-3.00	3.04×10^4	1.33
48.0	2.90×10^9	-3.33	3.04×10^4	1.33

Since the nonlinear forces affect the first mode more, excitation frequencies are selected around the first resonance of the system. It can be seen from Table 3.5 that more accurate estimates are obtained for the nonlinear parameters, cubic stiffness and frictional stiffness, when the excitation frequency is closer to the first resonance of the linear system. Although there are some exceptions, in general, the error in the

estimated nonlinear parameters tends to increase when excitation frequency deviates from the resonance frequency.

3.5 Comparison of the Performances of PRD and DDF Methods in Nonlinear Identification

In this case study, in order to compare DDF and proposed method, a SDOF system with cubic stiffness nonlinearity is used. The system used in the case study is shown in Figure 3.21.

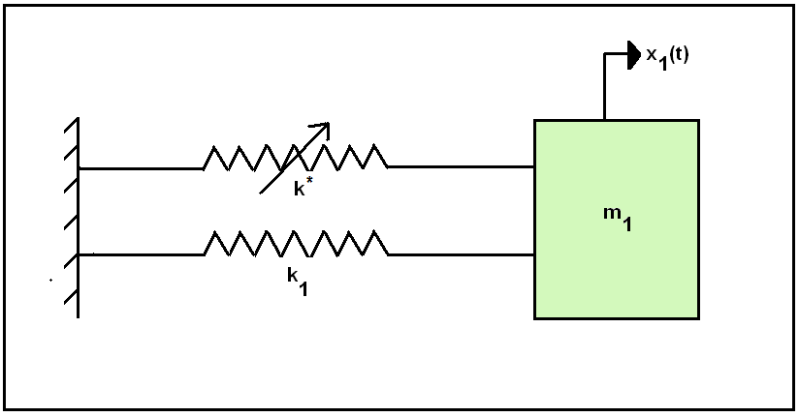

Figure 3.21 Nonlinear SDOF system

The parameters of these nonlinear elements and the properties of the system are given as follows:

$m_1 = 0.1\,kg,\ \ k_1 = 2x\,10^6\ N/m\ \ and\ \ \gamma\,(loss\ \ factor) = 0.01$

$k^* = 1x\,10^{10}\ N/m^3$

Nonlinear responses are calculated by using the harmonic balance method. In order to simulate the experimental measurements more realistically, polluted data is used in the analysis. The noise used in the case study has normal distribution and it has a standard deviation of 5% of the amplitude of the original response at that frequency.

3.5.1 Identification of Nonlinearity Using DDF Method

In this section, DDF method is applied for nonlinear identification by using different forcing sets and frequency ranges. In the analysis, 3 different forcing pairs (F_1=100N-F_2=450N, F_1=100N-F_2=350N, F_1=150N-F_2=450N) are used and for each of the forcing pairs, nonlinear parameter is identified using the DDF method. Furthermore since the method is dependent on the frequency used in the equations, different frequency ranges are considered for each force pair in the analysis. In Figure 3.22 and Figure 3.23, nonlinear response and linear response of the underlying linear system are shown for the forcing levels used in the analysis.

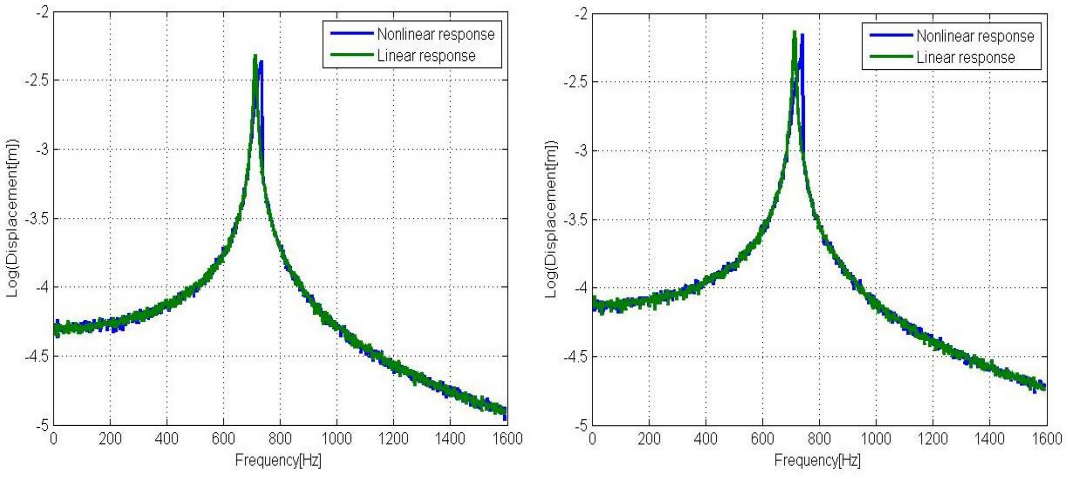

(a) (b)

Figure 3.22 Frequency response of the system with 5% noise
(a) F=100N, (b) F=150N

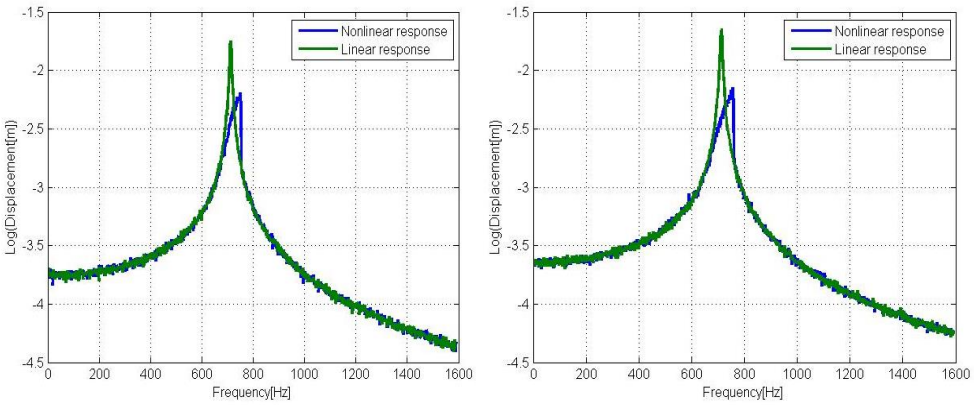

(a) (b)

Figure 3.23 Frequency response of the system with 5% noise

(a) F=350N, (b) F=450N

Then making use of these nonlinear responses, the nonlinear cubic stiffness parameter is identified using different frequency ranges. Comparison of the nonlinear parameters identified using different frequency ranges are given in Table 3.6 for the set of forcing F_1=100N-F_2=350N.

Table 3.6 Comparison of nonlinear parameters identified using different frequency ranges (F_1=100N-F_2=350N)

Frequency Range (Hz)	**600-850**	**650-900**	**700-950**
Identified Cubic Stiffness Value (N/m^3)	9.389×10^9	9.389×10^9	9.374×10^9
Error (%)	-6.11	-6.11	-6.26

As observed from Table 3.6 that using different frequency ranges does not affect the nonlinear parameters estimated for this forcing pair, but there is a considerable difference between the estimated and the actual cubic stiffness values, the error ranging between 6.11% and 6.26%, depending on the frequency range used.

Similarly, comparison of the nonlinear parameters identified using different frequency ranges are given in Table 3.7 for the set of forcing F_1=150N-F_2=450N.

Table 3.7 Comparison of nonlinear parameters identified using different frequency ranges (F_1=150N-F_2=450N)

Frequency Range (Hz)	**600-850**	**650-900**	**700-950**
Identified Cubic Stiffness Value (N/m^3)	9.828×10^9	9.827×10^9	9.823×10^9
Error (%)	-1.72	-1.73	-1.77

It is observed from Table 3.7 that using different frequency ranges does not affect the nonlinear parameters estimated for this forcing pair. For all cases there is a slight difference between the estimated and actual cubic stiffness values, the error ranging between 1.72% and 1.77%.

Finally, comparison of the nonlinear parameters identified using different frequency ranges are given in Table 3.8 for the set of forcing F_1=100N-F_2=450N.

Table 3.8 Comparison of nonlinear parameters identified using different frequency ranges (F_1=100N-F_2=450N)

Frequency Range (Hz)	**600-850**	**650-900**	**700-950**
Identified Cubic Stiffness Value (N/m^3)	1.026×10^{10}	1.026×10^{10}	1.027×10^{10}
Error (%)	2.6	2.6	2.7

As in the first and second forcing pair, it is observed that using different frequency ranges does not affect the nonlinear parameters estimated for this forcing pair. Estimated cubic stiffness values are close to the actual value, the error ranging between 2.6% and 2.7%.

If the results obtained for each of three forcing pairs are compared, it can be concluded that worst estimation of the nonlinear parameter is obtained for the set of forcing F_1=100N-F_2=350N where the difference between the low and high force is lowest.

3.5.2 Identification of Nonlinearity Using PRD Method

The nonlinear parameter is identified by using PRD method, by exciting the structure at 710 Hz at 12 different forcing levels ranging between F=50N and F=400N.

The regression curve used for nonlinear parameter estimation and the estimated nonlinear parameters are given in Figure 3.24 and Table 3.9, respectively.

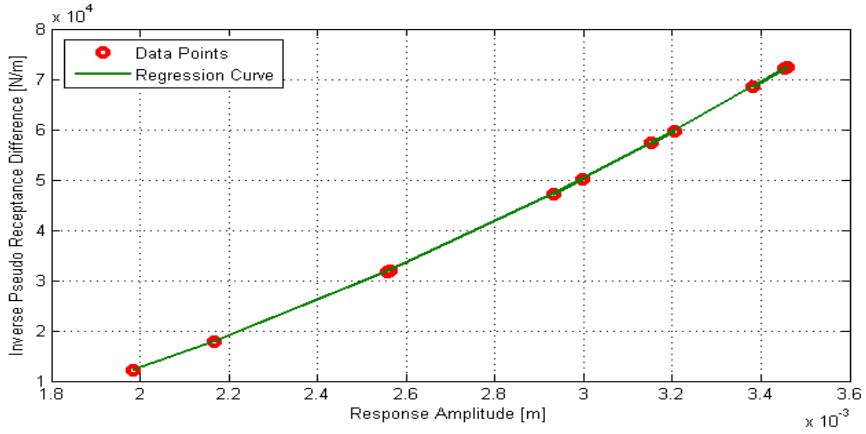

Figure 3.24 Regression curve

Table 3.9 Estimated nonlinear parameter

Nonlinear Parameters	Estimated	Actual	Error (%)
k* (N/m^3)	$9.99x\ 10^9$	$10\ x\ 10^9$	-0.1

As can be seen in Table 3.9, the nonlinear parameter is calculated very accurately. Furthermore, if the nonlinear parameter values identified by using PRD and DDF methods are compared, it can be seen that a better estimate is obtained for cubic stiffness value with PRD method for that case study.

CHAPTER 4

EXPERIMENTAL VALIDATION OF MODEL UPDATING APPROACH-APPLICATION TO A NONLINEAR T-BEAM

In this chapter, the proposed model updating approach for nonlinear systems is applied to a real test system. The test system is a nonlinear T-beam which is similar to the test structure used in the study of Ferreira [81], Siller [82] and also of Josefsson et al. [83]. Firstly, applying the PRD method, both linear FRFs and the nonlinearities in the system are obtained from experimentally measured nonlinear FRFs. Then, test structure is modelled in ANSYS and the linear FE model of T-beam is constructed. In the first section of this chapter, this linear FE model of the system is updated for the first mode of the structure by employing the inverse eigensensitivity method and also by using the linear FRFs calculated through PRD method. Combining the updated linear FE model with the identified nonlinearity, updated nonlinear model of the T-beam is obtained. Finally, in order to demonstrate the accuracy of the updated nonlinear model of the system, predicted nonlinear FRFs of the system are compared with the measured FRFs at different forcing levels. In the second section of this chapter, linear FRFs are obtained from experimentally measured nonlinear FRFs for the first, second and third global modes of the test system by using PRD method. Then the linear FE model of the test system is built in ANSYS and the linear FE model of the test structure is updated for the first three global modes of the structure by using the extracted linear FRFs employing first the PRD method and then using ANSYS Design Exploration Optimization. Using the identified nonlinearity and updated linear FE models, updated nonlinear models of the test structure are constructed. Finally, predicted and measured FRFs of the test

structure are compared at different forcing levels in order to show the accuracy of the updated nonlinear models of the system.

4.1 Experimental Study 1-Model Updating for a Single Mode

In the first experimental study, in order to validate the model updating approach for nonlinear systems, a nonlinear T-beam test system is used.

By applying the PRD method, both linear FRFs and the nonlinearities in the T-beam system are obtained from experimentally measured nonlinear FRFs. Then, linear FE model of the T-beam is constructed in ANSYS. For the first mode of the structure, the linear FE model of the system is updated by employing the inverse eigensensitivity method and using the obtained linear FRFs through the PRD method. By using the updated linear FE model and the identified nonlinearity, updated nonlinear mathematical model of the T-beam is obtained. Finally, nonlinear FRFs of the system are predicted at different forcing levels and they are compared with the experimental ones in order to show the accuracy and performance of the updated nonlinear model of the T-beam.

4.1.1 Experimental Setup

The T-beam test set-up consists of a fixed-free beam where its free end is maintained between two thin identical beams. The boundary conditions of the thin beams are fixed-fixed. Nonlinearity in the test structure is mainly due to thin beams that are assembled to the free end of the cantilever beam. Geometric details and the dimensions of the test system are shown in Figure 4.1.

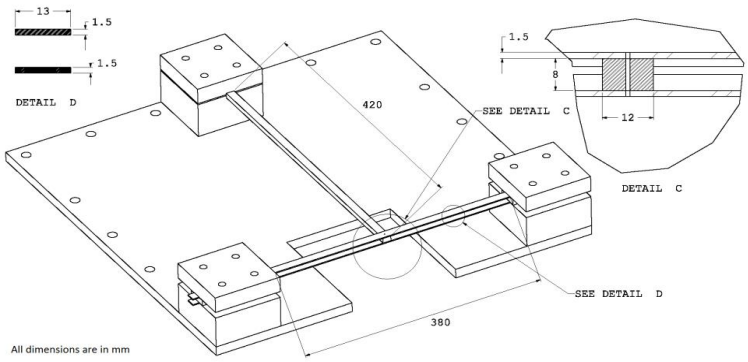

Figure 4.1 Nonlinear T-beam test system

Maintaining perfect fixed boundary conditions are very difficult in real life applications, therefore in order to maintain the fixed boundary conditions in the experimental setup, dimensions of the beams used in the experiments are longer than their effective length of 380 mm and 420 mm, so that adequate parts of the beams are clamped between fixture blocks. The material used for the beams is St37. The test rig used in the experiments is shown in Figure 4.2.

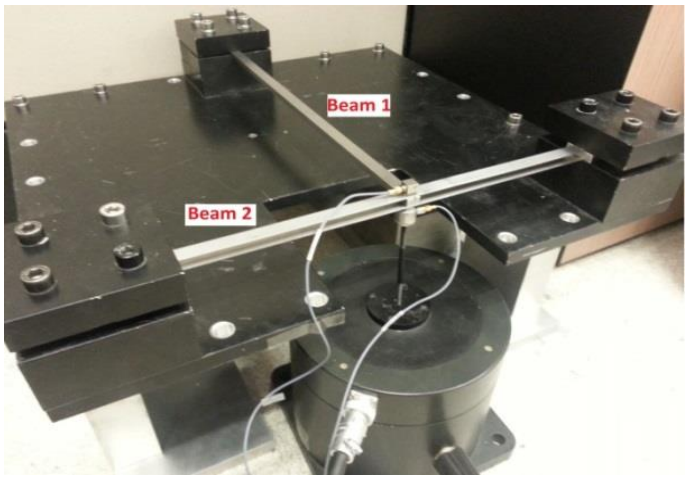

Figure 4.2 Test rig used in the experiment

In the experiments performed in this study, B&K Type 4808 modal shaker is used as an exciter. Since the voltage supplied from the signal generator is generally low, B&K Type 2712 power amplifier is used in order to increase the excitation force level of the shaker. Acceleration output and input force are measured with B&K Type 4507B accelerometer and B&K Type 8230-002 force transducer, respectively. As a data acquisition system, B&K Type 3560C frontend is used in all the experiments. The equipment used in the experiments is given Table 4.1 and it is shown in Figure 4.3.

Table 4.1 Equipment used in the modal testing

Data Acquisition System	Brüel&Kjaer Type 3560 C Frontend
Shaker	Brüel&Kjaer Type 4808
Force Transducer	Brüel&Kjaer Type 8230-002
Power Amplifier	Brüel&Kjaer Type 2712
Accelerometer	Brüel&Kjaer 4507B

Figure 4.3 View of the equipment used in the experiments

4.1.2 First Set of Experiments

In the first set of experiments, the test system is excited with a random input force. Since the accuracy of the PRD method depends on the frequency of excitation and it is shown that more accurate results are obtained when the system is excited at around the resonance frequency of the linear part of the system, a quick test that does not excite the nonlinearities considerably is selected. In random excitation, excitation force level is kept very low and driving point FRFs at the tip of beam 1 in transverse direction are measured. The flow chart defining the test procedure is given in Figure 4.4.

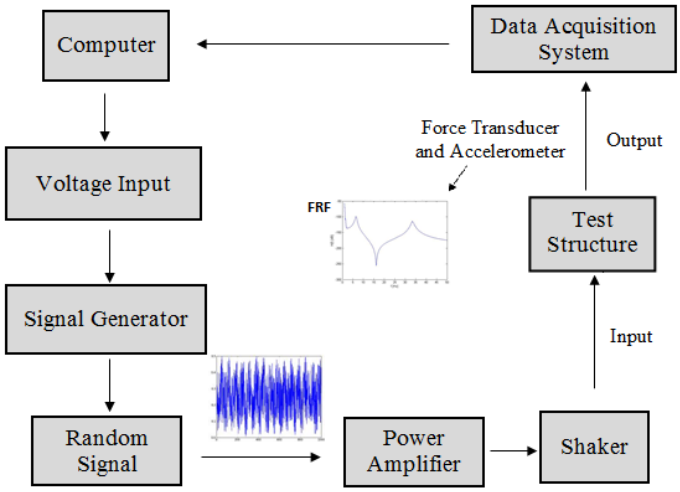

Figure 4.4 Experimental procedure followed in random excitation vibration test

The measurements are performed in the frequency range of 0-200 Hz and frequency resolution is 0.25 Hz. In order to minimize the noise in the experiment, 130 averages are taken. By using the force and acceleration measurements, driving point FRF

curve at the tip of beam 1 in transverse direction is obtained and it is shown in Figure 4.5.

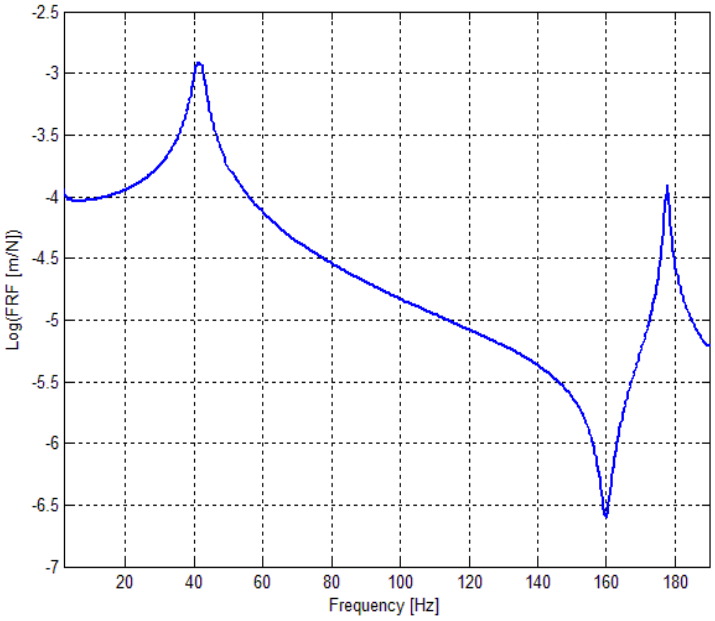

Figure 4.5 The driving point FRF at the tip of beam 1 in transverse direction

As seen from Figure 4.5, fundamental natural frequency of the structure in transverse direction is approximately 41 Hz. After finding the approximate linear fundamental natural frequency of the structure, T-beam is excited at around that frequency with a pure sine signal at a number of different forcing levels in order order to apply PRD method. Firstly the structure is excited at a low forcing level and then at a number of high forcing levels. The main advantage of PRD method is that, in order to apply the method, vibration controller is not necessary as in the cases of constant forcing or constant amplitude testing over a certain frequency range.

In order to demonstrate the effect of using different frequencies of excitation on the performance of PRD method, six different excitation frequencies (39 Hz, 39.5 Hz, 40 Hz, 40.5 Hz, 41 Hz and 41.5 Hz) are used. By applying PRD method that uses each of these frequencies, nonlinearities in the structure are obtained in the form of describing functions.

4.1.2.1 Application of PRD Method at 39 Hz for Identifying Nonlinearity

Real and imaginary parts of the describing function are obtained from experimental measurements at 39 Hz by applying PRD method. Curve fitting is performed for the calculated real and imaginary pats of describing function and the fitted curves are shown in Figure 4.6.

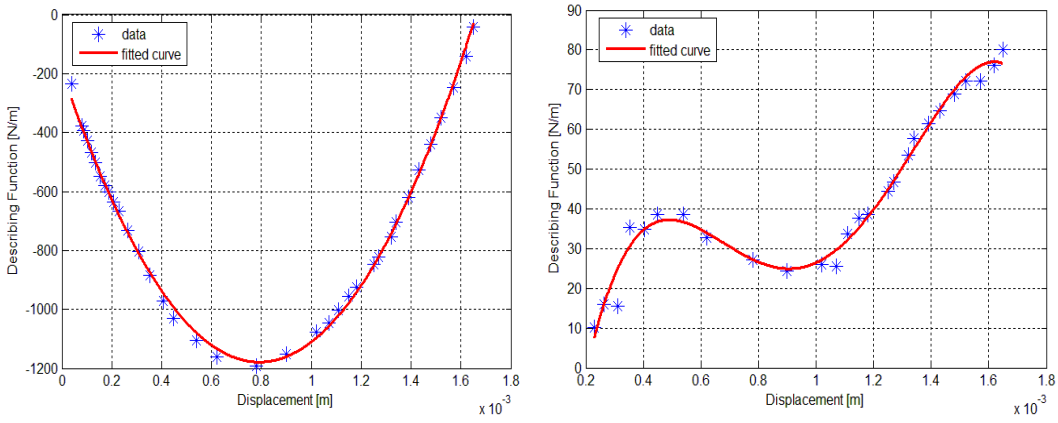

(a) (b)

Figure 4.6 Calculated describing function (a) Real part (b) Imaginary part

For the real part and imaginary part of describing function, 2nd order and 4th order polynomial functions are fit, respectively. Corresponding coefficients of the polynomial functions are given in Table 4.2.

Table 4.2 Coefficients of the polynomials fit to the data for real and imaginary parts of the describing function

	p_4	p_3	p_2	p_1	p_0
Real Part of Describing Function $p_2x^2 + p_1x + p_0$	---	---	$1.56\text{x}10^{9}$	$-2.48\ \text{x}10^{6}$	-190
Imaginary Part of Describing Function $p_4x^4 + p_3x^3 + p_2x^2 + p_1x + p_0$	$-2.7\text{x}10^{14}$	$1.1\text{x}10^{12}$	$-1.49\text{x}10^{9}$	$8.0\ \text{x}10^{5}$	-109

4.1.2.2 Application of PRD Method at 39.5 Hz for Identifying Nonlinearity

Real and imaginary parts of the describing function are obtained from experimental measurements at 39.5 Hz by applying PRD method. Curve fitting is performed for the calculated real and imaginary pats of describing function and the fitted curves are shown in Figure 4.7.

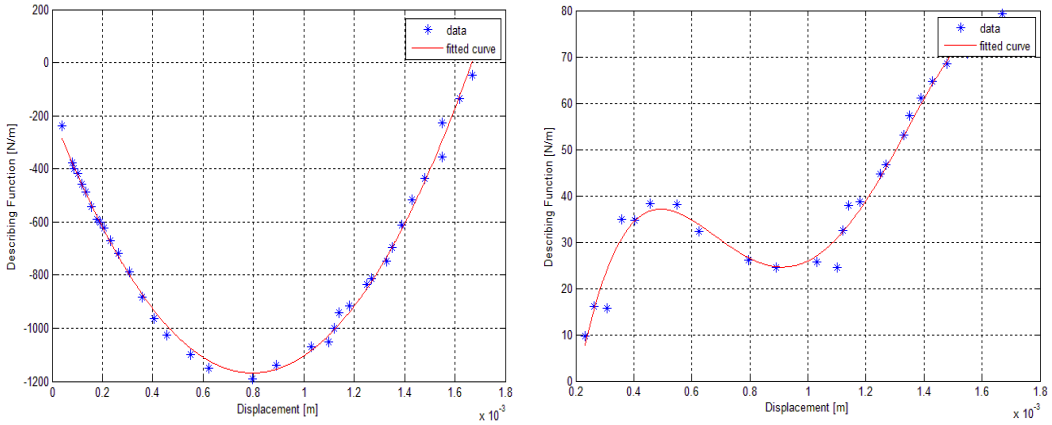

(a) (b)

Figure 4.7 Calculated describing function (a) Real part (b) Imaginary part

For the real part and imaginary part of describing function, 2nd order and 4th order polynomial functions are fit, respectively. Corresponding coefficients of the polynomial functions are given in Table 4.3.

Table 4.3 Coefficients of the polynomials fit to the data for real and imaginary parts of the describing function

	p_4	p_3	p_2	p_1	p_0
Real Part of Describing Function $p_2x^2 + p_1x + p_0$	---	---	1.54×10^9	-2.45×10^6	-190
Imaginary Part of Describing Function $p_4x^4 + p_3x^3 + p_2x^2 + p_1x + p_0$	-2.7×10^{14}	1.1×10^{12}	-1.51×10^9	8.1×10^5	-111

4.1.2.3 Application of PRD Method at 40 Hz for Identifying Nonlinearity

Real and imaginary parts of the describing function are obtained from experimental measurements at 40 Hz by applying PRD method. Curve fitting is performed for the calculated real and imaginary pats of describing function and the fitted curves are shown in Figure 4.8.

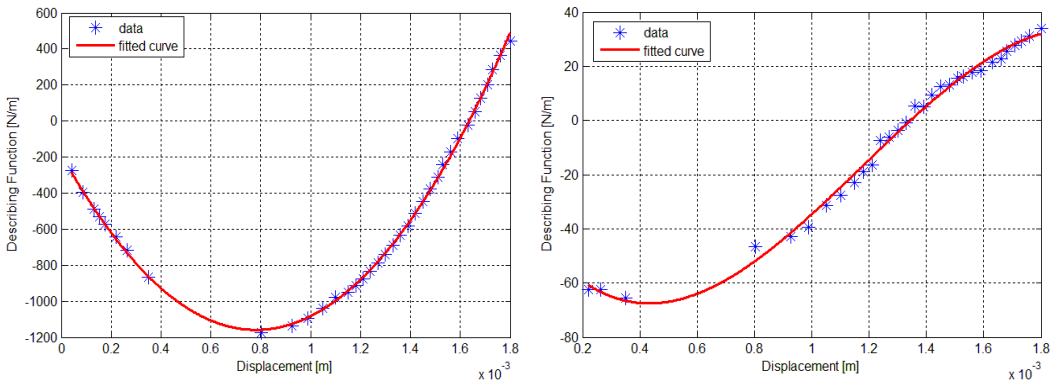

(a) (b)

Figure 4.8 Calculated describing function (a) Real part (b) Imaginary part

For the real part and imaginary part of describing function, 2nd order and 3rd order polynomial functions are fit, respectively. Corresponding coefficients of the polynomial functions are given in Table 4.4.

Table 4.4 Coefficients of the polynomials fit to the data for real and imaginary part of the describing function

	p_3	p_2	p_1	p_0
Real Part of Describing Function $p_2x^2 + p_1x + p_0$	---	$1.59\text{x}10^{9}$	$-2.49\text{x}10^{6}$	-181
Imaginary Part of Describing Function $p_3x^3 + p_2x^2 + p_1x + p_0$	$-6.0\text{x}10^{10}$	$2.15\text{x}10^{8}$	$-1.52\text{x}10^{5}$	-36

4.1.2.4 Application of PRD Method at 40.5 Hz for Identifying Nonlinearity

Real and imaginary parts of the describing function are obtained from experimental measurements at 40.5 Hz by applying PRD method. Curve fitting is performed for the calculated real and imaginary pats of describing function and the fitted curves are shown in Figure 4.9.

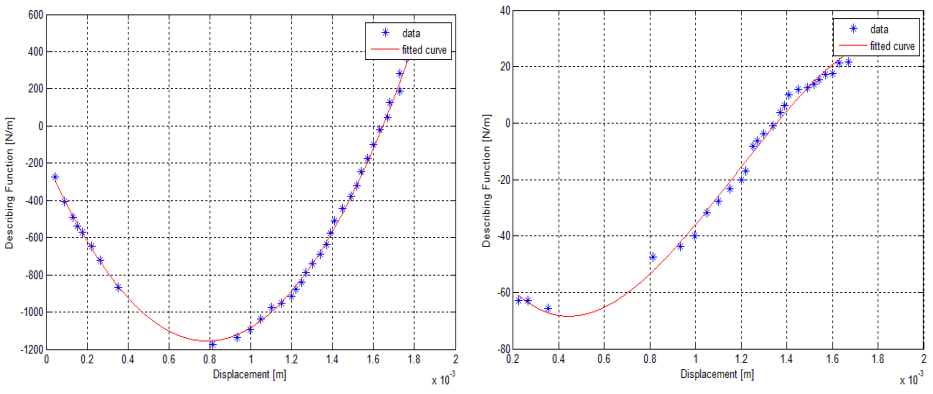

(a) (b)

Figure 4.9 Calculated describing function (a) Real part (b) Imaginary part

For the real part and imaginary part of describing function, 2nd order and 3rd order polynomial functions are fit, respectively. Corresponding coefficients of the polynomial functions are given in Table 4.5.

Table 4.5 Coefficients of the polynomials fit to the data for real and imaginary part of the describing function

	p_3	p_2	p_1	p_0
Real Part of Describing Function $p_2x^2 + p_1x + p_0$	---	$1.56\text{x}10^{9}$	$-2.46\text{x}10^{6}$	-188
Imaginary Part of Describing Function $p_3x^3 + p_2x^2 + p_1x + p_0$	$-6.4\text{x}10^{10}$	$2.26\text{x}10^{8}$	$-1.63\text{x}10^{5}$	-35

4.1.2.5 Application of PRD Method at 41 Hz for Identifying Nonlinearity

Real and imaginary parts of the describing function are obtained from experimental measurements at 41 Hz by applying PRD method. Curve fitting is performed for the calculated real and imaginary pats of describing function and the fitted curves are shown in Figure 4.10.

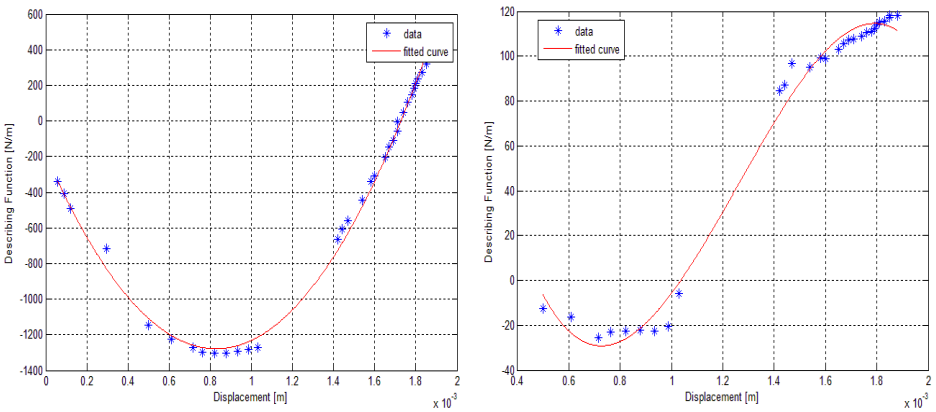

(a) (b)

Figure 4.10 Calculated describing function (a) Real part (b) Imaginary part

For the real part and imaginary part of describing function, 2nd order and 3rd order polynomial functions are fit, respectively. Corresponding coefficients of the polynomial functions are given in Table 4.6.

Table 4.6 Coefficients of the polynomials fit to the data for real and imaginary part of the describing function

	p_3	p_2	p_1	p_0
Real Part of Describing Function $p_2x^2 + p_1x + p_0$	---	$1.58\text{x}10^{9}$	$-2.62\text{x}10^{6}$	-191
Imaginary Part of Describing Function $p_3x^3 + p_2x^2 + p_1x + p_0$	$-2.38\text{x}10^{10}$	$9.0\text{x}10^{8}$	$-9.32\text{x}10^{5}$	264

4.1.2.6 Application of PRD Method at 41.5 Hz for Identifying Nonlinearity

Real and imaginary parts of the describing function are obtained from experimental measurements at 41.5 Hz by applying PRD method. Curve fitting is performed for the calculated real and imaginary pats of describing function and the fitted curves are shown in Figure 4.11.

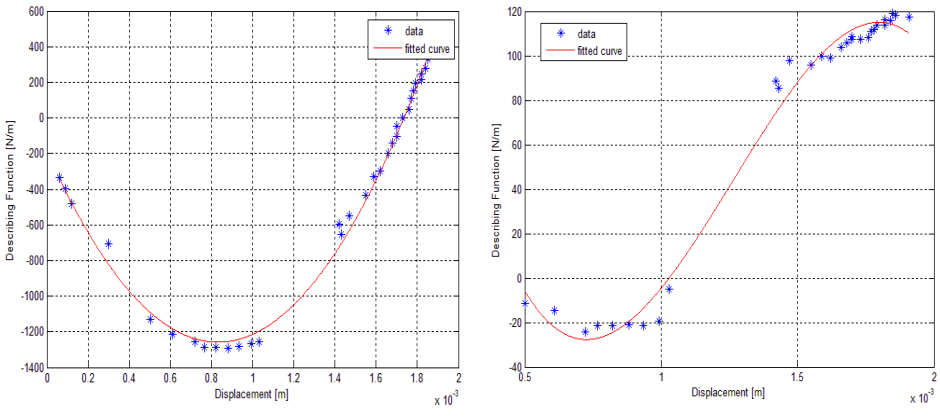

(a) (b)

Figure 4.11 Calculated describing function (a) Real part (b) Imaginary part

For the real part and imaginary part of describing function, 2nd order and 3rd order polynomial functions are fit, respectively. Corresponding coefficients of the polynomial functions are given in Table 4.7.

Table 4.7 Coefficients of the polynomials fit to the data for real and imaginary part of the describing function

	p_3	p_2	p_1	p_0
Real Part of Describing Function $p_2x^2 + p_1x + p_0$	---	$1.54\text{x}10^9$	$-2.56\text{x}10^6$	-190
Imaginary Part of Describing Function $p_3x^3 + p_2x^2 + p_1x + p_0$	$-2.32\text{x}10^{10}$	$8.8\text{x}10^8$	$-9.11\text{x}10^5$	259

If the coefficients for the real part of describing functions obtained using the measurements at 39 Hz, 39.5 Hz, 40 Hz, 40.5 Hz, 41 Hz and 41.5 Hz are compared, we can see that estimated coefficients are very similar. However, when we compare the imaginary parts of describing functions obtained by using the measurements at 39 Hz, 39.5 Hz, 40 Hz, 40.5 Hz, 41 Hz and 41.5, it is observed that there are considerable differences between the functions.

Final test in the first set of experiments is the measurement of frequency responses between 37 Hz and 47 Hz at a number of constant forcing levels. In the experiments stepped sine signal is used. In the frequency range of interest, the resolution of the frequency is set as 0.25 Hz. However, in order to perform constant force vibration testing over the desired frequency range, it is necessary to control the force level. Since there is no automatic controller in the experiments, for every frequency point this control is maintained manually by checking the measured force and adjusting voltage signal generated by the signal generator. The flow chart defining the test procedure is given in Figure 4.12. Measured FRFs for F=0.05N are also shown in Figure 4.13.

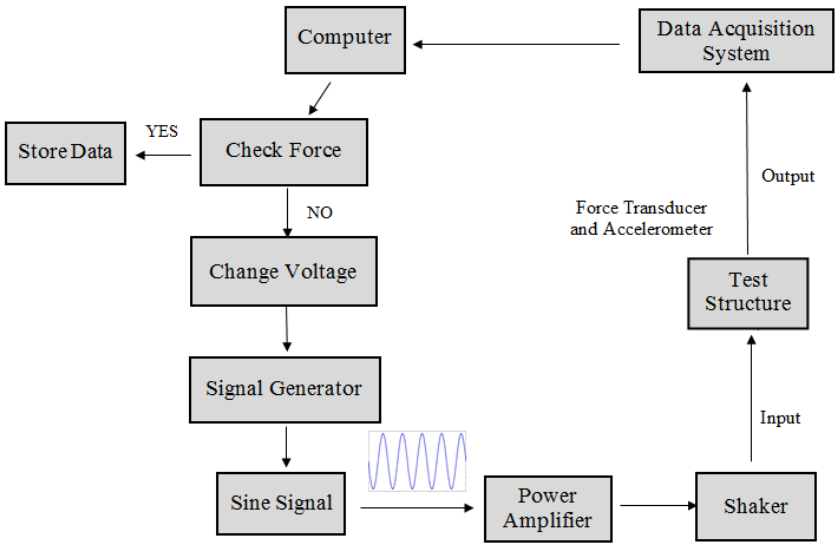

Figure 4.12 Experimental procedure followed in constant force vibration test

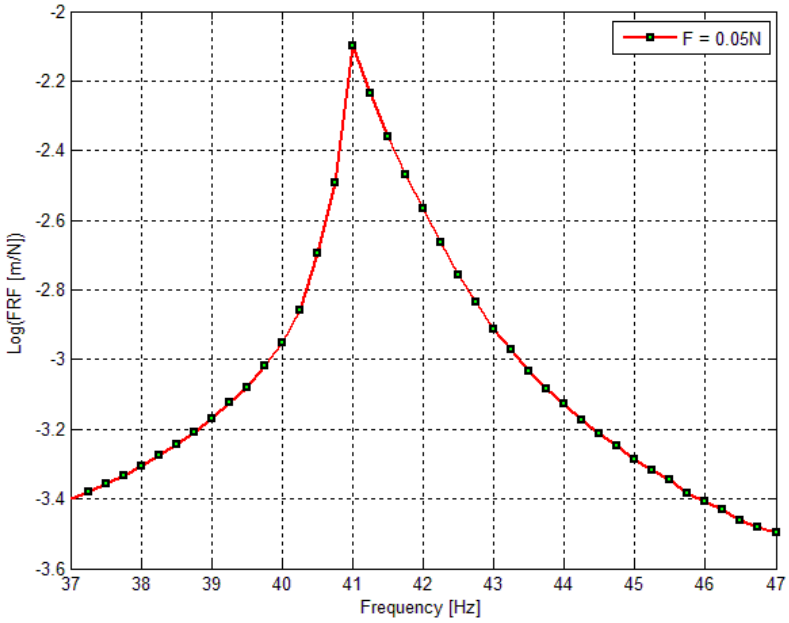

Figure 4.13 Measured FRF at F=0.05N

As seen from Figure 4.13, the FRF curve measured at F=0.05N looks like a linear FRF curve, as expected. However, as it will be shown later that, even though the forcing level used in the experiment is very low, the measured FRF curve is different from the linear FRF curve of the system.

4.1.3 Second Set of Experiments

Main purpose of the second set of experiments is to obtain measured nonlinear FRFs that will be used for the verification of PRD method and of the proposed model updating approach.

Stepped sine testing is used with a frequency resolution of 0.25 Hz at constant force levels. Similarly, for every frequency point force control is maintained manually by checking the measured force and adjusting voltage signal generated by the signal generator. In the experiments, 3 different forcing levels (F=0.6N, F=0.7N, F=0.8N) are used. The corresponding FRFs for F=0.6N, F=0.7N, F=0.8N are shown in Figure 4.14.

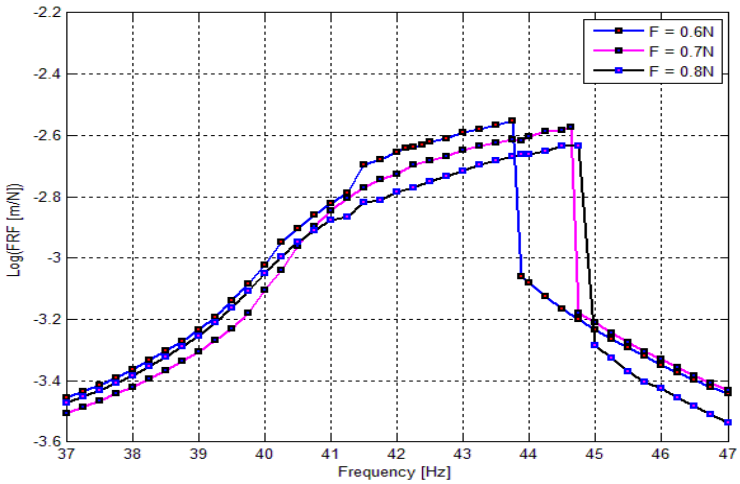

Figure 4.14 Measured FRFs at F=0.6N, F=0.7N, F=0.8N

4.1.4 Application of PRD Method for Obtaining Linear FRFs

In this section, PRD method is used in order to predict the linear FRF of the structure by using the measured FRF values at F=0.05N and the describing functions obtained in Section 4.1.2. Since, different describing functions are obtained for each of six different excitation frequencies, in order to investigate the effects of excitation frequency on the performance of the PRD method; six separate linear FRF curves are predicted. Each FRF curves predicted by using the describing functions obtained from experiments made at 39 Hz, 39.5 Hz, 40 Hz, 40.5 Hz, 41 Hz and 41.5 Hz are compared with the measured FRFs at F=0.05N in Figure 4.15, and with each other in Figure 4.16 at the first mode.

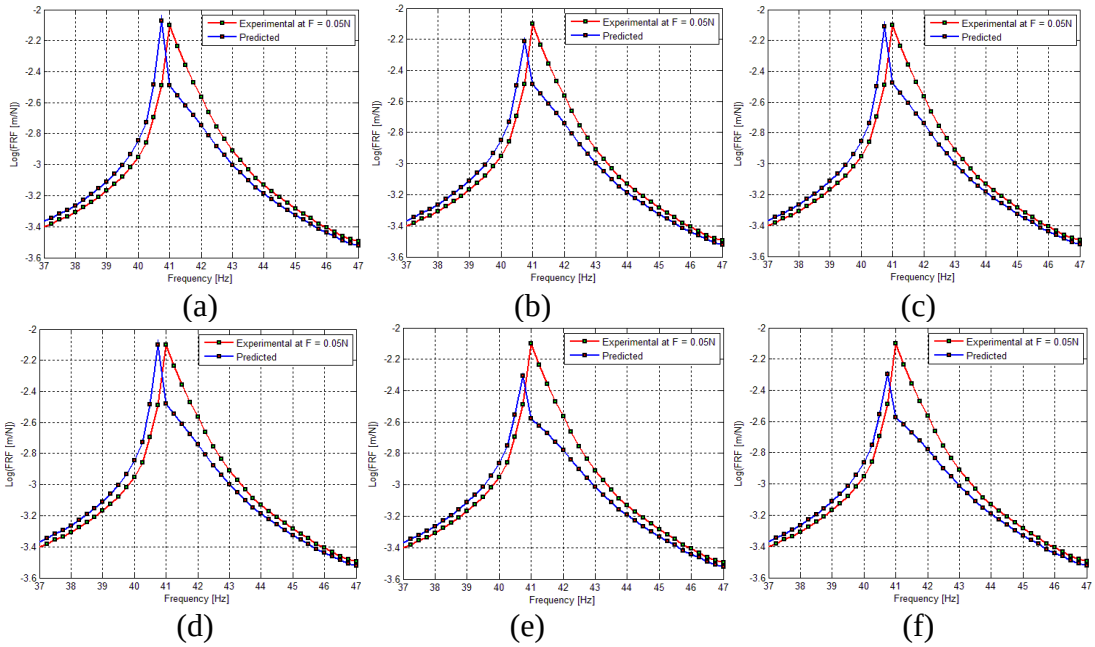

Figure 4.15 Comparison of measured FRF at F=0.05N and predicted linear FRFs by using PRD method using experiments conducted at (a) 39 Hz (b) 39.5 Hz (c) 40 Hz (d) 40.5 Hz (e) 41 Hz (f) 41.5 Hz

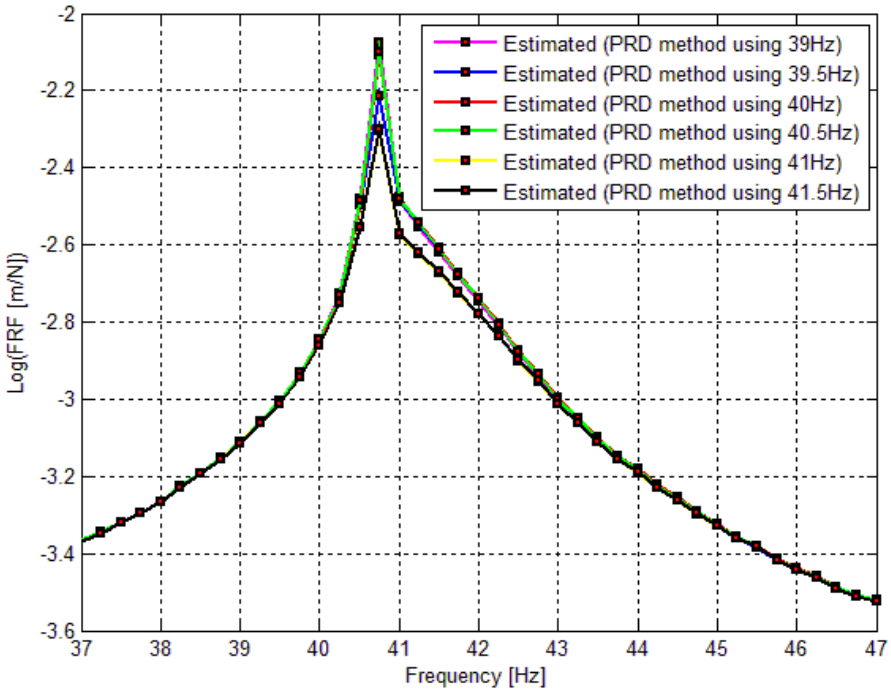

Figure 4.16 Comparison of predicted linear FRFs by using PRD method using experiments conducted at 39 Hz, 39.5 Hz, 40 Hz, 40.5 Hz, 41 Hz and 41.5 Hz

It is seen from Figure 4.15 that, the linear FRF curves of the system that are predicted by applying the PRD method proposed, are not accurately represented by the FRF curve measured at low forcing level (F = 0.05N). As it was shown in Chapter 3 that PRD method yields the FRFs of the underlying linear system in a nonlinear system accurately, it can be concluded that even a very low forcing level is used in the experiments, the FRFs of the underlying linear system cannot be accurately represented by the FRFs measured at low forcing levels. Furthermore, as seen from Figure 4.16 that linear FRFs obtained using the describing functions identified from the tests made at 39 Hz, 39.5 Hz, 40 Hz, 40.5 Hz, 41 Hz and 41.5 Hz do not differ much from each other, even though identified imaginary parts of the describing functions from these tests are rather different from each other.

4.1.5 Model Updating of the Test System and Verification of the Updated Model

In this section, firstly the structure is modelled in ANSYS and the linear FE model of the structure is built. Then this linear FE model of the test structure is updated by using the obtained linear FRFs employing first the PRD and then the inverse eigensensitivity method. Once the updated linear FE model is built then it is possible to have the updated nonlinear model of the test system. Therefore by combining updated linear FE model and the identified nonlinearity, updated nonlinear model of the test structure is constructed. As a final step, in order to show the accuracy of the updated nonlinear model, FRFs of the test structure calculated by using the updated nonlinear model are compared with the measured nonlinear FRFs at different forcing levels.

In Figure 4.17, the FE model of the test structure built in ANSYS is shown. Material properties used in the analysis of the initial FE model are also given in Table 4.8.

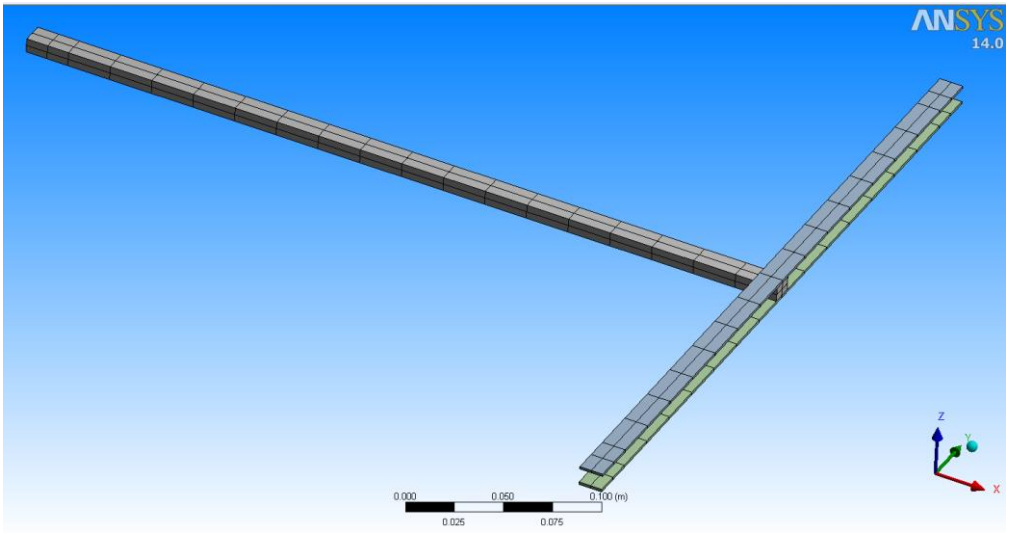

Figure 4.17 FE model of the test structure

Table 4.8 Material properties used in the initial FE model

	Modulus of Elasticity (E) (GPa)	**Poisson's Ratio (ν)**	**Density (ρ) (kg/m^3)**
Beam1	210	0.3	7850
Beam2	210	0.3	7850

By performing modal analysis in ANSYS, the first natural frequency and the driving point FRF at the tip of beam 1 in Z (transverse) direction are calculated for the initial FE model of the structure. In ANSYS, sufficient number of modes (100) is used to calculate FRFs, in order to minimize truncation error. Comparisons of the linear FRFs obtained from FE analysis with those obtained from experiments by using PRD method are shown in Figure 4.18.

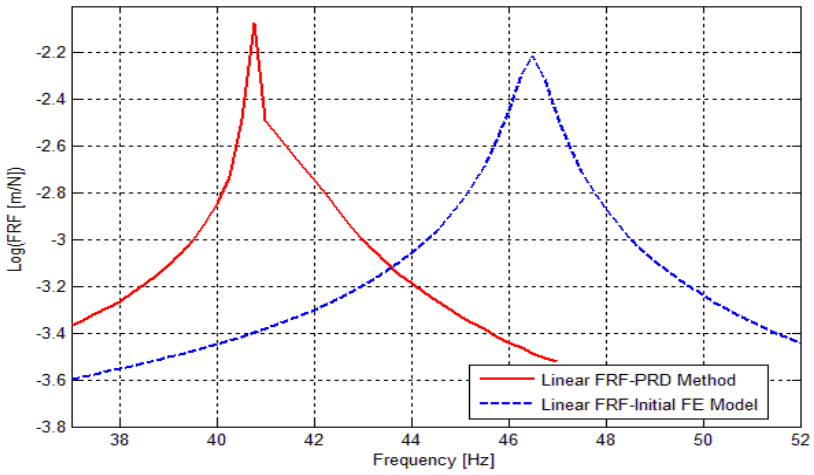

Figure 4.18 Comparison of the linear FRFs obtained from initial FE model with those obtained by using PRD method

In Table 4.9, the natural frequency obtained from FE analysis is also compared with the one obtained from experiments.

Table 4.9 Comparison of the first natural frequency obtained from initial FE model with the experimental value obtained by using PRD method

Mode Number	Natural Frequency (PRD Method) (Hz)	Natural Frequency (Initial FE Model) (Hz)	Error (%)
1	40.75	46.48	14.06

As can be observed from Table 4.9 and Figure 4.18, the results are considerably different; therefore it is necessary to update the FE model of the structure. Since generally modulus of elasticity (E) of the materials has considerable uncertainties the modulus of elasticity is selected as an updating parameter in the FE model. For the selected parameter, element of the sensitivity matrix is calculated by using the following central difference approximation with $O(h^4)$, at each iteration step.

$$r'(p_i) = \frac{-r(p_{i+2}) + 8r(p_{i+1}) - 8r(p_{i-1}) + r(p_{i-2})}{12\Delta h} \tag{4.1}$$

In Equation (4.1), Δh is the step size used. After 5 iterations, updating parameter is converged to 161.5 GPa. The convergence graph of this parameter is given in Figure 4.19.

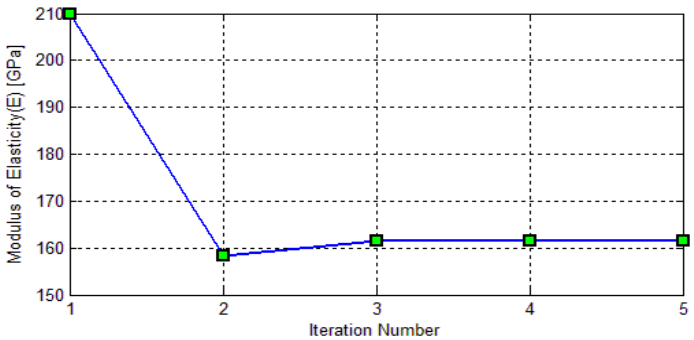

Figure 4.19 Convergence of the modulus of elasticity of the beams

Using the converged value for the modulus of elasticity, the FE model is updated. Performing modal analysis in ANSYS for the updated FE model of the structure, the first natural frequency of the updated linear model is calculated. The comparisons of the first natural frequency obtained from updated model with that of initial FE model, as well as with the natural frequency obtained from experiments by using PRD method are given in Table 4.10.

Table 4.10 Comparison of the first natural frequency obtained from initial and updated FE models with experimental value obtained by using PRD method

Mode Number	Natural Frequency (PRD Method) (Hz)	Natural Frequency (Initial FE Model) (Hz)	Error (%)	Natural Frequency (Updated FE Model) (Hz)	Error (%)
1	40.75	46.48	14.06	40.75	0.00

As can be seen in Table 4.10 the first natural frequency is very accurately estimated by using the updated FE model.

In order to see the performance of the updated FE model in the prediction of other natural frequencies which are not used in updating the FE model, the second natural frequency of the system is calculated by using the updated linear model and it is compared with that obtained from the initial FE model, as well as with the measured one (Table 4.11).

Table 4.11 Comparison of the second natural frequency obtained from initial and updated FE models with experimental value obtained by using PRD method

Mode Number	Natural Frequency (Experimental) (Hz)	Natural Frequency (Initial FE Model) (Hz)	Error (%)	Natural Frequency (Updated FE Model) (Hz)	Error (%)
2	177.75	198.05	11.42	173.63	-2.32

As can be seen in Table 4.11 , there is a considerable improvement in the calculated value of the second natural frequency.

In Figure 4.20, the comparasion of the linear FRFs calculated from experimentally measured nonlinear FRFs by using PRD method with those obtained from the initial and updated FE models is given. It is observed from Figure 4.20 that, there is a considerable improvement when updated FE model is used.

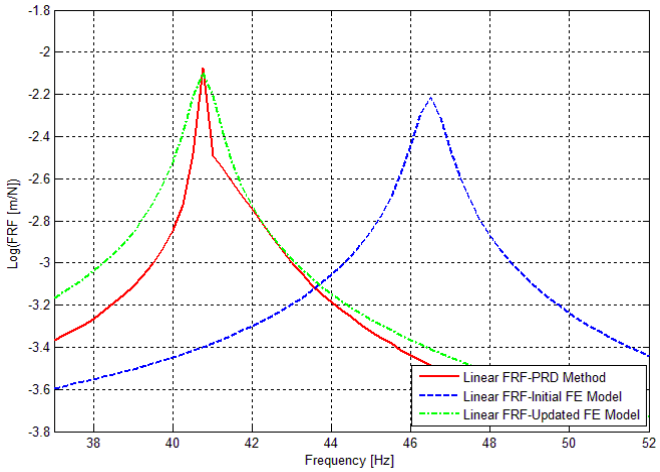

Figure 4.20 Comparison of the linear FRF obtained by using PRD method from experimentally measured values, with those calculated from, initial and updated FE models

Since the ultimate goal is to predict nonlinear responses accurately from the updated model, for F=0.6N, F=0.7N and F=0.8N, experimentally measured nonlinear FRFs are compared with those obtained from the initial and updated models (composed of original and updated FE models, respectively, combined with identified nonlinearity). The results obtained are shown in Figure 4.21. It is seen from Figure

4.21 that, considerable improvements are obtained for the FRFs calculated with the updated model for all forcing levels.

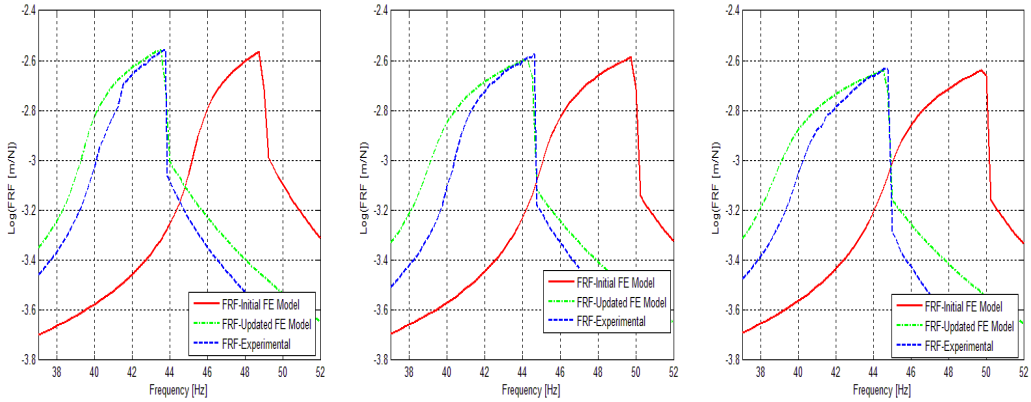

(a) (b) (c)

Figure 4.21 Comparison of FRFs obtained from initial and updated models with the experimental ones for (a) F=0.6N (b) F=0.7N (c) F=0.8N

4.1.6 Investigation of Effect of Finite Difference Formula Used for Sensitivity Calculation on the Model Updating Performance

As mentioned in the theory part, in the inverse eigensensitivity method, $S_{r_n}^{\ p_m}$ (element of a Modal sensitivity matrix $[S]$) which stands for the sensitivity of the nth response to the mth updating parameter is mathematically obtained by calculating the partial differential of the nth response to the mth updating parameter. In this section, in order to calculate the sensitivities, different numerical differentiation formulas are used, and the effect of using different finite difference formulas on the model updating performance is investigated.

In this analysis, the same initial FE model of the T-beam test structure is used. The FE model of the test structure is shown in Figure 4.17, and the material properties used in the initial FE model are given in Table 4.8.

In the model updating of the FE model, four different finite difference formulas are used in turn, in order to calculate numerical differentiation and approximate the sensitivities. Numerical differentiation formulas used in the analysis are given below.

1. Central difference formula with error order of $O(h^4)$:

$$r'(p_i) = \frac{-r(p_{i+2}) + 8r(p_{i+1}) - 8r(p_{i-1}) + r(p_{i-2})}{12\Delta h} \tag{4.2}$$

2. Central difference formula with error order of $O(h^2)$:

$$r'(p_i) = \frac{r(p_{i+1}) - r(p_{i-1})}{2\Delta h} \tag{4.3}$$

3. Backward difference formula with error order of $O(h)$:

$$r'(p_i) = \frac{r(p_i) - r(p_{i-1})}{\Delta h} \tag{4.4}$$

4. Forward difference formula with error order of $O(h)$:

$$r'(p_i) = \frac{r(p_{i+1}) - r(p_i)}{\Delta h} \tag{4.5}$$

where Δh is the step size used for the parameter in the analysis.

Since most of the uncertainty is generally in the modulus of elasticity (E) of the materials, again, the modulus of elasticity is selected as an updating parameter in FE model. For the selected parameter, element of the sensitivity matrix is calculated using each of the finite difference formula at each iteration step. For all of the cases, after 5 iterations, updating parameter is converged to 161.5 GPa. The convergence graphs of this parameter by using the numerical differentiation with central difference formula with error order of $O(h^4)$, central difference formula with error order of $O(h^2)$, backward difference formula with error order of $O(h)$ and forward difference formula with error order of $O(h)$, are given in Figure 4.22, Figure 4.23, Figure 4.24 and Figure 4.25, respectively.

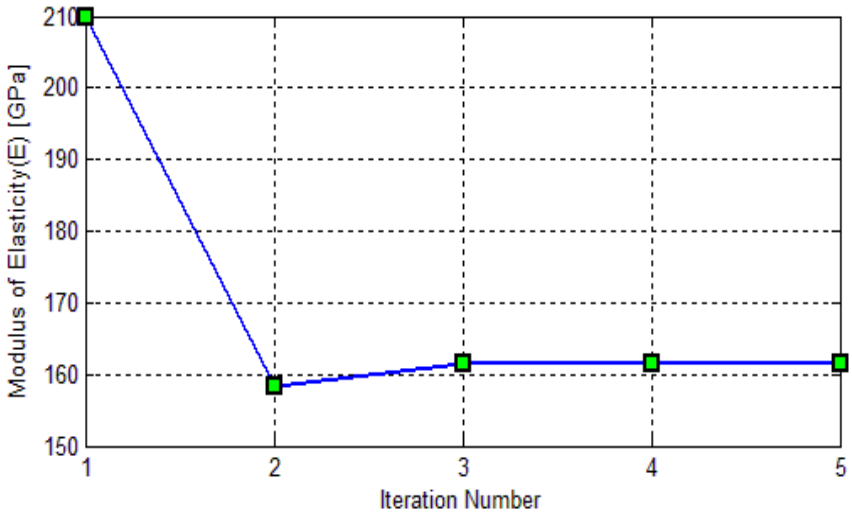

Figure 4.22 Convergence of the modulus of elasticity of the beams, for the numerical differentiation with central difference formula with error order of $O(h^4)$

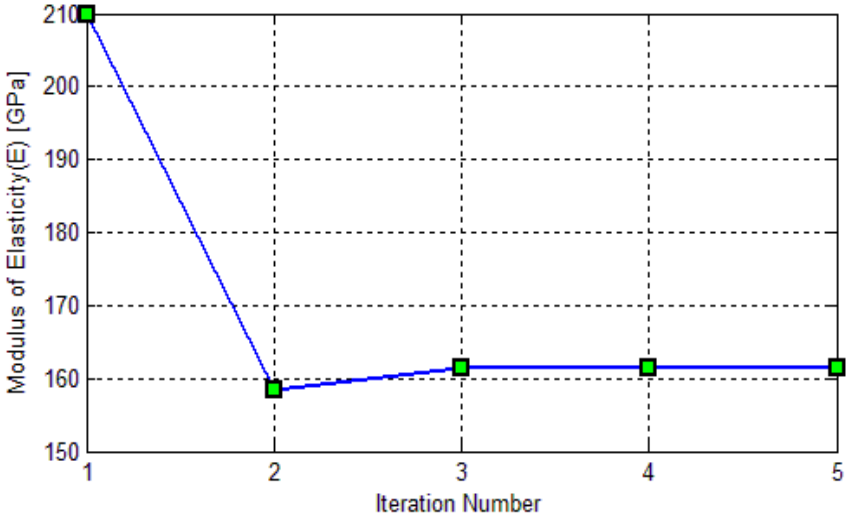

Figure 4.23 Convergence of the modulus of elasticity of the beams for the numerical differentiation central difference formula with error order of $O(h^2)$

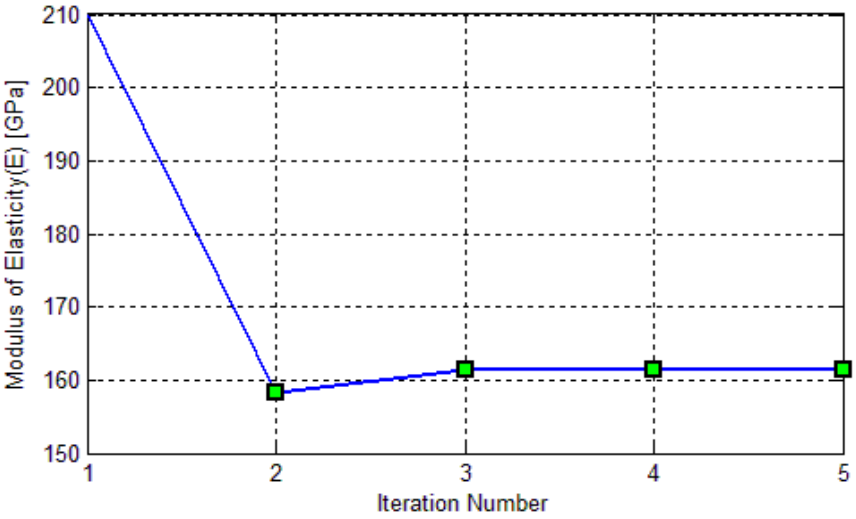

Figure 4.24 Convergence of the modulus of elasticity of the beams for the numerical differentiation with backward difference formula with error order of $O(h)$

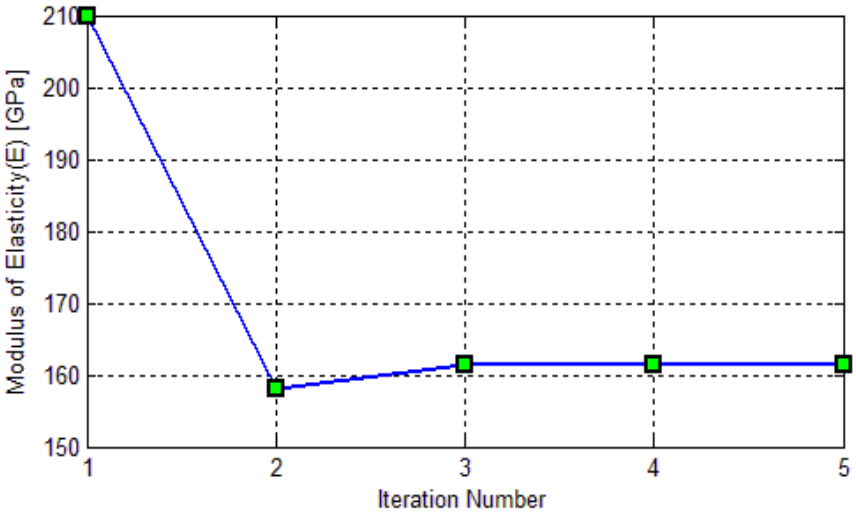

Figure 4.25 Convergence of the modulus of elasticity of the beams for the numerical differentiation with forward difference formula with error order of *O(h)*

For the calculation of the sensitivities, the number of FE analysis that needs to be run is different for each of the finite difference formula. Therefore, the total computation time that is used in the model updating procedure is compared for each of the finite difference formula. The results are given in Table 4.12.

Table 4.12 Computation time comparison of the different finite difference formulas

Finite Difference Formula	**# of FE Analysis Performed**	**# of Iteration Performed**	**Computation Time (s)**
Central difference formula with error order of $O(h^4)$	21	5	640.5
Central difference formula with error order of $O(h^2)$	13	5	396.5
Backward difference formula with error order of $O(h)$	10	5	305
Forward difference formula with error order of $O(h)$	10	5	305

As seen from Table 4.12, although the number of iteration is same for all the cases, total computation time is much larger for updating procedure that uses central difference formula with error order of $O(h^4)$, due to the number of FE analysis that needs to be done at each iteration step. Also, updating procedure that uses first order forward and backward difference formula has the smallest computation time. Based on these results, it is recommended that in updating of FE models forward or backward difference formula should be used in order to reduce computational effort which is consistent with the recommendations given in [84].

4.2 Experimental Study 2-Model Updating for Three Modes

In this section, the approach suggested for model updating of a nonlinear system is applied again on the nonlinear experimental T-beam test system given in Section 4.1. The main difference of the study in this section from the study given in Section 4.1 is that, the first three global modes of the T-beam are considered in the model updating in this section. First, using identified nonlinearities obtained by the PRD method in the previous test, linear FRFs are obtained from experimentally measured nonlinear FRFs for the first, second and third global modes of the test system. Then, linear FE model of the test system is built in ANSYS and the linear FE model of the test structure is updated for the first three global modes of the structure by using the extracted linear FRFs employing the PRD method and then using ANSYS Design Exploration Optimization. Combining the updated linear FE model and the identified nonlinearity, updated nonlinear model of the test structure is obtained. Finally, in order to show the accuracy of the updated nonlinear model of the system, for different forcing levels, FRFs calculated using the updated nonlinear model are compared with the measured FRFs of the test structure.

4.2.1 First Set of Experiments

In the first set of experiments, the structure is excited with a random input force. In random excitation, low excitation signal level is selected. The measurements are performed in the frequency range of 0-300 Hz and frequency resolution is 0.25 Hz. In order to minimize the noise in the experiment, 130 averages are taken. By using the force and acceleration measurements, driving point FRFs at the tip of beam 1 in transverse direction are obtained and they are shown in Figure 4.26.

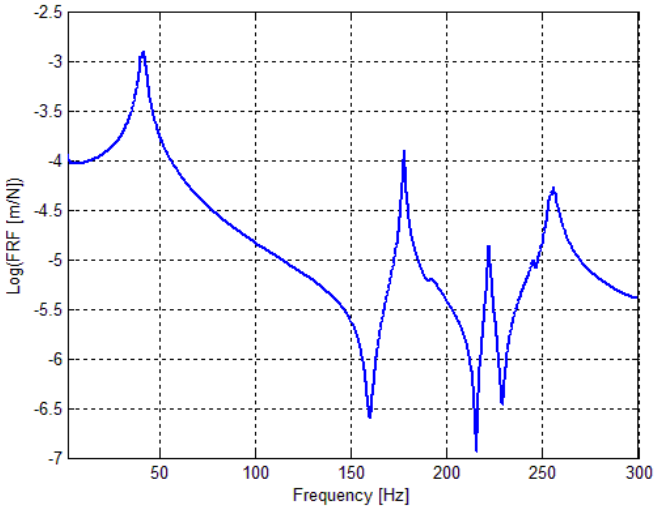

Figure 4.26 The measured driving point FRF at the tip of beam 1 in transverse direction (random excitation)

It is observed from the results, that first three natural frequency of the global modes of the structure is in between 0-300 Hz. It will be shown in Section 4.2.4.1 that, a local mode exists in between the second and third global mode of system. Therefore this local mode is not considered in the next set of experiments.

As a final test in this set of experiments, a constant low forcing level excitation experiment is performed between 175 Hz and 181 Hz (around the second natural frequency) and between 257 Hz and 267 Hz (around the third natural frequency). Stepped sine constant force test is performed for the given test set-up. In the frequency range of interest, the resolution of the frequency is set as 0.25 Hz. However, in order to perform constant force vibration testing over the desired frequency range, it is necessary to control the force level. Since there is no automatic controller in the experiments, for every frequency point this control is maintained manually by checking the measured force and adjusting voltage signal generated by the signal generator. In Figure 4.27 and Figure 4.28, measured FRFs at F=0.05N are shown for the second and third modes, respectively.

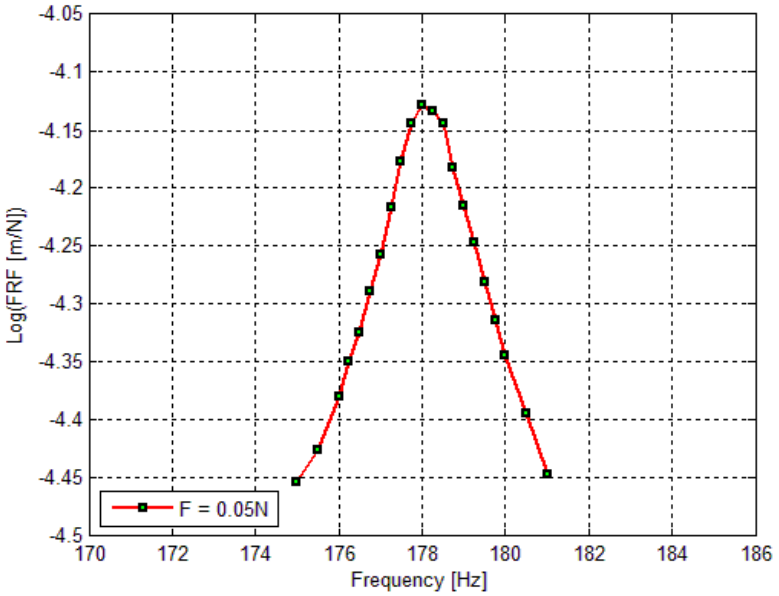

Figure 4.27 Measured FRF at F=0.05N

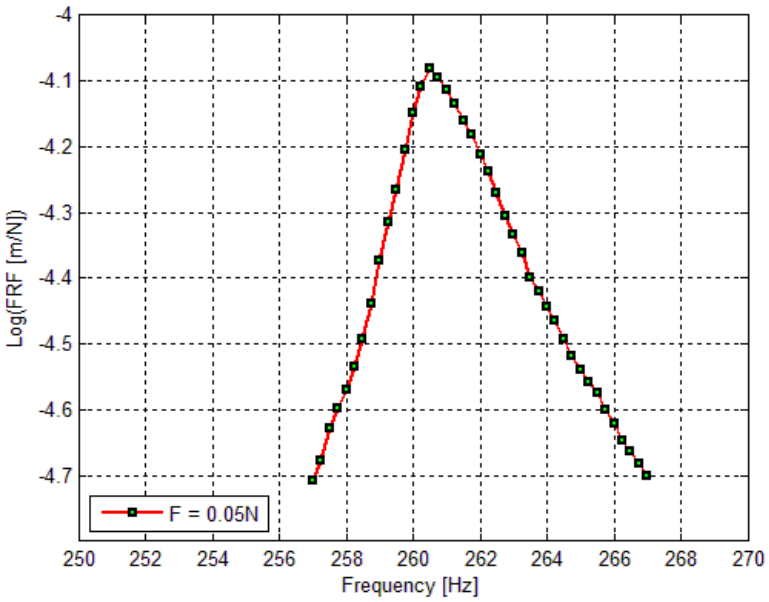

Figure 4.28 Measured FRF at F=0.05N

It is observed from the Figure 4.27 and Figure 4.28 that, the FRFs measured at F=0.05N seem like a linear FRF.

4.2.2 Second Set of Experiments

Main purpose of the second set of experiments is to obtain the measurement data that will be used for the verification of PRD method and the proposed model updating approach. Stepped sine testing is performed with a frequency resolution of 0.25 Hz at constant force levels. Similarly, for every frequency point force control is maintained manually by checking the measured force and adjusting voltage signal generated by the signal generator. In the experiments, 3 different forcing levels (F=0.6N, F=0.7N, F=0.8N) are used. The measured FRFs are shown in Figure 4.29 and Figure 4.30 for the second and third modes of the structure, respectively.

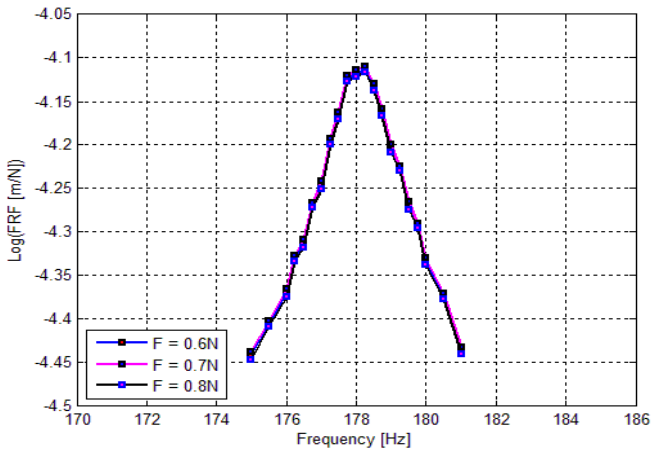

Figure 4.29 Measured FRF at F=0.6N, F=0.7N, F=0.8N

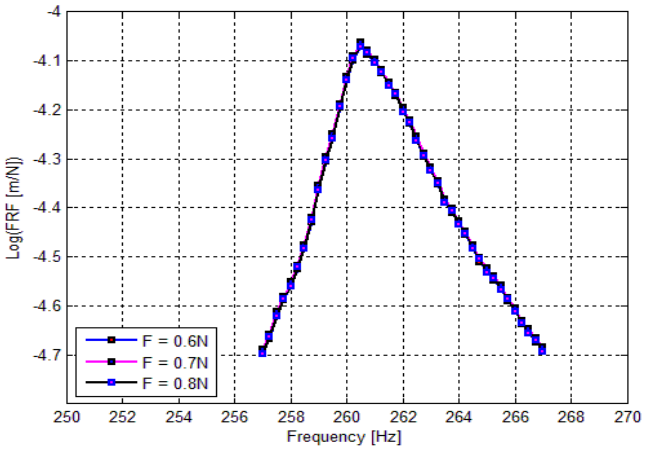

Figure 4.30 Measured FRF at F=0.6N, F=0.7N, F=0.8N

From Figure 4.29 and Figure 4.30, it is observed that measured FRFs are very similar to each other. In order to compare these FRFs with the FRFs measured at F=0.05N, these FRFs are also plotted in the same graph with the FRFs measured at F=0.05N and they are shown in Figure 4.31 and Figure 4.32 for the second and third modes of the structure, respectively.

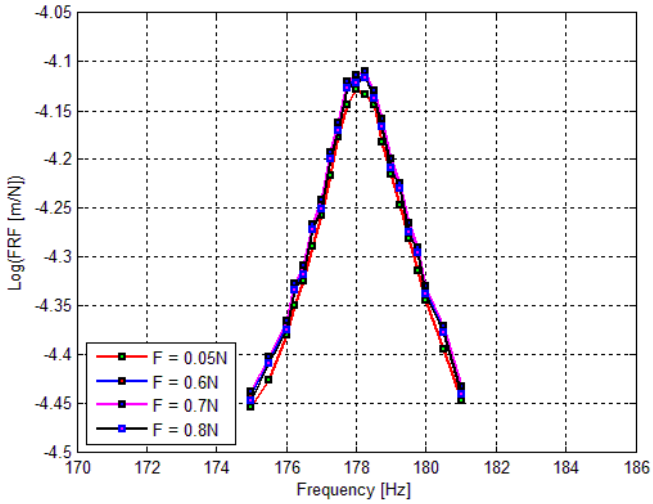

Figure 4.31 Measured FRF at F=0.05N, F=0.6N, F=0.7N, F=0.8N

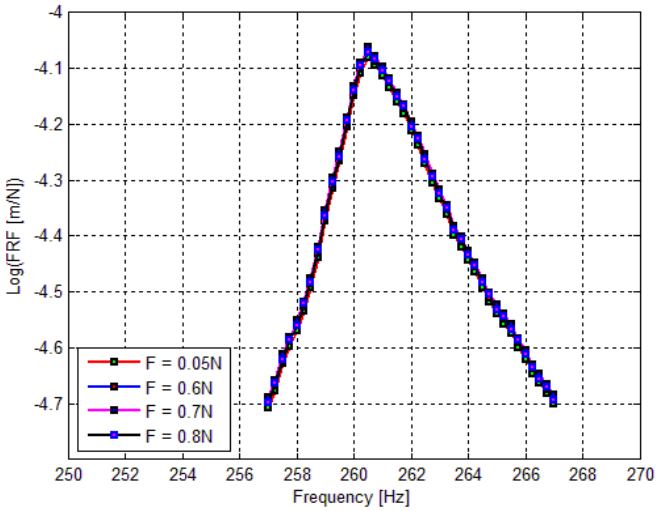

Figure 4.32 Measured FRF at F=0.05N, F=0.6N, F=0.7N, F=0.8N

From Figure 4.31 and Figure 4.32, it is observed that, the FRFs are very similar at low and high forcing levels, which indicates that nonlinearity in the structure does not affect these modes significantly.

4.2.3 Application of PRD Method for Obtaining Linear FRFs

In this section, PRD method is used in order to predict the linear FRF of the structure by using the measured FRF values at F=0.05N and the describing function values obtained in Section 4.1.2. Since, different describing function values are obtained for each of six different excitation frequencies, in order to investigate the effects of excitation frequency on the performance of the PRD method; six separate linear FRF curves are predicted. FRF curves predicted by using the describing functions obtained from experiments made at 39 Hz, 39.5 Hz, 40 Hz, 40.5 Hz, 41 Hz and 41.5 Hz are compared with the measured FRFs at F=0.05N in Figure 4.33, as well as with each other (Figure 4.34) for the second natural frequency. Similar comparisons are shown in Figure 4.35 and Figure 4.36 for the third natural frequency. Since similar comparisons were also given in Section 4.1.4 for the first natural frequency, they are not given here again.

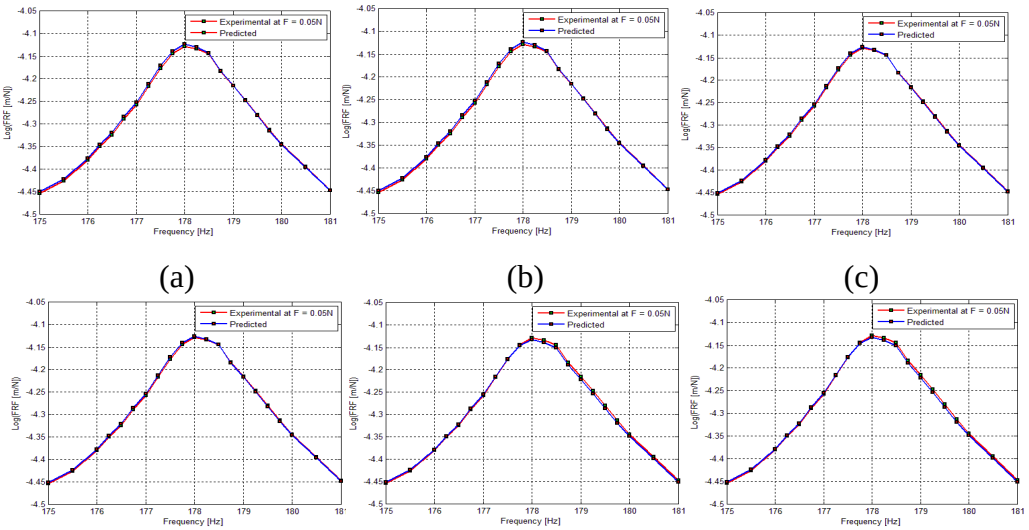

Figure 4.33 Comparison of measured FRF at F=0.05N and predicted linear FRFs by using PRD method using experiments conducted at (a) 39 Hz (b) 39.5 Hz (c) 40 Hz (d) 40.5 Hz (e) 41 Hz (f) 41.5 Hz

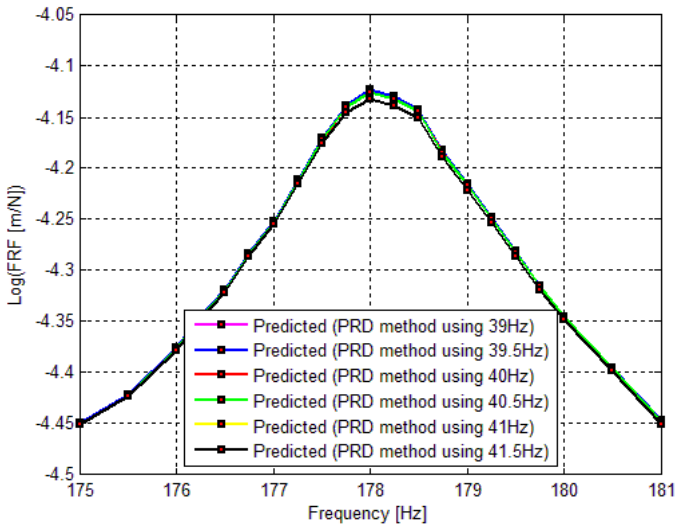

Figure 4.34 Comparison of predicted linear FRFs by using PRD method using experiments conducted at 39 Hz, 39.5 Hz, 40 Hz, 40.5 Hz, 41 Hz and 41.5 Hz

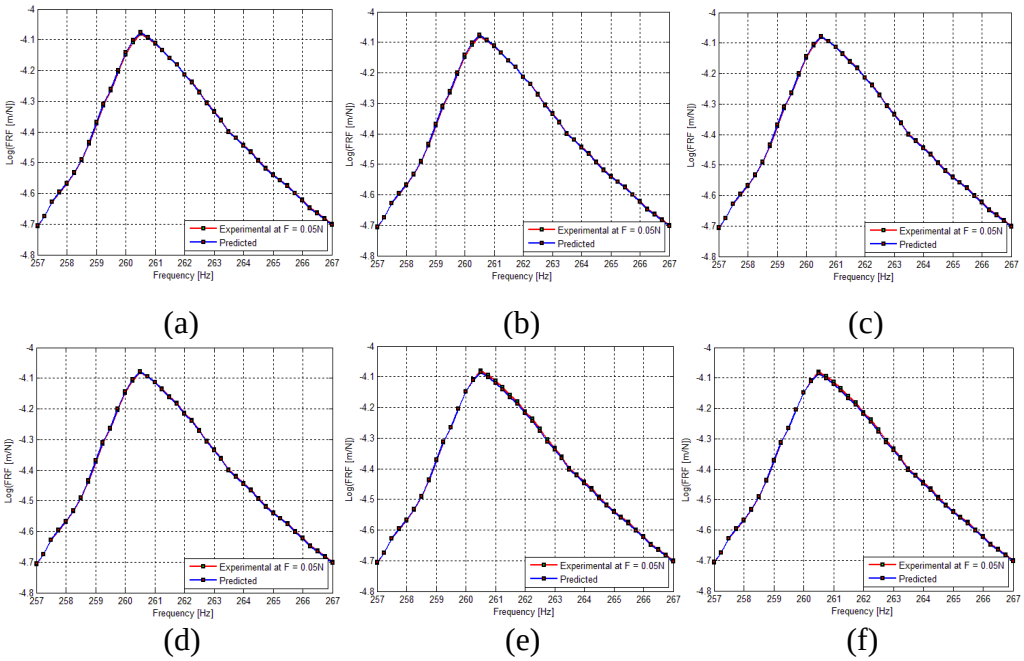

Figure 4.35 Comparison of measured FRF at F=0.05N and predicted linear FRFs by using PRD method using experiments conducted at (a) 39 Hz (b) 39.5 Hz (c) 40 Hz (d) 40.5 Hz (e) 41 Hz (f) 41.5 Hz

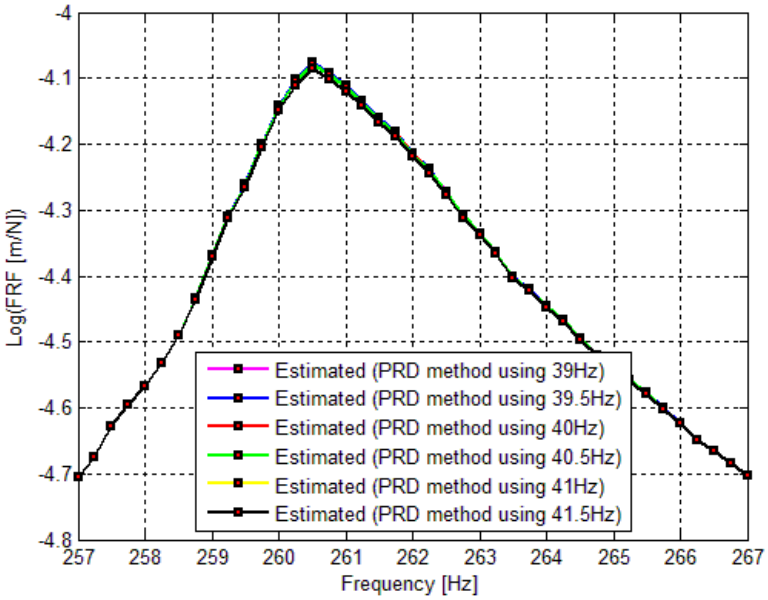

Figure 4.36 Comparison of predicted linear FRFs by using PRD method using experiments conducted at 39 Hz, 39.5 Hz, 40 Hz, 40.5 Hz, 41 Hz and 41.5 Hz

As can be seen from Figure 4.33 and Figure 4.35, linear FRFs obtained by using the PRD method is very close to the FRFs measured at low forcing level (F=0.05N) for the second and third modes of the structure. Also it is observed from Figure 4.34 and Figure 4.36 that linear FRFs obtained using the describing functions identified from the tests made at six different frequencies are very close to each other. These observations indicate that nonlinearity in the structure does not affect the second and third modes significantly.

4.2.4 Model Updating of the Test System and Verification of the Updated Model

In this section, linear FE model of the test system is built in ANSYS and then the linear FE model is updated by employing the approach proposed. Before the construction of the initial FE model, mesh sensitivity analysis is performed for the

linear FE model of the structure. Then, the linear FE model of the test structure is updated by using the extracted linear FRFs employing the PRD method and then using ANSYS Design Exploration Optimization.

In the updating of the FE model, different updating parameter sets are used and for these updating parameters, different candidates for the updated FE model are obtained by using ANSYS. Measured and predicted FRFs for all the updated linear FE models are compared to each other and the performance of the updated models are investigated. Using the identified nonlinearity and updated linear FE models, updated nonlinear models of the test structure are constructed. Finally, predicted and measured FRFs of the test structure are compared at different forcing levels in order to show the accuracy of the updated nonlinear models of the system.

4.2.4.1 Mesh Sensitivity Analysis for the FE Model of the Structure

In this section before the construction of the initial FE model in ANSYS, mesh sensitivity analysis is performed in order to see the effect of the mesh sizing on the estimation of the first three natural frequencies of the global modes of the structure. FE model of the test structure used in the mesh sensitivity analysis is same as the one used in Section 4.1.5. In the mesh sensitivity analysis, firstly an initial modal analysis is performed in order to find the first three global modes of the system. The results are shown in Figure 4.37.

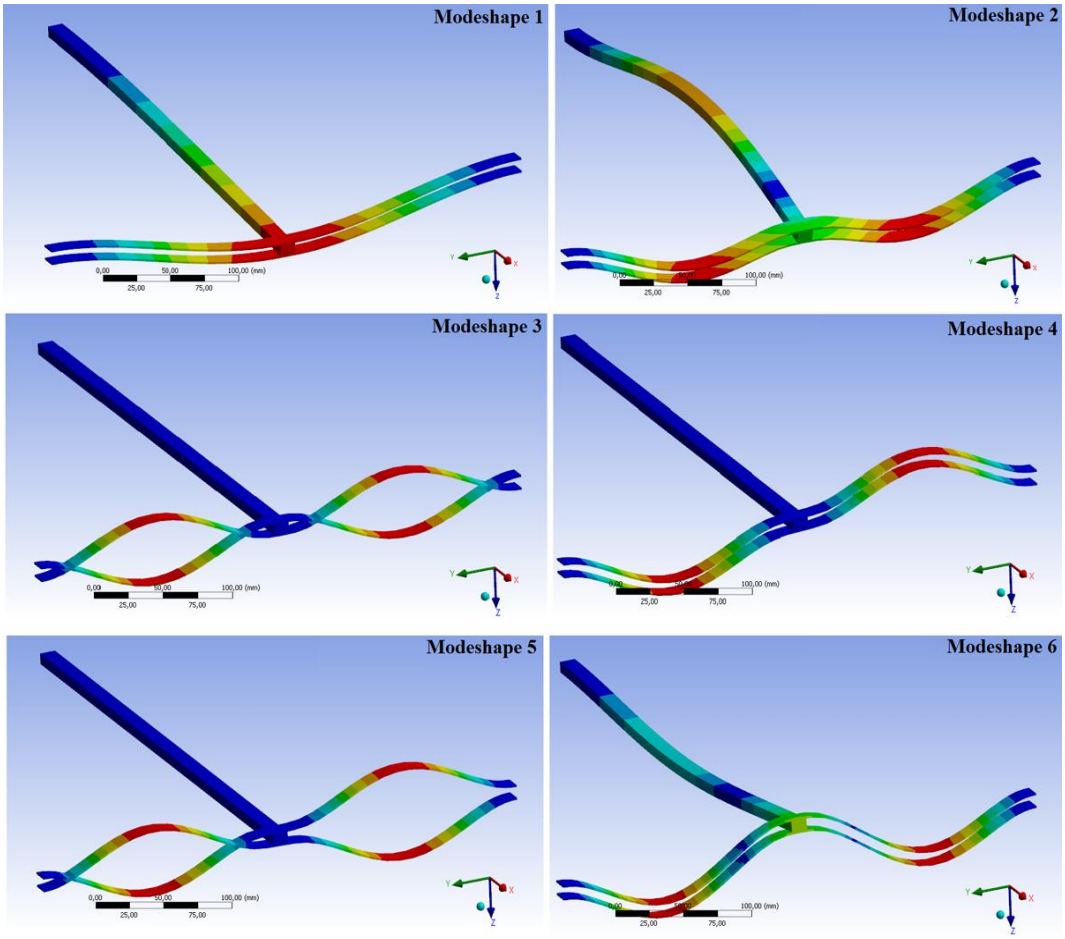

Figure 4.37 The modeshapes of the T-beam structure

It is observed from Figure 4.37 that, the first three global modes of the system are the first, second and sixth modes of structure calculated by ANSYS. Third, fourth and fifth modes are local modes of the thin beam (beam 2) since beam 1 does not move in these modes.

After finding the first three global modes of the structure, several modal analyses are performed in ANSYS and for each of the cases, the first three natural frequencies of the global modes of the structure are obtained. Parameters of the sizing of the mesh are organized according to the Table 4.13.

Table 4.13 Parameters of the sizing of the mesh

h_1/H	w_1/W	w_2/W	l_1/L & l_2/L
6	6	6	40-210
7	7	7	40-210
8	8	8	40-210
9	9	9	40-210
10	10	10	40-210

In Table 4.13, h_1, w_1, w_2, l_1, l_2 are the height of the beam 1, width of beam 1, width of beam 2, length of beam 1 and length of beam 2, respectively. H, W, and L are the height, width and length of the mesh element. In the analysis, SOLID 186 element is used. The variation of the first natural frequency with respect to mesh sizing parameters is shown in Figure 4.38, Figure 4.39 and Figure 4.40.

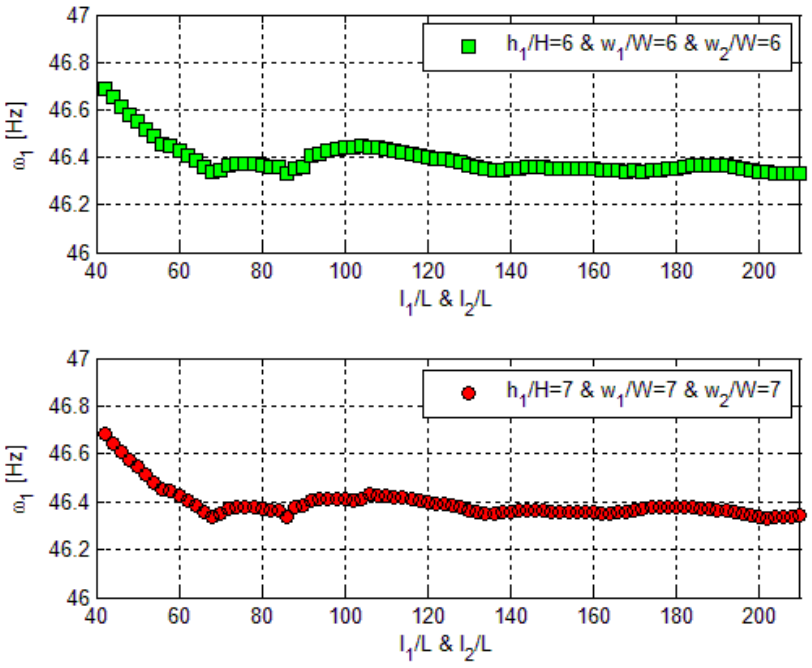

Figure 4.38 Variation of the first natural frequency with respect to mesh sizing

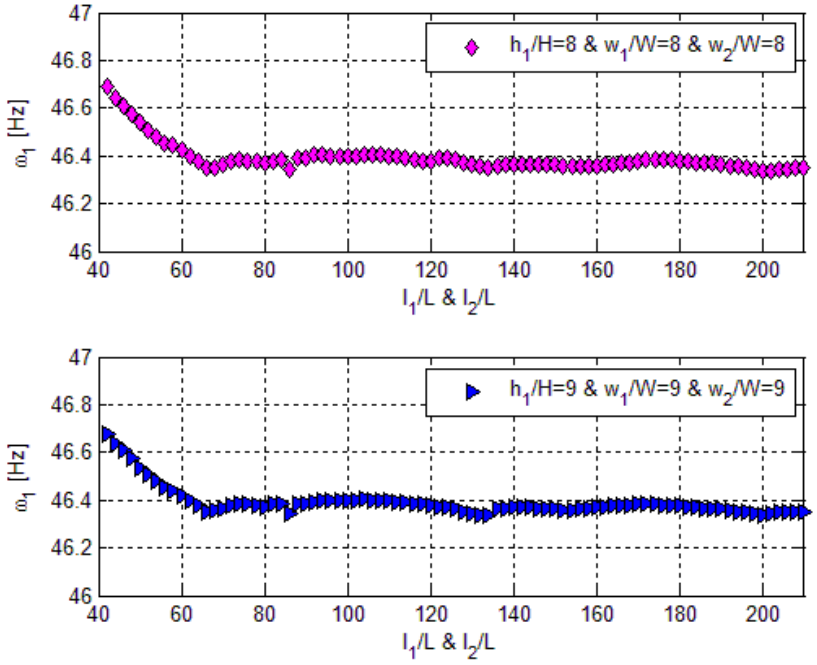

Figure 4.39 Variation of the first natural frequency with respect to mesh sizing

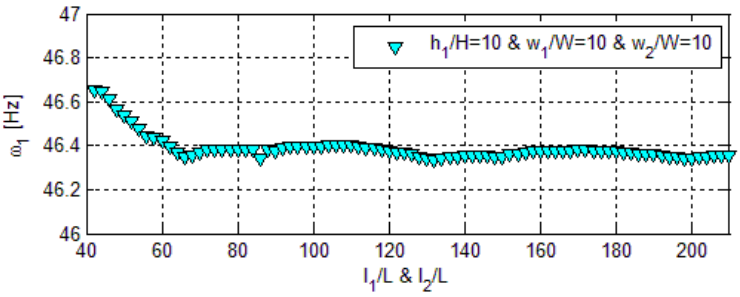

Figure 4.40 Variation of the first natural frequency with respect to mesh sizing

As seen from Figure 4.38, Figure 4.39 and Figure 4.40, the first natural frequency is converged approximately to 46.4 Hz after l_1/L and l_2/L reach to approximately 60-80 range. Similarly, the variation of the second natural frequency with respect to mesh sizing parameters is shown in Figure 4.41, Figure 4.42 and Figure 4.43.

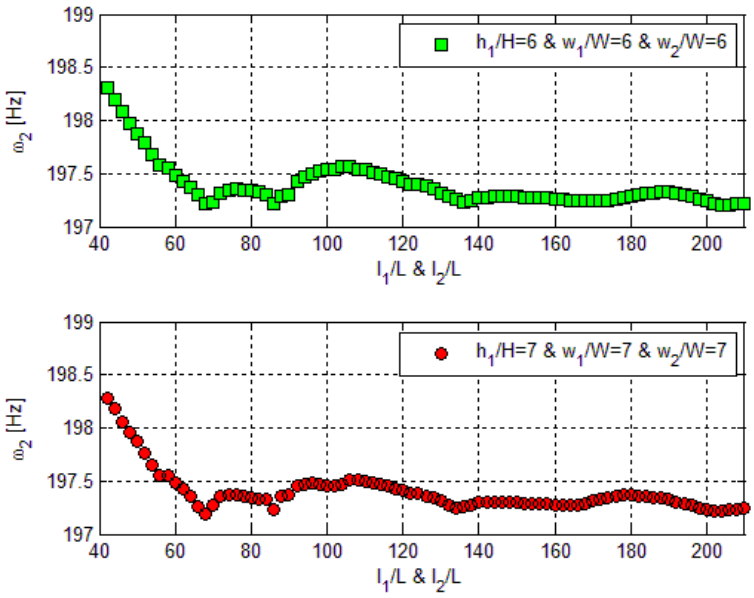

Figure 4.41 Variation of the second natural frequency with respect to mesh sizing

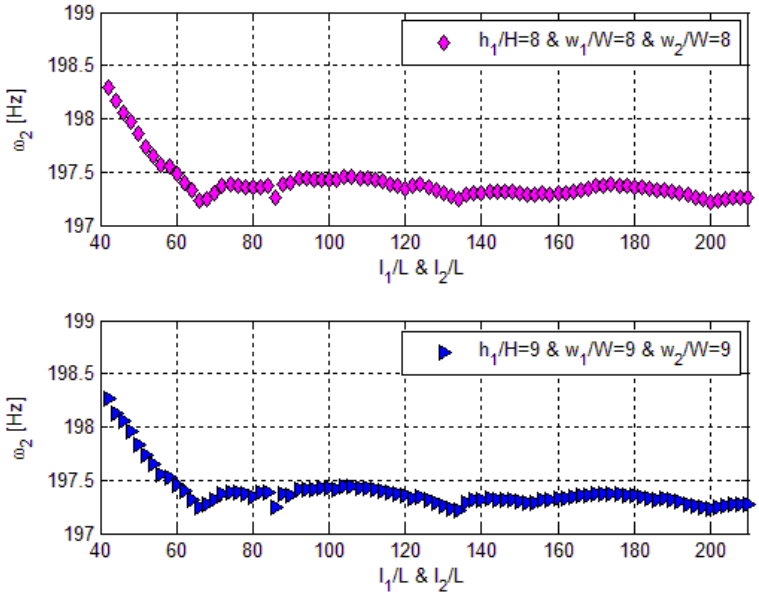

Figure 4.42 Variation of the second natural frequency with respect to mesh sizing

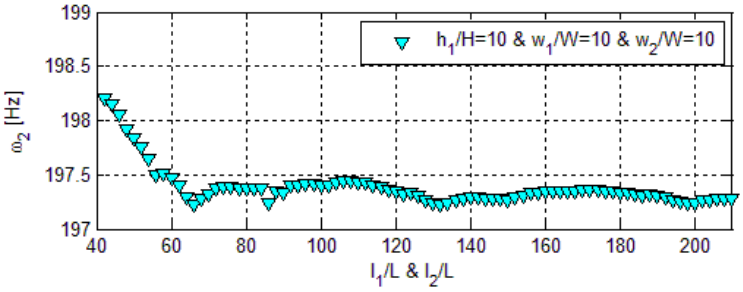

Figure 4.43 Variation of the second natural frequency with respect to mesh sizing

As seen from Figure 4.41, Figure 4.42 and Figure 4.43, the second natural frequency is converged to the frequency band of 197-197.5 Hz, after l_1/L and l_2/L reach to approximately 60-80 range. Finally, the variation of the third natural frequency with respect to mesh sizing parameters is shown in Figure 4.44, Figure 4.45 and Figure 4.46.

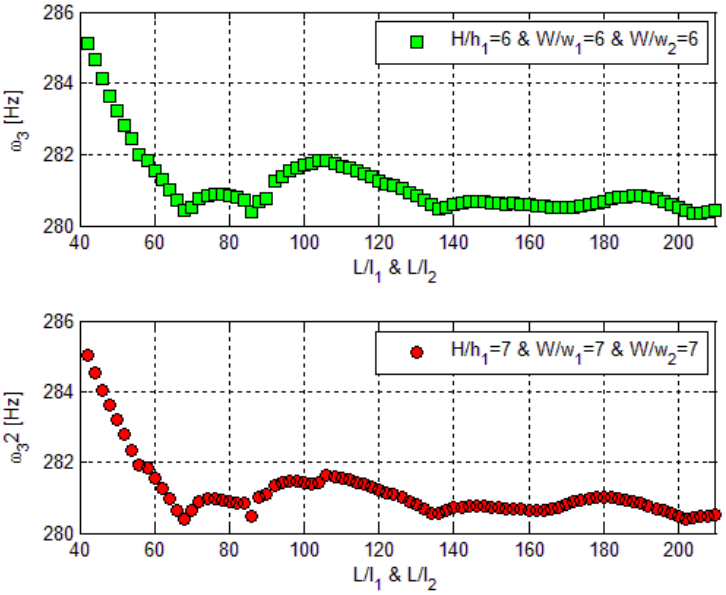

Figure 4.44 Variation of the third natural frequency with respect to mesh sizing

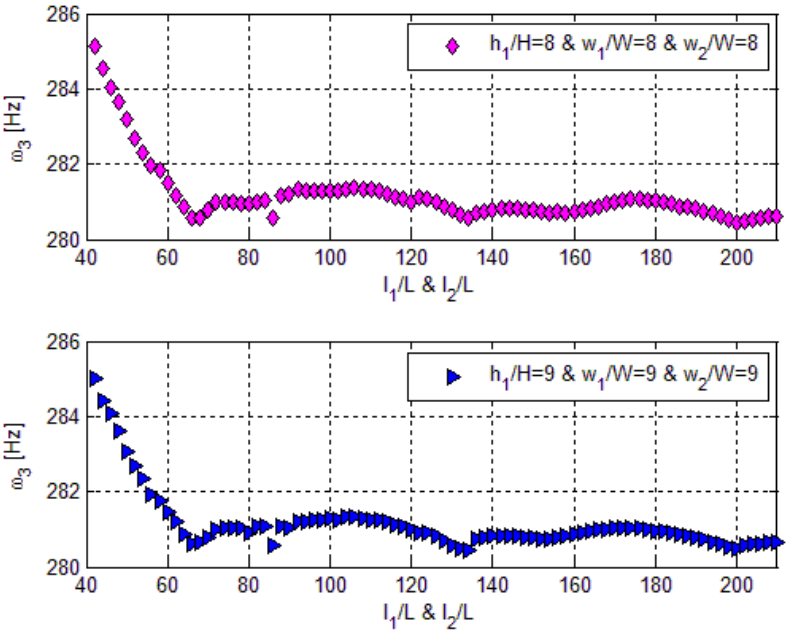

Figure 4.45 Variation of the third natural frequency with respect to mesh sizing

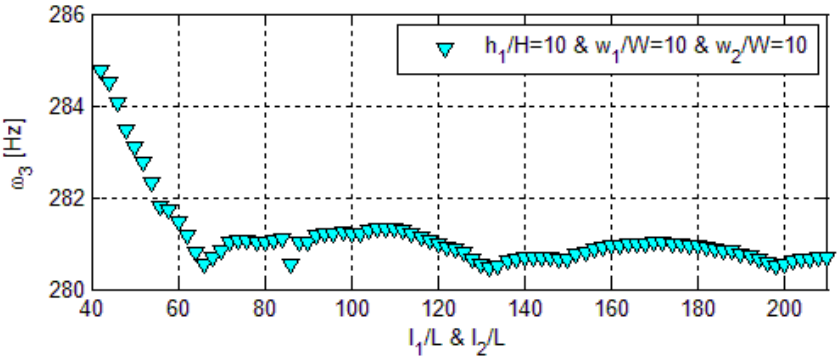

Figure 4.46 Variation of the third natural frequency with respect to mesh sizing

As seen from Figure 4.44, Figure 4.45 and Figure 4.46, the third natural frequency is converged to the frequency band of 280-282 Hz, after l_1/L and l_2/L reach to approximately 60-80 range. From these observations, l_1/L and l_2/L values are kept

approximately in 60-80 range in the mesh sizing of the FE model used in the further analysis.

4.2.4.2 Model Updating of the Test System

In this section, by using the observations made from mesh sensitivity analysis, initial linear FE model of the test system is built in ANSYS and then the linear FE model is updated by using the measured nonlinear FRFs and employing the approach proposed. The linear FE model of the test structure is updated by using the calculated linear FRFs employing first the PRD method and then by using the ANSYS Design Exploration Optimization. In the updating of the FE model, different updating parameter sets are used. For these updating parameter sets, different candidates for the updated FE model are obtained by using ANSYS.

In order to investigate the performance of the updated linear FE models, measured and predicted linear FRFs are compared for all updated FE models. Using the identified nonlinearity and updated FE models, updated nonlinear mathematical models of the test structure are built. Finally, in order to demonstrate the accuracy of the updated nonlinear models of the system, for all the updated nonlinear mathematical models, predicted FRFs of the test structure are compared with the measured FRFs at different forcing levels.

Initial FE model of the test structure is shown in Figure 4.47 and the material properties used for the beams in the initial FE model are the same as the ones used in Section 4.1.5 (Table 4.8).

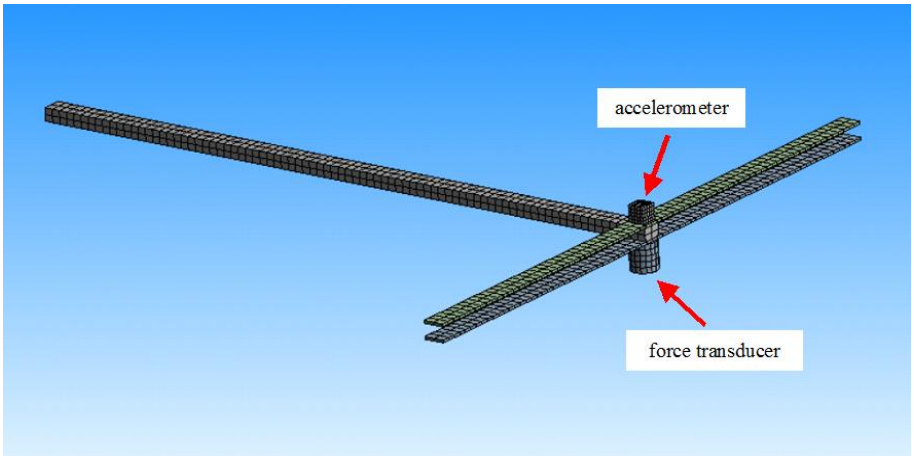

Figure 4.47 FE model of the test structure

In the initial FE model, in order to minimize the modeling errors, accelerometer and force transducer used in the experiments are modeled as rigid masses. Since they are modeled as rigid, modulus of elasticity for the accelerometer and force transducer are taken 10 times larger than the modulus of elasticity of the beams. Mass values are obtained from the datasheet of the accelerometer and force transducer. These values are given in Table 4.14.

Table 4.14 Mass of the accelerometer and force transducer

Transducer Type		**Mass (gr)**
Force Transducer	Brüel&Kjaer Type 8230-002	30.2
Accelerometer	Brüel&Kjaer Type 4507B	4.8

The first three natural frequency of the global modes of the structure and the driving point FRFs at the tip of beam 1 in Z (transverse) direction are calculated by performing modal analysis in ANSYS. Comparisons of the natural frequencies obtained from FE analysis with those obtained from experiments by using PRD method are given in Table 4.15. Linear FRFs obtained from measured nonlinear

FRFs by using PRD method are compared with linear FRFs obtained from FE analysis. This comparison is shown in Figure 4.48.

Table 4.15 Comparison of the first three natural frequencies obtained from initial FE model with those obtained from measured nonlinear FRFs by using PRD method

Mode Number	Natural Frequency (PRD Method) (Hz)	Natural Frequency (Initial FE Model) (Hz)	Error (%)
1	40.75	41.4	1.595
2	178	193.3	8.596
3	260.5	266.0	2.115

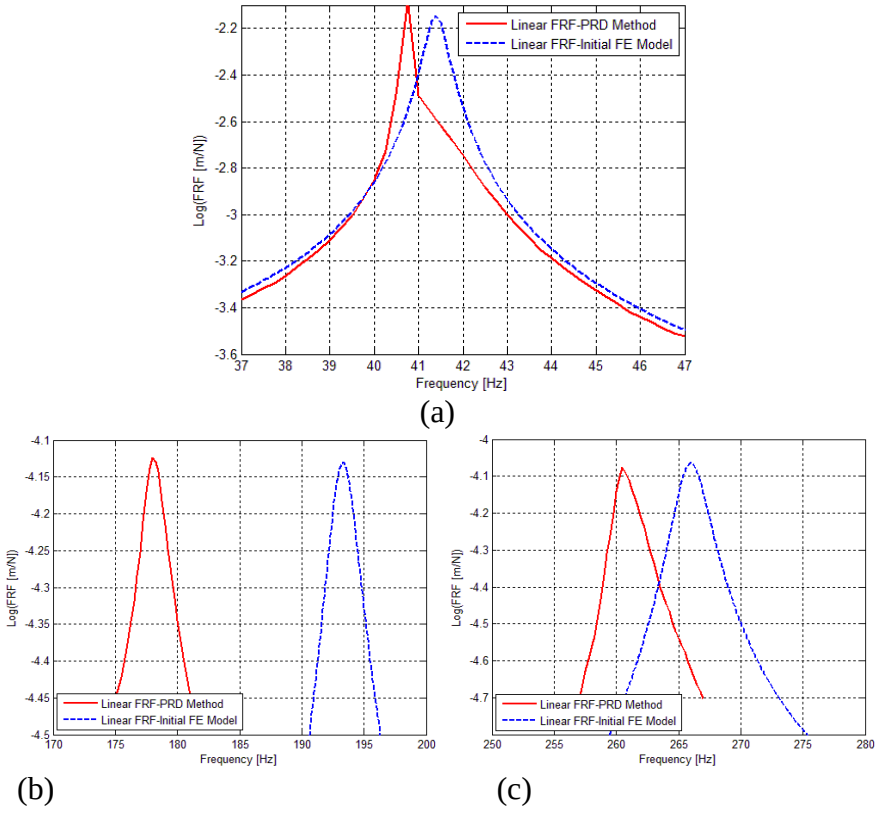

Figure 4.48 Comparison of the linear FRFs obtained from initial FE model with those obtained by using PRD method for the (a) first mode (b) second mode (c) third mode

As can be seen in Table 4.15 and Figure 4.48, there are considerable discrepancies between the results; therefore it is necessary to update the FE model of the test structure.

As an updating parameter set, two sets of parameters are selected. In the first set, modulus of elasticity (E), height of beam 1 (h1), height of beam 2 (h2) are selected as updating parameters, in the second set, modulus of elasticity (E), height of beam 2 (h2), width of beam 1 (w1) are selected as updating parameters. Since most of the uncertainty is generally in modulus of elasticity of the materials, this parameter exists in both of the parameter sets. Furthermore variation in the height of beam (h2) has a considerable effect on the natural frequencies; this parameter also exists in both of the parameter sets. Using these parameter sets, FE model of the structure is updated by employing ANSYS Design Exploration Optimization.

Based on manufacturing tolerances and variation of modulus of elasticity of St37, the bounds given Table 4.16 are defined for the parameters used in the analysis.

Table 4.16 Bounds for the updating parameters

	Modulus of Elasticity (E) (GPa)	**h_2 (mm)**	**h_1 (mm)**	**w_1 (mm)**
Lower Bound	185	1.35	7.7	11.7
Upper Bound	210	1.65	8.3	12.3

For those parameter sets, 5 different updated FE model candidates are calculated by ANSYS.

4.2.4.2.1 Updated FE Model 1

For the updated FE model 1, the updating parameters are calculated as given in Table 4.17.

Table 4.17 Updating parameters for updated FE model 1

Modulus of Elasticity (E) (GPa)	**h_2 (mm)**	**h_1 (mm)**
189.4	1.600	7.727

Using these parameter values, the first three natural frequencies of the updated linear model are calculated. The comparisons of the results with those of initial FE model, as well as with the natural frequencies obtained from experiments by using PRD method are given in Table 4.18.

Table 4.18 Comparison of the first three natural frequencies obtained from initial and updated FE models with experimental values obtained by using PRD method

Mode Number	**Natural Frequency (PRD Method) (Hz)**	**Natural Frequency (Initial FE Model) (Hz)**	**Error (%)**	**Natural Frequency (Updated FE Model 1) (Hz)**	**Error (%)**
1	40.75	41.4	1.595	40.76	0.025
2	178	193.3	8.596	178.69	0.389
3	260.5	266.0	2.115	268.07	2.907

As can be seen in Table 4.18, the first and second natural frequencies are very accurately estimated by using the updated FE model. However for the third natural frequency, updated model gave poor results.

In Figure 4.49, the linear FRFs calculated from experimentally measured nonlinear FRFs by using PRD method are compared with those obtained from initial and updated FE models. As can be seen in Figure 4.49, there is a considerable improvement for the first and second modes of the structure when updated FE model is used.

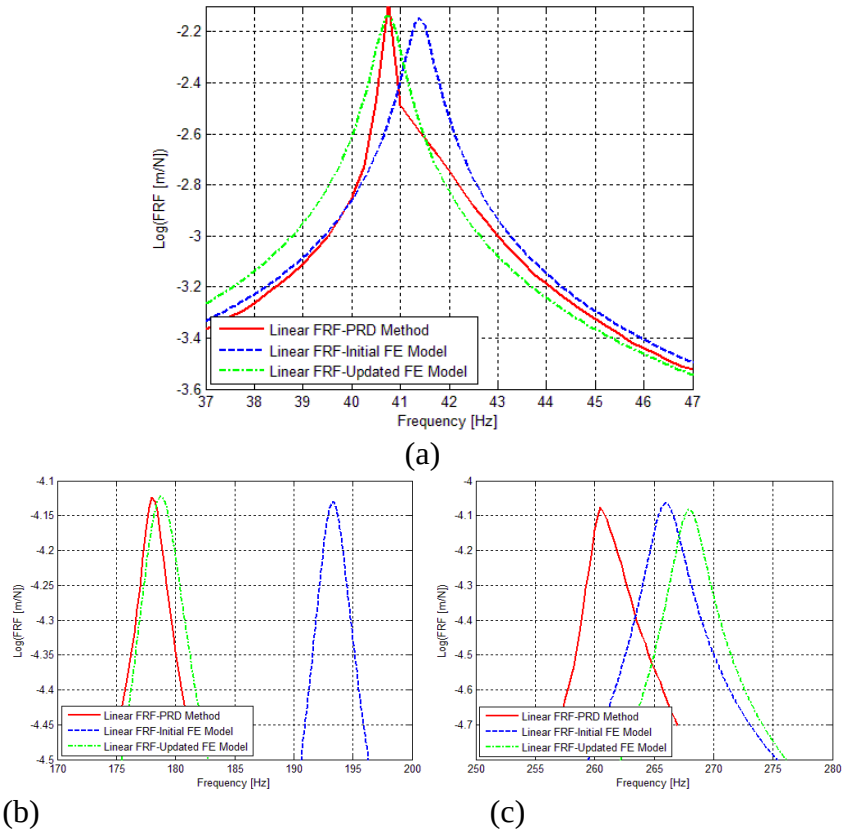

Figure 4.49 Comparison of the linear FRFs obtained from experimentally measured values by using PRD method, with those calculated from initial and updated FE models for (a) first mode (b) second mode (c) third mode

4.2.4.2.2 Updated FE Model 2

For the updated FE model 2, the updating parameters are calculated as given in Table 4.19.

Table 4.19 Updating parameters for updated FE model 2

Modulus of Elasticity (E) (GPa)	**h_2 (mm)**	**h_1 (mm)**
186.9	1.596	7.826

Using these parameter values, the first three natural frequencies of the updated linear model are calculated. The comparisons of the results with those of initial FE model, as well as with the natural frequencies obtained from experiments by using PRD method are given in Table 4.20.

Table 4.20 Comparison of the first three natural frequencies obtained from initial and updated FE models with experimental values obtained by using PRD method

Mode Number	**Natural Frequency (PRD Method) (Hz)**	**Natural Frequency (Initial FE Model) (Hz)**	**Error (%)**	**Natural Frequency (Updated FE Model 2) (Hz)**	**Error (%)**
1	40.75	41.4	1.595	40.57	-0.434
2	178	193.3	8.596	179.66	0.932
3	260.5	266.0	2.115	265.70	1.996

As can be seen in Table 4.20, there is a considerable improvement in the first and second natural frequencies and a slight improvement in the third natural frequency when the updated FE model is used.

In Figure 4.50, the linear FRFs calculated from experimentally measured nonlinear FRFs by using PRD method are compared with those obtained from initial and updated FE models. As can be seen in Figure 4.50, considerable improvement is obtained for the first and second modes of the structure when updated FE model is used. However for the third mode, almost no improvement is obtained.

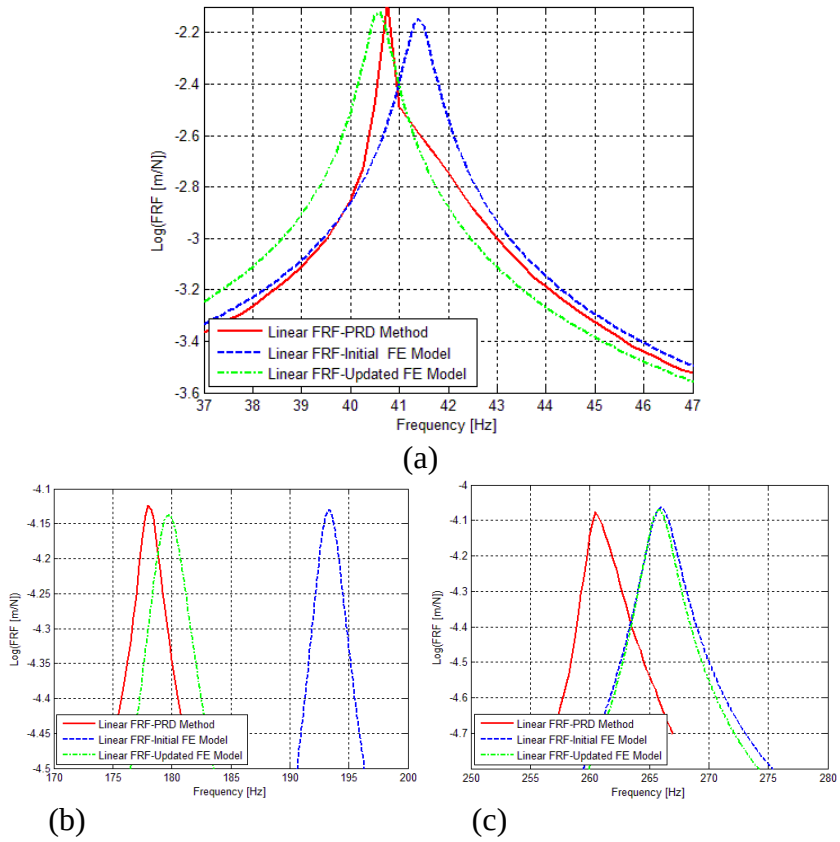

Figure 4.50 Comparison of the linear FRFs obtained from experimentally measured values by using PRD method, with those calculated from initial and updated FE models for (a) first mode (b) second mode (c) third mode

4.2.4.2.3 Updated FE Model 3

For the updated FE model 3, the updating parameters are calculated as given in Table 4.21.

Table 4.21 Updating parameters for updated FE model 3

Modulus of Elasticity (E) (GPa)	**h_2 (mm)**	**h_1 (mm)**
193.6	1.559	7.726

Using these parameter values, the first three natural frequencies of the updated linear model are calculated. The comparisons of the results with those of initial FE model, as well as with the natural frequencies obtained from experiments by using PRD method are given in Table 4.22.

Table 4.22 Comparison of the first three natural frequencies obtained from initial and updated FE models with experimental values obtained by using PRD method

Mode Number	**Natural Frequency (PRD Method) (Hz)**	**Natural Frequency (Initial FE Model) (Hz)**	**Error (%)**	**Natural Frequency (Updated FE Model 3) (Hz)**	**Error (%)**
1	40.75	41.4	1.595	40.39	-0.894
2	178	193.3	8.596	180.32	1.304
3	260.5	266.0	2.115	264.24	1.437

As can be seen in Table 4.22, there is a considerable improvement in the second natural frequency. Also the error for the first natural frequency decreased to the half of its initial value. Furthermore a better estimate is obtained for the the third natural frequency when the updated FE model is used.

In Figure 4.51, the linear FRFs calculated from experimentally measured nonlinear FRFs by using PRD method are compared with those obtained from initial and updated FE models. As can be seen in Figure 4.51, considerable improvement is obtained for the second mode of the structure when updated FE model is used. However, for the first and third modes, the improvement is less compared to the improvement in the second mode.

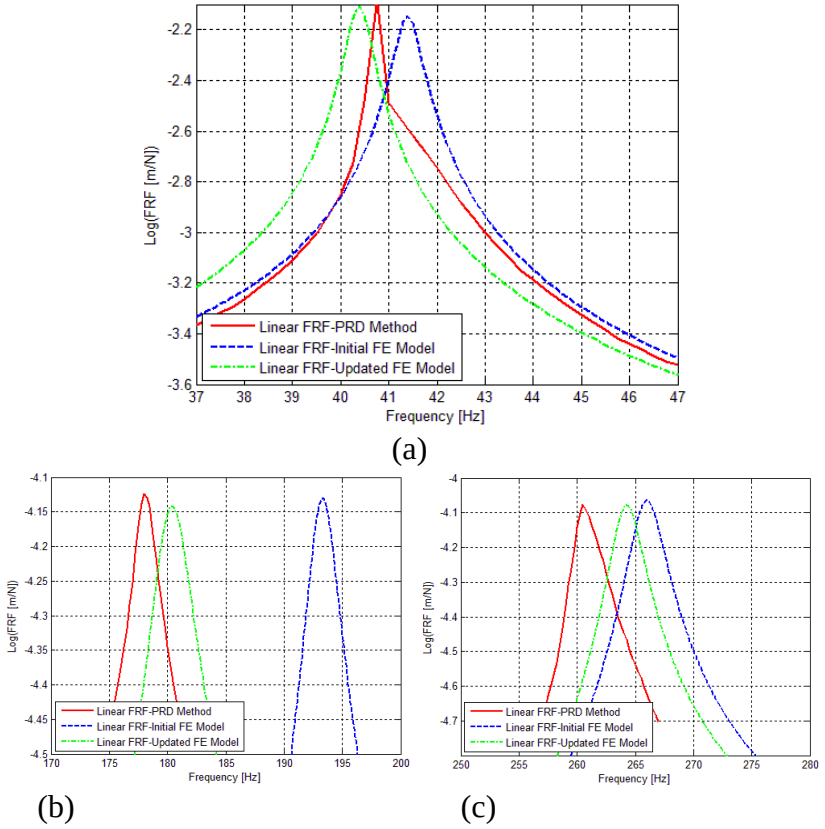

Figure 4.51 Comparison of the linear FRFs obtained from experimentally measured values by using PRD method, with those calculated from initial and updated FE models for (a) first mode (b) second mode (c) third mode

4.2.4.2.4 Updated FE Model 4

For the updated FE model 4, the updating parameters are calculated as given in Table 4.23.

Table 4.23 Updating parameters for updated FE model 4

Modulus of Elasticity (E) (GPa)	**h_2 (mm)**	**w_1 (mm)**
185.3	1.594	11.868

Using these parameter values, the first three natural frequencies of the updated linear model are calculated. The comparisons of the results with those of initial FE model, as well as with the natural frequencies obtained from experiments by using PRD method are given in Table 4.24.

Table 4.24 Comparison of the first three natural frequencies obtained from initial and updated FE models with experimental values obtained by using PRD method

Mode Number	**Natural Frequency (PRD Method) (Hz)**	**Natural Frequency (Initial FE Model) (Hz)**	**Error (%)**	**Natural Frequency (Updated FE Model 4) (Hz)**	**Error (%)**
1	40.75	41.4	1.595	40.64	-0.258
2	178	193.3	8.596	182.60	2.582
3	260.5	266.0	2.115	264.54	1.550

As can be seen in Table 4.24, there is a considerable improvement in the first natural frequency. Also the error for the second natural frequency decreased considerably. Furthermore a better estimate is obtained for the the third natural frequency when the updated FE model is used.

In Figure 4.52, the linear FRFs calculated from experimentally measured nonlinear FRFs by using PRD method are compared with those obtained from initial and updated FE models. As can be seen in Figure 4.52, considerable improvement is obtained for the first mode of the structure when updated FE model is used. However, for the second and third modes, the improvement is less compared to the improvement in the first mode.

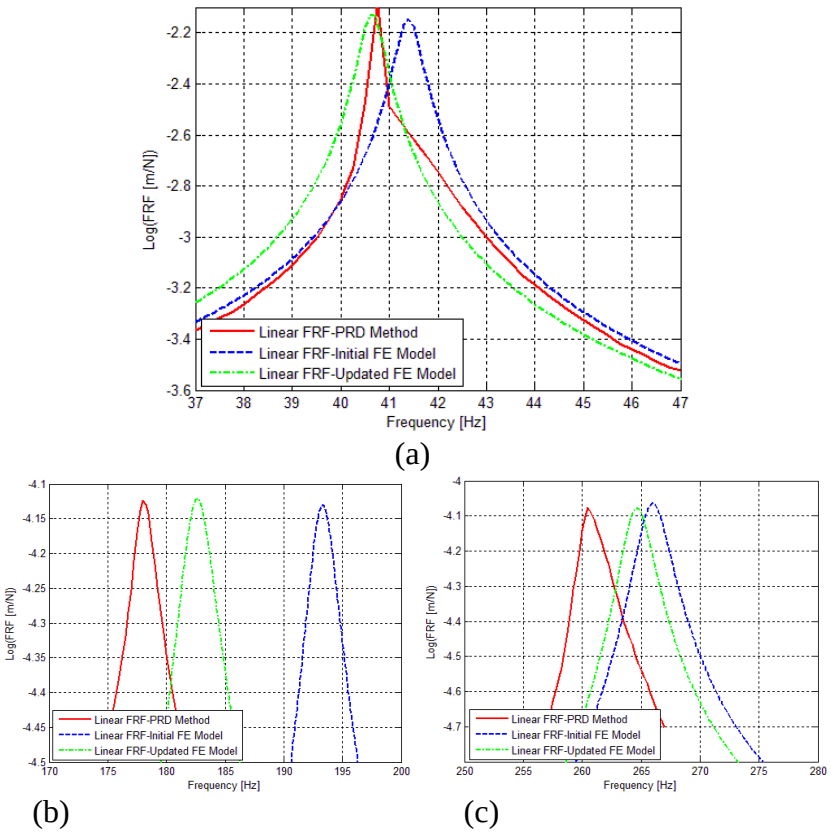

Figure 4.52 Comparison of the linear FRFs obtained from experimentally measured values by using PRD method, with those calculated from initial and updated FE models for (a) first mode (b) second mode (c) third mode

4.2.4.2.5 Updated FE Model 5

For the updated FE model 5, the updating parameters are calculated as given in Table 4.25.

Table 4.25 Updating parameters for updated FE model 5

Modulus of Elasticity (E) (GPa)	**h_2 (mm)**	**w_1 (mm)**
190.5	1.551	12.124

Using these parameter values, the first three natural frequencies of the updated linear model are calculated. The comparisons of the results with those of initial FE model, as well as with the natural frequencies obtained from experiments by using PRD method are given in Table 4.26.

Table 4.26 Comparison of the first three natural frequencies obtained from initial and updated FE models with experimental values obtained by using PRD method

Mode Number	**Natural Frequency (PRD Method) (Hz)**	**Natural Frequency (Initial FE Model) (Hz)**	**Error (%)**	**Natural Frequency (Updated FE Model 5) (Hz)**	**Error (%)**
1	40.75	41.4	1.595	40.38	-0.914
2	178	193.3	8.596	184.72	3.774
3	260.5	266.0	2.115	261.26	0.293

As can be seen in Table 4.26, there is a considerable improvement for the third natural frequency. However, improvement is less in the first and second natural frequencies when the updated FE model is used

In Figure 4.53, the linear FRFs calculated from experimentally measured nonlinear FRFs by using PRD method are compared with those obtained from initial and updated FE models. As can be seen in Figure 4.53, considerable improvement is obtained for the third mode of the structure when updated FE model is used. However, for the first and second modes, the improvement is less compared to the improvement in the third mode.

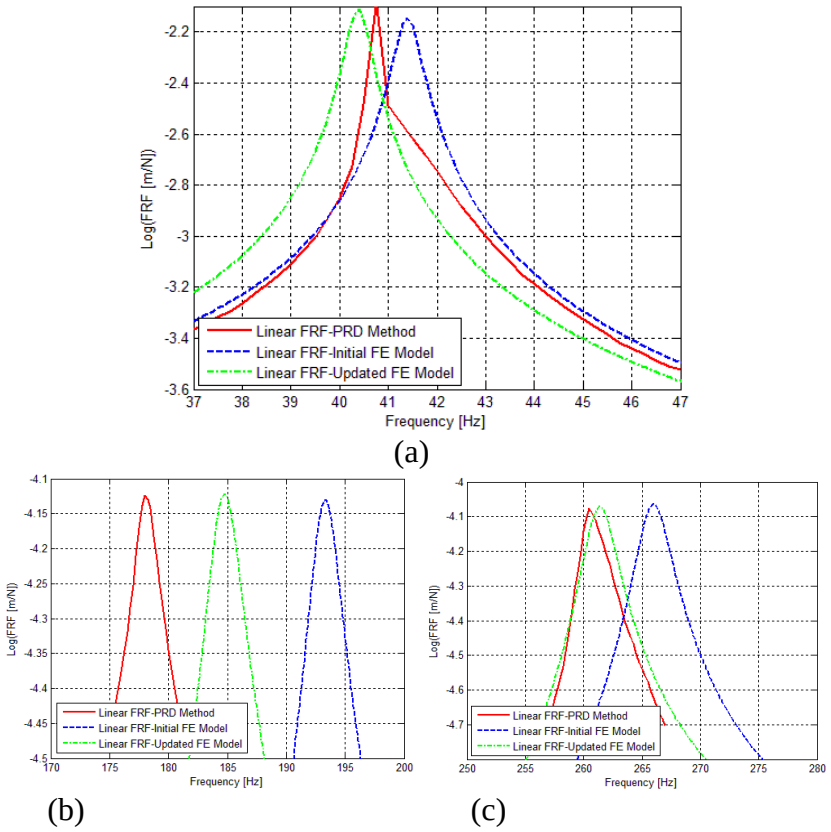

Figure 4.53 Comparison of the linear FRFs obtained from experimentally measured values by using PRD method, with those calculated from initial and updated FE models for (a) first mode (b) second mode (c) third mode

4.2.4.2.6 Comparison of the Updated FE Models

In this section, each of natural frequencies and FRFs obtained by the updated FE models are compared to each other as well as with those of initial FE model, and also with the ones obtained from measured nonlinear FRFs by using PRD method.

In Table 4.27, the first natural frequencies obtained from each updated linear model are compared with each other as well as with that of initial FE model. The natural frequency obtained from measured nonlinear FRFs by using PRD method are also given in the same table.

Table 4.27 Comparison of the first natural frequency obtained from initial and updated FE models with experimental value obtained by using PRD method

Natural Frequency (PRD Method) (Hz)	**Natural Frequency (Initial FE Model) (Hz)**	**Error (%)**	**Updated FE Models**	**Natural Frequency (Hz)**	**Error (%)**
40.75	41.4	1.595	Updated FE model 1	40.76	0.025
			Updated FE model 2	40.57	-0.434
			Updated FE model 3	40.39	-0.894
			Updated FE model 4	40.64	-0.258
			Updated FE model 5	40.38	-0.914

As can be seen from Table 4.27, updated model 1 gives the best value and the updated model 5 gives the worst value for the first natural frequency. In Figure 4.54, the linear FRFs obtained by using PRD method from experimentally measured nonlinear FRFs are compared with those calculated from initial and updated FE models.

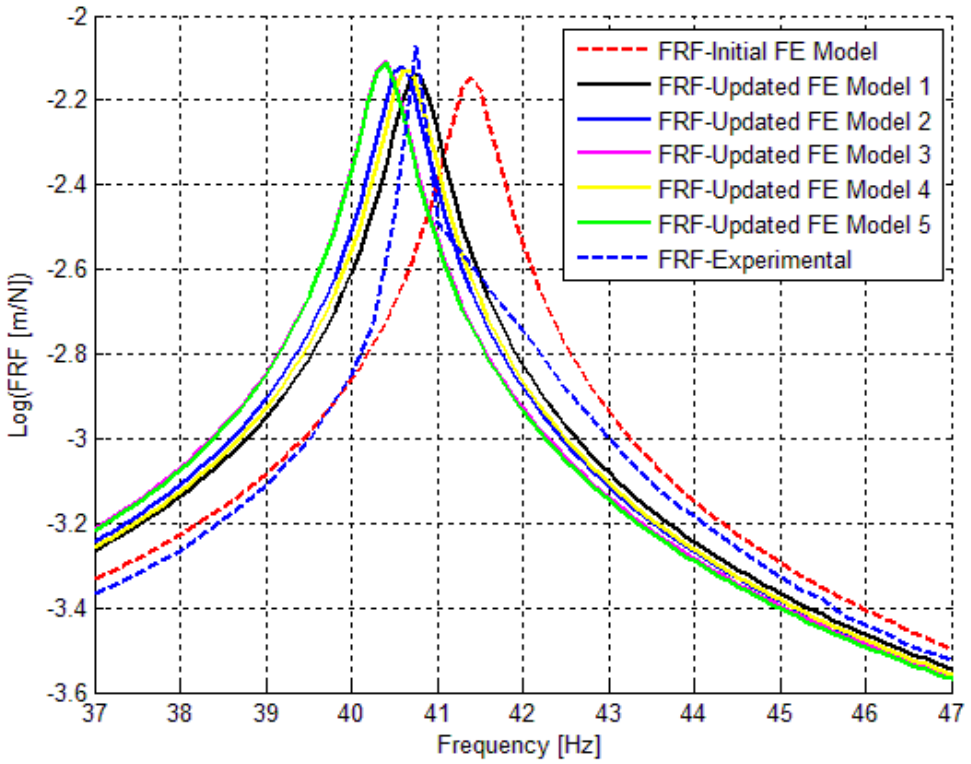

Figure 4.54 Comparison of the linear FRFs obtained from experimentally measured nonlinear FRFs by using PRD method, with those calculated from initial and updated FE models

As can be seen from Figure 4.54, similar conclusions can be obtained for linear FRFs as well. That is, updated model 1 is the best as far as the linear FRF prediction is concerned.

The second and third natural frequencies of the updated linear models are compared with each other as well as with those of the initial FE model. The second and third natural frequencies obtained from measured nonlinear FRFs by using PRD method are also given in Table 4.28 and Table 4.29, respectively.

Table 4.28 Comparison of the second natural frequency obtained from initial and updated FE models with experimental value obtained by using PRD method

Natural Frequency (PRD Method) (Hz)	Natural Frequency (Initial FE Model) (Hz)	Error (%)	Updated FE Models	Natural Frequency (Hz)	Error (%)
178	193.3	8.596	Updated FE model 1	178.69	0.389
			Updated FE model 2	179.66	0.932
			Updated FE model 3	180.32	1.304
			Updated FE model 4	182.60	2.582
			Updated FE model 5	184.72	3.774

Table 4.29 Comparison of the third natural frequency obtained from initial and updated FE models with experimental value obtained by using PRD method

Natural Frequency (PRD Method) (Hz)	Natural Frequency (Initial FE Model) (Hz)	Error (%)	Updated FE Models	Natural Frequency (Hz)	Error (%)
260.5	266.0	2.115	Updated FE model 1	268.07	2.907
			Updated FE model 2	265.70	1.996
			Updated FE model 3	264.24	1.437
			Updated FE model 4	264.54	1.550
			Updated FE model 5	261.26	0.293

As can be seen from Table 4.28, updated model 1 gives the best value, and the updated model 5 gives the worst value for the second natural frequency. However it is observed from Table 4.29 that updated model 5 gives the best value, and the updated model 1 gives the worst value for the third natural frequency.

In Figure 4.55, the linear FRFs obtained by using PRD method from experimentally measured nonlinear FRFs are compared with those calculated from initial and updated FE models.

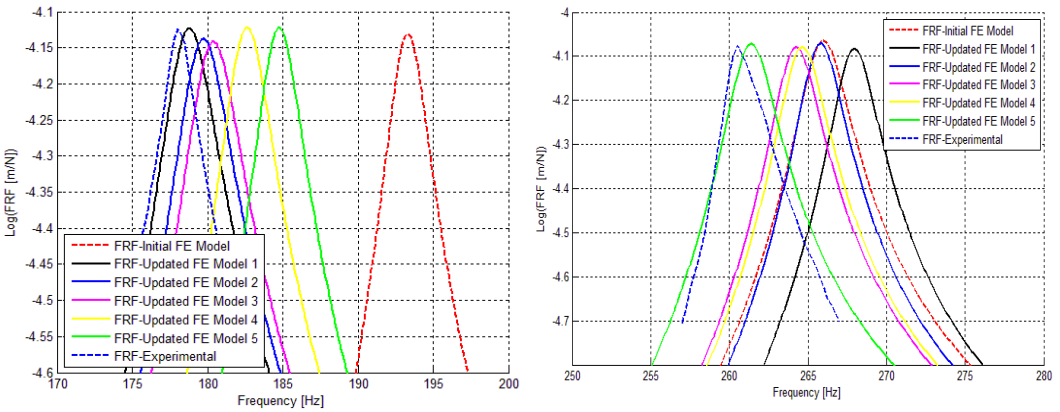

(a) (b)

Figure 4.55 Comparison of the linear FRFs obtained from experimentally measured nonlinear FRFs by using PRD method, with those calculated from initial and updated FE models for (a) second mode (b) third mode

As can be seen from Figure 4.55, similar conclusions can be obtained for linear FRFs as well. That is, updated model 1 is the best in the second mode and updated model 5 is the best in the third mode, as far as the linear FRF predictions are concerned.

Since the ultimate goal is to have accurate nonlinear response predictions from the updated model, nonlinear FRFs measured experimentally for F=0.6N, F=0.7N and F=0.8N are compared with those obtained from the initial and updated models (composed of original and updated FE models combined with identified nonlinearity). The results are given in Figure 4.56, Figure 4.57 and Figure 4.58, for the first, second and third modes of the structure, respectively.

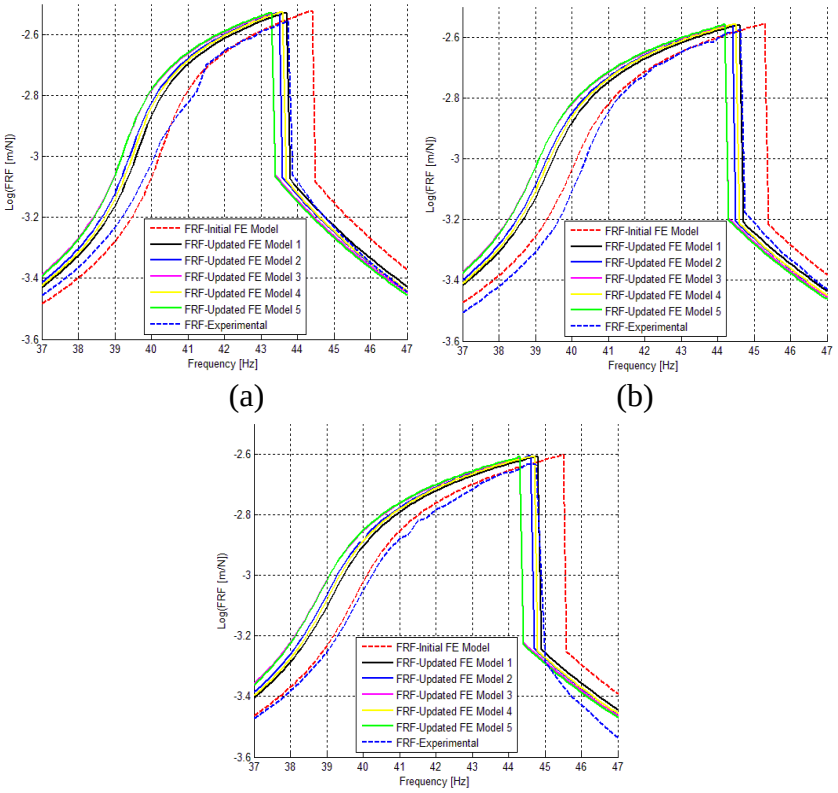

(a) (b)

(c)

Figure 4.56 Comparison of FRFs obtained from initial and updated models with the experimental ones for (a) F=0.6N (b) F=0.7N (c) F=0.8N

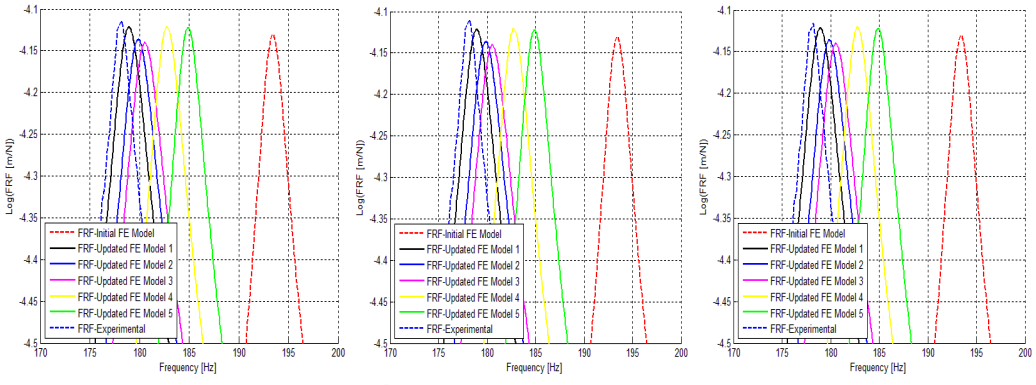

(a) (b) (c)

Figure 4.57 Comparison of FRFs obtained from initial and updated models with the experimental ones for (a) F=0.6N (b) F=0.7N (c) F=0.8N

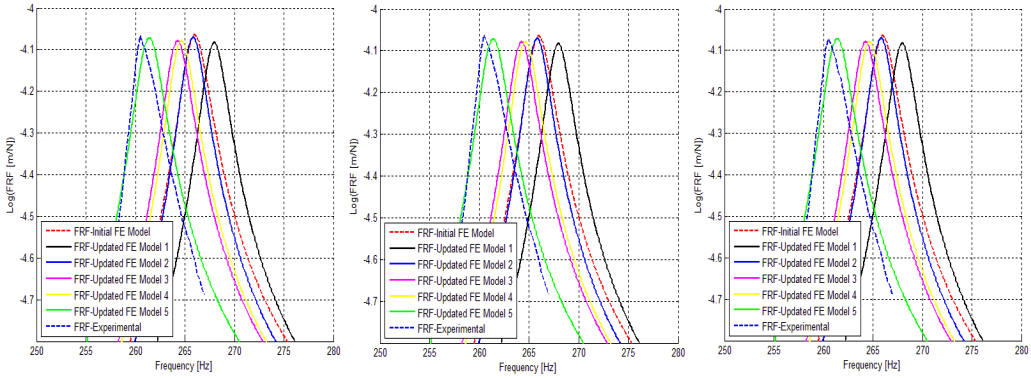

(a) (b) (c)

Figure 4.58 Comparison of FRFs obtained from initial and updated models with the experimental ones for (a) F=0.6N (b) F=0.7N (c) F=0.8N

For the first mode, as can be seen in Figure 4.56, the best match between measured and predicted FRFs is observed when the updated model 1 is used. For the second mode, as can be seen in Figure 4.57, again the updated model 1 gives the best prediction. However, as observed from Figure 4.58, updated model 5 gives the best predictions for nonlinear FRFs around third mode of the structure. From these results we can conclude that depending on the candidate updating parameter sets, best response prediction may vary. Therefore, it is recommended to construct different updated models, and choose the one which represents the actual system in the mode(s) we are interested in, or give priority to.

CHAPTER 5

MODEL UPDATING OF A NONLINEAR GUN BARREL OF A BATTLE TANK

Predicting the dynamic behavior of the tip of a gun barrel especially at the fundamental mode is critical when the shooting and stabilization performance of the tank is considered. In this perspective, detailed model of the gun barrel at the fundamental mode is studied in this chapter. The method developed for model updating of nonlinear systems is applied to a gun barrel of a battle tank. An equivalent single degree of freedom nonlinear model of the system is built for the fundamental mode of system. First, using the PRD method, both linear FRFs and the nonlinearities in the system are obtained from experimentally measured nonlinear FRFs. Afterwards, linear FE model of the test structure is built in ANSYS and it is updated by using the linear FRFs obtained through the PRD method. Thus, an updated nonlinear model of the test structure is constructed by using the identified nonlinearity and updated linear FE model of the system. Finally, predicted and measured FRFs of the test structure are compared at different forcing levels in order to demonstrate the accuracy of the updated nonlinear model of the system. Furthermore, in order to compare the performance of PRD method with that of DDF method, both linear FRFs and the nonlinearities in the system are also obtained by using the DDF method.

5.1 Experimental Setup

The test set-up, which consists of the gun barrel of a battle tank, is shown in Figure 5.1.

Figure 5.1 Gun barrel test setup

In the experiments performed in this study, the structure is excited with B&K Type 4808 modal shaker via a push-rod. In order to increase the excitation level of the shaker, B&K Type 2712 power amplifier is used. Acceleration responses and the forces applied are measured with B&K Type 4507B accelerometer and B&K Type 8230-002 force transducer, respectively. In all the measurements, as a data acquisition system, B&K Type 3560C frontend is used. The equipment used in the experiments is given in Table 5.1 and it is shown in Figure 5.2.

Table 5.1 Equipment used in the experiments

Data Acquisition System	Brüel&Kjaer Type 3560 C Frontend
Shaker	Brüel&Kjaer Type 4808
Force Transducer	Brüel&Kjaer Type 8230-002
Power Amplifier	Brüel&Kjaer Type 2712
Accelerometer	Brüel&Kjaer 4507B

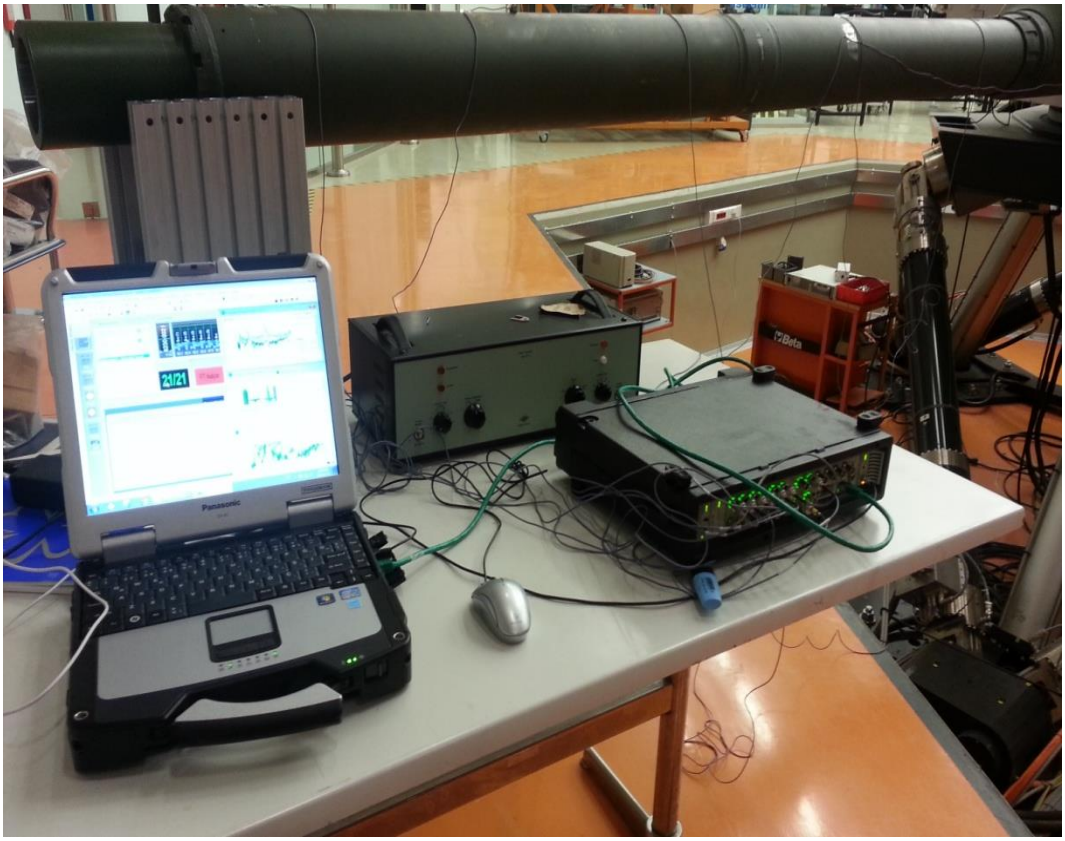

Figure 5.2 Equipment used in the experiments

5.2 First Set of Experiments

In the first set of experiments, the structure is excited with a random force. In random excitation tests, 6 different force levels are used starting from a very low to high forcing levels. Since the accuracy of the PRD method proposed for obtaining linear FRFs and nonlinear identification depends on the excitation frequency and it is shown that when the structure is excited at around the linear resonance frequency of the structure method gives more accurate results, in the first random excitation test low excitation signal level is selected.

In all the random excitation tests, the frequency range is selected between 0-100 Hz and a frequency resolution of 0.0625 Hz is used in measurements. In order to minimize the noise in measurements, 21 averages are taken. In all the random excitation tests, 6 accelerometers are used and the gun barrel is excited with the shaker located at the tip of the gun barrel.

The accelerometer and the shaker locations and geometry constructed in the PULSE software are shown in Figure 5.3.

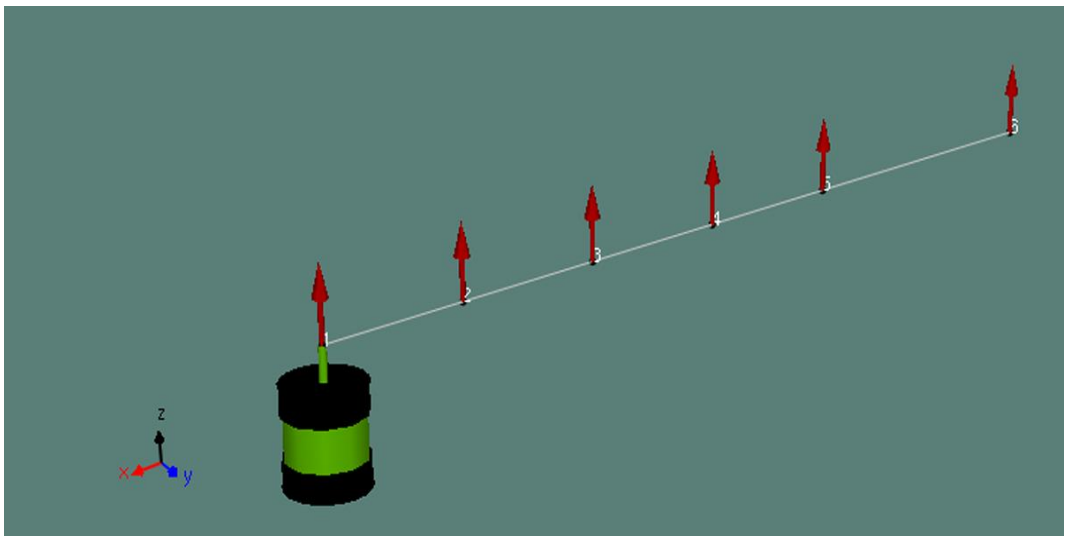

Figure 5.3 Test geometry constructed in PULSE software

The node numbering starts from the tip of gun barrel (node number 1) and continues till the root end of the gun barrel (node number 6) that is accessible from outside of the tank. The shaker is located at node 1 as shown in Figure 5.3.

The force levels used in the random excitation tests are shown in Figure 5.4, and their root mean square (rms) values are given in Table 5.2.

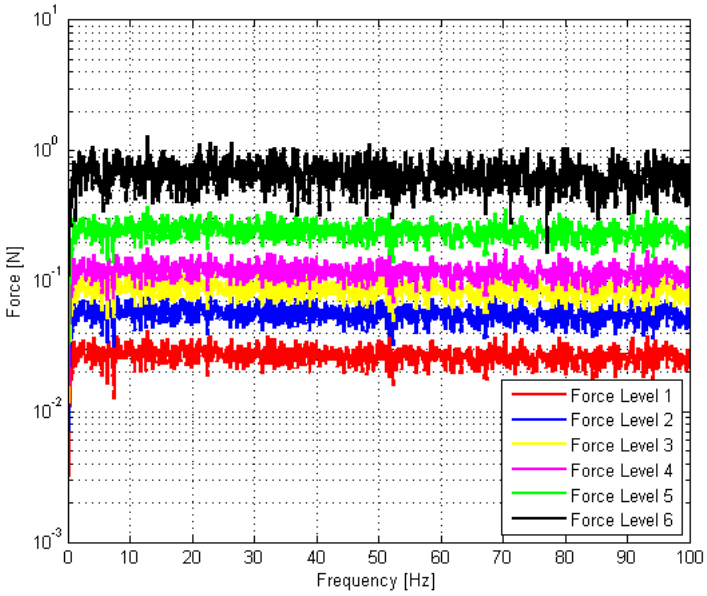

Figure 5.4 Force levels used in random excitation tests

Table 5.2 Force levels used in random excitation tests

Force Level	Rms (N)
1	0.88
2	1.829
3	2.809
4	3.859
5	7.888
6	21.851

For the given excitation levels, FRFs are measured by using B&K Pulse software, the FRF at node 1 (tip of gun barrel) and corresponding coherences are shown in Figure 5.5 and Figure 5.6, respectively.

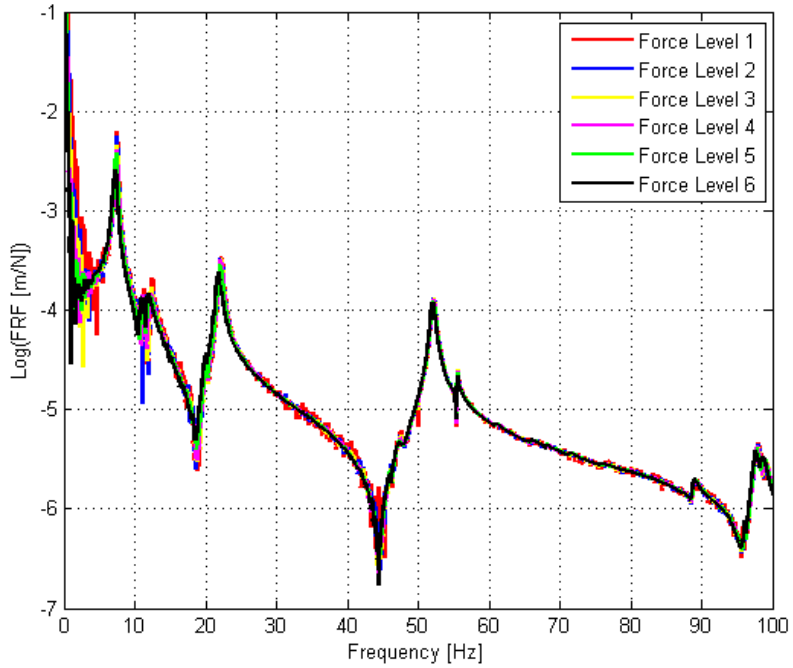

Figure 5.5 Measured FRFs at node 1

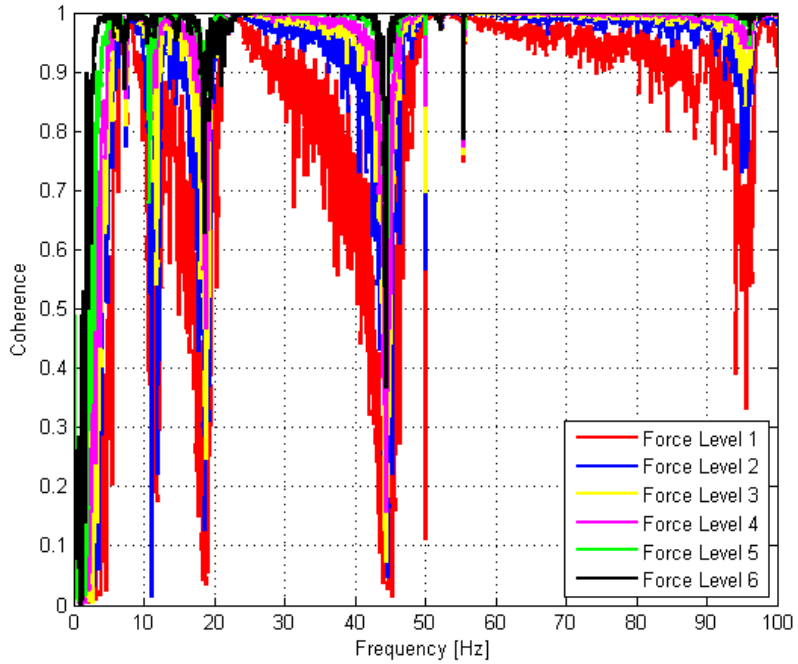

Figure 5.6 Coherence of the FRFs measured at node 1

As the first observation from Figure 5.5, it can be said that FRFs are slightly different for different random excitation force levels. Therefore in order to see differences more clearly, resonance regions are zoomed in and shown in Figure 5.7, Figure 5.8 and Figure 5.9, respectively.

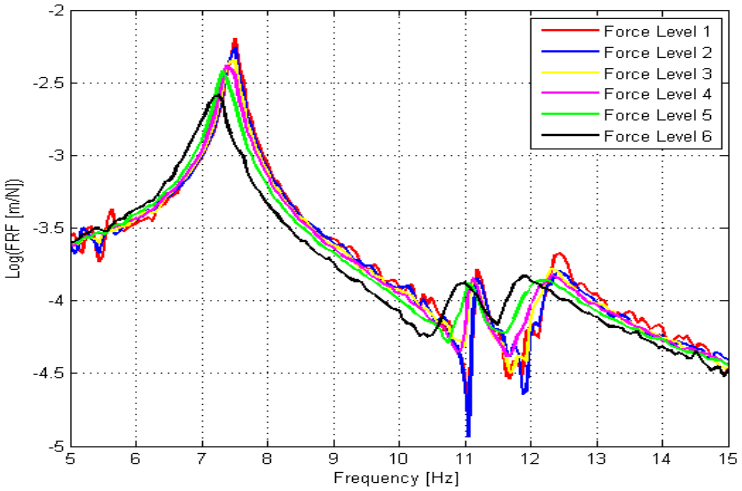

Figure 5.7 Measured FRFs at node 1 between 5-15 Hz

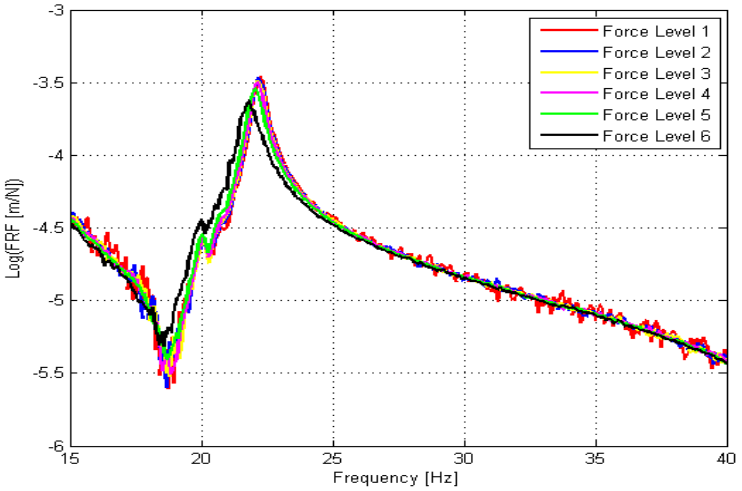

Figure 5.8 Measured FRFs at node 1 between 15-40 Hz

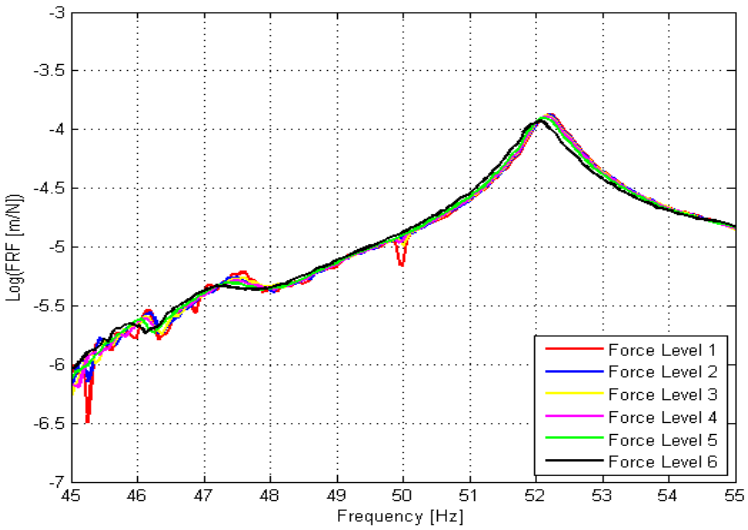

Figure 5.9 Measured FRFs at node 1 between 45-55 Hz

As can be seen from Figure 5.7, Figure 5.8 and Figure 5.9, natural frequencies are shifted when the force level changes. Especially at the fundamental mode of the gun barrel this effect is much more pronounced. These observations give a clear indication of nonlinearity in the structure. In order to see the dynamical characteristic of the gun barrel in more detail, for each of the force levels, modal analysis is performed and the corresponding modal parameters are extracted by using ME'scope modal analysis software.

5.2.1 Modal Analysis of the Gun Barrel for the Random Excitation Force Level 1

After performing the measurements, the modal analysis is performed between 0-55 Hz in ME'scope modal analysis software. By using the stabilization diagram (Figure 5.10) algorithm modal parameters are extracted and they are given in Table 5.3.

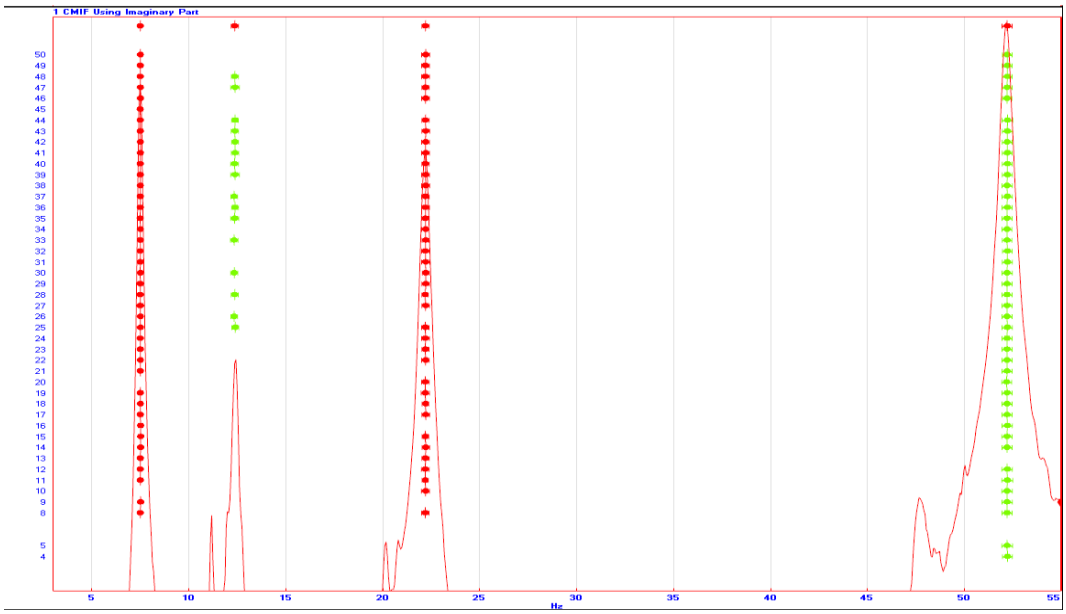

Figure 5.10 Stability diagram

Table 5.3 Extracted modal parameters

Mode Number	Natural Frequency (Hz)	Modal Damping Ratio (%)
1	7.501	0.955
2	12.368	1.531
3	22.203	0.870
4	52.191	0.499

After extracting the modal parameters, FRFs are synthesized and these synthesized FRFs are shown together with the measured FRFs for nodes 1 and 2 in Figure 5.11, and for nodes 3, 4, 5 and 6 in Figure 5.12.

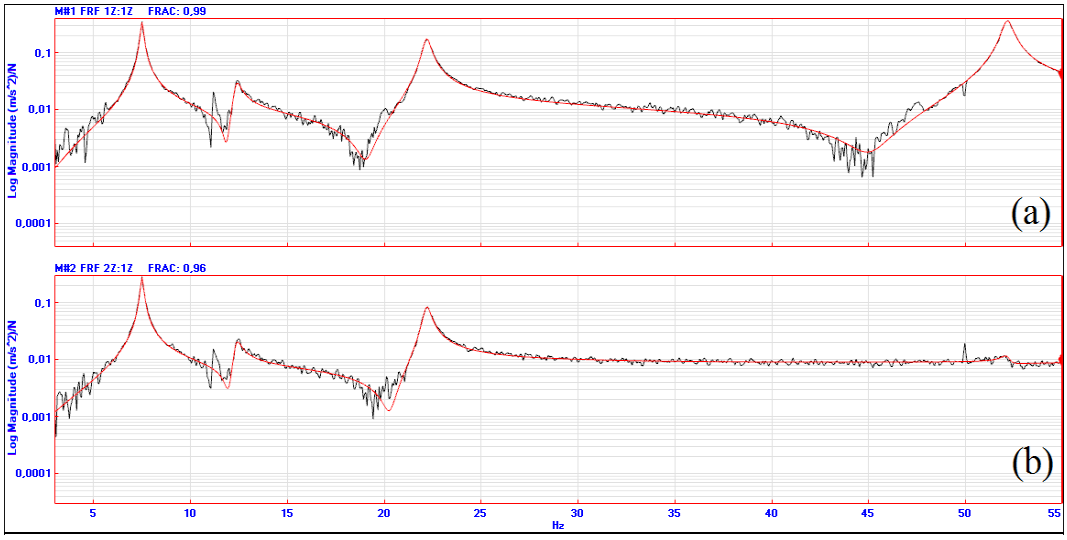

Figure 5.11 Synthesized and measured FRFs at nodes (a) 1 and (b) 2

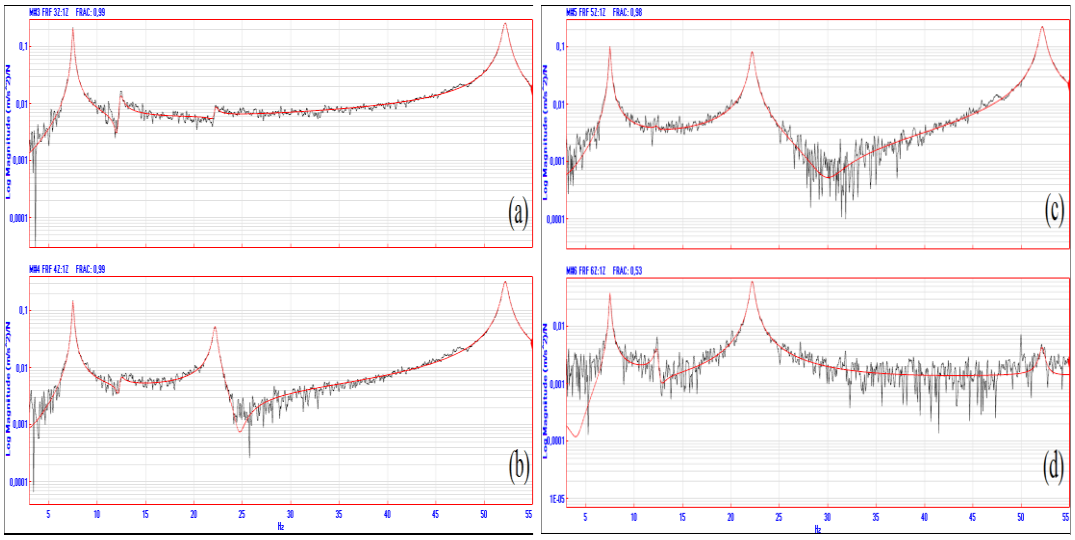

Figure 5.12 Synthesized and measured FRFs at nodes (a) 3, (b) 4, (c) 5 and (d) 6

The modeshapes of the gun barrel are also obtained and they are shown in Figure 5.13.

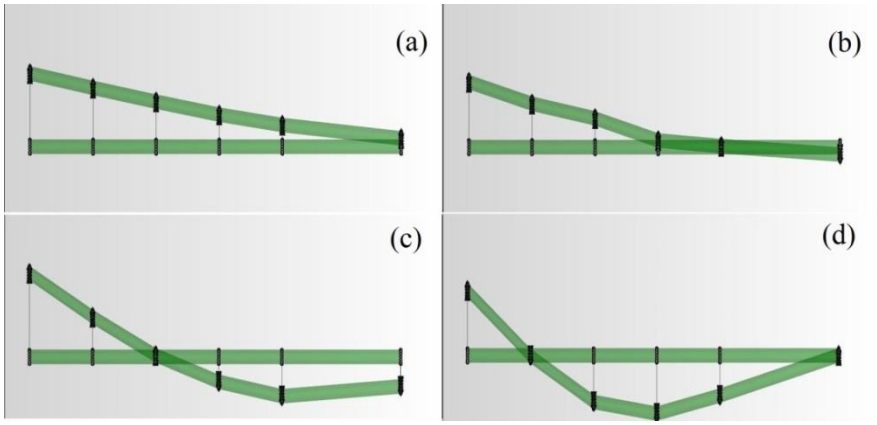

Figure 5.13 (a) First (b) second (c) third (d) fourth modeshapes

When the modeshapes of the gun barrel are studied, the first, second and fourth modes of the structure are found to be dominant modes. Second mode may be related with flexibility of joint at the root however it is not a dominant mode which can be observed from the FRF curves. In order to check the complexity of the modes, complexity plots of modes are drawn and shown in Figure 5.14.

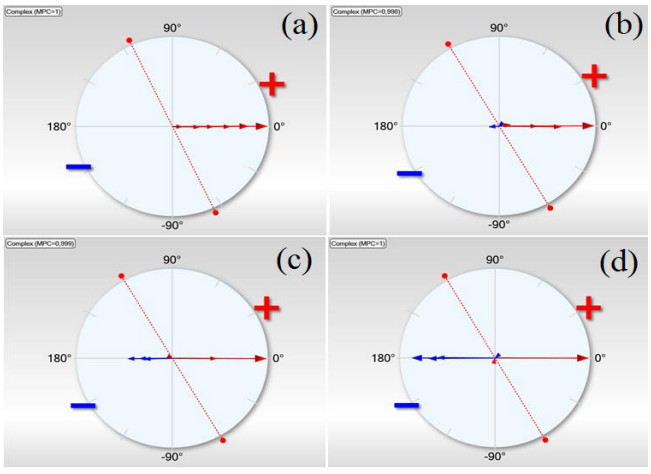

Figure 5.14 Complexity plot of (a) first (b) second (c) third (d) fourth modeshapes

It is observed from the complexity plots that all the modes are almost real since all the modeshape components stand on the horizontal line (0-180 phase angle line) of the complexity plot.

Furthermore, in order to see how the modes are correlated to each other, MAC diagram and the corresponding MAC matrix values are given in Figure 5.15 and in Table 5.4, respectively.

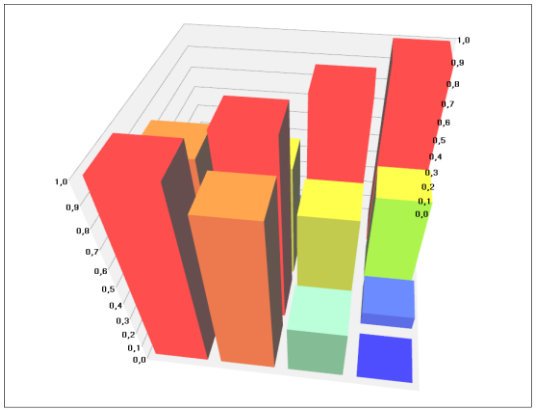

Figure 5.15 MAC diagram

Table 5.4 MAC matrix values

Modeshape	**1**	**2**	**3**	**4**
1	1.0000	0.8760	0.3050	0.0001
2	0.8760	1.0000	0.6520	0.0845
3	0.3050	0.6520	1.0000	0.5350
4	0.0001	0.0845	0.5350	1.0000

As seen from MAC matrix, second modeshape is very similar to first and third modehaspes of the structure.

5.2.2 Modal Analysis of the Gun Barrel for the Random Excitation Force Level 2

Similarly, by using the stabilization diagram (Figure 5.16) algorithm, modal parameters are extracted for this modal test and they are given in Table 5.5.

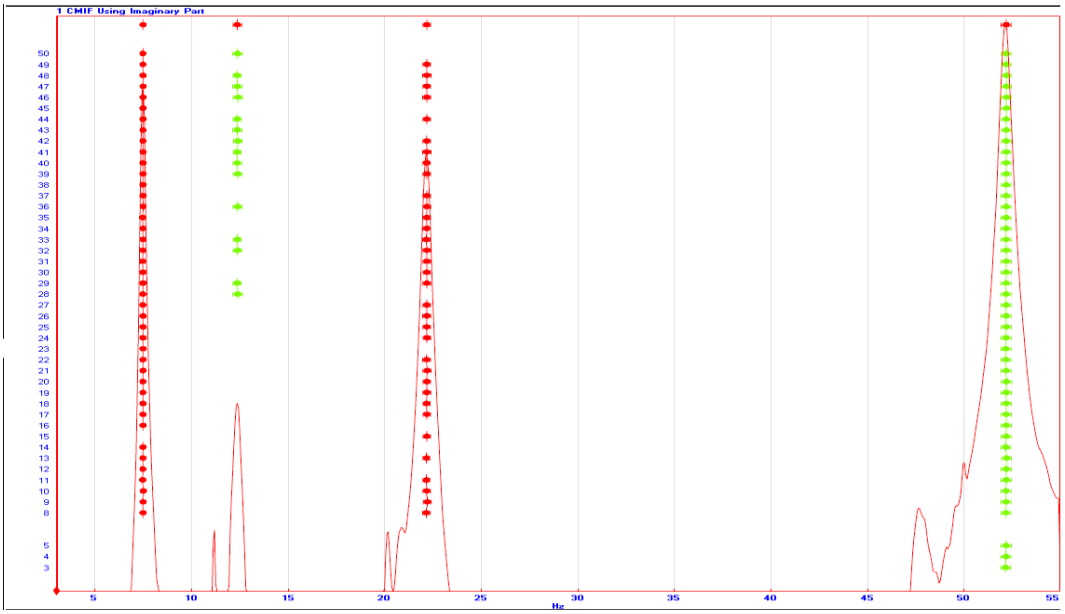

Figure 5.16 Stability diagram

Table 5.5 Extracted modal parameters

Mode Number	Natural Frequency (Hz)	Modal Damping Ratio (%)
1	7.473	1.033
2	12.364	1.837
3	22.169	0.903
4	52.174	0.496

After extracting the modal parameters, FRFs are synthesized and these synthesized FRFs are shown together with the measured FRFs for nodes 1 and 2 in Figure 5.17, and for nodes 3, 4, 5 and 6 in Figure 5.18.

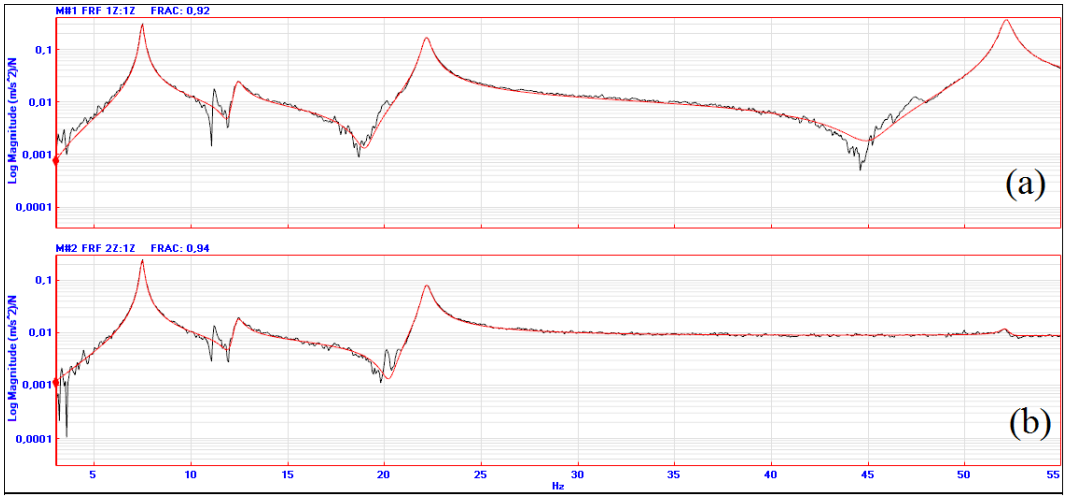

Figure 5.17 Synthesized and measured FRFs at nodes (a) 1 and (b) 2

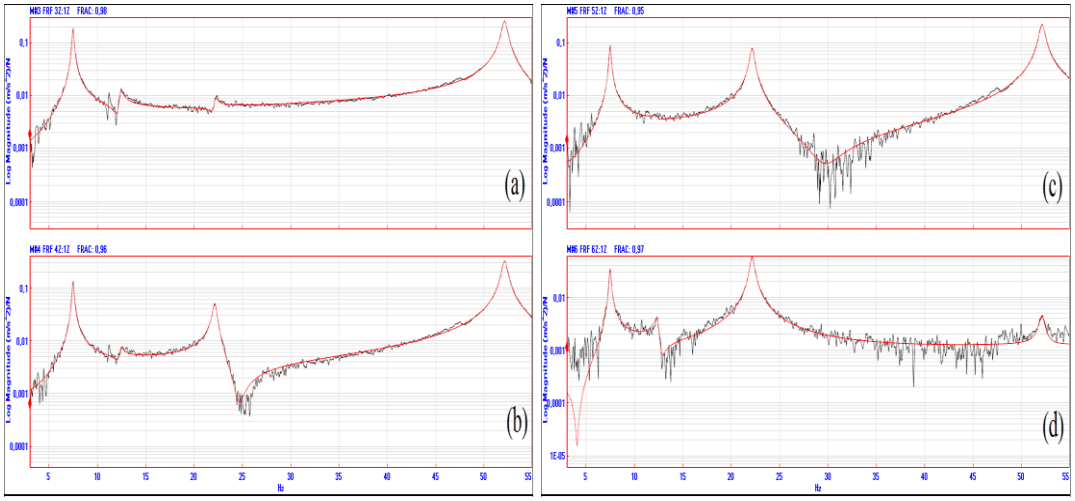

Figure 5.18 Synthesized and measured FRFs at nodes (a) 3, (b) 4, (c) 5 and (d) 6

Very similar modeshapes, complexity plots and MAC matrices are obtained as in the random excitation force level 2 test case.

5.2.3 Modal Analysis of the Gun Barrel for the Random Excitation Force Level 3

Modal parameters are extracted for this modal test, similarly, by using the stabilization diagram (Figure 5.19) algorithm and they are given in Table 5.6.

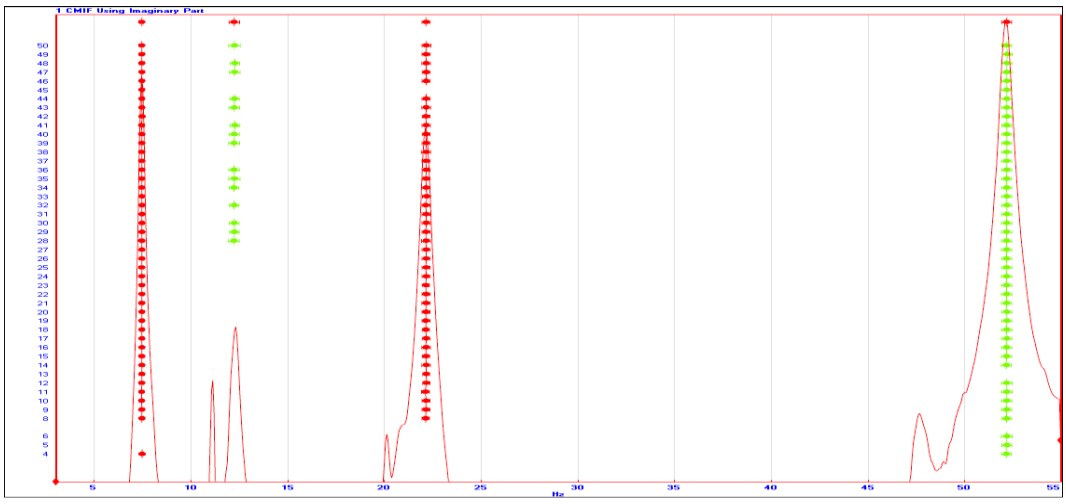

Figure 5.19 Stability diagram

Table 5.6 Extracted modal parameters

Mode Number	Natural Frequency (Hz)	Modal Damping Ratio (%)
1	7.449	1.171
2	12.229	2.193
3	22.144	0.941
4	52.161	0.504

After extracting the modal parameters, FRFs are synthesized and these synthesized FRFs are shown together with the measured FRFs for nodes 1 and 2 in Figure 5.20, and for nodes 3, 4, 5 and 6 in Figure 5.21.

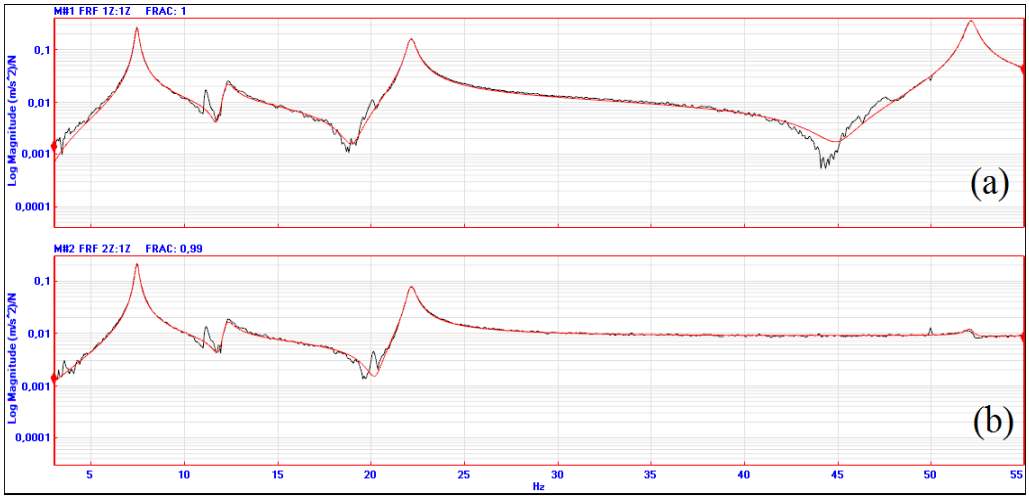

Figure 5.20 Synthesized and measured FRFs at nodes (a) 1 and (b) 2

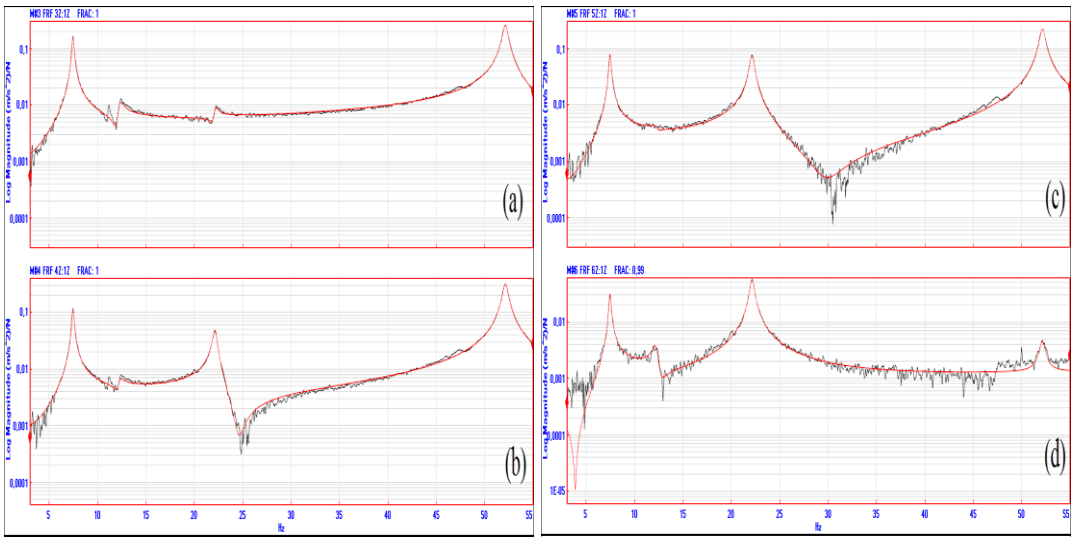

Figure 5.21 Synthesized and measured FRFs at nodes (a) 3, (b) 4, (c) 5 and (d) 6

Very similar modeshapes, complexity plots and MAC matrices are obtained as in the random excitation force level 2 test case.

5.2.4 Modal Analysis of the Gun Barrel for the Random Excitation Force Level 4

Similarly, by using the stabilization diagram (Figure 5.22) algorithm, modal parameters are extracted for this modal test and they are given in Table 5.7.

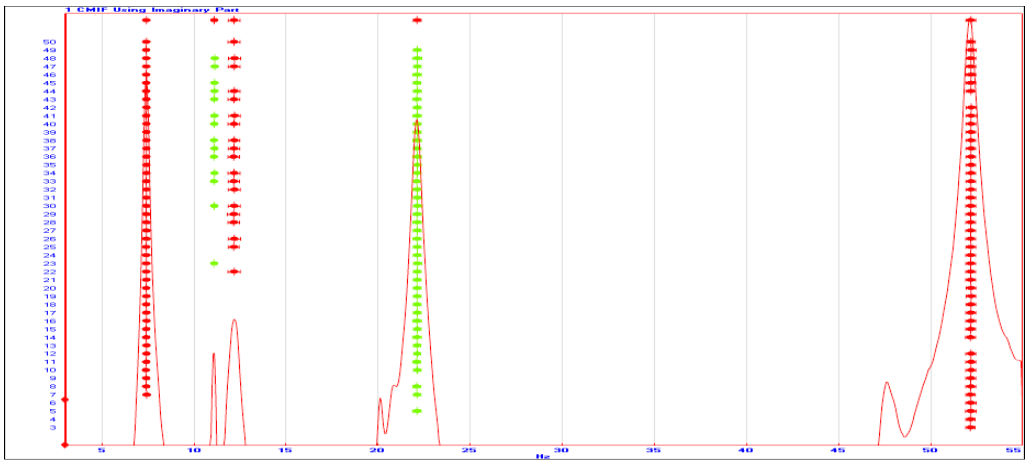

Figure 5.22 Stability diagram

Table 5.7 Extracted modal parameters

Mode Number	Natural Frequency (Hz)	Modal Damping Ratio (%)
1	7.416	1.345
2	11.105	0.769
3	12.177	2.637
4	22.111	0.985
5	52.150	0.513

Different from the previous results, 5 modes are extracted from the stabilization diagram algorithm. After extracting the modal parameters, FRFs are synthesized and these synthesized FRFs are shown together with the measured FRFs for nodes 1 and 2 in Figure 5.23, and for nodes 3, 4, 5 and 6 in Figure 5.24.

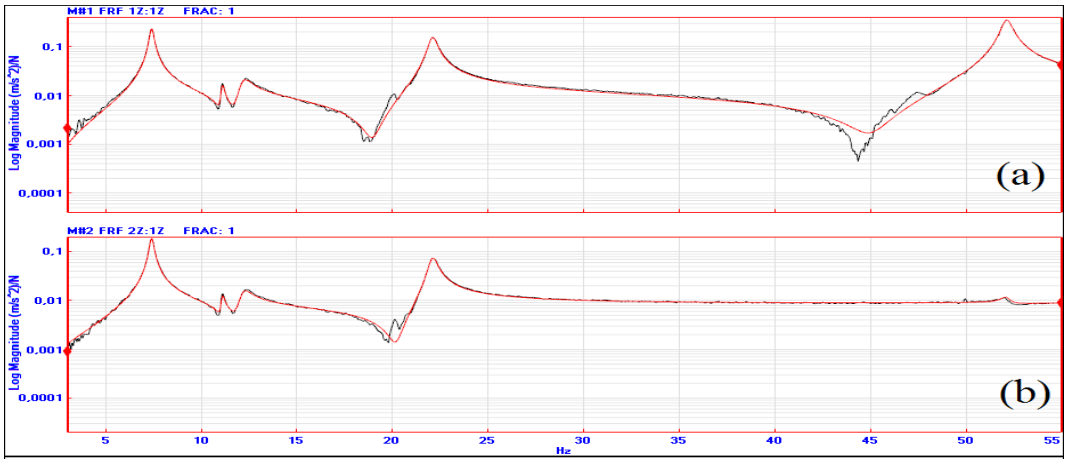

Figure 5.23 Synthesized and measured FRFs at nodes (a) 1 and (b) 2

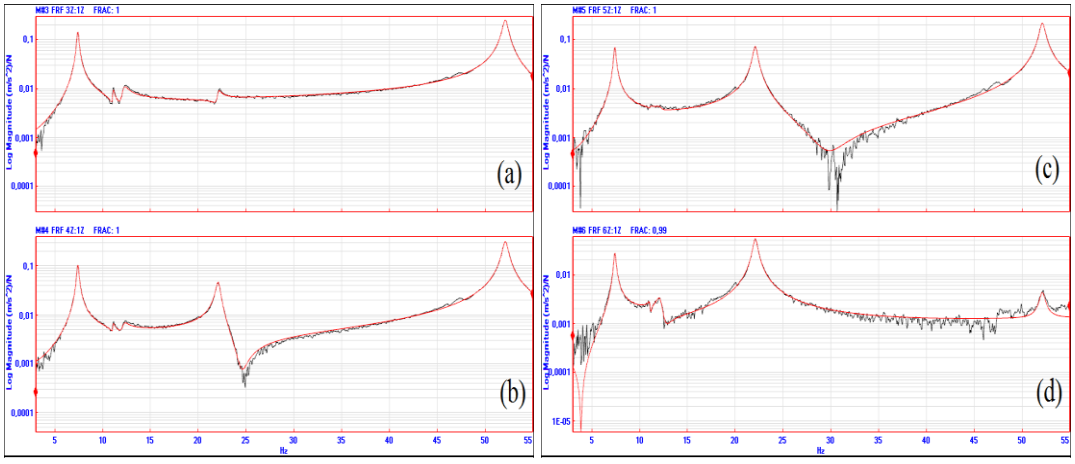

Figure 5.24 Synthesized and measured FRFs at nodes (a) 3, (b) 4, (c) 5 and (d) 6

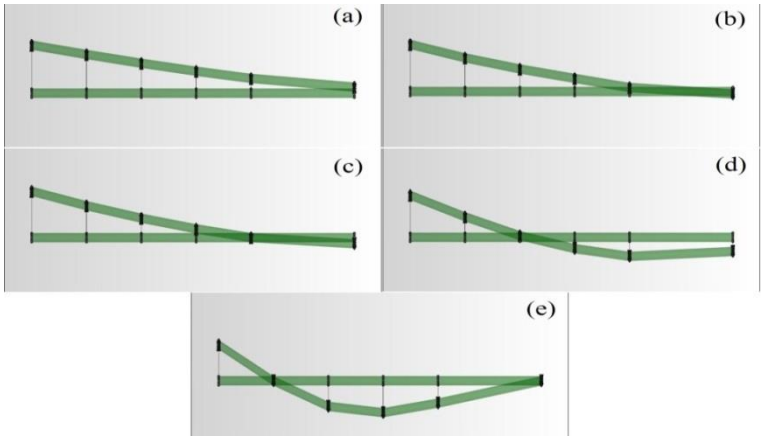

Figure 5.25 (a) First (b) second (c) third (d) fourth (e) fifth modeshapes

When the modeshapes of the gun barrel are studied, the first, fourth and fifth modes of the structure are found to be dominant modes. However, the second and third mode may be related with flexibility of joint at the root however they are not dominant modes which can be observed from the FRF curves. In order to check the complexity of the modes, complexity plots of modes are drawn and shown in Figure 5.26.

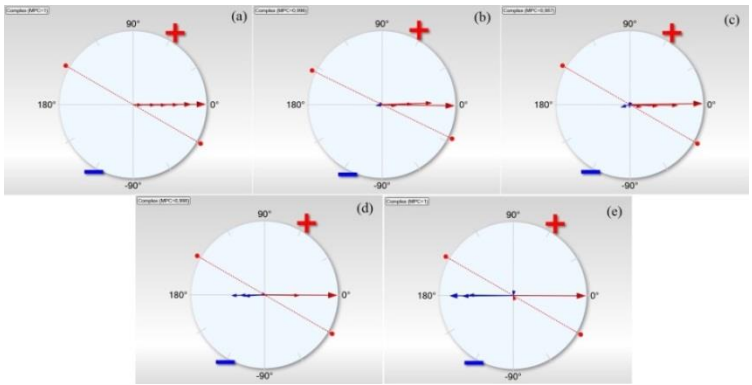

Figure 5.26 Complexity plot of (a) first (b) second (c) third (d) fourth (e) fifth modeshapes

It is observed from the complexity plots that, all the modes are almost real since all the modeshape components lie on the horizontal line (0-180 phase angle line) of the complexity plot.

Furthermore in order to see how these modes are correlated to each other, MAC diagram and the corresponding MAC matrix values are given in Figure 5.27 and in Table 5.8.

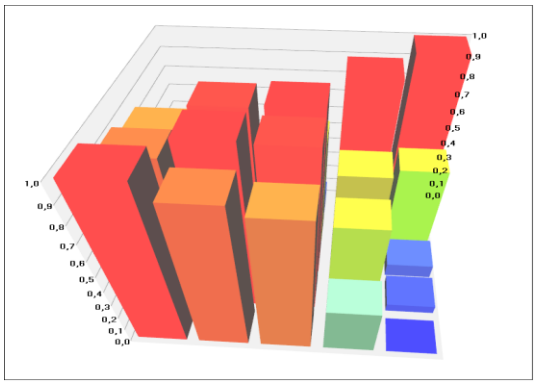

Figure 5.27 MAC diagram

Table 5.8 MAC matrix values

Modeshape	1	2	3	4	5
1	1.0000	0.9110	0.8600	0.3050	0.0001
2	0.9110	1.0000	0.9880	0.5920	0.0541
3	0.8600	0.9880	1.0000	0.6750	0.0897
4	0.3050	0.5920	0.6750	1.0000	0.5320
5	0.0001	0.0541	0.0897	0.5320	1.0000

As seen from MAC matrix, the first, second and third modeshapes have very similar shapes.

5.2.5 Modal Analysis of the Gun Barrel for the Random Excitation Force Level 5

After performing the measurements for that force level, the modal analysis is performed between 0-55 Hz in ME'scope modal analysis software. By using the stabilization diagram (Figure 5.28) algorithm modal parameters are extracted and they are given in Table 5.9.

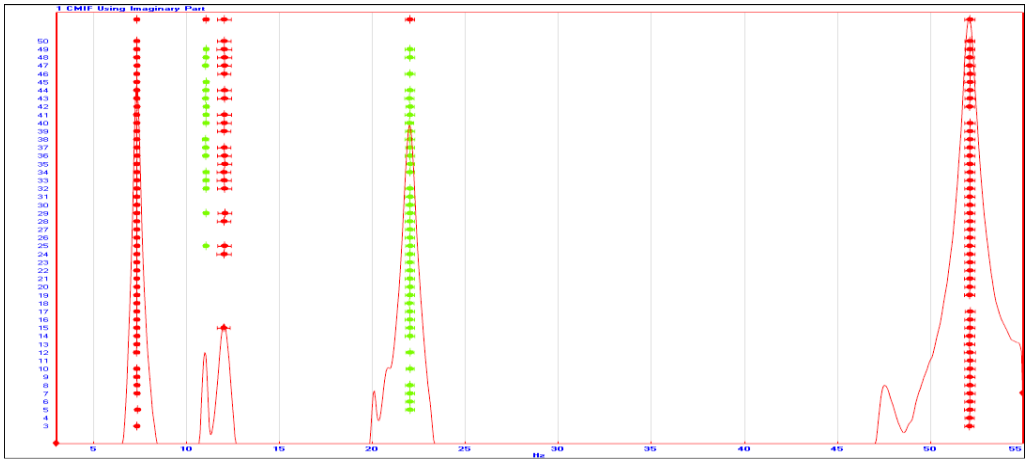

Figure 5.28 Stability diagram

Table 5.9 Extracted modal parameters

Mode Number	Natural Frequency (Hz)	Modal Damping Ratio (%)
1	7.341	1.621
2	11.053	1.187
3	12.044	3.093
4	22.018	1.115
5	52.112	0.533

After extracting the modal parameters, FRFs are synthesized and these synthesized FRFs are shown together with the measured FRFs for nodes 1 and 2 in Figure 5.29, and for nodes 3, 4, 5 and 6 in Figure 5.30.

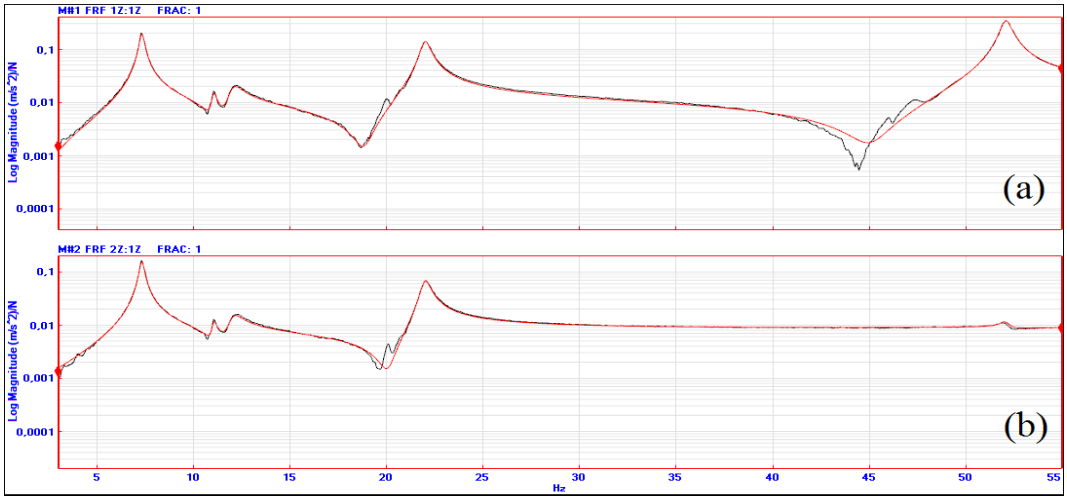

Figure 5.29 Synthesized and measured FRFs at nodes (a) 1 and (b) 2

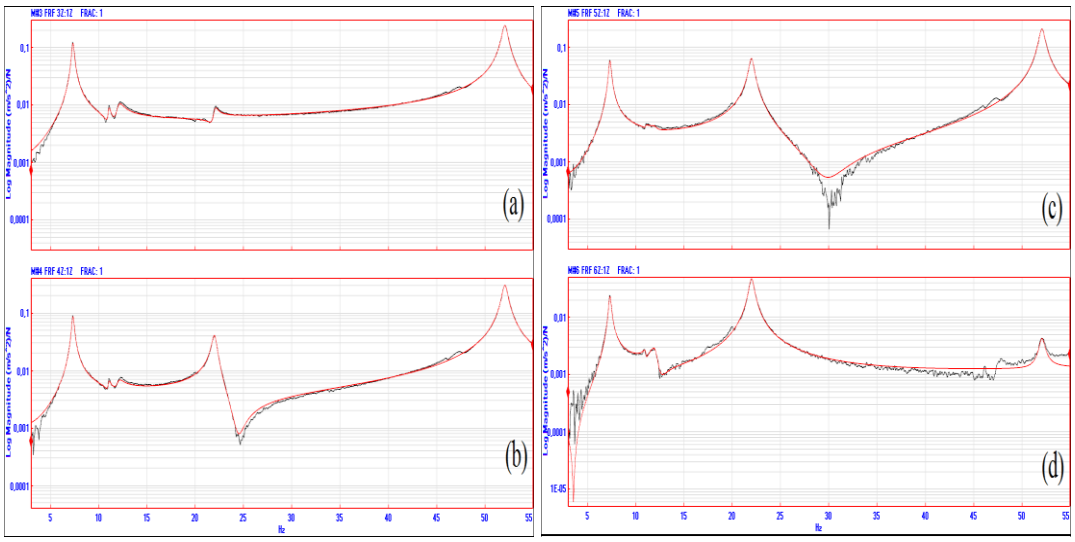

Figure 5.30 Synthesized and measured FRFs at nodes (a) 3, (b) 4, (c) 5 and (d) 6

In this analysis, very similar modeshapes, complexity plots and MAC matrices are obtained as in the random excitation force level 4 test case.

5.2.6 Modal Analysis of the Gun Barrel for the Random Excitation Force Level 6

Similarly, by using the stabilization diagram (Figure 5.31) algorithm, modal parameters are extracted for this modal test and they are given in Table 5.10.

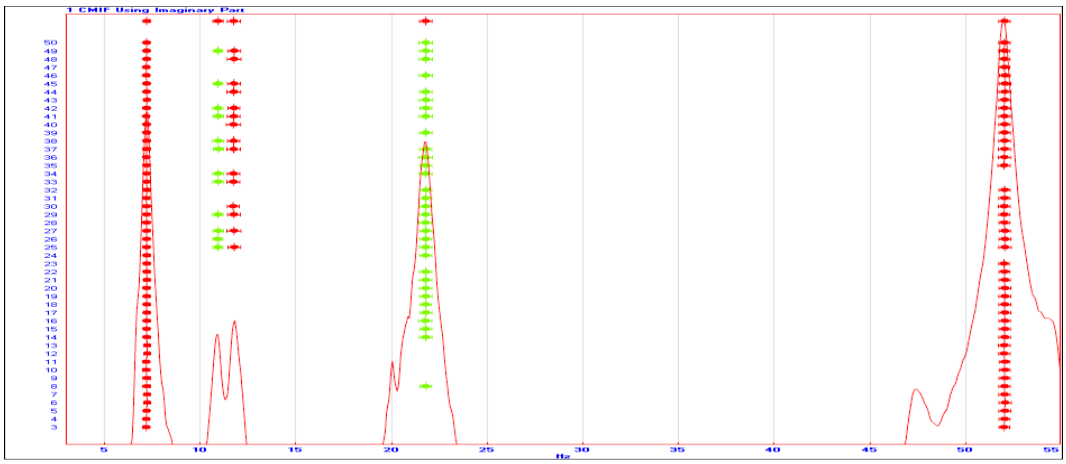

Figure 5.31 Stability diagram

Table 5.10 Extracted modal parameters

Mode Number	Natural Frequency (Hz)	Modal Damping Ratio (%)
1	7.196	2.368
2	10.929	2.498
3	11.755	2.926
4	21.785	1.483
5	52.034	0.580

After extracting the modal parameters, FRFs are synthesized and these synthesized FRFs are shown together with the measured FRFs for nodes 1 and 2 in Figure 5.32, and for nodes 3, 4, 5 and 6 in Figure 5.33.

Figure 5.32 Synthesized and measured FRFs at nodes (a) 1 and (b) 2

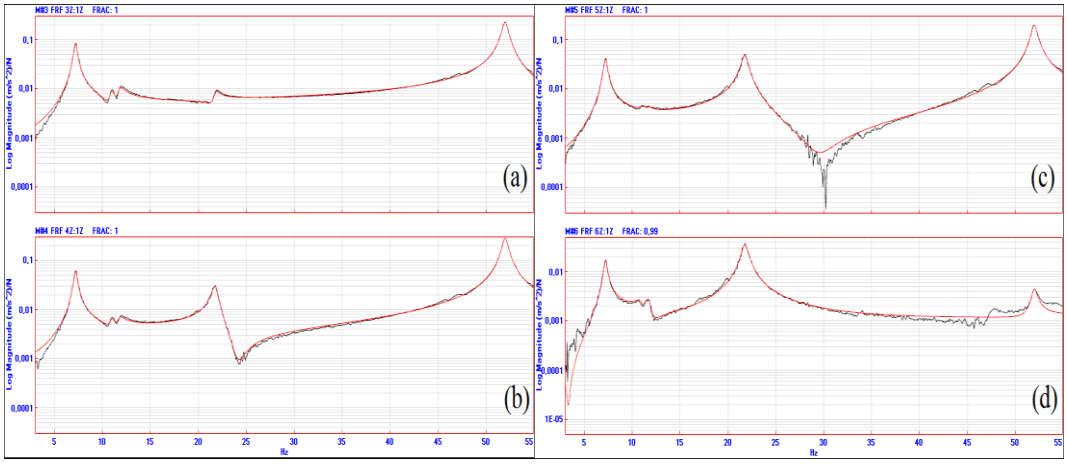

Figure 5.33 Synthesized and measured FRFs at nodes (a) 3, (b) 4, (c) 5 and (d) 6

Similar modeshapes, complexity plots and MAC matrices are obtained for this test case as in the random excitation force level 4 test case as well.

5.2.7 Comparisons of the Modal Analysis Results of Each Random Excitation Force Level

In this section modal parameters extracted are compared to each other for all the random excitation force level cases. The natural frequency comparison is given in Table 5.11 and it is shown in Figure 5.34.

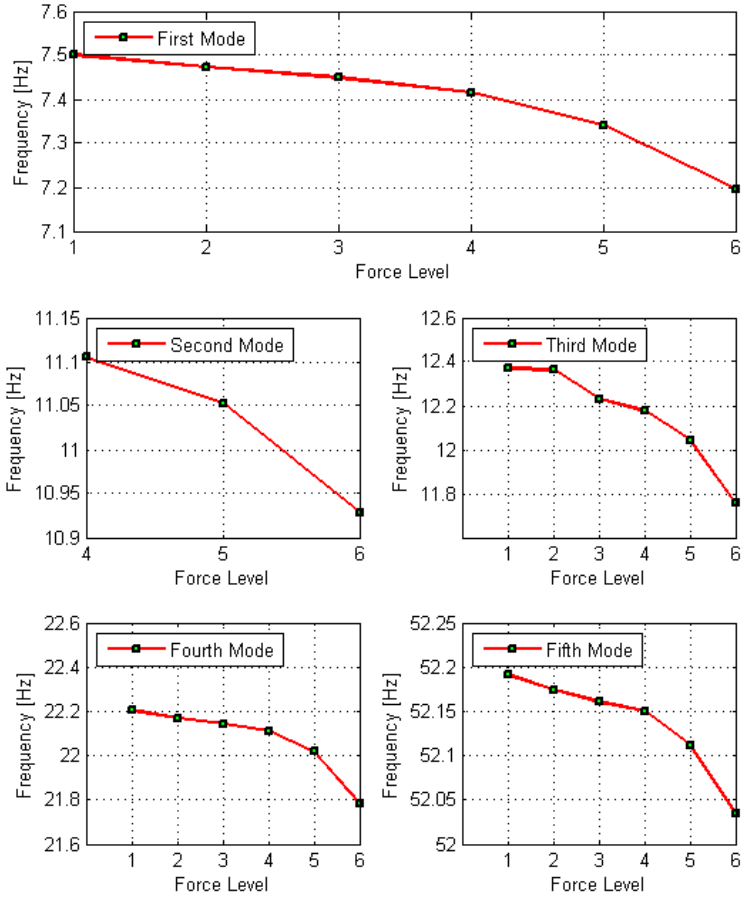

Figure 5.34 Natural frequency comparison for different force levels

Table 5.11 Natural frequency comparison for different force levels

	Force Level 1	**Force Level 2**	**Force Level 3**	**Force Level 4**	**Force Level 5**	**Force Level 6**
Mode Number	**Natural Frequency (Hz)**					
1	7.501	7.473	7.449	7.416	7.341	7.196
2	***	***	***	11.105	11.053	10.929
3	12.368	12.364	12.229	12.177	12.044	11.755
4	22.203	22.169	22.144	22.111	22.018	21.785
5	52.191	52.174	52.161	52.15	52.112	52.034

As seen from Figure 5.34 and Table 5.11, for the first three force levels, the second mode of the structure cannot be extracted from modal analysis. Also it is clearly seen that as the force level increases the natural frequencies tend to decrease for all the modes.

Similar comparison can be made for the damping values extracted from the analysis. The comparison of the damping values for each of the force levels is given in Table 5.12 and shown in Figure 5.35.

Table 5.12 Damping ratio comparison for different force levels

	Force Level 1	**Force Level 2**	**Force Level 3**	**Force Level 4**	**Force Level 5**	**Force Level 6**
Mode Number	**Modal Damping Ratio (%)**					
1	0.955	1.033	1.171	1.345	1.621	2.368
2	***	***	***	0.769	1.187	2.498
3	1.531	1.837	2.193	2.637	3.093	2.926
4	0.87	0.903	0.941	0.985	1.115	1.483
5	0.499	0.496	0.504	0.513	0.533	0.58

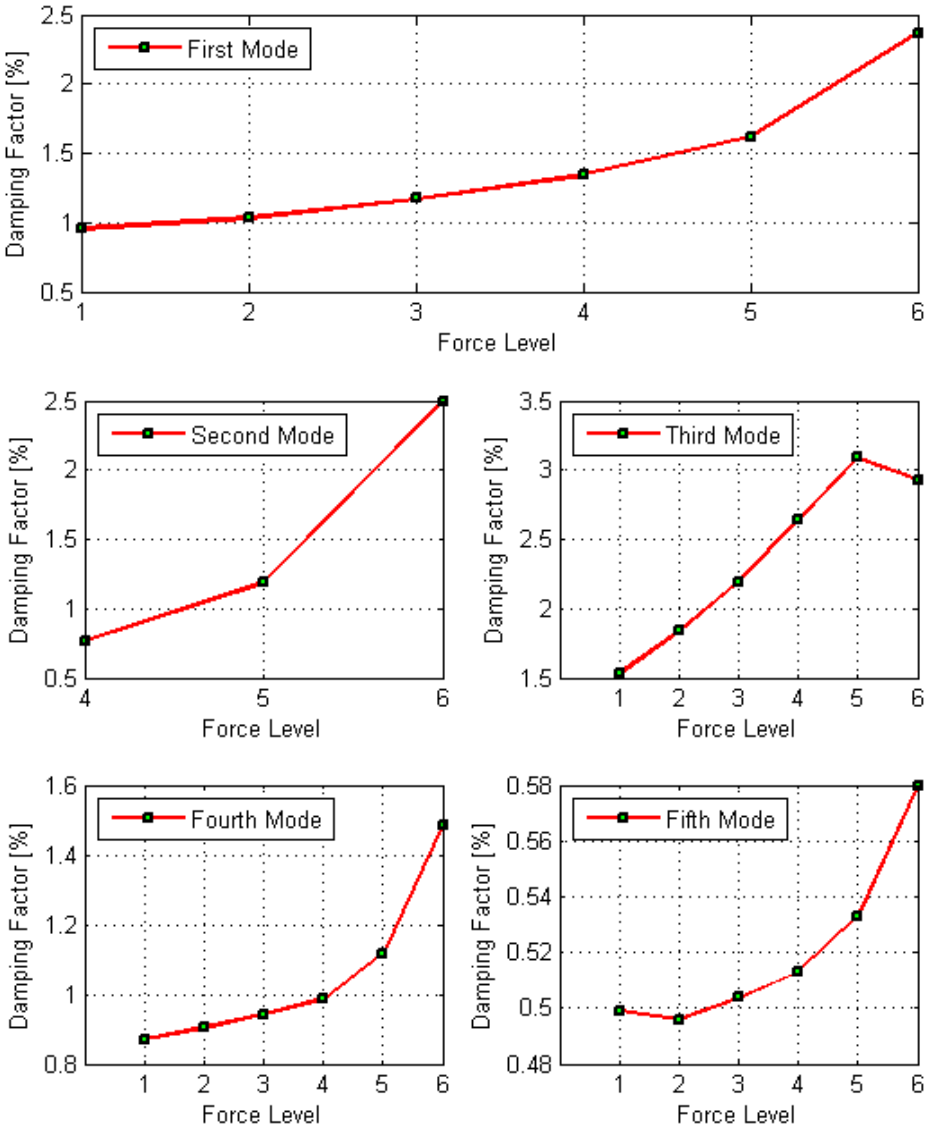

Figure 5.35 Damping ratio comparison for different force levels

As observed from Figure 5.35 and Table 5.12, as the force level increases damping values of the modes tend to increase for all the modes except the third mode. Only in the third mode the damping value drops for force level 6.

From results of random excitation tests, clear indication of the existence of nonlinearity in the system is seen. Since the fundamental mode of the gun barrel is under consideration, we can also conclude that, for the fundamental mode, as the force level increases in the random excitation tests, damping value of the fundamental mode increases and natural frequency decreases.

It is also observed that, fundamental frequency of the gun barrel is around 7.5 Hz for lowest excitation force level. In order to apply the PRD method, the structure is excited at around that frequency with a pure sine excitation at different forcing levels. The structure is excited at a low forcing level and then at a number of high forcing levels. The advantage of this method is that, there is no need for any vibration controller as in the cases of constant forcing or constant amplitude testing over a certain frequency range.

In order to see the effect of choosing different frequencies of excitation on the performance of the method, five different excitation frequencies (7.5 Hz, 7 Hz, 7.125 Hz, 7.25 Hz, and 7.375 Hz) are used, and for each of these excitation frequencies, describing functions of the nonlinearities are obtained by using PRD method.

5.2.8 Application of PRD Method at 7.5 Hz for Identifying Nonlinearity

Real and imaginary parts of the describing function are obtained from experimental measurements at 7.5 Hz by applying PRD method. Curve fitting is performed for the calculated real and imaginary parts of describing function and the fitted curves are shown in Figure 5.36.

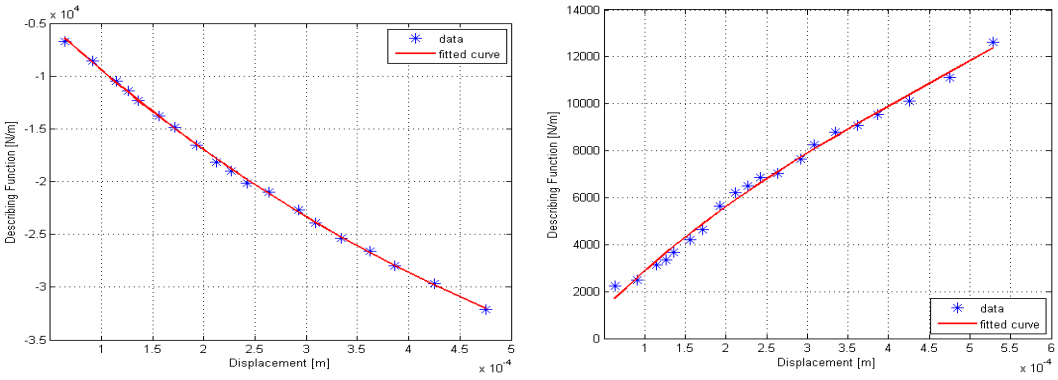

(a) (b)

Figure 5.36 Calculated describing function (a) Real part (b) Imaginary part

For the real and imaginary parts of the describing function, 3rd order polynomial functions are fit. Corresponding coefficients of the polynomial functions are given in Table 5.13.

Table 5.13 Coefficients of the polynomials fit to the data for real and imaginary parts of the describing function

	p_3	p_2	p_1	p_0
Real Part of Describing Function $p_3x^3 + p_2x^2 + p_1x + p_0$	$-2.62\text{x}10^{13}$	$7.62\text{x}10^{10}$	$-9.64\text{x}10^{7}$	-565
Imaginary Part of Describing Function $p_3x^3 + p_2x^2 + p_1x + p_0$	$3.12\text{x}10^{13}$	$-4.18\text{x}10^{10}$	$3.77\text{x}10^{7}$	-518

5.2.9 Application of PRD Method at 7 Hz for Identifying Nonlinearity

Real and imaginary parts of the describing function are obtained from experimental measurements at 7 Hz by applying PRD method. Curve fitting is performed for the calculated real and imaginary parts of describing function and the fitted curves are shown in Figure 5.37.

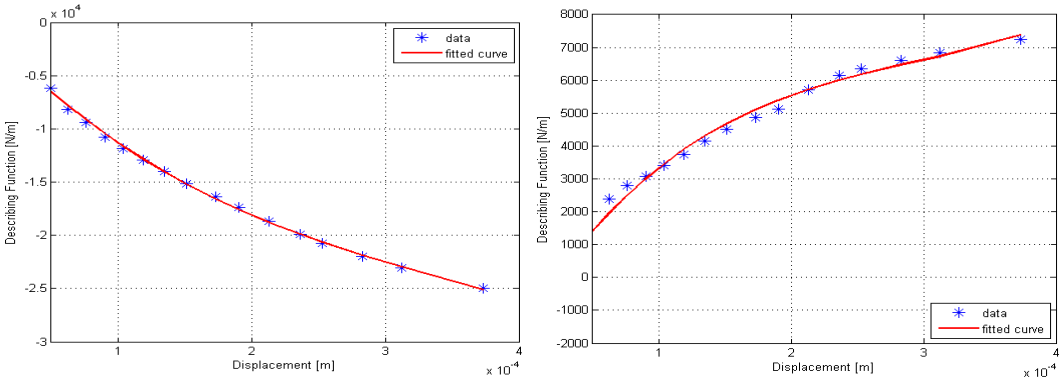

(a) (b)

Figure 5.37 Calculated describing function (a) Real part (b) Imaginary part

For the real and imaginary parts of the describing function, 3rd order polynomial functions are fit. Corresponding coefficients of the polynomial functions are given in Table 5.14.

Table 5.14 Coefficients of the polynomials fit to the data for real and imaginary part of the describing function

	p_3	p_2	p_1	p_0
Real Part of Describing Function $p_3x^3 + p_2x^2 + p_1x + p_0$	-2.52x10^{14}	2.72x10^{11}	-1.32x10^{8}	-579
Imaginary Part of Describing Function $p_3x^3 + p_2x^2 + p_1x + p_0$	2.03x10^{14}	-1.79x10^{11}	6.17x10^{7}	-1260

5.2.10 Application of PRD Method at 7.125 Hz for Identifying Nonlinearity

Real and imaginary parts of the describing function are obtained from experimental measurements at 7.125 Hz by applying PRD method. Curve fitting is performed for the calculated real and imaginary parts of describing function and the fitted curves are shown in Figure 5.38.

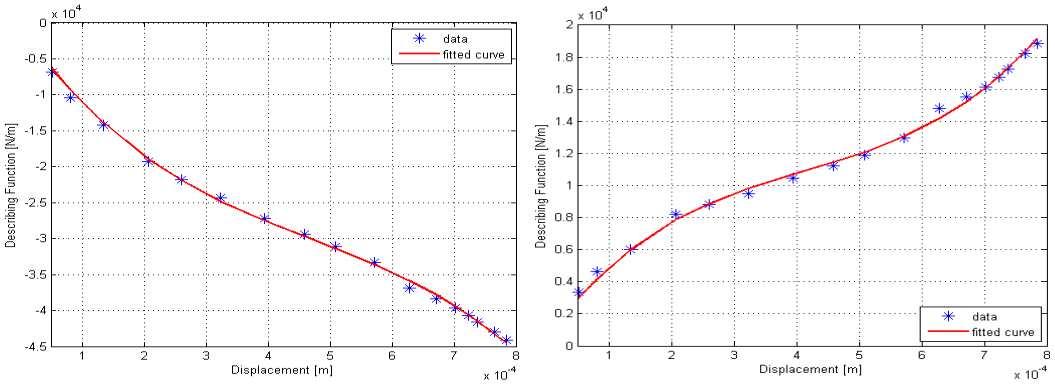

(a) (b)

Figure 5.38 Calculated describing function (a) Real part (b) Imaginary part

For the real and imaginary parts of the describing function, 3rd order polynomial functions are fit. Corresponding coefficients of the polynomial functions are given in Table 5.15.

Table 5.15 Coefficients of the polynomials fit to the data for real and imaginary part of the describing function

	p_3	p_2	p_1	p_0
Real Part of Describing Function $p_3x^3 + p_2x^2 + p_1x + p_0$	-1.33x10^{14}	1.88x10^{11}	-1.21x10^{8}	-608
Imaginary Part of Describing Function $p_3x^3 + p_2x^2 + p_1x + p_0$	7.84x10^{13}	-9.78x10^{10}	5.21x10^{7}	523

5.2.11 Application of PRD Method at 7.25 Hz for Identifying Nonlinearity

Real and imaginary parts of the describing function are obtained from experimental measurements at 7.25 Hz by applying PRD method. Curve fitting is performed for the calculated real and imaginary parts of describing function and the fitted curves are shown in Figure 5.39.

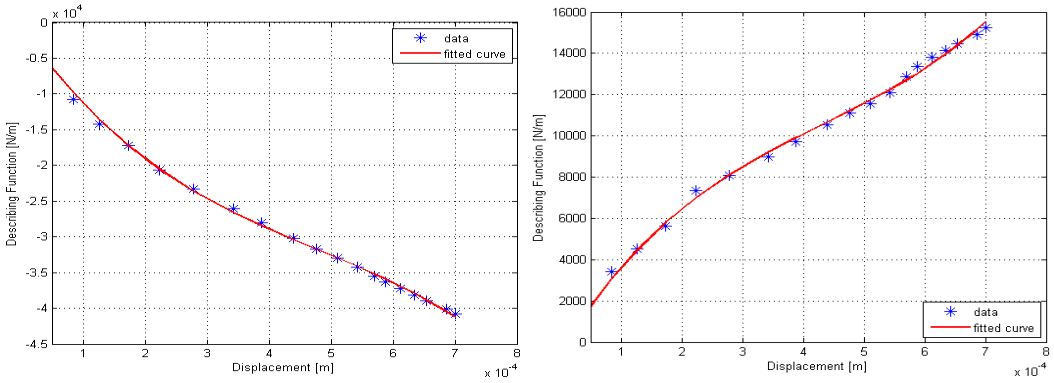

(a) (b)

Figure 5.39 Calculated describing function (a) Real part (b) Imaginary part

For the real and imaginary parts of the describing function, 3rd order polynomial functions are fit. Corresponding coefficients of the polynomial functions are given in Table 5.16.

Table 5.16 Coefficients of the polynomials fit to the data for real and imaginary part of the describing function

	p_3	p_2	p_1	p_0
Real Part of Describing Function $p_3x^3 + p_2x^2 + p_1x + p_0$	-1.30x10^{14}	1.85x10^{11}	-1.24x10^{8}	-618
Imaginary Part of Describing Function $p_3x^3 + p_2x^2 + p_1x + p_0$	5.84x10^{13}	-7.62x10^{10}	4.75x10^{7}	-483

5.2.12 Application of PRD Method at 7.375 Hz for Identifying Nonlinearity

Real and imaginary parts of the describing function are obtained from experimental measurements at 7.375 Hz by applying PRD method. Curve fitting is performed for the calculated real and imaginary parts of describing function and the fitted curves are shown in Figure 5.40.

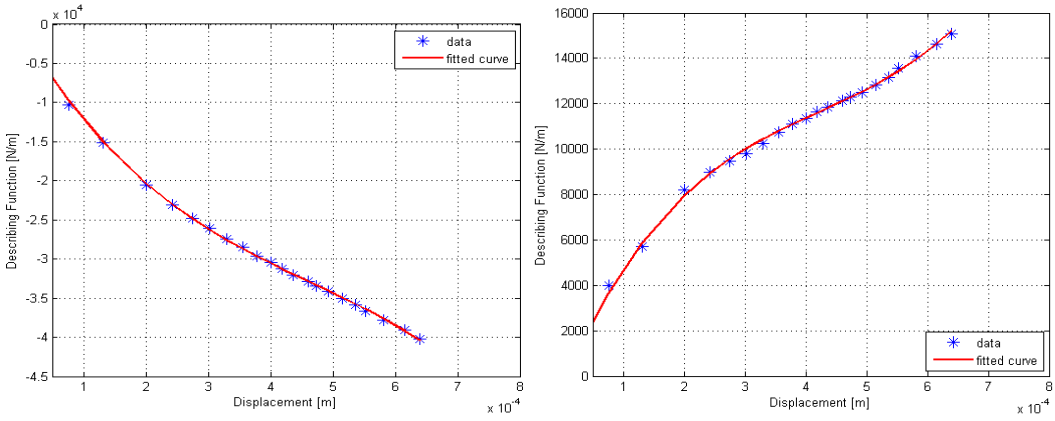

(a) (b)

Figure 5.40 Calculated describing function (a) Real part (b) Imaginary part

For the real and imaginary parts of the describing function, 3rd order polynomial functions are fit. Corresponding coefficients of the polynomial functions are given in Table 5.17.

Table 5.17 Coefficients of the polynomials fit to the data for real and imaginary part of the describing function

	p_3	p_2	p_1	p_0
Real Part of Describing Function $p_3x^3 + p_2x^2 + p_1x + p_0$	$-1.51\text{x}10^{14}$	$2.1\text{x}10^{11}$	$-1.34\text{x}10^{8}$	-628
Imaginary Part of Describing Function $p_3x^3 + p_2x^2 + p_1x + p_0$	$1.05\text{x}10^{14}$	$-1.27\ \text{x}10^{11}$	$6.36\text{x}10^{7}$	-498

5.2.13 Comparison of Nonlinearities Identified by Using PRD Method at Different Frequencies

In this section, the real and imaginary parts of the describing function obtained from experimental measurements at 7 Hz, 7.125 Hz, 7.25 Hz, 7.375 Hz and 7.5 Hz by

using PRD method are compared to each other. Comparisons of the real and imaginary parts of the describing functions are shown in Figure 5.41 and Figure 5.42, respectively.

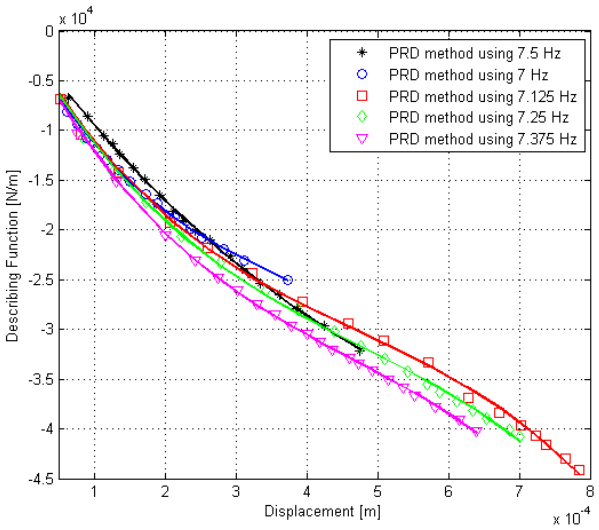

Figure 5.41 Comparison of identified real parts of the describing function

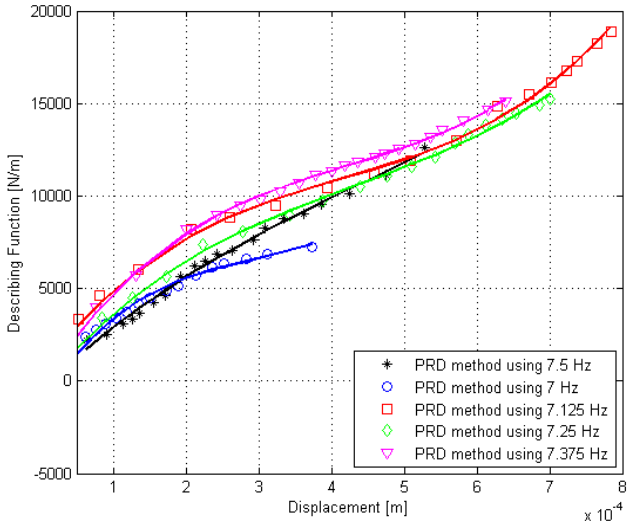

Figure 5.42 Comparison of identified imaginary parts of the describing function

When we compare the real part of describing functions obtained using the measurements at 7 Hz, 7.125 Hz, 7.25 Hz, 7.375 Hz and 7.5 Hz, it can be observed from Figure 5.41 that identified functions are similar to each other. As seen from Figure 5.42, the identified imaginary parts of describing functions are also similar to each other. However, we can see larger deviations in the describing function obtained when the measurement at 7 Hz is used, especially at larger response amplitudes. From the results we can conclude that the excitation frequency used in PRD method, does not have significant effect on the identified nonlinearity, if the excitation frequency is approximately in the 5% range of the resonance of the underlying linear system.

As a final test in this set of experiments, frequency responses between 6 Hz and 8 Hz are measured for a constant low forcing level excitation. Stepped sine test is used as an excitation type by using the given test set-up. Frequency resolution of 0.03125 Hz is used around the resonance region, and a frequency resolution of 0.25 Hz is used elsewhere. Excitation signal is a pure sinusoidal signal. However, in order to perform constant force vibration testing over the frequency range, a manual control strategy is used in the experiments. This control is maintained by checking the forcing level and changing the excitation voltage supplied to the shaker. In Figure 5.43, measured FRFs for F=0.5N are shown.

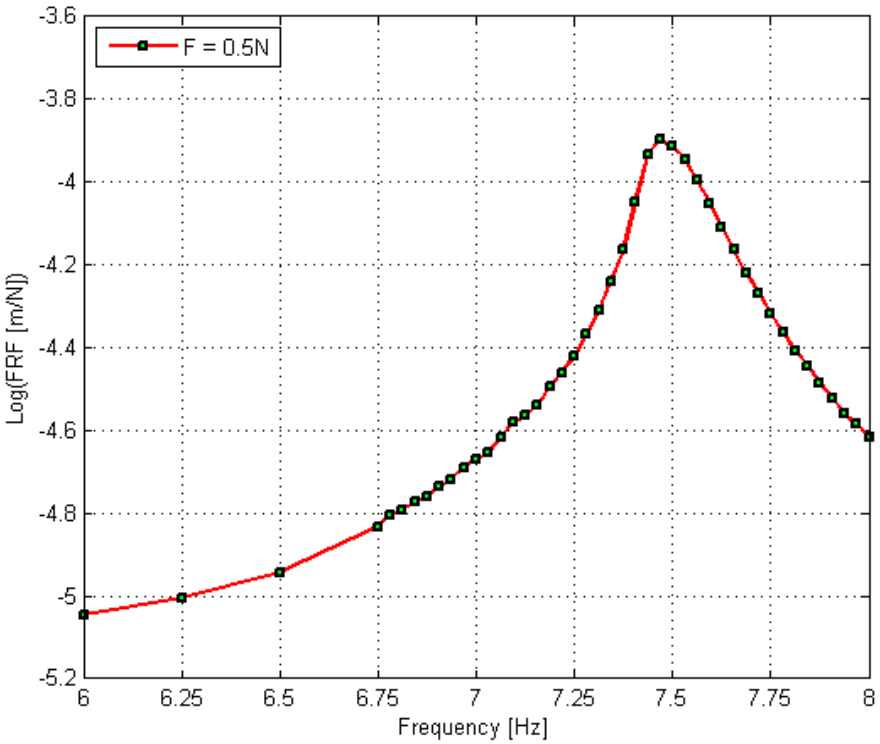

Figure 5.43 Measured FRF at F=0.5N

It is observed from Figure 5.43 that the FRF curve obtained for F=0.5N seems like a linear FRF curve, as expected. However, as it will be shown below, the measured FRF and the linear FRF curves of the system are different from each other even though a very low forcing is used in the experiment.

5.3 Second Set of Experiments

In the second set of experiments, the main purpose is to perform measurements which will be used to study the performance of the PRD method and the model updating approach proposed. A set of stepped sine constant force tests is used in the experiments. Frequency resolution of resolution of 0.03125 Hz is used around the resonance region and away from the resonance region larger frequency resolution is

used. Similarly, the constant force excitation is maintained by manually checking the forcing level and changing the excitation voltage supplied to the shaker at each frequency point. The structure is excited at 3 different forcing levels (F=5N, F=10.4N, F=15N).The measured FRFs are shown in Figure 5.44.

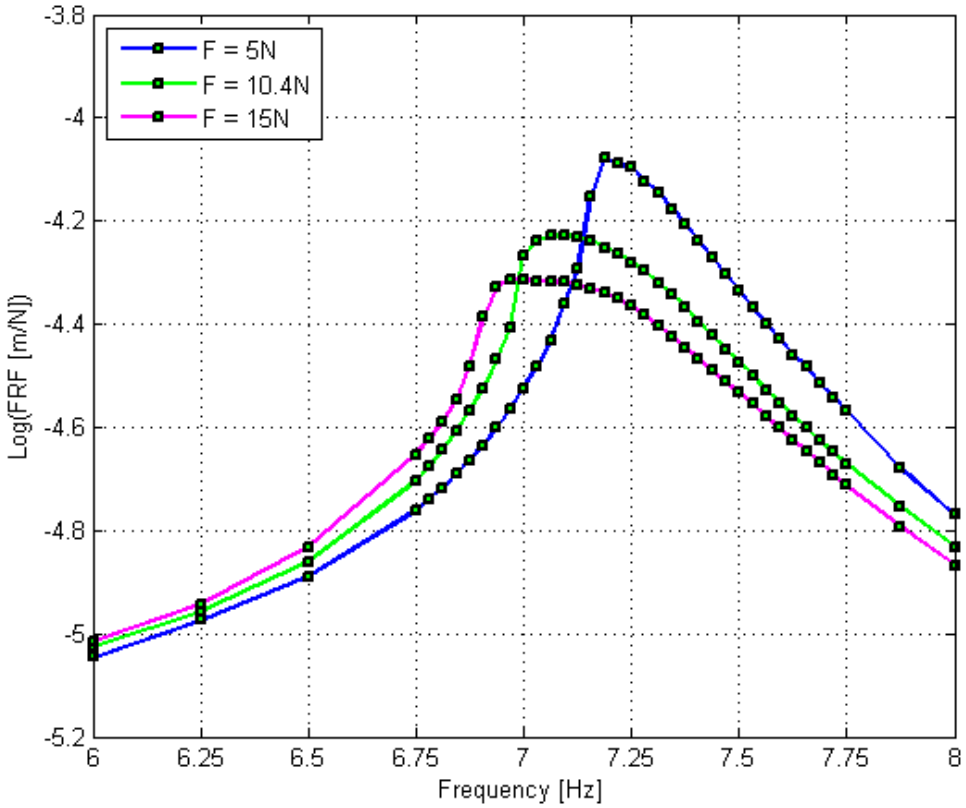

Figure 5.44 Measured FRF at F=5N, F=10.4N, F=15N

Also, these measured FRFs are shown with the FRF obtained at low forcing level (F=0.5N) in the same graph (Figure 5.45).

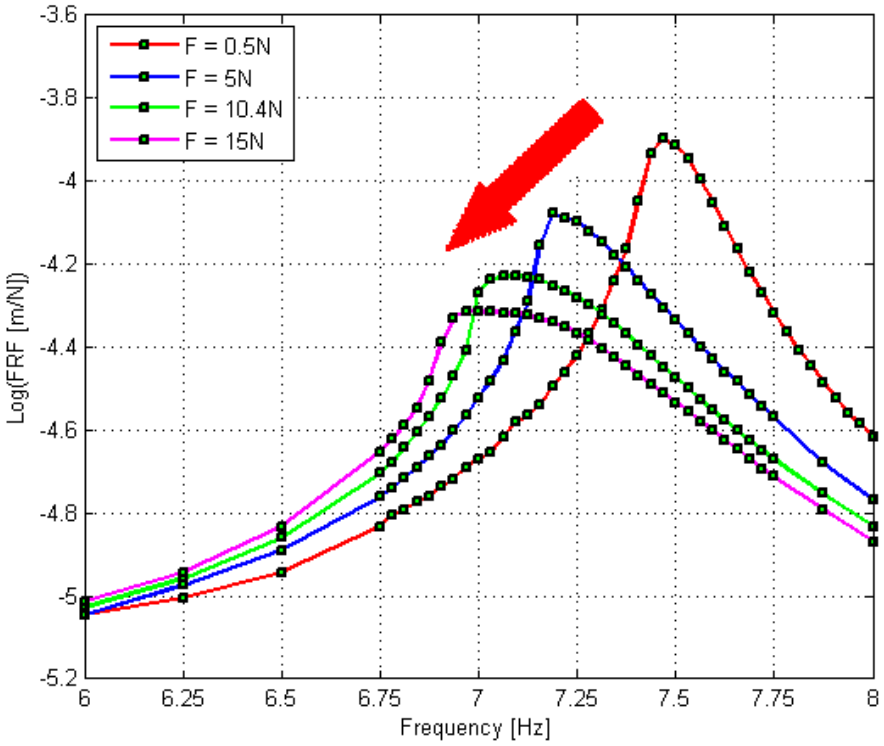

Figure 5.45 Measured FRF at F=0.5N, F=5N, F=10.4N, F=15N

5.4 Application of PRD Method for Obtaining Linear FRFs

Using the describing function values obtained by applying PRD method and the FRF values measured at F=0.5N in the first set of experiments, linear FRFs of the structure are predicted. Since, describing functions are obtained at 5 different excitation frequencies, in order to study the effects of test frequency on the performance of the method; five separate linear FRF curves are predicted. The linear FRF curves predicted by using the describing functions obtained from experiments made at 7 Hz, 7.125 Hz, 7.25 Hz, 7.375 Hz and 7.5 Hz are compared with the FRFs measured at F=0.5N in Figure 5.46, Figure 5.47 and Figure 5.48 and with each other in Figure 5.49.

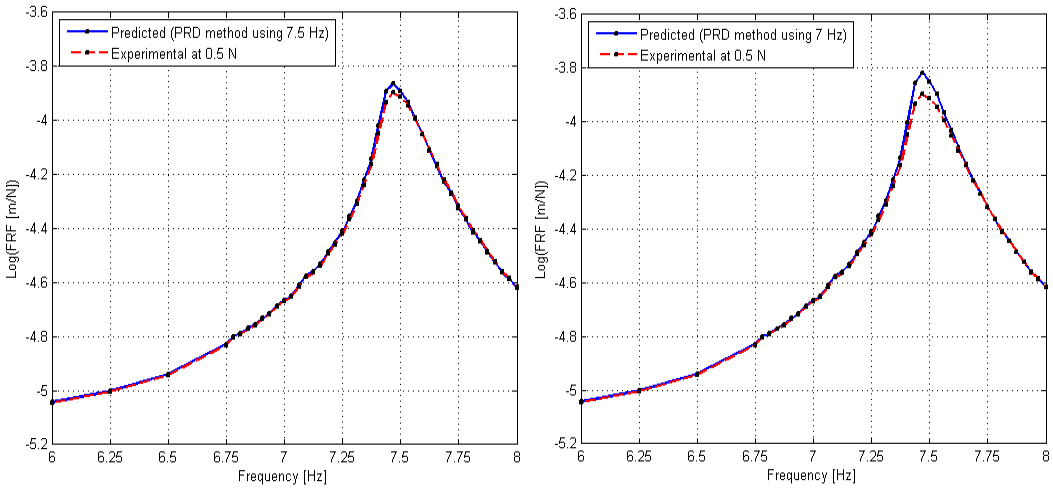

(a) (b)

Figure 5.46 Comparison of measured FRFs at F=0.5N with predicted linear FRFs by using PRD method at (a) 7.5 Hz (b) 7 Hz

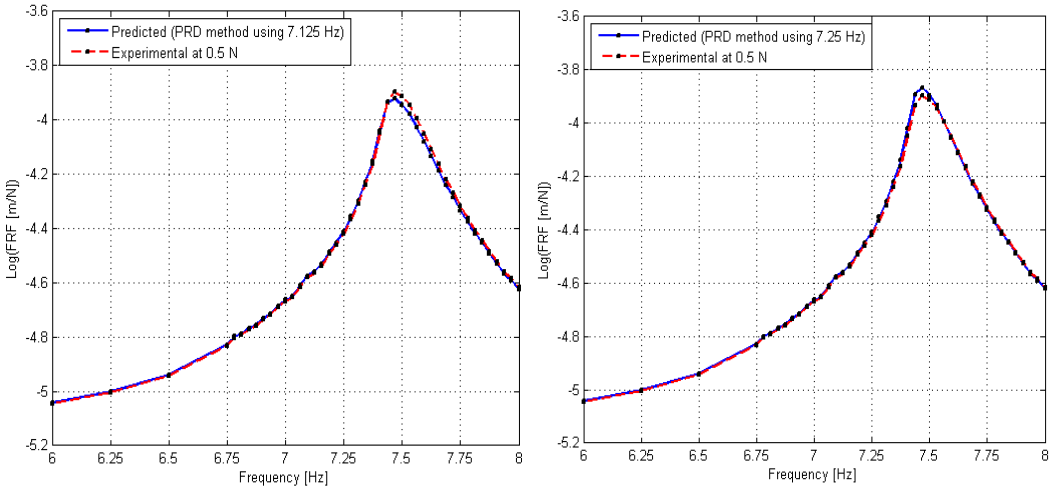

(a) (b)

Figure 5.47 Comparison of measured FRFs at F=0.5N with predicted linear FRFs by using PRD method at (a) 7.125 Hz (b) 7.25 Hz

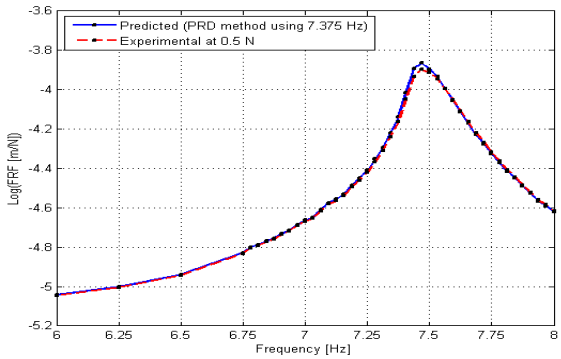

Figure 5.48 Comparison of measured FRFs at F=0.5N with predicted linear FRFs by using PRD method at 7.375 Hz

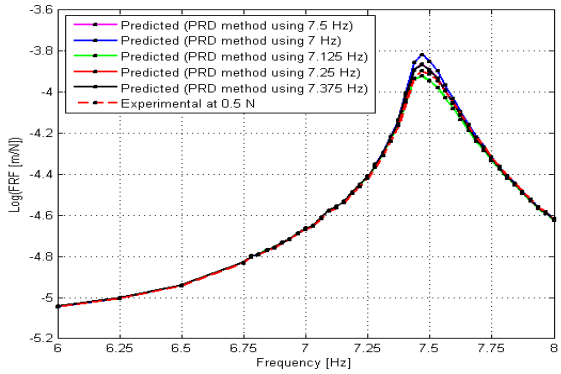

Figure 5.49 Comparison of predicted linear FRFs by using PRD method at 7 Hz, 7.125 Hz, 7.25 Hz, 7.375 Hz and 7.5 Hz

As can be observed from Figure 5.46, Figure 5.47 and Figure 5.48, FRFs measured at low forcing level (F = 0.5N) do not accurately represent the linear FRFs of the system which can be obtained by using the PRD method proposed. FRFs measured at even a very low forcing level may not represent the linear FRF accurately. It is also observed from Figure 5.49 that linear FRFs obtained using the describing functions identified from the tests made at 7 Hz, 7.125 Hz, 7.25 Hz, 7.375 Hz and 7.5 Hz have

discrepancies around the resonance (deviation of the peak amplitude from the mean amplitude value is approximately less than 9%). Based on these observations, if the excitation frequency used in PRD method is approximately in the 5% range of the resonance of the underlying linear system, there are no large discrepancies in the predicted linear FRFs. In the next section, in order to further investigate the effects of test frequency on the performance of the method, predicted nonlinear FRFs (regenerated nonlinear FRFs by using linear FRFs and identified nonlinearity obtained by PRD method) are compared with experimental nonlinear FRFs at F=5N, F=10.4N and F=15N.

5.5 Prediction of Nonlinear FRFs by Using Linear FRFs and Identified Nonlinearity Obtained by PRD Method

In this section, by using the identified nonlinearity and linear FRFs predicted by using the PRD method at 7 Hz, 7.125 Hz, 7.25Hz, 7.375 Hz and 7.5 Hz, the nonlinear FRFs at F=5N, F=10.4N and F=15N are calculated (regenerated). The regenerated FRFs are compared with the experimental measurements for F=5N. The results are given in Figure 5.50, Figure 5.51 and Figure 5.52.

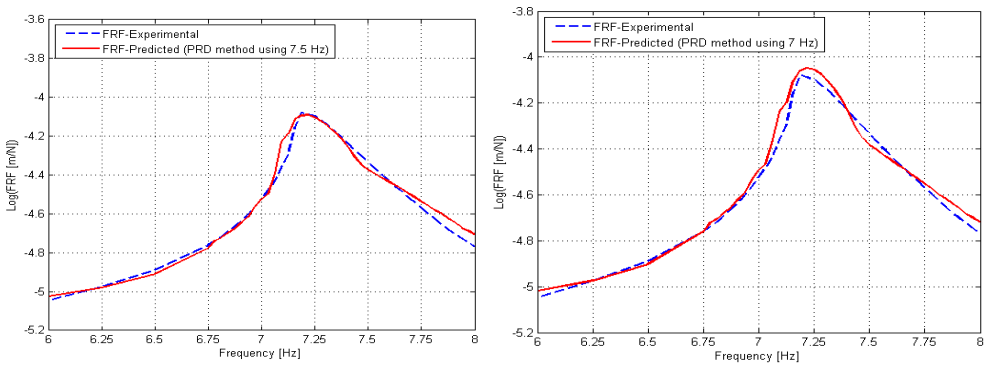

(a) (b)

Figure 5.50 Comparison of measured and predicted FRFs at F=5N (PRD method is used at (a) 7.5 Hz (b) 7 Hz)

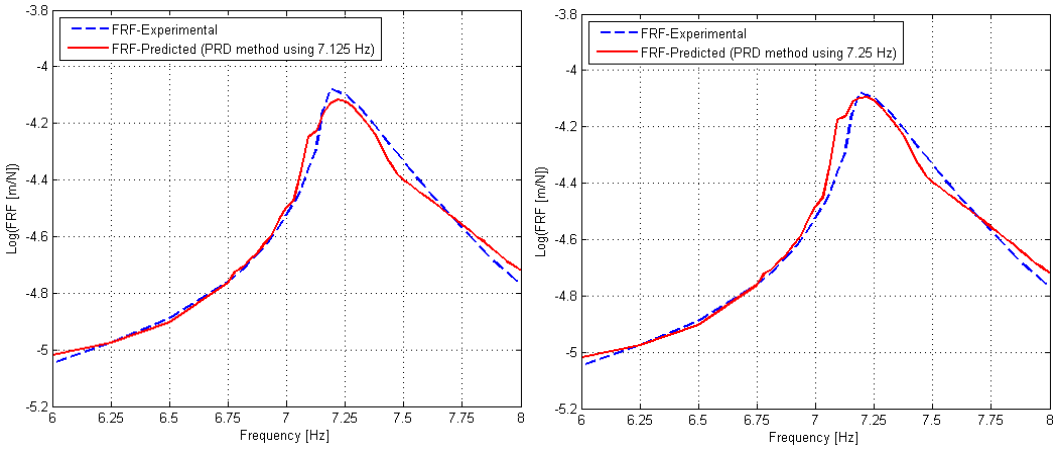

(a) (b)

Figure 5.51 Comparison of measured and predicted FRFs at F=5N (PRD method is used at (a) 7.125 Hz (b) 7.25 Hz)

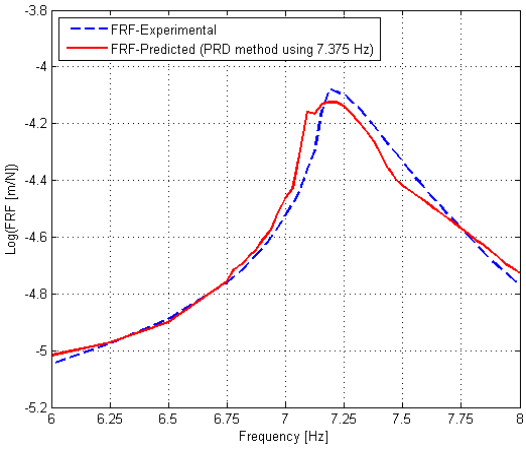

Figure 5.52 Comparison of measured and predicted FRFs at F=5N (PRD method is used at 7.375 Hz)

Regenerated nonlinear FRF curves are also compared with each other as well as with the experimental one for F=5N as shown in Figure 5.53.

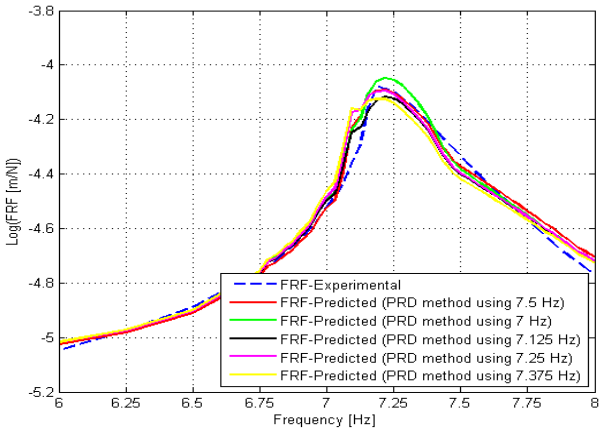

Figure 5.53 Comparison of experimental and regenerated FRFs by using PRD method at 7 Hz, 7.125 Hz, 7.25 Hz, 7.375 Hz and 7.5 Hz

As can be seen from Figure 5.53, regenerated nonlinear FRFs match very good with the experimental nonlinear FRFs at F=5N. Similarly, the comparison of the regenerated and experimental nonlinear FRF curves at F=10.4N are given in Figure 5.54, Figure 5.55 and Figure 5.56.

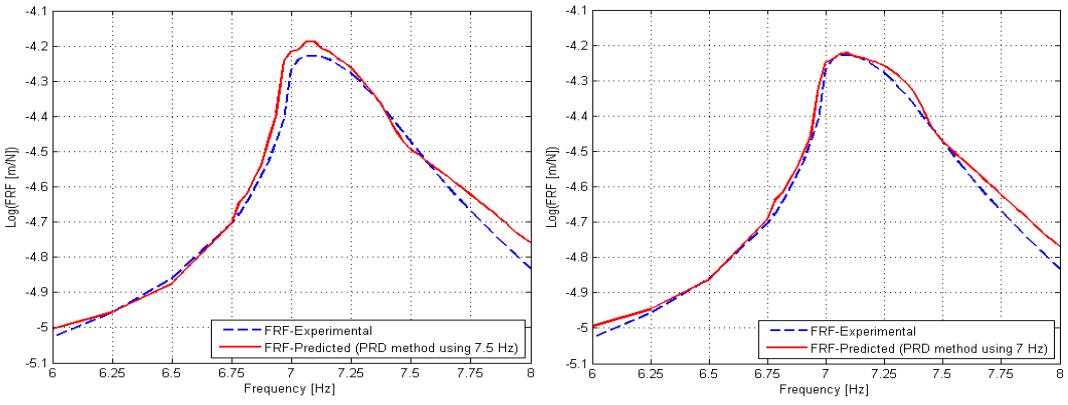

(a) (b)

Figure 5.54 Comparison of measured and predicted FRFs at F=10.4N (PRD method is used at (a) 7.5 Hz (b) 7 Hz)

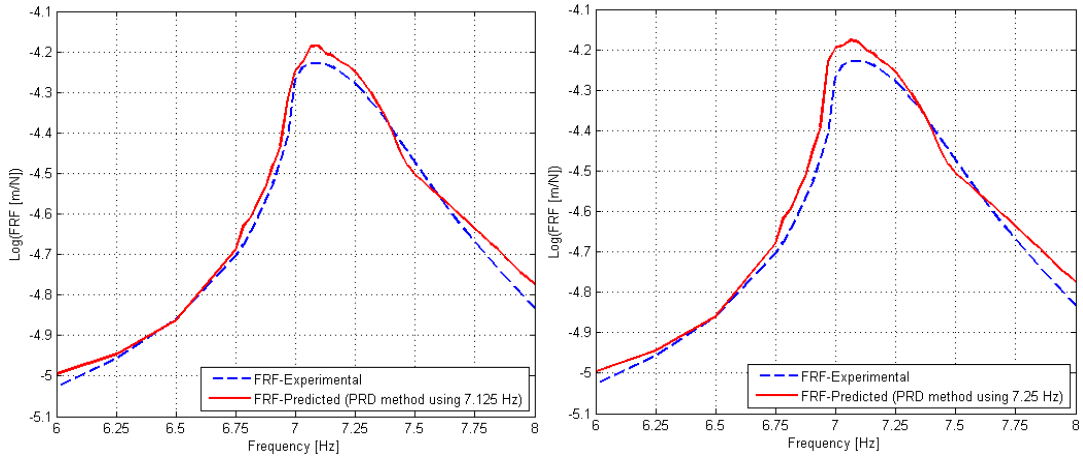

(a) (b)

Figure 5.55 Comparison of measured and predicted FRFs at F=10.4N (PRD method is used at (a) 7.125 Hz (b) 7.25 Hz)

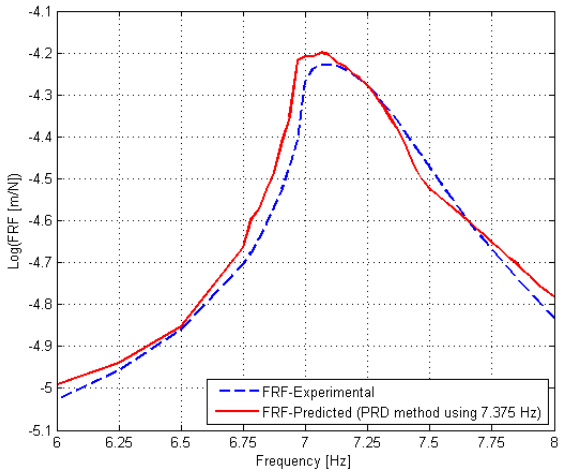

Figure 5.56 Comparison of measured and predicted FRFs at F=10.4N (PRD method is used at 7.375 Hz)

Regenerated nonlinear FRF curves are also compared with each other as well as with the experimental one for F=10.4N as shown in Figure 5.57.

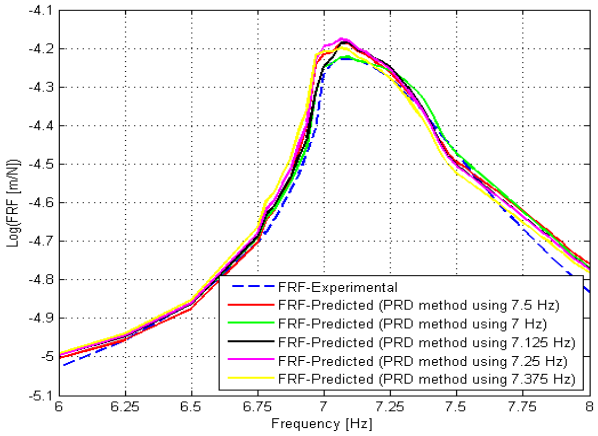

Figure 5.57 Comparison of experimental and regenerated FRFs by using PRD method at 7 Hz, 7.125 Hz, 7.25 Hz, 7.375 Hz and 7.5 Hz

As can be observed from the Figure 5.57, regenerated nonlinear FRFs and experimental nonlinear FRFs matches are in good agreement at F=10.4N. Finally, the comparison of the predicted and experimental nonlinear FRFS at F=15N are given in Figure 5.58, Figure 5.59 and Figure 5.60.

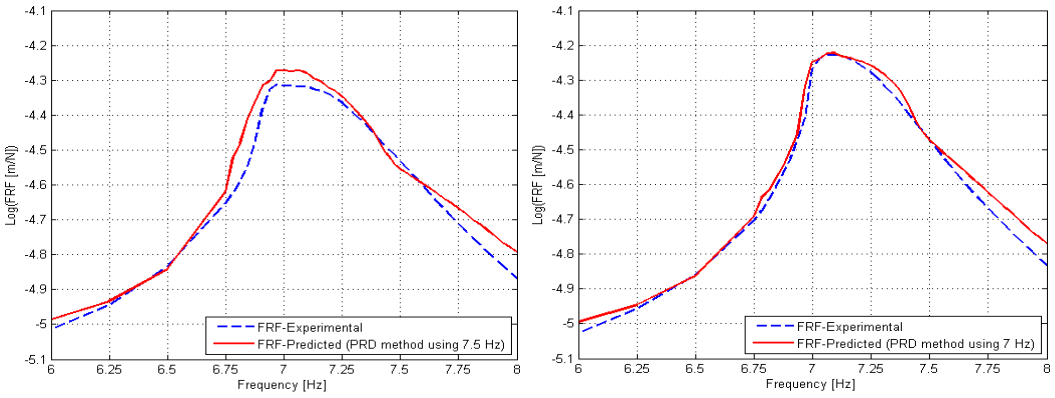

(a) (b)

Figure 5.58 Comparison of measured and predicted FRFs at F=15N (PRD method is used at (a) 7.5 Hz (b) 7 Hz)

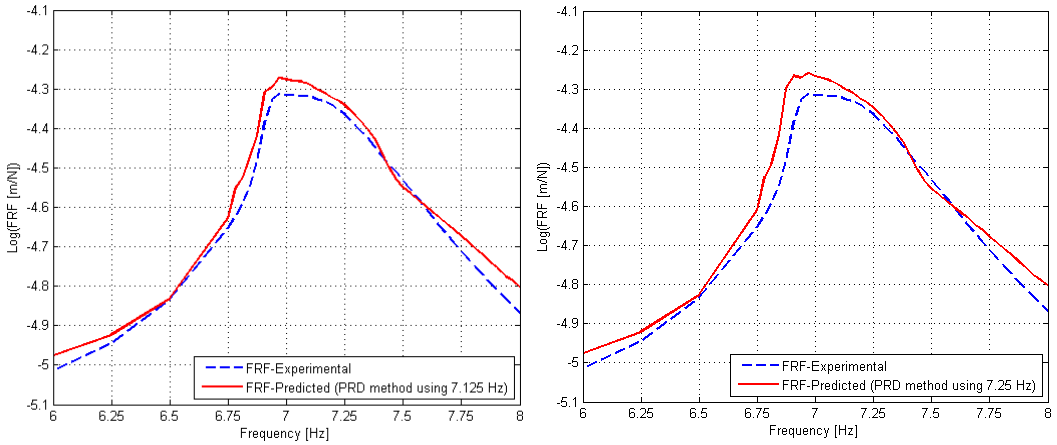

(a) (b)

Figure 5.59 Comparison of measured and predicted FRFs at F=15N (PRD method is used at (a) 7.125 Hz (b) 7.25 Hz)

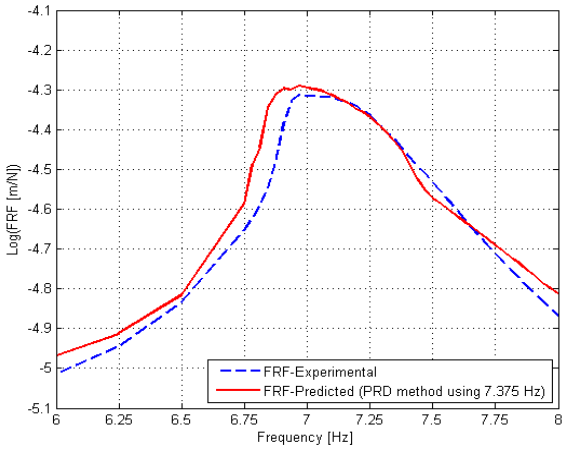

Figure 5.60 Comparison of measured and predicted FRFs at F=15N (PRD method is used at 7.375 Hz)

Similarly, regenerated nonlinear FRF curves are also compared with each other as well as with the experimental one for F=15N as shown in Figure 5.61.

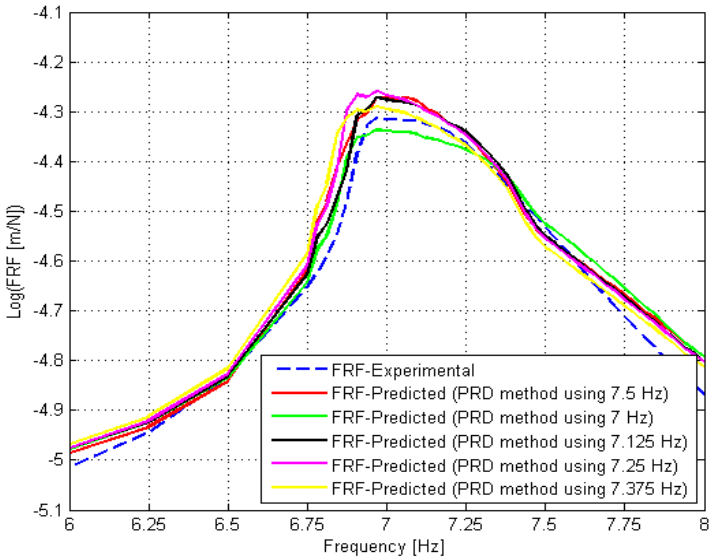

Figure 5.61 Comparison of experimental and regenerated FRFs by using PRD method at 7 Hz, 7.125 Hz, 7.25 Hz, 7.375 Hz and 7.5 Hz

From Figure 5.61, it is seen that there is a very good agreement between the regenerated and experimental nonlinear FRFs at F=15N.

Since the predicted FRFs are close to each other regardless of the frequency used in PRD method, it is better to quantify the similarity between the regenerated and experimental FRFs, by using the Frequency Response Assurance Criteria (FRAC) given below [85].

$$FRAC = \frac{\left|\left\{H_{Xrj}(\omega)\right\}^{H}\left\{H_{Arj}(\omega)\right\}\right|^{2}}{\left(\left\{H_{Xrj}(\omega)\right\}^{H}\left\{H_{Xrj}(\omega)\right\}\right)\left(\left\{H_{Arj}(\omega)\right\}^{H}\left\{H_{Arj}(\omega)\right\}\right)} \tag{5.1}$$

In Equation (5.1) $\left\{H_{Xrj}(\omega)\right\}$ and $\left\{H_{Arj}(\omega)\right\}$ are the experimental and calculated FRFs over the frequency spectrum ω respectively. Superscript H represents the

complex conjugate transpose. FRAC value changes between zero and one. FRAC value of unity represents full correlation between experimental and calculated FRFs and FRAC value of zero indicates no correlation between experimental and calculated FRFs.

By using the Equation (5.1) FRAC values are calculated for all the excitation frequency cases at all forcing levels. The results are given in Table 5.18.

Table 5.18 FRAC values for PRD method

Forcing Level	PRD Method				
	Used at 7.5Hz	**Used at 7Hz**	**Used at 7.125Hz**	**Used at 7.25Hz**	**Used at 7.375Hz**
5N	0.9823	0.9922	0.9820	0.9678	0.9429
10.4N	0.9826	0.9945	0.9902	0.9788	0.9622
15N	0.9843	0.9748	0.9864	0.9486	0.9492

From Table 5.18, it is seen that the FRAC values are very close to 1 for most of the cases at all forcing levels the worst value being approximately 0.95. At F=5N and F=10.4N, the FRFs predicted by PRD method using 7 Hz have slightly larger value compared to the other cases. Similarly, at F=15N, the FRFs predicted by PRD method using 7.125 Hz has slightly larger FRAC value compared to the other cases. The worst results are obtained at 7.375 Hz. However, it may not be possible to observe a trend.

5.6 Application of DDF Method for Identifying Nonlinearity

In this section, nonlinearity of the gun barrel is identified by using DDF method [79]. As mentioned in theory part, since nonlinear FRF measurements at two constant forcing levels are necessary for the application of the method, we can construct a total of 3 force combinations by using the experimental measurements made at 3 forcing levels. These force combinations are given in Table 5.19.

Table 5.19 Force combinations used in DDF method

Force Combination	Low Forcing Level	High Forcing Level
1	F=5N	F=10.4N
2	F=5N	F=15N
3	F=10.4N	F=15N

In order to investigate the effect of choosing different force levels on the accuracy of the DDF method, for each of force combination case, nonlinearities are identified and are compared to each other.

5.6.1 Force Combination 1

Real and imaginary parts of the describing function are obtained from experimental measurements by applying DDF method. Curves fitted to the real and imaginary parts of the describing function values obtained through DDF method are shown in Figure 5.62.

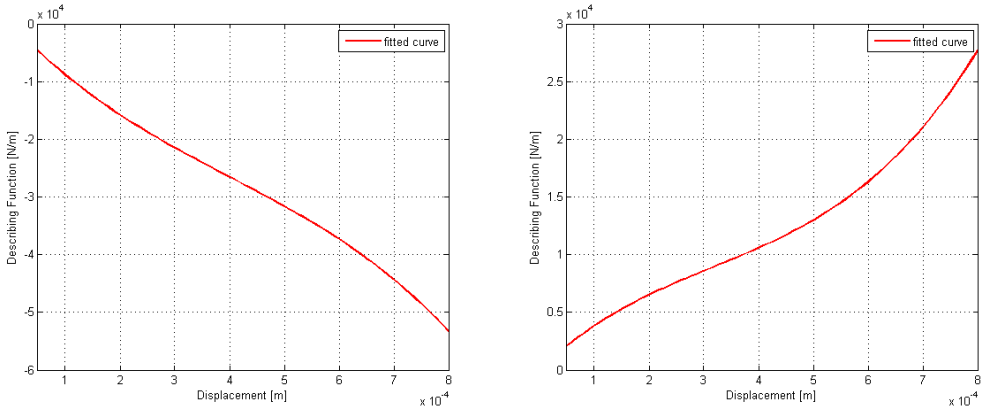

(a) (b)

Figure 5.62 Calculated describing function (a) Real part (b) Imaginary part

For the real and imaginary parts of describing function, 3rd order polynomial functions are fit. Corresponding coefficients of the polynomial functions are given in Table 5.20.

Table 5.20 Coefficients of the polynomials fit to the data for the real and imaginary parts of the describing function

	p_3	p_2	p_1
Real Part of Describing Function $p_3x^3 + p_2x^2 + p_1x$	$-1.06\text{x}10^{14}$	$1.26\text{x}10^{11}$	$-1.00\text{x}10^{8}$
Imaginary Part of Describing Function $p_3x^3 + p_2x^2 + p_1x$	$8.43\text{x}10^{13}$	$-8.08\ \text{x}10^{10}$	$4.52\text{x}10^{7}$

5.6.2 Force Combination 2

Real and imaginary parts of the describing function are obtained from experimental measurements by applying DDF method. Curves fitted to the real and imaginary parts of the describing function values obtained through DDF method are shown in Figure 5.63.

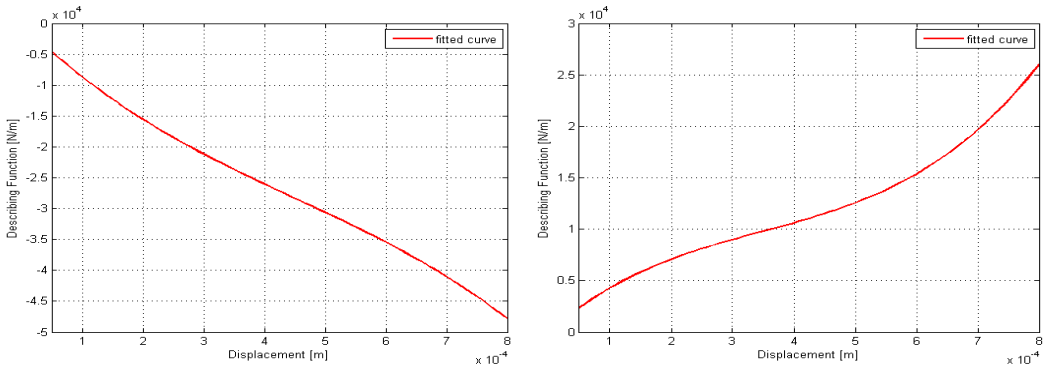

(a) (b)

Figure 5.63 Calculated describing function (a) Real part (b) Imaginary part

For the real and imaginary parts of describing function, 3rd order polynomial functions are fit. Corresponding coefficients of the polynomial functions are given in Table 5.21.

Table 5.21 Coefficients of the polynomials fit to the data for the real and imaginary parts of the describing function

	p_3	p_2	p_1
Real Part of Describing Function $p_3x^3 + p_2x^2 + p_1x$	$-8.42\text{x}10^{13}$	$1.14\text{x}10^{11}$	$-9.73\text{x}10^{7}$
Imaginary Part of Describing Function $p_3x^3 + p_2x^2 + p_1x$	$9.83\text{x}10^{13}$	$-1.03\text{ x}10^{11}$	$5.20\text{x}10^{7}$

5.6.3 Force Combination 3

Real and imaginary parts of the describing function are obtained from experimental measurements by applying DDF method. Curves fitted to the real and imaginary parts of the describing function values obtained through DDF method are shown in Figure 5.64.

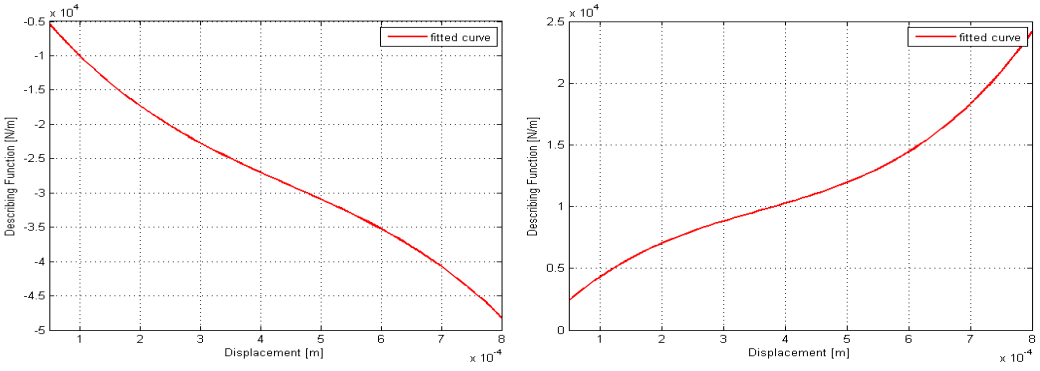

(a) (b)

Figure 5.64 Calculated describing function (a) Real part (b) Imaginary part

For the real and imaginary parts of describing function, 3rd order polynomial functions are fit. Corresponding coefficients of the polynomial functions are given in Table 5.22.

Table 5.22 Coefficients of the polynomials fit to the data for the real and imaginary parts of the describing function

	p_3	p_2	p_1
Real Part of Describing Function $p_3x^3 + p_2x^2 + p_1x$	$-1.27\text{x}10^{14}$	$1.71\text{x}10^{11}$	$-1.15\text{x}10^{8}$
Imaginary Part of Describing Function $p_3x^3 + p_2x^2 + p_1x$	$9.74\text{x}10^{13}$	$-1.05\ \text{x}10^{11}$	$5.23\text{x}10^{7}$

5.7 Comparison of Identified Nonlinearity Using DDF Method with Each of the Force Combinations

In this section, calculated real and imaginary parts of the describing function obtained from experimental measurements by using DDF method are compared to each other for each of the force combinations employed. The comparisons are shown in Figure 5.65 and Figure 5.66 for the real and imaginary parts of the describing functions, respectively.

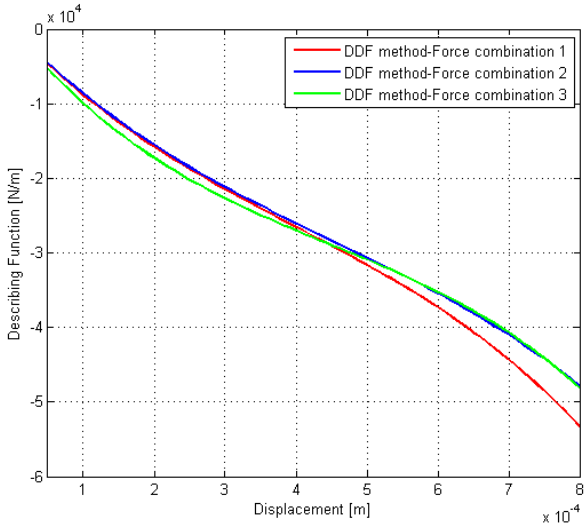

Figure 5.65 Comparison of identified real parts of describing functions

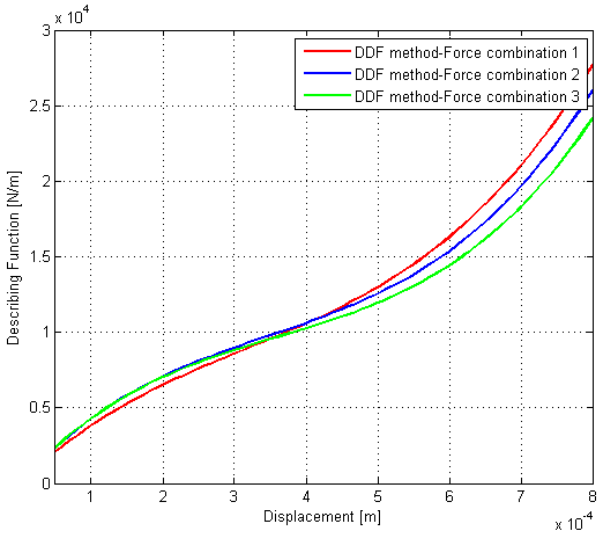

Figure 5.66 Comparison of identified imaginary parts of describing functions

As seen from Figure 5.65 and Figure 5.66, calculated real and imaginary parts of the describing functions are quite similar for different force combinations, therefore it

can be concluded that the forcing level used in the application of the DDF method does not have a significant effect on the identified nonlinearities. However, it is more important to compare the predicted nonlinear FRFs by using the nonlinearities identified employing different force combinations.

5.8 Application of DDF Method for Obtaining Linear FRFs

Using the describing function values obtained and the measured nonlinear FRF values, linear FRFs of the structure are predicted by applying DDF method for each force combination. For each force combination, there are two possibilities for obtaining the linear FRFs: Either of the low forcing or high forcing levels can be used. These possibilities are shown in Table 5.23.

Table 5.23 Possible linear FRF calculation

Force Combination	Force Level Used to Calculate Linear FRF	Case No
1	F=5N	1
	F=10.4N	2
2	F=5N	3
	F=15N	4
3	F=10.4N	5
	F=15N	6

Both of the low forcing level or high forcing levels are used separately in the prediction of the linear FRF, in order to study the effects of choosing low or high forcing levels on the performance of the linear FRF prediction of the method. Six different linear FRF curves predicted are compared with the FRFs measured at F=0.5N in Figure 5.67 and Figure 5.68, and with each other in Figure 5.69.

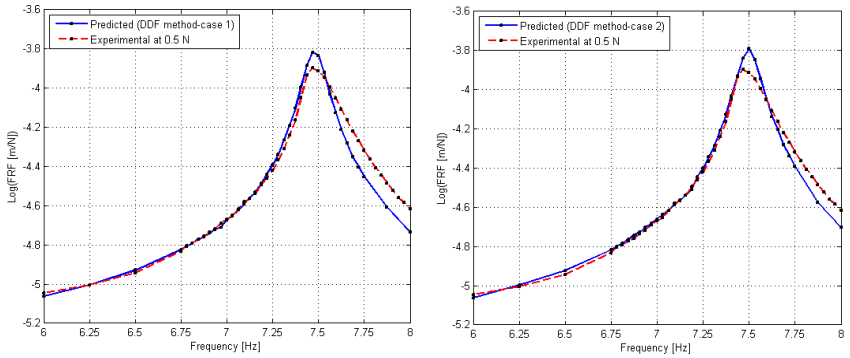

(a) (b)

Figure 5.67 Comparison of measured FRFs at F=0.5N with predicted linear FRFs by using (a) DDF method-case 1 (b) DDF method-case 2

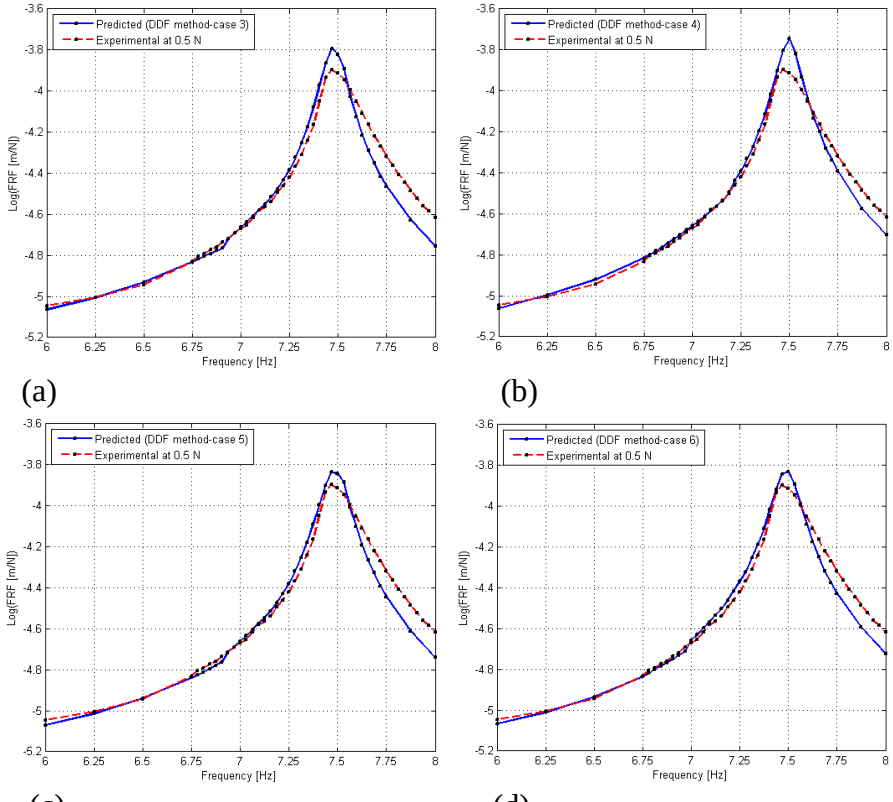

(a) (b)

(c) (d)

Figure 5.68 Comparison of measured FRFs at F=0.5N with predicted linear FRFs by using (a) DDF method-case 3 (b) DDF method-case 4 (c) DDF method-case 5 (d) DDF method-case 6

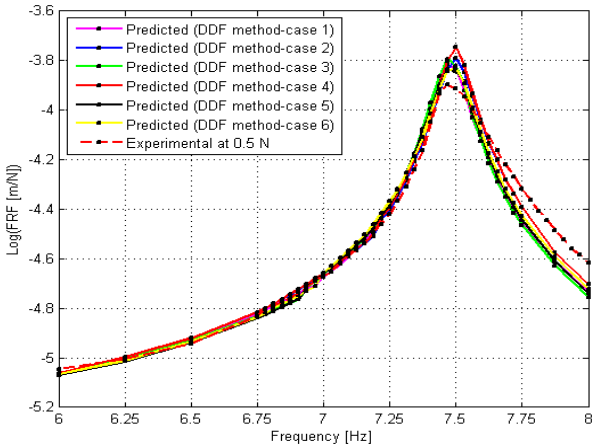

Figure 5.69 Comparison of measured FRFs at F=0.5N with predicted linear FRFs by using DDF method

As can be observed from Figure 5.67 and Figure 5.68, FRFs measured at low forcing level (F=0.5N) deviate from the linear FRFs of the system which can be obtained by using the DDF method. It is observed from Figure 5.69 that there are slight differences at the resonance region for each of six linear FRFs obtained by using DDF method (deviation of the peak amplitude from the mean amplitude value is approximately 10%). Therefore we can conclude that force combinations and using either of low or high forcing levels to calculate linear FRFs do not have considerable effects on the predicted linear FRFs.

5.9 Prediction of Nonlinear FRFs by Using Linear FRFs and Identified Nonlinearity Obtained from DDF Method

In this section, by using the identified nonlinearity and linear FRFs by using the DDF method, the nonlinear FRFs at F=5N, F=10.4N and F=15N are regenerated for all the six different combinations. Firstly, the results are compared with nonlinear FRFs experimentally measured at F=5N. The results are given in Figure 5.70, Figure 5.71 and Figure 5.72.

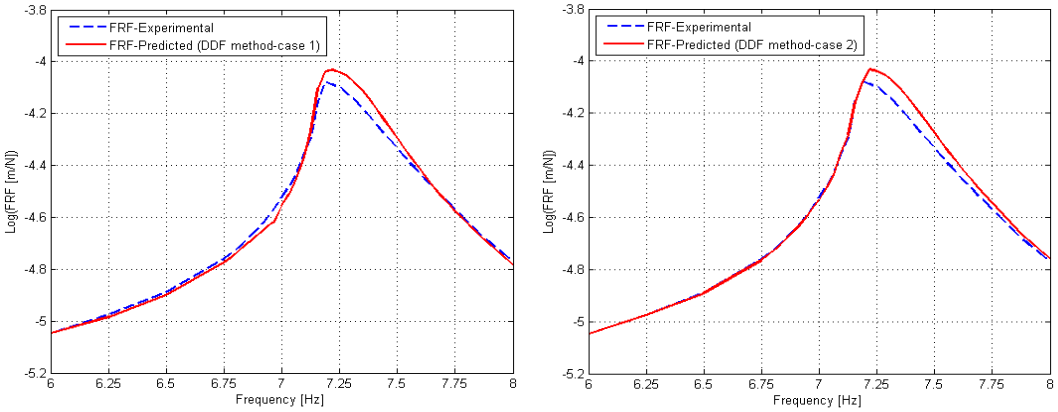

(a) (b)

Figure 5.70 Comparison of measured FRFs at F=5N with predicted nonlinear FRFs by using (a) DDF method-case 1 (b) DDF method-case 2

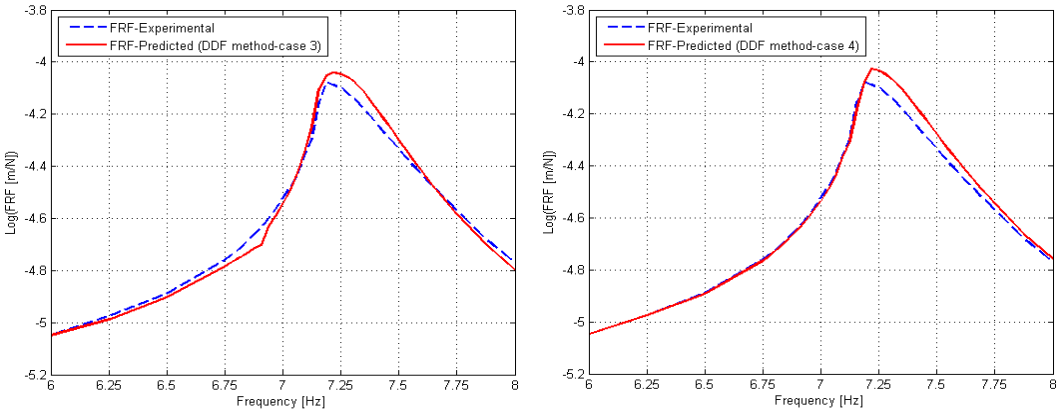

(a) (b)

Figure 5.71 Comparison of measured FRFs at F=5N with predicted nonlinear FRFs by using (a) DDF method-case 3 (b) DDF method-case 4

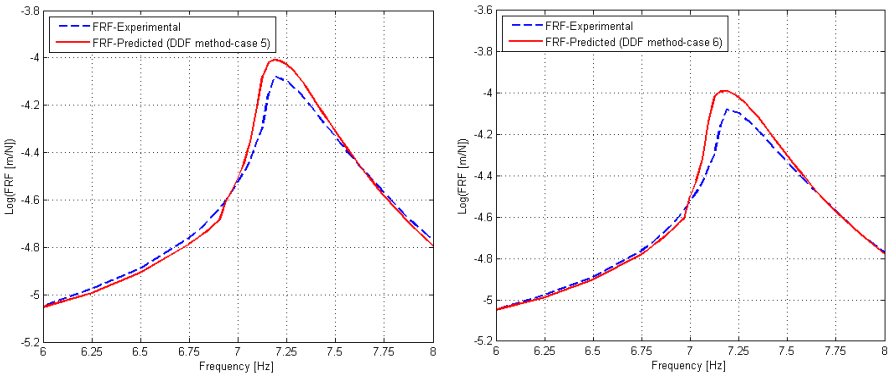

(a) (b)

Figure 5.72 Comparison of measured FRFs at F=5N with predicted nonlinear FRFs by using (a) DDF method-case 5 (b) DDF method-case 6

From these results, it can be concluded that the regenerated nonlinear FRFs match pretty well with experimentally measured ones at F=5N. The nonlinear FRFs regenerated in 6 different cases are also compared with each other as well as with the experimental one and it is shown in Figure 5.73.

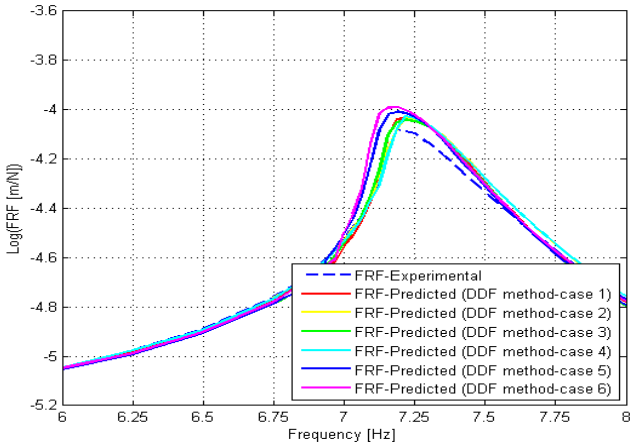

Figure 5.73 Comparison of measured FRFs at F=5N with predicted nonlinear FRFs by using DDF method

As can be seen from Figure 5.73, around the resonance frequency there are discrepancies between 6 different nonlinear FRF curves and the experimental nonlinear FRF curve at F=5N.

Similarly, the comparison of the regenerated and experimental nonlinear FRF curves at F=10.4N are given in Figure 5.74, Figure 5.75 and Figure 5.76.

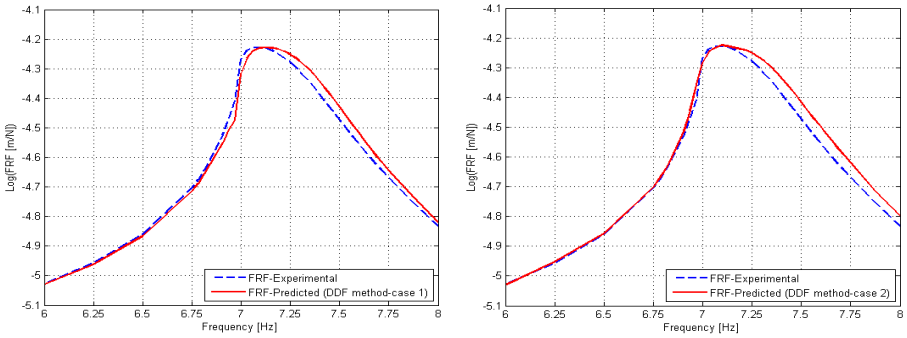

(a) (b)

Figure 5.74 Comparison of measured FRFs at F=10.4N with predicted nonlinear FRFs by using (a) DDF method-case 1 (b) DDF method-case 2

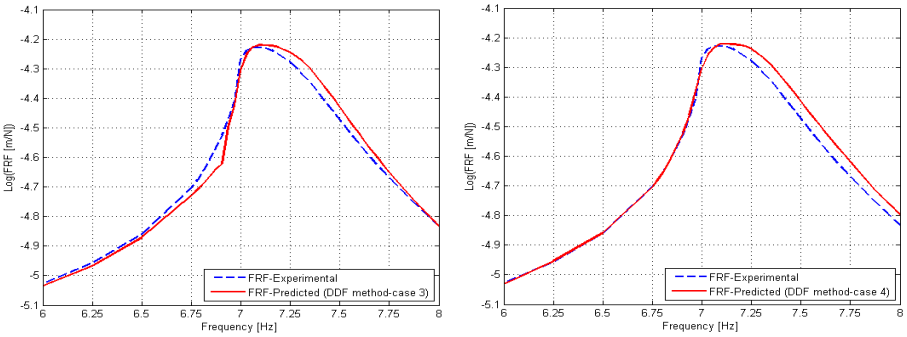

(a) (b)

Figure 5.75 Comparison of measured FRFs at F=10.4N with predicted nonlinear FRFs by using (a) DDF method-case 3 (b) DDF method-case 4

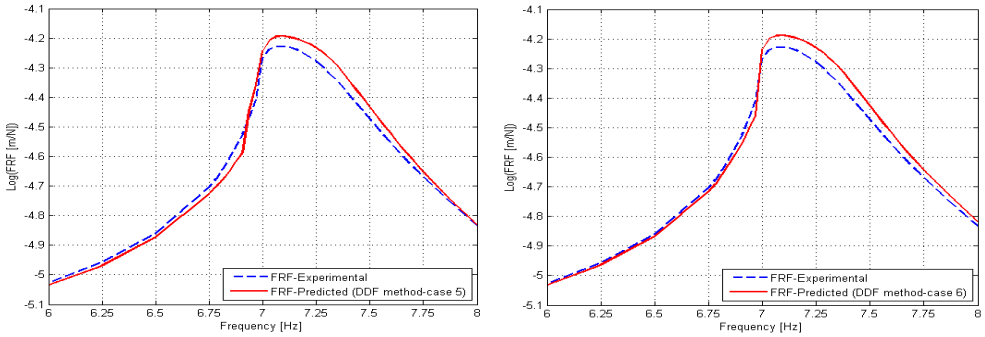

(a) (b)

Figure 5.76 Comparison of measured FRFs at F=10.4N with predicted nonlinear FRFs by using (a) DDF method-case 5 (b) DDF method-case 6

From the results, it can be concluded that there is a good agreement between the regenerated nonlinear FRFs and measured ones at F=10.4N. The nonlinear FRFs regenerated in 6 different cases are also compared with each other as well as with the experimental one and it is shown in Figure 5.77.

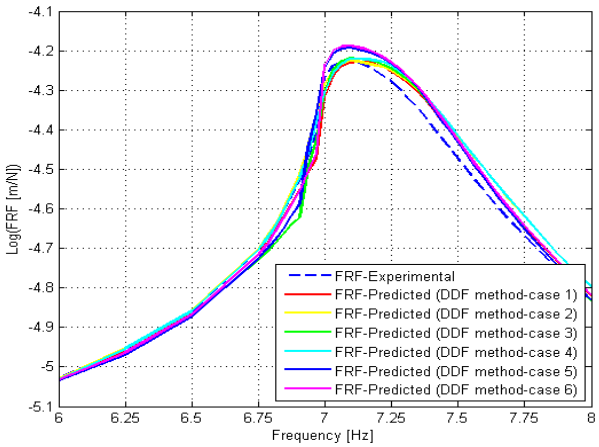

Figure 5.77 Comparison of measured FRFs at F=10.4N with predicted nonlinear FRFs by using DDF method

As can be seen from the Figure 5.77, around the resonance frequency there are slight discrepancies between 6 different regenerated nonlinear FRF curves and the experimental nonlinear FRF curve at F=10.4N.

Finally, the comparison of the regenerated and experimental nonlinear FRF curves at F=15N are given in Figure 5.78, Figure 5.79 and Figure 5.80.

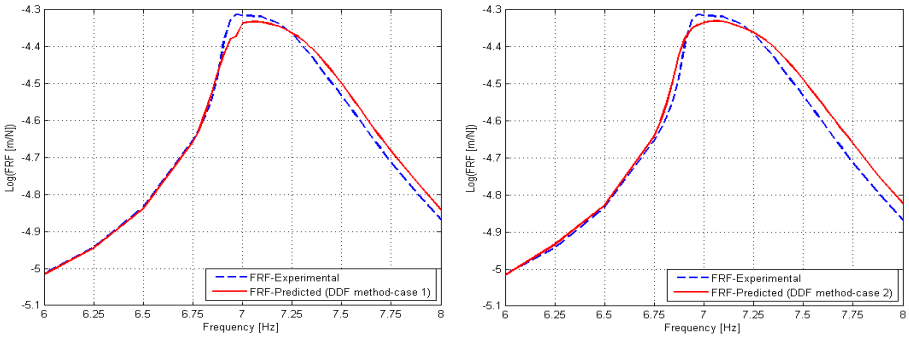

(a) (b)

Figure 5.78 Comparison of measured FRFs at F=15N with predicted nonlinear FRFs by using (a) DDF method-case 1 (b) DDF method-case 2

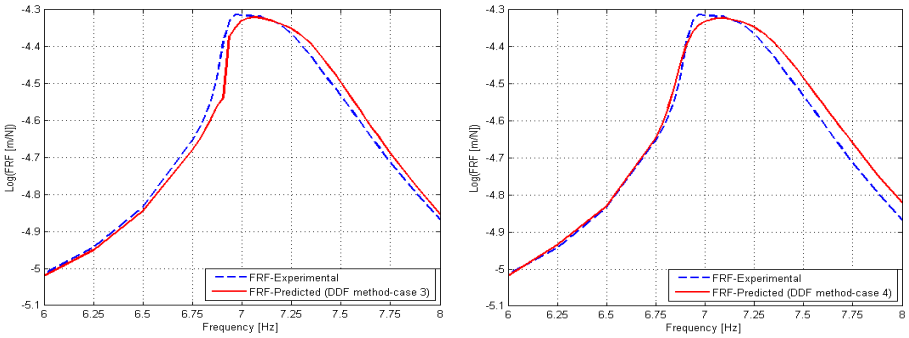

(a) (b)

Figure 5.79 Comparison of measured FRFs at F=15N with predicted nonlinear FRFs by using (a) DDF method-case 3 (b) DDF method-case 4

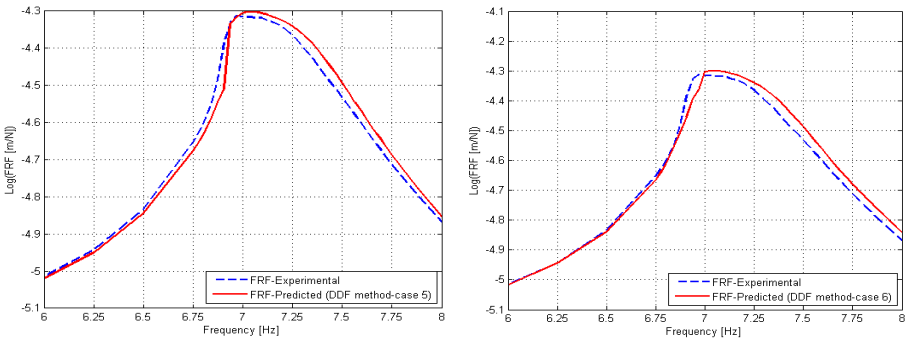

(a) (b)

Figure 5.80 Comparison of measured FRFs at F=15N with predicted nonlinear FRFs by using (a) DDF method-case 5 (b) DDF method-case 6

It is observed from the figures given above that, regenerated nonlinear FRFs match pretty well with experimentally measured ones at F=15N. The nonlinear FRFs regenerated in 6 different cases are also compared with each other as well as with the experimental ones and it is shown in Figure 5.81.

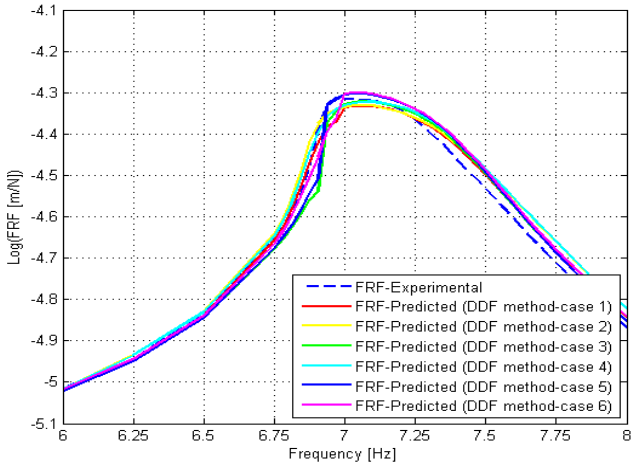

Figure 5.81 Comparison of measured FRFs at F=15N with predicted nonlinear FRFs by using DDF method

As can be seen from Figure 5.81, regenerated nonlinear FRFs and the experimental nonlinear FRFs are similar at F=15N.

If we compare the results shown in Figure 5.73, Figure 5.77 and Figure 5.81, the nonlinear FRFs regenerated in 6 different cases seem to match better with the experimental measurements as the force level increases. In order to have better observations, the similarity between the regenerated and experimental FRFs is quantified. At all forcing levels, FRAC values are calculated for all cases and the calculated FRAC values are given in Table 5.24.

Table 5.24 FRAC values for DDF method

Forcing Level	**DDF Method**					
	Case 1	**Case 2**	**Case 3**	**Case 4**	**Case 5**	**Case 6**
5N	0.9631	0.9483	0.9681	0.9555	0.9624	0.9475
10.4N	0.9669	0.9773	0.9665	0.9669	0.9803	0.9856
15N	0.9763	0.9793	0.9711	0.9753	0.9803	0.9642

From Table 5.24, it is observed that the FRAC values are very close to 1 for all cases. The highest FRAC value in each forcing level is obtained in a different case. However, there is no significant change in the FRAC values for the combinations used in DDF method. Furthermore, we cannot see a clear increasing trend in FRAC value as the force level increases, which is consistent with the observations made in the results shown in Figure 5.73, Figure 5.77 and Figure 5.81. Therefore we can say that, force combinations and the force level used to calculate linear FRF do not have a significant effect on the predicted FRFs.

5.10 Comparison of PRD and DDF Method for Identifying Nonlinearity and Obtaining Linear FRFs

In this section, firstly, real and imaginary parts of the describing functions identified from experimentally measured nonlinear FRFs by using PRD and DDF methods are

compared to each other. This comparison is shown in Figure 5.82 and Figure 5.83 for the real and imaginary parts of the describing functions, respectively.

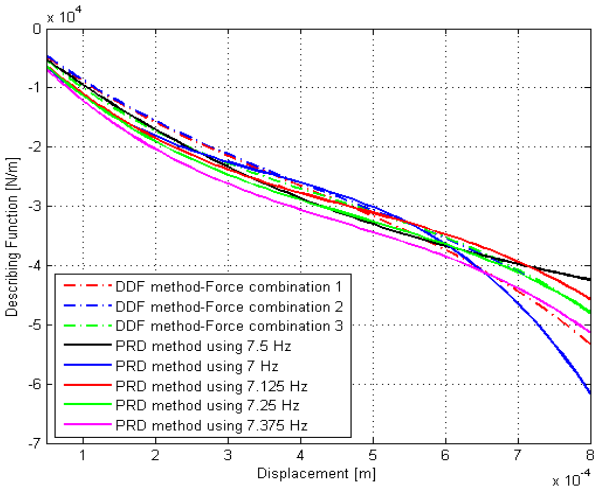

Figure 5.82 Comparison of real parts of describing functions identified by using DDF and PRD method

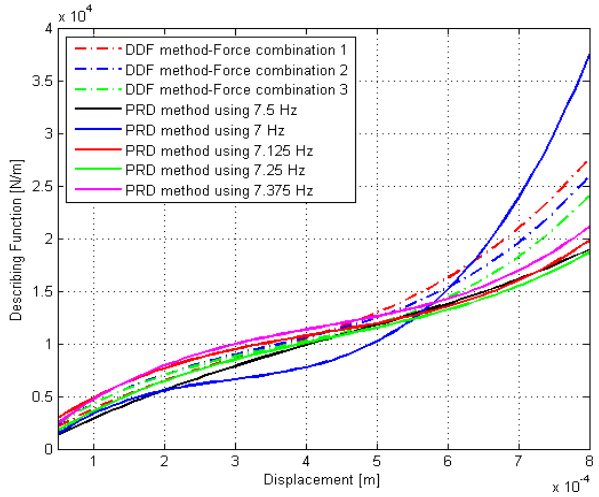

Figure 5.83 Comparison of imaginary parts of describing functions identified by using DDF and PRD method

As can be seen from Figure 5.82 and Figure 5.83, real and imaginary parts of the describing functions identified from experimentally measured nonlinear FRFs by using PRD and DDF methods are pretty close to each other. However, it is seen that, the real and imaginary parts of describing functions identified from measured FRFs at 7 Hz by using PRD method deviates from the other identified nonlinearities, especially at higher displacement values.

Secondly, predicted linear FRFs obtained by using PRD and DDF methods are compared in Figure 5.84.

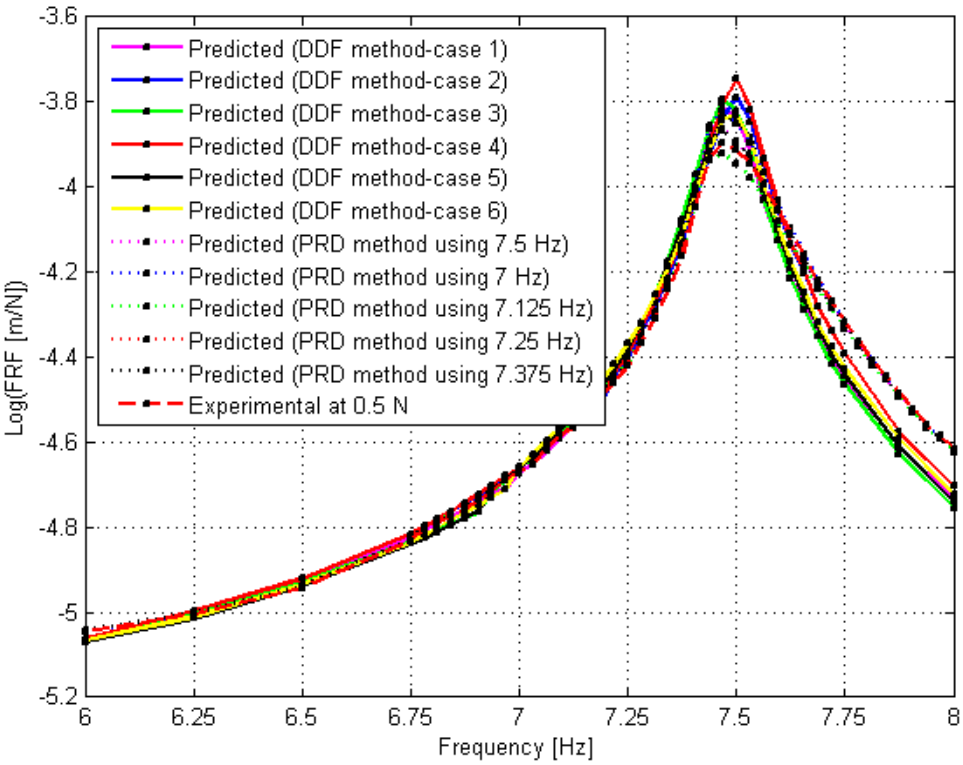

Figure 5.84 Comparison of predicted linear FRFs obtained by using PRD and DDF methods

As can be observed from Figure 5.84, there are some discrepancies between predicted linear FRFs obtained by using PRD and DDF methods especially around the resonance region. One of the reasons of these discrepancies is the differences in the identified imaginary part of the describing functions. Therefore we can say that the methods are more sensitive to damping nonlinearity predictions.

As a final comparison, regenerated nonlinear linear FRFs calculated by using PRD and DDF methods at F=5N, F=10.4N and F=15N are compared. The comparison is given in Figure 5.85, Figure 5.86 and Figure 5.87 for F=5N, F=10.4N and F=15N, respectively.

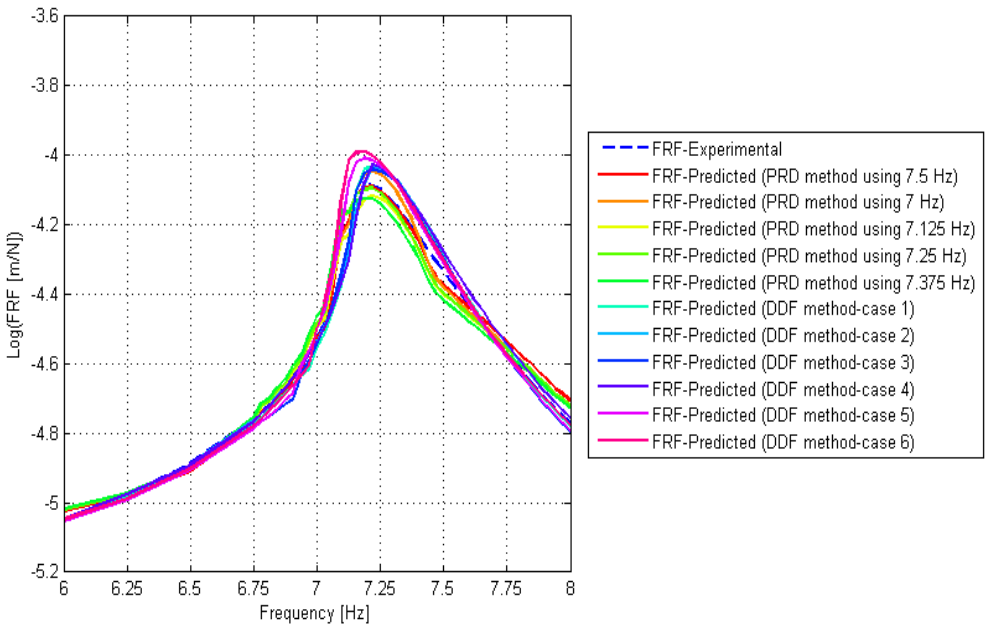

Figure 5.85 Comparison of predicted nonlinear FRFs by using PRD and DDF methods at F=5N

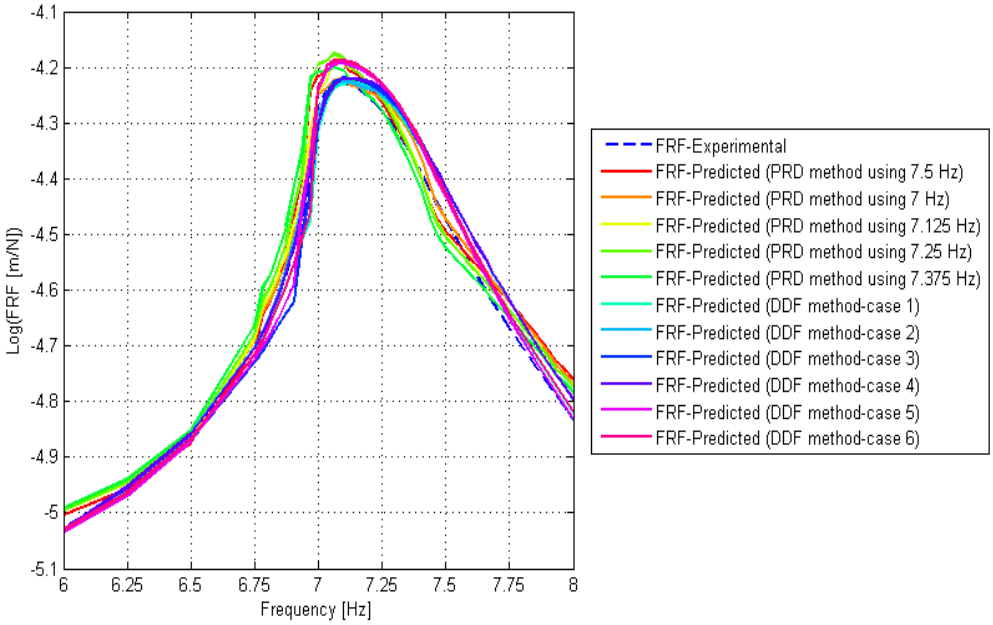

Figure 5.86 Comparison of predicted nonlinear FRFs by using PRD and DDF methods at F=10.4N

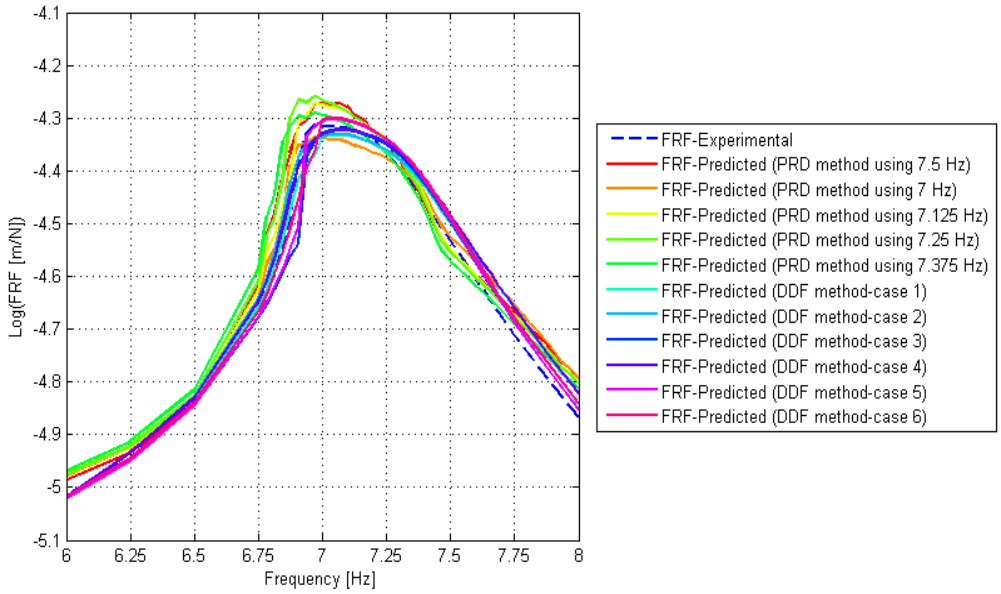

Figure 5.87 Comparison of predicted nonlinear FRFs by using PRD and DDF methods at F=15N

As can be observed from Figure 5.85, Figure 5.86 and Figure 5.87, although there are discrepancies around the resonance region between FRF curves, in general, regenerated nonlinear FRFs seems to be similar to each other for all the forcing levels tested (F=5N, F=10.4N and F=15N). In order to make better observations, the similarity between the regenerated and experimental FRFs is quantified. FRAC values are calculated and given in Table 5.25, in order to compare the regenerated FRFs at all forcing levels.

Table 5.25 FRAC values for PRD and DDF methods

PRD Method	**Using**	**Forcing Level 5N**		**Forcing Level 10.4N**		**Forcing Level 15N**
	7.5Hz	0.9823		0.9826		0.9843
	7Hz	0.9922		0.9945		0.9748
	7.125Hz	0.9820		0.9902		0.9864
	7.25Hz	0.9678		0.9788		0.9486
	7.375Hz	0.9429		0.9622		0.9492
DDF Method	**Case No**		**Case No**		**Case No**	
	5	0.9624	3	0.9665	1	0.9763
	6	0.9475	4	0.9669	2	0.9793

At F=5N, only FRAC values of DDF method-cases 5 and 6 are compared to the ones of PRD method because, as mentioned earlier, DDF method-cases 5 and 6 use F=10.4N and F=15N to obtain the linear FRF and nonlinearity, therefore it is more meaningful to compare only FRAC values of DDF method-cases 5 and 6 with FRAC values of PRD method. At F=10.4N and F=15N, only FRAC values of DDF method-cases 3 and 4 and DDF method-cases 1 and 2 are compared to the corresponding ones obtained by PRD method, because of a similar reason. As seen from Table 5.25, at all forcing levels, PRD method has higher FRAC values and therefore PRD method give a better prediction for nonlinear FRFs.

5.11 Model Updating of the FE Model of the Gun Barrel

In this section firstly linear FE model of the gun barrel is constructed and then it is updated by using the linear FRFs obtained through the PRD method and by applying inverse eigensensitivity method. The updated nonlinear model of the gun barrel is constructed by using the identified nonlinearity and updated linear FE model of the system. Then the nonlinear FRFs of the system are calculated at different forcing levels by using the updated model. Finally, predicted and measured FRFs of the system are compared and thus the accuracy of the updated nonlinear model of the system is studied.

5.11.1 FE Modeling of the Gun Barrel

In order to model the gun barrel in FE analysis software, firstly the components and the mechanism of the gun barrel should be understood. Typical gun barrel of a battle tank is shown in Figure 5.88.

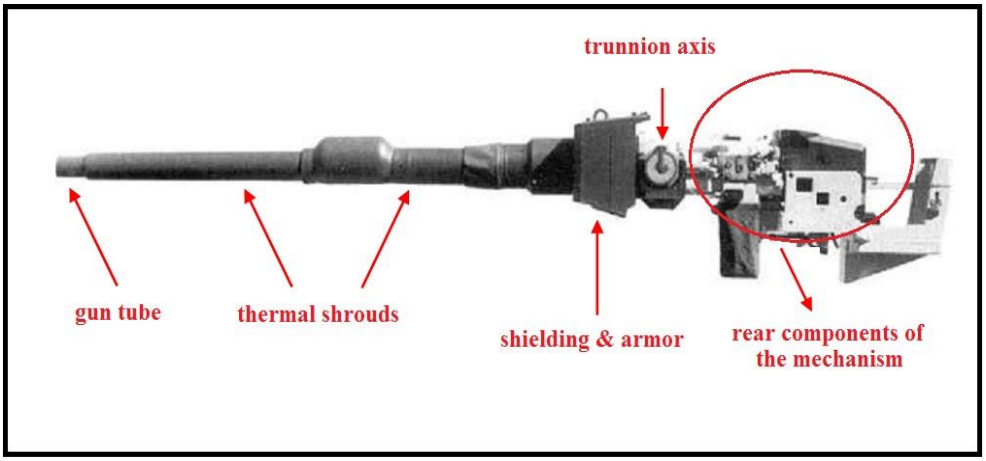

Figure 5.88 Gun barrel of a battle tank

As seen from Figure 5.88, gun barrel is mainly composed of gun tube, thermal shrouds, shielding-armor and rear components of the mechanism. The main part of the rear components is the elevation motor assembly and which drives the gun barrel around the trunnion axis. The simplified model of the gun barrel system is shown in Figure 5.89.

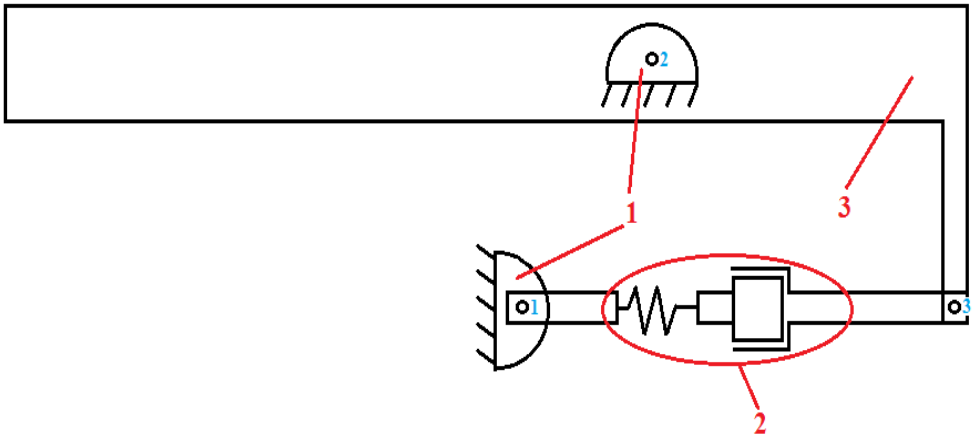

Figure 5.89 Simplified model of gun barrel system

Simplified model of the gun barrel system is composed of turret, elevation motor assembly and gun tube. Elevation motor assembly is modelled by a linear stiffness which acts force along the gun tube axis. The link names and the joints between the links are given in Table 5.26 and Table 5.27, respectively.

Table 5.26 Link names of the system

Link No	**1**	Turret
	2	Elevation Motor Assembly
	3	Gun Tube

Table 5.27 Joint locations in the gun barrel system

Joint No	**1**	Pin Joint	Turret-Elevation Motor Assembly
	2	Pin Joint (at trunnion axis)	Turret-Gun Tube
	3	Pin Joint	Gun Tube-Elevation Motor Assembly

The geometric and material properties of the gun tube (Figure 5.90) of the gun barrel system are also given in Table 5.28.

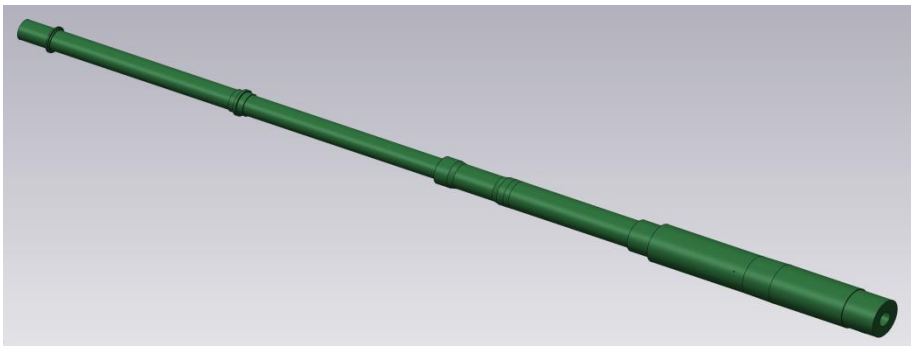

Figure 5.90 Gun Tube

Table 5.28 Geometrical and material properties of the gun tube

Material	Carbon Steel (0.4 % Carbon)
Modulus of Elasticity (GPa)	207
Length (m)	6.6
Inner Diameter (mm)	120

In the FE model constructed, mass of the thermal shrouds are neglected. The shielding-armor and the rear components of the system are modelled as point masses with mass and inertia properties given in Table 5.29 [86].

Table 5.29 Mass and inertia properties

	Mass (kg)	**Inertia (kg.m^2)**
Shielding-Armor	650	29.6
Rear Components of the System	1845	667

The stiffness of the elevation motor is taken as $140x10^6$ N/m by using similar elevation motor properties used to drive a different gun barrel system [86]. However, there is an uncertainty in the value of stiffness of the elevation motor, therefore this parameter will be used as the updating parameter in FE model updating.

5.11.2 Mesh Sensitivity Analysis for the FE Model of Gun Barrel

In this section before the construction of the initial FE model of the gun barrel in ANSYS, mesh sensitivity analysis is performed in order to see the effect of mesh sizing on the estimation of the fundamental natural frequencies of the structure. Constructed geometry and the FE model of the gun barrel used in the mesh sensitivity analysis is shown in Figure 5.91 and Figure 5.92, respectively.

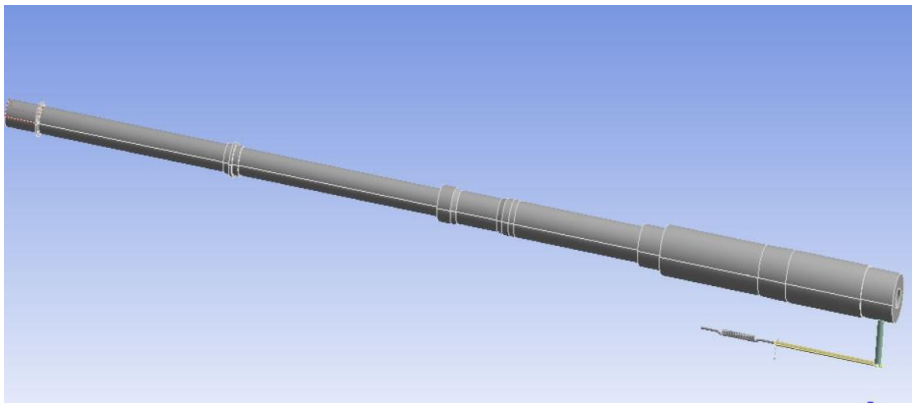

Figure 5.91 Constructed geometry of the gun barrel in ANSYS

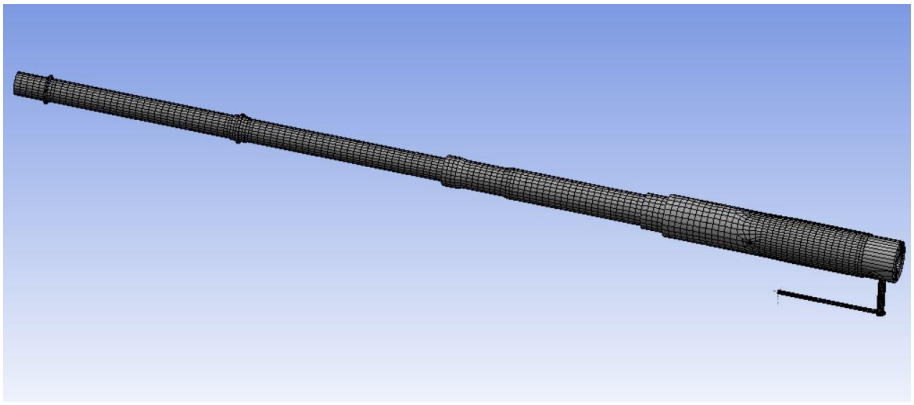

Figure 5.92 FE model of the gun barrel

Global mesh size for the FE model is varied between 0.1-0.01m, and for each of the global mesh size, modal analyses are performed in ANSYS. Fundamental natural frequency of the gun barrel is calculated for each case. In the analysis SOLID 186 element is used. The variation of the fundamental natural frequency with respect to global mesh sizing and the fundamental modeshape is shown in Figure 5.93 and Figure 5.94, respectively.

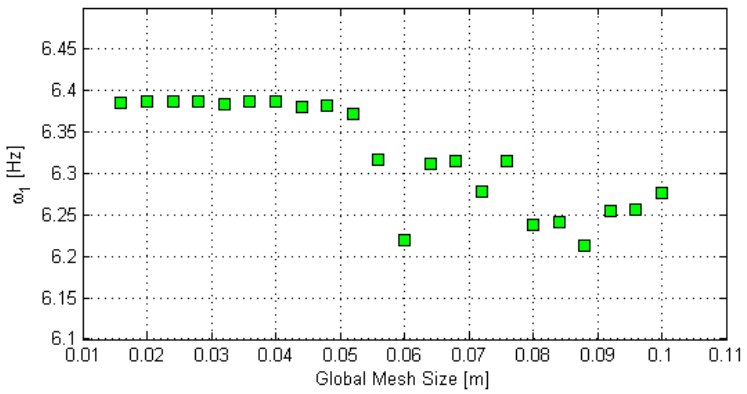

Figure 5.93 Variation of the fundamental natural frequency of the gun barrel with respect to global mesh sizing

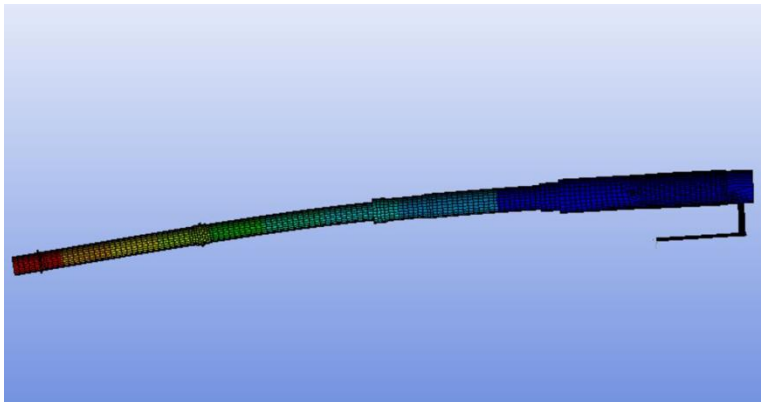

Figure 5.94 Fundamental modeshape of the gun barrel

As seen from Figure 5.93, fundamental natural frequency is converged approximately to 6.38 Hz after global mesh size reaches to approximately 0.05m. From the observations made for the mesh sensitivity analysis, mesh sizing of the initial FE model is selected as 0.05m.

5.11.3 Model Updating of the FE Model of Gun Barrel System

In this section, by using the observations made from mesh sensitivity analysis, initial linear FE model of the gun barrel is built in ANSYS and then the linear FE model is updated by employing the approach proposed. Since the best FRAC value is obtained for the PRD method using 7 Hz (shown in Section 5.10), the linear FE model of the gun barrel is updated by using the extracted linear FRFs employing the PRD method at 7 Hz and then applying inverse eigensensitivity method. Furthermore, FE model of the gun barrel is also updated by using ANSYS Design Exploration Optimization and the results obtained by two different updating techniques are compared with each other. In order to investigate the performance of the updated linear FE model, predicted FRFs are compared with the measured ones. Using the identified nonlinearity and updated linear FE model, updated nonlinear mathematical model of the gun barrel system is built. Finally, in order to demonstrate the accuracy of the

updated nonlinear model of the system, predicted and measured FRFs of the gun barrel are compared at different forcing levels.

In the initial FE model, the stiffness of the elevation motor is taken as $140x10^6$ N/m. The fundamental natural frequency and the driving point FRF at the tip of gun barrel (node 1 in the experiments) in transverse direction are calculated in ANSYS by using the FE model. In ANSYS, sufficient number of modes (100) is used to calculate FRFs, in order to minimize truncation error. Comparisons of the fundamental natural frequency and the linear FRFs obtained from FE analysis with those obtained from experiments by using PRD method are given in Table 5.30 and Figure 5.95, respectively.

Table 5.30 Comparison of the fundamental natural frequency obtained from initial FE model with the one obtained from experimental FRFs by using PRD method

Mode Number	Natural Frequency (PRD Method) (Hz)	Natural Frequency (Initial FE Model) (Hz)	Error (%)
1	7.46875	6.375	-14.64

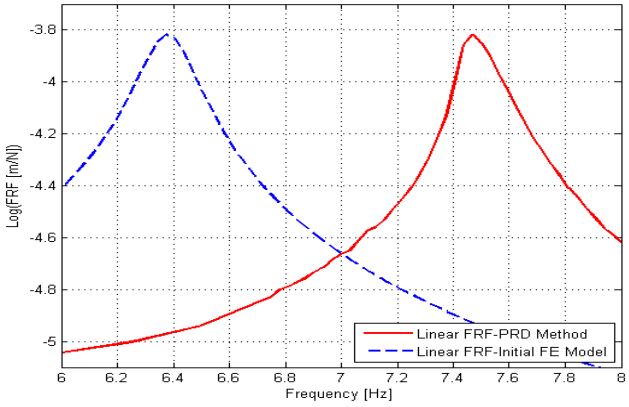

Figure 5.95 Comparison of the linear FRFs obtained from initial FE model with those obtained from experimental FRFs by using PRD method

As can be seen in Table 5.30 and Figure 5.95, there are considerable differences between two results; therefore the FE model of the gun barrel needs to be updated. As mentioned earlier there is a considerable uncertainty in the elevation motor stiffness, therefore elevation motor stiffness is selected as the updating parameter in the FE model. For the selected parameter, element of the sensitivity matrix is calculated by using the forward difference approximation with *O(h)* which is given by Equation (5.2), at each iteration step.

$$r'(p_i) = \frac{r(p_{i+1}) - r(p_i)}{\Delta h} \tag{5.2}$$

After 9 iterations, stiffness of the elevation motor is converged to 499x10^6 N/m. The convergence graph of stiffness of the elevation motor is given in Figure 5.96.

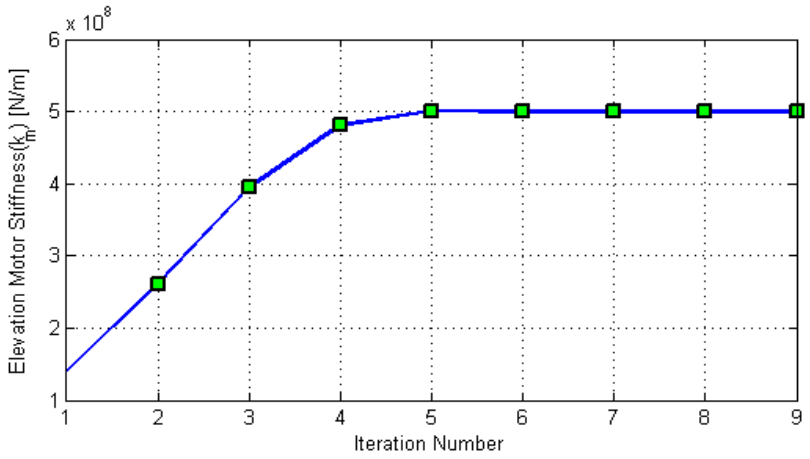

Figure 5.96 Convergence of the stiffness of the elevation motor

The same stiffness value (499x10^6 N/m) is also found by using ANSYS Design Exploration Optimization. Using the elevation motor stiffness value, the FE model is

updated. Then, the fundamental natural frequency of the updated linear model of the gun barrel is calculated and compared with that of the initial FE model, as well as with the fundamental natural frequency obtained from experiments by using PRD method, in Table 5.31.

Table 5.31 Comparison of the fundamental natural frequency obtained from initial and updated FE models with the value obtained from measurements by using PRD method

Mode Number	Natural Frequency (PRD Method) (Hz)	Natural Frequency (Initial FE Model) (Hz)	Error (%)	Natural Frequency (Updated FE Model) (Hz)	Error (%)
1	7.46875	6.375	-14.64	7.46875	0.00

As can be seen in Table 5.31, the fundamental natural frequency of the gun barrel is perfectly estimated by using the updated FE model.

In order to see the performance of the updated FE model in the prediction of other natural frequencies which are not used in updating the FE model, the second and third natural frequency of the gun barrel in transverse direction are calculated by using the updated linear FE model and it is compared with those obtained from the initial FE model, as well as with the measured ones (Table 5.32).

Table 5.32 Comparison of the second and third natural frequency obtained from initial and updated FE models with experimental values

Mode Number	Natural Frequency (Experimental) (Hz)	Natural Frequency (Initial FE Model) (Hz)	Error (%)	Natural Frequency (Updated FE Model) (Hz)	Error (%)
2	22.203	17.777	-19.94	21.816	-1.742
3	52.191	43.897	-15.89	45.694	-12.45

As can be seen in Table 5.32, there is a considerable improvement in the calculated value of the second natural frequency, and only a slight improvement in the calculated value of the third natural frequency of the gun barrel.

In Figure 5.97, the linear FRFs obtained from experimentally measured nonlinear FRFs by using PRD method are compared with those calculated from the initial and updated FE models of the gun barrel. As can be seen in Figure 5.97 again a considerable improvement is obtained for the updated FE model.

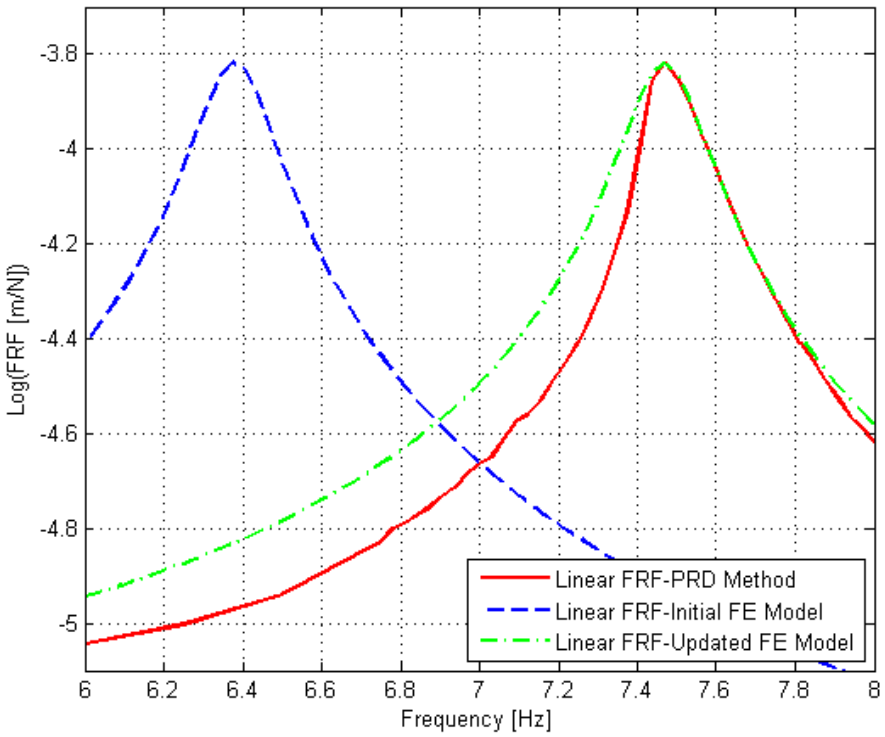

Figure 5.97 Comparison of the linear FRF obtained by using PRD method from experimentally measured nonlinear FRFs, with those calculated from, initial and updated FE models

Since the ultimate goal is to have accurate nonlinear response predictions from the updated FE model of the gun barrel, nonlinear FRFs experimentally measured at F=5N, F=10.4N and F=15N are compared with those obtained from the initial and FE updated models (composed of original and updated FE models, respectively, combined with identified nonlinearity). The results are given in Figure 5.98, Figure 5.99 and Figure 5.100 for the forcing levels F=5N, F=10.4N and F=15N, respectively.

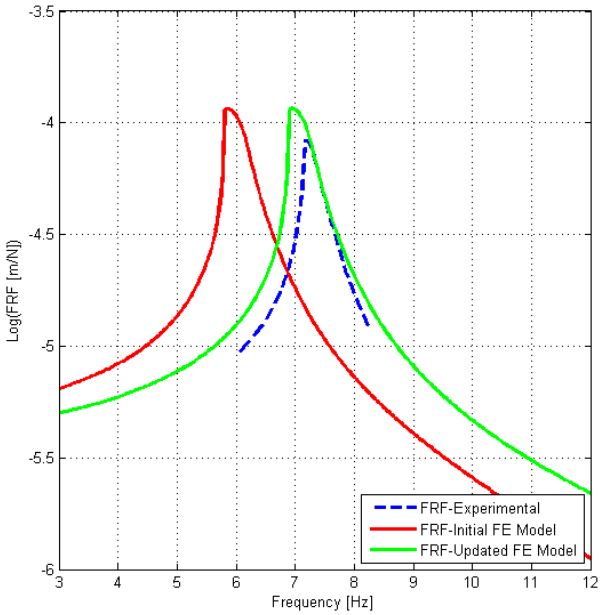

Figure 5.98 Comparison of FRFs obtained from initial and updated models with the experimental ones for F=5N

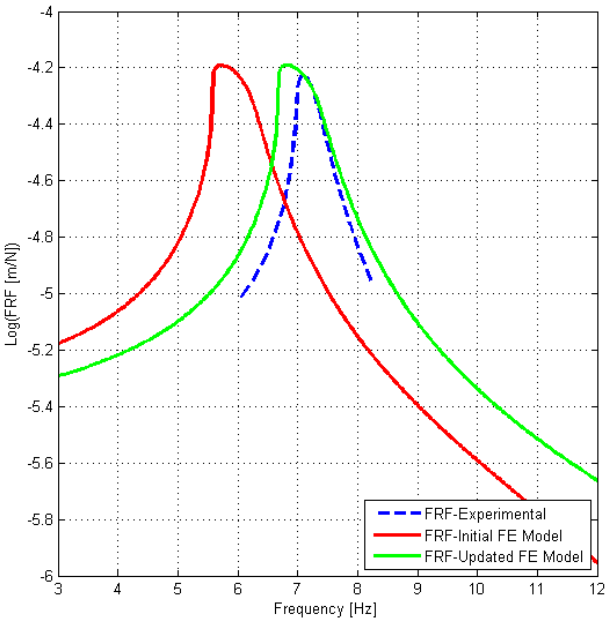

Figure 5.99 Comparison of FRFs obtained from initial and updated models with the experimental ones for F=10.4N

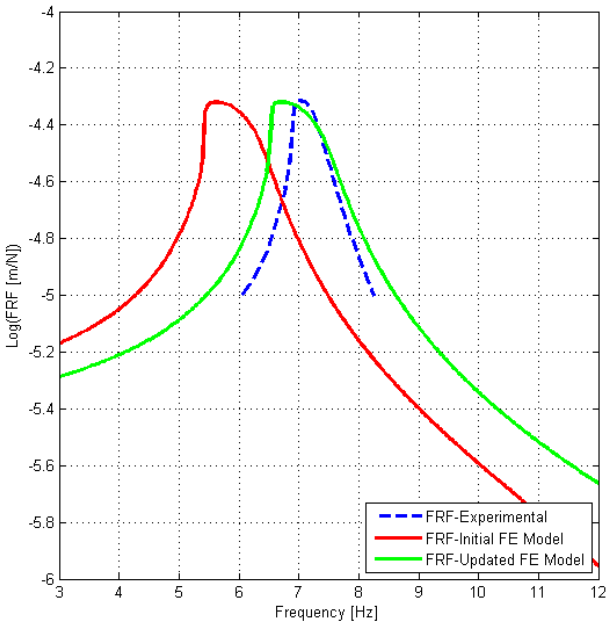

Figure 5.100 Comparison of FRFs obtained from initial and updated models with the experimental ones for F=15N

As can be observed in Figure 5.98, Figure 5.99 and Figure 5.100, considerable improvements are obtained with the updated FE model of the structure at all forcing levels. If the peak responses of the nonlinear FRF curves are observed, better match is obtained with the updated FE model at F=15N. From these results it can be concluded that, the developed model updating approach for nonlinear system is very successfully applied to a complicated real engineering problem (gun barrel of a battle tank) and a very good nonlinear model of the gun barrel system is constructed for the fundamental mode of the system.

CHAPTER 6

SUMMARY AND CONCLUSION

In this thesis, a new model updating technique for nonlinear structures having local nonlinearities is developed. As it is not easy to accurately model nonlinearity in a structure theoretically, it is a usual practice to identify nonlinearity from experimental measurements. Still the linear part of the model may need to be updated when theoretical and experimental responses do not mach. When there are multiple nonlinearities including friction in a structure; it is not possible to obtain the linear FRF of the system accurately by using low forcing levels in the experiments. In this thesis, a model updating approach for nonlinear structures having multiple nonlinearities including friction type of nonlinearity is presented. The approach is based on the method developed (PRD method) to calculate linear FRFs of a nonlinear structure by using nonlinear FRFs measured at various forcing levels. The method simultaneously identifies multiple nonlinearities in the system parametrically as well. Although there are various nonlinear identification methods, the method proposed here has the feature of extracting the FRFs of the underlying linear system while identifying nonlinearity in the system. After obtaining linear FRFs, inverse eigensensitivity method is employed to update the FE model of the linear part of the nonlinear structure.

Firstly, verifications of the PRD method for nonlinear lumped SDOF, MDOF systems and a nonlinear structure are demonstrated by using simulated experimental data, and thus the accuracy of the method is studied. It is clearly observed that for the lumped case studies with and without polluting data, PRD method is very successful in the estimation of nonlinear parameters and linear FRFs, even for systems with multiple nonlinearities including friction type of nonlinearity. As a more complex

case study, the application of PRD method to a nonlinear experimental structure (T-beam which has cubic stiffness and dry friction nonlinearities) is given. Again, in this case study, simulated experimental results are used. In order to simulate the nonlinear response of the system, first FE model of the linear part of the T-beam is built in ANSYS, and linear FRFs are obtained by performing modal analysis in ANSYS. Then using the nonlinear parameters for cubic stiffness and dry friction and calculated linear FRFs, nonlinear responses are obtained by employing the harmonic balance method. The calculated FRF values are polluted and used as measured nonlinear FRF data. Then employing PRD method, the nonlinearities in the system are identified and the FRFs are calculated. It is observed that identified nonlinearities and calculated linear FRFs match quite well with actual values. The effect of the excitation frequency (at which measurements are made) on the accuracy of PRD method is also investigated by using the nonlinear T-beam. By using PRD method at a different excitation frequency each time, the values of the nonlinear parameters are calculated and it is shown that, more accurate identification is possible when the excitation frequency is closer to the resonance of the underlying linear system. Although there are some exceptions, in general, the error in the estimated nonlinear parameter values tends to increase when excitation frequency deviates from the resonance frequency. As a final case study, in order to compare the proposed PRD method with the recently developed DDF method which identifies nonlinearity and simultaneously extracts the linear FRFs, the value of nonlinear parameter is calculated for a SDOF system with cubic stiffness nonlinearity. When the results obtained from PRD and DDF method are compared, it is seen that, better estimates are obtained for the nonlinearity by using PRD method for that case study. When only the results of DDF method is investigated, it is also observed that, worst estimation of the nonlinear parameter for the DDF is obtained for the force set where the difference between the low and high force used in DDF method is minimum.

After verifying the accuracy of PRD method by using simulated case studies, PRD method is applied to a real test system (T-beam) for model updating of a real

nonlinear system. Firstly, applying PRD method, both linear FRFs and the nonlinearities in the system are obtained from experimentally measured nonlinear FRFs. In order to demonstrate the effect of using different frequencies of excitation on the performance of PRD method, six different excitation frequencies are used. By applying PRD method that uses each of these frequencies at a time, nonlinearities in the structure are identified in the form of describing functions, and linear FRFs are obtained. It is seen that linear FRFs obtained using the describing functions identified from the tests conducted at different frequencies are not considerably different from each other, even though identified imaginary parts of the describing functions from these tests are rather different from each other. Linear FE model of the system modeled in ANSYS is updated for the first mode of the structure by employing the inverse eigensensitivity method and also by using the linear FRFs calculated through PRD method. It is observed that very good match is obtained between the results of updated model and experimental ones. Combining the updated linear FE model with the identified nonlinearity, updated nonlinear model of the T-beam is obtained. It is shown that, considerable improvements are obtained for the FRFs calculated with the updated model for all forcing levels. Consequently, the proposed method is successfully applied to a real test system and the accuracy of the method is verified by using this set up.

As a next experimental work, for the same T-beam, linear FRFs are obtained from experimentally measured nonlinear FRFs for the first, second and third global modes of the test system by using PRD method. The linear FE model of the test structure is updated for the first three global modes of the structure by using the extracted linear FRFs employing first the PRD method and then using ANSYS Design Exploration Optimization. From these sets of experiments it is observed that the linear FRFs of the system that are obtained by applying the PRD method proposed, are not accurately represented by the FRFs measured at low forcing level (F = 0.05N). As it was shown in Chapter 3 that PRD method yields the FRFs of the underlying linear system in a nonlinear system accurately, it can be concluded even a very low forcing

level is used in the experiments, the measured FRFs at this low forcing level may not represent the linear FRFs accurately.

As a next study on the T-beam, the effect of using different finite difference formula on the model updating performance is investigated. In order to calculate the sensitivities, different numerical differentiation formulas are used. It is seen that although the number of iteration is same for all the cases, total computation time is smaller for the updating procedure that uses the first order forward and backward difference formula. So it is concluded that, in the model updating of FE models, forward or backward difference formula should be used in the sensitivity calculations in order to reduce computational effort.

Finally, model updating approach proposed is applied to a real engineering structure, which is the gun barrel of a battle tank. In the first set of experiments, the structure is excited with random forcing. Since the fundamental natural frequency of the gun barrel is under consideration, it is clearly shown that as the force level increases in the random excitation tests damping value of the fundamental mode increases and natural frequency decreases. From the results of random excitation tests, the nonlinearity in the system is clearly detected. In order to study the effect of using different frequencies of excitation on the performance of PRD method, once again, different excitation frequencies are used. By applying PRD method that uses each of these frequencies at a time, nonlinearities in the structure are parametrically identified in the form of describing functions, and also the linear FRFs are obtained. It is observed that FRFs measured at low forcing levels do not accurately represent the linear FRFs of the system. However, they can be obtained by using the PRD method proposed. FRFs measured at even a very low forcing level may not represent the linear FRFs accurately. It is also observed that linear FRFs obtained through PRD method which use the describing functions identified from the tests made at different frequencies have discrepancies around the resonance (deviation of peak amplitude from the mean amplitude value is approximately less than 9%). Based on these

observations, it can be concluded that if the excitation frequency used in PRD method is approximately in the 5% range of the resonance of the underlying linear system, there are no significant differences in the predicted linear FRFs. As a further study, nonlinearity of the gun barrel is identified by using DDF method. It is observed that the real and imaginary parts of the describing functions calculated by using different force combinations are very similar. Therefore it is concluded that forcing levels used in the method do not have a significant effect on the identified nonlinearities. Although it is also observed that the FRF values at the resonance region are slightly different for each of six linear FRFs obtained by the using DDF method, it can be concluded that force combinations and using either of low or high forcing levels to calculate linear FRFs do not have a considerable effect on the predicted linear FRFs. From the study of the nonlinear FRFs regenerated employing the identified nonlinearity and linear FRFs obtained from DDF method, it is observed that force combinations and using either of low or high forcing levels to calculate linear FRFs do not have a considerable effect on the predicted nonlinear FRFs. When the regenerated nonlinear FRFs obtained from PRD and DDF method are compared with experimentally measured nonlinear FRFs, by using FRAC values, it is observed that PRD method has higher FRAC values and therefore it is concluded that PRD method gives better results, as far as regeneration of nonlinear FRFs from identified nonlinearities and predicted linear FRFs are concerned.

After obtaining linear FRFs through the PRD method, linear FE model of the gun barrel constructed in ANSYS is updated by using inverse eigensensitivity method. It is observed that the fundamental natural frequency of the gun barrel is perfectly estimated by using the updated FE model. Furthermore there is a considerable improvement in the calculated value of the second natural frequency, and a slight improvement in the calculated value of the third natural frequency of the gun barrel. Then the updated nonlinear model of the test structure is constructed by using the identified nonlinearity and updated linear FE model of the system. Finally, predicted and measured FRFs of the test structure are compared at different forcing levels and

it is seen that considerable improvement is obtained for the updated FE model of the gun barrel at all forcing levels.

In conclusion the model updating approach is validated with different simulated case studies, a real experimental test system and an engineering structure. The main advantage of PRD method is that, for the application of the method there is no need for any vibration controller as in the cases of constant forcing or constant amplitude testing over a certain frequency range. Furthermore, the method simultaneously identifies multiple nonlinearities in the system parametrically and it has a feature of extracting the FRFs of the underlying linear system simultaneously. It is thus concluded that the method proposed can successfully be applied to complex engineering problems for obtaining accurate nonlinear models.

As a future work, model updating of nonlinear structures that have distributed nonlinearities over the structure rather than local nonlinearities may be studied. In this case, all the elements of the nonlinear FRF matrix need to be obtained experimentally, which may be a difficult task. Therefore a detailed investigation would be necessary to handle this difficulty. Also, as a further improvement, rotational DOFs can be included in the formulation for the updating of more complex structures. Finally, the possibility of using random excitation or impact testing should be investigated to obtain accurate linear FRFs of nonlinear structures.

REFERENCES

[1] E. Dascotte, P. Vanhonacker, Development of an Automatic Mathematical Model Updating Program, Proceedings of the 7th International Modal Analysis Conference, Las Vegas, Nevada,1989, 596-602.

[2] N.G. Nalitolela., J.E.T. Penny, M.I. Friswell, Updating Structural Parameters of a Finite Element Model by Adding Mass or Stiffness to the System, in: Proceedings of the 8th International Modal Analysis Conference, Kissimmee, Florida, 1990, 836-842.

[3] N.A. Roy, A. Girard, P.E. Dupuis, A Direct Energy Approach for Updating Dynamic Finite Element Models, in: Proceedings of the 9th International Modal Analysis Conference, Florence, Italy, 1991, 51-57.

[4] M. Brughmans, G. Hrycko, J. Wyzykowski, Application of FEM Model Correlation and Updating Techniques on an Aircraft Using Test Data of a Ground Vibration Survey, in: Proceedings of the 9th International Modal Analysis Conference, Florence, Italy, 1991, 517-525.

[5] M. Link, L. Zhang, Experience with Different Procedures for Updating Structural Parameters of Analytical Models Using Test Data, in: Proceedings of the 10th International Modal Analysis Conference, San Diego, California, 1992, 730-738.

[6] S.R. Ibrahim, W. D'Ambrogio, P. Salvani, A.J. Sestieri, Direct Updating of Nonconservative Finite Element Models Measured Input-Output, Proceedings of the 10th International Modal Analysis Conference, San Diego, California, 1992, 202-210.

[7] A. Aiad, P. Level, Y. Ravalard, A Global Updating Procedure to Improve Finite Elements Models, Proceedings of the10th International Modal Analysis Conference, San Diego, California, 1992, 992-998.

[8] H. Jung, D.J. Ewins, Error Sensitivity of the Inverse Eigensensitivity Method for Model Updating, in: Proceedings of the 10th International Modal Analysis Conference, San Diego, California, 1992, 1051-1056.

[9] G. Miccoli, F. Agostoni, Modal updating using sensitivity analysis, in: Proceedings of the 11th International Modal Analysis Conference, Kissimmee, Florida, 1993, pp.683-689.

[10] E. Dascotte, J. Strobbe, H. Hua, Sensitivity Based Model Updating Using Multiple Types of Simultaneous State Variables, Proceedings of the 13th International Modal Analysis Conference, Nashville, Tennessee, 1995, 1035-1040.

[11] M. Imregun, W.J. Visser, D.J. Ewins, Finite Element Model Updating Using Frequency Response Function Data: I. Theory and Initial Investigation, Mechanical Systems and Signal Processing, 9 (2) (1995) 187–202.

[12] M. Imregun, W.J. Visser, D.J. Ewins, Finite Element Model Updating Using Frequency Response Function Data: II. Case Study on a Medium-Size Finite Element Model, Mechanical Systems and Signal Processing, 9 (2) (1995) 203-213.

[13] F.M. Hemez, Advanced Tools for Updating Damped Finite Element Models Using Static Modal and Flexibility Data, in: Proceedings of the 14th International Modal Analysis Conference, Dearborn, Michigan, 1996, 511-517.

[14] D. Lenoir, S. Cogan, G. Lallement, J.N. Bricout, Model Updating by Modal Synthesis of Experimental Forced Responses, in: Proceedings of the 16th International Modal Analysis Conference, Santa Barbara, California, 1998, 399-405.

[15] J.E. Mottershead, C. Mares, M.I. Friswell, S. James, Selection and Updating of Parameters for an Aluminium Space Frame Model, Mechanical Systems and Signal Processing, 14 (6) (2000) 923-944.

[16] W.L. Li, A new Method for Structural Model Updating and Joint Stiffness Identification, Mechanical Systems and Signal Processing, 16 (1) (2002) 155-167.

[17] S.V. Modak, T.K. Kundra, B.C. Nakra, Use of an Updated Finite Element Model for Dynamic Design, Mechanical Systems and Signal Processing, 16 (2002) 303–322.

[18] G.H. Kim, Y.S. Park, An Improved Updating Parameter Selection Method and Finite Element Model Update Using Multiobjective Optimization Technique, Mechanical System and Signal Processing, 18 (2004) 59-78.

[19] N. Cottin, J. Reetz , Accuracy of Multiparameter Eigenvalues Used for Dynamic Model Updating with Measured Natural Frequencies Only, Mechanical Systems and Signal Processing, 20 (2006) 65–77.

[20] R.M. Lin, J. Zhu, Model Updating of Damped Structures Using FRF Data, Mechanical Systems and Signal Processing, 20 (2006) 2200–2218.

[21] J. Carvalho, B.N. Datta, A. Gupta, M. Lagadapati, A Direct Method for Model Updating with Incomplete Measured Data and without Spurious Modes, Mechanical Systems and Signal Processing, 21 (2007) 2715–2731.

[22] V. Arora, S.P.Singh, T.K. Kundra, On the Use of Damped Updated FE Model for Dynamic Design, Mechanical Systems and Signal Processing, 23 (2009) 580–587.

[23] V. Arora, S.P.Singh, T.K. Kundra, Comparative Study of Damped FE Model Updating , Mechanical Systems and Signal Processing, 23 (2009) 2113–2129.

[24] M.T. Kozak, M. Öztürk, H.N. Özgüven, A Method in Model Updating Using Miscorrelation Index Sensitivity, Mechanical Systems and Signal Processing, 23 (2009) 1747-1758.

[25] P.A. Tarazaga, Y. Halevi, D.J. Inman, Modified Quadratic Compression Method for Mass and Stiffness Updating, Mechanical Systems and Signal Processing, 23 (2009) 1773–1783.

[26] S. Adhikari, M.I. Friswell, Distributed Parameter Model Updating Using the Karhunen-Loève Expansion, Mechanical Systems and Signal Processing, 24 (2010) 326–339.

[27] J.L. Zapico-Valle, R. Alonso-Camblor, M.P. González-Martínez, M. García-Diéguez, A New Method for Finite Element Model Updating in Structural Dynamics, Mechanical Systems and Signal Processing, 24 (2010) 2137–2159.

[28] J.E. Mottershead, M.Link, M.I. Friswell, The Sensitivity Method in Finite Element Model Updating: A Tutorial, Mechanical Systems and Signal Processing, 25 (2011) 2275–2296.

[29] K. Yuen, Updating Large Models for Mechanical Systems Using Incomplete Modal Measurement, Mechanical Systems and Signal Processing, 28 (2012) 297–308.

[30] J.D. Sipple, M.Sanayei, Finite Element Model Updating of the UCF Grid Benchmark Using Measured Frequency Response Functions, Mechanical Systems and Signal Processing 46(2014)179–190.

[31] I. Boulkaibet, L. Mthembu, T. Marwala, M.I. Friswell, S. Adhikari, Finite Element Model Updating Using the Shadow Hybrid Monte Carlo Technique, Mechanical Systems and Signal Processing, 52-53 (2015) 115–132.

[32] T.K. Hasselman, M.C. Anderson, W. Gan, Principal Components Analysis for Nonlinear Model Correlation, Updating and Uncertainty Evaluation, in: Proceedings of the 16th International Modal Analysis Conference, Santa Barbara, California, 1998, 644-651.

[33] M.C. Anderson, T.G. Carne, Model Correlation and Updating of a Nonlinear Finite Element Model Using Crush Test Data, Proceedings of the 17th International Modal Analysis Conference, Kissimmee, Florida, 1999, 1511-1517.

[34] M.C. Anderson, T.K. Hasselman, Minimizing Parameter Correlation in Nonlinear Model Updating, in: Proceedings of the 18th International Modal Analysis Conference, San Antonio, Texas, 2000, 109-115.

[35] T.D. Burton, F.M. Hemez, W. Rhee, Combined Model Reduction/SVD Approach to Nonlinear Model Updating, in: Proceedings of the 18th International Modal Analysis Conference, San Antonio, Texas, 2000, 116-123.

[36] V. Lenaerts, G. Kerschen, J.C. Golinval, Proper Orthogonal Decomposition for Model Updating of Non-linear Mechanical Systems, Mechanical Systems and Signal Processing, 15 (1) (2001) 31–43.

[37] F.M. Hemez, S.W. Doebling, Review and Assessment of Model Updating for Non-linear, Transient Dynamics, Mechanical Systems and Signal Processing, 15 (1) (2001) 45–74.

[38] S. Meyer, M. Link, Modelling and Updating of Local Non-linearities Using Frequency Response Residuals, Mechanical Systems and Signal Processing, 17 (1) (2003) 219–226.

[39] I. Isasa, A. Hot, S. Cogan, E. Sadoulet-Reboul, Model Updating of Locally Non-linear Systems Based on Multi-harmonic Extended Constitutive Relation Error, Mechanical Systems and Signal Processing, 25 (2011) 2413–2425.

[40] S.F. Masri, H. Sass, T.K. Caughey, A Nonparametric Identification of Nearly Arbitrary Nonlinear Systems, Journal of Applied Mechanics, 49 (1982) 619–628.

[41] E.F. Crawley, A.C. Aubert, Identification of Nonlinear Structural Elements by Force-State Mapping, AIAA Journal 24 (1986) 155–162 (Sections 3.2, 6.1).

[42] E.F. Crawley, K.J. O'Donnell, Identification of Nonlinear System Parameters in Joints Using the Force-State Mapping Technique, AIAA Paper 86-1013 (1986) 659–667 (Sections 3.2, 6.1).

[43] K. Yasuda, S. Kawamura, K. Watanabe, Identification of Nonlinear Multi-Degree-of-Freedom Systems (Presentation of an Identification Technique), JSME International Journal Series III, 31 (1988) 8–14.

[44] Y. Benhafsi, J.E.T. Penny, M.I. Friswell, A Parameter Identification Method for Discrete Nonlinear Systems Incorporating Cubic Stiffness Elements, International Journal of Analytical and Experimental Modal Analysis, Volume 7, Issue 3, (1992) 179-196.

[45] H.J. Rice, Identification of Weakly Non-linear Systems Using Equivalent Linearization, Journal of Sound and Vibration, 185 (3) (1995) 473–481.

[46] C. Soize, Stochastic Linearization Method with Random Parameters for SDOF Nonlinear Dynamical Systems: Prediction and Identification Procedures, Probabilistic Engineering Mechanics, 10 (1995) 143–152.

[47] F. Thouverez, L. Jezequel, Identification of a Localized Non-linearity, International Journal of Non-Linear Mechanics, 33 (1998) 935–945.

[48] C.M. Richards, R. Singh, Identification of Multi-Degree-of-Freedom Non-linear Systems Under Random Excitations by the Reverse-Path Spectral Method, Journal of Sound and Vibration, 213 (1998) 673–708.

[49] G. Kerschen, J.C. Golinval, K. Worden, Theoretical and Experimental Identification of a Non-linear Beam, Journal of Sound and Vibration, 244 (2001) 597–613.

[50] M.B. Özer, H.N. Özgüven, A New Method for Localization and Identification of Nonlinearities in Structures, 6th Biennial Conference on Engineering Systems Design and Analysis, Istanbul, Turkey, 2002.

[51] M.B Özer, H.N. Özgüven, T.J Royston, Identification of Structural Non-linearities Using Describing Functions and the Sherman–Morrison Method, Mechanical Systems and Signal Processing, 23 (2009) 30–44.

[52] G. Kerschen, V. Lenaerts, J.C. Golinval, VVT Benchmark: Application of the Restoring Force Surface Method, Mechanical Systems and Signal Processing 17(1) (2003) 189-193.

[53] S. Bellizzi, M. Defilippi, Non-linear Mechanical Systems Identification Using Linear Systems with Random Parameters, Mechanical Systems and Signal Processing, 17 (2003) 203–210.

[54] M. Thothadri, R.A. Casas, F.C. Moon, R.D'andrea, C.R. Johnson Jr., Nonlinear System Identification of Multi-Degree-of-Freedom Systems, Nonlinear Dynamics, 32 (2003) 307–322.

[55] A.A. Muravyov, S.A. Rizzi, Determination of Nonlinear Stiffness with Application to Random Vibration of Geometrically Nonlinear Structures, Computers and Structures, 81 (2003) 1513–1523.

[56] G. Kerschen, V. Lenaerts, J.C. Golinval, Identification of a Continuous Structure with a Geometrical Non-linearity, Part I: Conditioned Reverse Path Method, Journal of Sound and Vibration, 262 (2003) 889–906.

[57] M. Haroon, D.E. Adams, Y.W. Luk, A.A. Ferri, A Time and Frequency Domain Approach for Identifying Nonlinear Mechanical System Models in the Absence of an Input Measurement, Journal of Sound and Vibration, 283 (2005) 1137–1155.

[58] G. Kerschen, K. Worden, A.F. Vakakis, J.C. Golinval, Past, Present and Future of Nonlinear System Identification in Structural Dynamics, Mechanical Systems and Signal Processing, 20 (2006) 505-592.

[59] S. M. Spottswood, R. J. Allemang, Identification of Nonlinear Parameters for Reduced Order Models, Journal of Sound and Vibration 295 (2006) 226-245.

[60] P.F. Pai, A.N. Palazotto, Detection and Identification of Nonlinearities by Amplitude and Frequency Modulation Analysis, Mechanical Systems and Signal Processing, 22 (2008) 1107–1132.

[61] S. Marchesiello, L. Garibaldi, Identification of Clearance-type Nonlinearities, Mechanical Systems and Signal Processing, 22 (2008) 1133–1145.

[62] C. Xueqi, L. Qiuhai, H. Zhichao, G. Tieneng, A Two-step Method to Identify Parameters of Piecewise Linear Systems, Journal of Sound and Vibration, 320 (2009) 808–821.

[63] K. Worden, D. Hickey, M. Haroon, D.E. Adams, Nonlinear System Identification of Automotive Dampers: A Time and Frequency-domain Analysis, Mechanical Systems and Signal Processing 23 (2009) 104-126.

[64] A. Carrella, D.J. Ewins, Identifying and Quantifying Structural Nonlinearities in Engineering Applications from Measured Frequency Response Functions, Mechanical Systems and Signal Processing, 25 (2011) 1011–1027.

[65] Ö. Arslan, M.Aykan, H.N.Özgüven, Parametric Identification of Structural Nonlinearities from Measured Frequency Response Data, Mechanical Systems and Signal Processing, 25(2011) 1112–1125.

[66] H. Jalali, B.T. Bonab, H. Ahmadian, Identification of Weakly Nonlinear Systems Using Describing Function Inversion, Experimental Mechanics, 51 (2011) 739–747.

[67] M. Aykan, H.N. Özgüven, Parametric Identification of Nonlinearity in Structural Systems Using Describing Function Inversion, Mechanical Systems and Signal Processing, 40 (2013) 356–376.

[68] M. Eriten, M. Kurt, G. Luo, D.M. McFarland, L.A. Bergman, A.F. Vakakis, Nonlinear System Identification of Frictional Effects in a Beam with a Bolted Joint Connection, Mechanical Systems and Signal Processing, 39 (2013) 245–264.

[69] M. Aykan, H.N. Özgüven, Identification of Restoring Force Surfaces in Nonlinear MDOF Systems from FRF Data Using Nonlinearity Matrix, Topics in Nonlinear Dynamics, Volume 1: Proceedings of the 31st IMAC, A Conference on Structural Dynamics, 2013, 65-76.

[70] G. Canbaloglu, H.N. Özgüven, Obtaining Linear FRFs for Model Updating in Structures with Multiple Nonlinearities Including Friction, Topics in Nonlinear Dynamics, Volume 1: Proceedings of the 31st IMAC, A Conference on Structural Dynamics, 2013, 145-157.

[71] G. Canbaloglu, H.N. Özgüven, Model Updating of Nonlinear Structures, Nonlinear Dynamics, Volume 2: Proceedings of the 32nd IMAC, A Conference and Exposition on Structural Dynamics, 2014, 69-182.

[72] G. Canbaloglu, H.N. Özgüven, Experimental Validation of Pseudo Receptance Difference (PRD) Method for Nonlinear Model Updating, Nonlinear Dynamics, Volume 1: Proceedings of the 33rd IMAC, A Conference and Exposition on Structural Dynamics, 2015.

[73] A. Gelb, W.E. Vander Velde, Multiple-Input Describing Functions and Nonlinear System Design, McGraw Hill, New York, 1968.

[74] E. Budak, H.N. Özgüven, Iterative Receptance Method for Determining Harmonic Response of Structures with Symmetrical Non-linearities, Mechanical Systems and Signal Processing, 7 (1) (1993) 75–87.

[75] B. Kuran, H. N. Özgüven, A Modal Superposition Method for Non-Linear Structures, Journal of Sound and Vibration 189 (1996) 315–339.

[76] E. Ciğeroğlu, H.N. Özgüven, Non-linear Vibration Analysis of Bladed Disks with Dry Friction Dampers, Journal of Sound and Vibration, 295 (2006) 1028-1043.

[77] Ö. Tanrıkulu, B. Kuran, H.N. Özgüven, M. Imregün, Forced Harmonic Response Analysis of Non-linear Structures Using Describing Functions, AIAA Journal, 31 (7) (1993) 1313-1320.

[78] E. Ciğeroğlu, ME709 Lecture Notes, Middle East Technical University

[79] M. Aykan, Identification of Localized Nonlinearity for Dynamic Analysis of Structures, Ph.D. Thesis, Middle East Technical University, Graduate School of Natural and Applied Sciences, 2013.

[80] J.D. Collins, G.C. Hart, T.K. Hasselman, B. Kennedy, Statistical Identification of Structure, AIAA Journal, (12) (2) (1974) 185-190.

[81] J.V. Ferreira, Dynamic Response Analysis of Structures with Nonlinear Components, Ph.D. Thesis, Department of Mechanical Engineering, Imperial College London,1998.

[82] H.R.E. Siller, Non-linear Modal Analysis Methods for Engineering Structures, Ph.D. Thesis, Department of Mechanical Engineering, Imperial College London, 2004.

[83] A. Josefsson, M. Magnevall, K. Ahlin, On Nonlinear Parameter Estimation with Random Noise Signals, Proceedings of the 25th International Modal Analysis Conference, Orlando, USA, 2007.

[84] C.T. Kelly, Iterative Methods for Optimization, SIAM Press, Philadelphia, 1999.

[85] W. Heylen, S. Lammens, FRAC: a Consistent Way of Comparing Frequency Response Functions, Identification in Engineering Systems, Proceedings of the Conference Swansea, 1996.

[86] F. Büyükcivelek, Analysis and Control of Gun Barrel Vibrations, M.Sc. Thesis, Middle East Technical University, Graduate School of Natural and Applied Sciences, 2011.

APPENDIX A

PUBLISHED PAPERS DURING PHD

Obtaining Linear FRFs for Model Updating in Structures with Multiple Nonlinearities Including Friction*

Güvenç Canbaloğlu[1,2], H. Nevzat Özgüven[1]
[1]Department of Mechanical Engineering, Middle East Technical University, 06800 Ankara, TURKEY
[2]MGEO Division, ASELSAN Inc., 06750 Ankara, TURKEY
e-mail: gcanbal@aselsan.com.tr, ozguven@metu.edu.tr

ABSTRACT

Most of the model updating methods used in structural dynamics are for linear systems. However, in real life applications structures may have nonlinearity. In order to apply model updating techniques to a nonlinear structure, linear FRFs of the structure have to be obtained. The linear dynamic behavior of a nonlinear structure can be obtained experimentally by using low forcing level excitations, if friction type of nonlinearity does not exist in the structure. However when the structure has multiple nonlinearities including friction type of nonlinearity, nonlinear forces due to friction will be more pronounced at low forcing level excitations. Then it will not be possible to measure linear FRFs by using low level forcing. In this study a method is proposed to obtain linear FRFs of a nonlinear structure having multiple nonlinearities including friction type of nonlinearity by using experimental measurements made at low and high forcing levels. The motivation is to obtain FRFs of the linear part of the system that can be used in model updating of a nonlinear system. The method suggested can also be used as a nonlinear identification method for nonlinear systems. The proposed method is validated with different case studies using SDOF and lumped MDOF systems and simulated experimental data. The effect of the excitation frequency, at which experiments are carried out, on the accuracy of the proposed method, is also demonstrated.

KEYWORDS

Nonlinear identification, nonlinearity, friction nonlinearity, model updating, nonlinear structures

1 INTRODUCTION

Structural modeling is one of the most important stages in the design of a structure. Since design stage is iterative, the need for structural modeling has come into prominence and accurate prediction of the dynamic response of a structure has become a vital step in the design stage. With the development of computation technology, finite element (FE) method has established itself as the most common numerical method used for obtaining the dynamic response of engineering structures. However, application of FE method may yield inaccuracies arising from numerical and modeling errors. Due to these errors, there are always discrepancies between the dynamic responses obtained by FE method and experiment; therefore FE models need to be updated by using the experimental results and changing some of the parameters used in the FE model.

Over the last three decades various model updating methods have been developed in order to have correct analytical models that reflect the real dynamic responses better. However, most of the model updating methods available in the literature are for linear systems. Berman [1] updated the analytical mass matrix by using incomplete set of measured modes in order to achieve the orthogonality of the mass matrix. In order to correlate the FE model and test results of an aerospace structure, Sidhu and Ewins [2] proposed a method in which the error matrix equation was used. Caesar [3] used Berman's direct system matrix update method, suggested improvements on this method and applied the extended method to a test model. In a later study, Caesar [4] described the methods for updating mass and stiffness matrices based on the eigendynamic behavior of linear structures. Visser and Imregun [5] investigated the use of a model updating technique by using FRFs. They discussed the requirement for minimum measured data for successful implementation of the technique and applied the updating technique to different systems in order to demonstrate the effectiveness of the method. Larsson and Sas [6] worked on model updating

---

*G. Canbaloglu, H.N. Özgüven, Obtaining Linear FRFs for Model Updating in Structures with Multiple Nonlinearities Including Friction, Topics in Nonlinear Dynamics, Volume 1: Proceedings of the 31st IMAC, A Conference on Structural Dynamics, pp.145-157, 2013.

technique employing forced vibration testing. They proposed a set of updating equations based on force response data and investigated the limitation in the measurements and numerical aspects in the formulations. Bollinger [7] presented constrained optimization theory in order to improve FE model. Lammens et al. [8] optimized reduced analytical dynamic stiffness matrix by solving a linearized set of equations, and updated the FE model of an engine sub frame. Girard et al. [9] extended energy approach for the model updating of a rotating shaft mounted on hydrodynamic bearings. They applied the method to a simple shaft model including mass, stiffness and damping parameters. Billet et al. [10] used an updating method based on minimization of an error in constitutive relation in order to update a nuclear reactor building scale model. Mottershead et al. [11] compared the selection of different updating parameters in the model updating of an aluminum space frame. In a more recent work, Kozak et al. [12] presented a new error localization method and an updating routine and they applied the routine to different case studies.

Since most of the structures have nonlinear behavior, it is vital to have model updating techniques for nonlinear structures as well. In order to apply model updating techniques developed for linear systems to nonlinear structures and to correct linear system matrices, linear dynamic behaviors of the structure have to be experimentally obtained which may require identification of nonlinearity first. In early 1990's Benhafsi et al. [13] worked on the parametric identification of nonlinearities in structures by using describing function method. In a later study, Richards and Singh [14] studied on the identification of nonlinearities that are in the form of polynomial forms and they approximated the nonlinear elastic forces as polynomial functions. Chong and Imregun [15, 16] presented an identification procedure in terms of variable modal parameters for nonlinear systems. Adams and Allemang [17] derived a method for estimating the parameters of nonlinear models and demonstrate the implementation of this method on simulated data for SDOF and MDOF lumped parameter systems. One of most detailed nonlinear system identification literature survey was performed by Kerschen et al. [18] in which more than 400 papers are cited. Özer et al. [20] extended their previous study [19] and identified the nonlinearity in structures by using describing functions and Sherman-Morrison method. Jalali et al. [21] used the inversion of describing functions in order to identify the nonlinearities in the structure.

In a recent study by Arslan et al. [22], two different methods which are capable of identifying nonlinearities in structures are implemented on a test rig containing a nonlinear element. They used low forcing level excitations in the experiments in order to obtain the linear FRFs of the structure. However, when there are multiple nonlinearities including friction type of nonlinearity, it will not be possible to measure the linear FRFs at low level of force excitation. Since most of the model updating methods are applied to linear analytical models it is important to obtain linear FRFs of a nonlinear structure first. In the present study a method is proposed to obtain linear FRFs in order to update linear model parameters of a nonlinear structure having multiple nonlinearities including friction type of nonlinearity. The proposed method is validated with different case studies using SDOF and lumped MDOF systems. In these case studies simulated experimental data is used. The effect of the excitation frequency, at which experiments are carried out, on the accuracy of the proposed method, is also demonstrated with a case study. The method suggested can also be used as a nonlinear identification method.

2 THEORY

The proposed method in this study is based on the theory developed by Budak and Özgüven [23, 24] for expressing the nonlinear forcing vector in a nonlinear structure as a matrix multiplication form for harmonically excited nonlinear MDOF systems. They expressed the nonlinear internal force vector in a nonlinear MDOF system as

$$\{N(x,\dot{x})\} = [\Delta(x,\dot{x})]\{X\}e^{i\omega t} \tag{1}$$

where $\{N(x,\dot{x})\}$ stands for the nonlinear internal forcing vector, $\{X\}$ is a complex response amplitude vector and $[\Delta(x,\dot{x})]$ is the "nonlinearity matrix" which was first presented by Budak and Özgüven [23, 24] for certain types of nonlinearities, and later by Tanrıkulu et al. [25] for any type of nonlinearity by using describing functions. The elements of nonlinearity matrix are written in terms of describing functions, such that the describing function ν_{rj} represents the nonlinearity in the system by giving the best average restoring force between coordinates r and j.

The elements of $[\Delta(x,\dot{x})]$ are given as follows [25]:

$$\Delta_{rr} = \nu_{rr} + \sum_{\substack{j=1 \\ j\neq r}} \nu_{rj}, \quad r = 1, 2, ..., n \tag{2}$$

$$\Delta_{rj} = -v_{rj}, \quad r \neq j, \quad r = 1, 2, ..., n \tag{3}$$

The response level dependent nonlinear FRF matrix (in the form of receptances) for a nonlinear system can be written as follows:

$$\left[H^{NL}\right] = \left[-\omega^2[M] + i\omega[C] + i[D] + [K] + \Delta\right]^{-1} \tag{4}$$

where $[M]$, $[C]$, $[D]$, $[K]$ represent the mass, viscous damping, structural damping and stiffness matrices, respectively. Considering the linear part of this nonlinear system, the linear FRF matrix (in the form of receptances) can be written as follows:

$$\left[H^{L}\right] = \left[-\omega^2[M] + i\omega[C] + i[D] + [K]\right]^{-1} \tag{5}$$

Taking the inverses of $\left[H^{NL}\right]$ and $\left[H^{L}\right]$ matrices given in equations (4) and (5), and then subtracting the second from the first, the following equation is obtained:

$$[\Delta] = \left[H^{NL}\right]^{-1} - \left[H^{L}\right]^{-1} \tag{6}$$

After some matrix manipulations, the linear FRF matrix can be obtained as

$$\left[H^{L}\right] = \left[\left[H^{NL}\right]^{-1} - [\Delta]\right]^{-1} \tag{7}$$

For a nonlinear MDOF system with multiple nonlinearities including friction type of nonlinearity, nonlinearity matrix $[\Delta]$ can be partitioned as

$$[\Delta] = \left[\Delta_f\right] + [\Delta_{HF}] \tag{8}$$

where $\left[\Delta_f\right]$ is the nonlinearity matrix due to friction and $[\Delta_{HF}]$ is the nonlinearity matrix due to remaining nonlinearities that are dominant at high forcing levels of excitation. Substituting equation (8) into equation (6), the following equation can be obtained:

$$\left[\Delta_f\right] + [\Delta_{HF}] = \left[H^{NL}\right]^{-1} - \left[H^{L}\right]^{-1} \tag{9}$$

When the structure is excited at low forcing levels, $\left[\Delta_f\right]$ will be dominant and $[\Delta_{HF}]$ will have negligible terms. Then, at low forcing levels equation (9) can be approximated as

$$\left[\Delta_f\right] \cong \left[H^{NL}\right]^{-1} - \left[H^{L}\right]^{-1} \tag{10}$$

On the other hand, for high forcing levels, $[\Delta_{HF}]$ will be more pronounced compared to frictional nonlinear forces, therefore equation (9) can be approximated at high forcing levels as

$$[\Delta_{HF}] \cong \left[H^{NL}\right]^{-1} - \left[H^{L}\right]^{-1} \tag{11}$$

Then, by using equations (10) and (11), and measuring FRFs experimentally several times at the same frequency but at different forcing levels, the linear FRFs can be obtained and the nonlinearities can be identified as explained below.

Let us assume that a certain set of experiments are performed at a constant frequency ω, at different forcing levels. Firstly, let the system be excited at a low forcing level, and then (*n-1*) times at different high forcing levels. Using equations (10) and (11), the following equations can be written:

$$\left[\Delta_f\right]_1 = \left[H^{NL}\right]_1^{-1} - \left[H^{L}\right]_1^{-1} \tag{12}$$

$$\left[\Delta_{HF}\right]_2 = \left[H^{NL}\right]_2^{-1} - \left[H^{L}\right]_2^{-1} \tag{13}$$

$$\left[\Delta_{HF}\right]_3 = \left[H^{NL}\right]_3^{-1} - \left[H^{L}\right]_3^{-1} \tag{14}$$

$$\left[\Delta_{HF}\right]_4 = \left[H^{NL}\right]_4^{-1} - \left[H^{L}\right]_4^{-1} \tag{15}$$

$$\vdots$$

$$\left[\Delta_{HF}\right]_n = \left[H^{NL}\right]_n^{-1} - \left[H^{L}\right]_n^{-1} \tag{16}$$

where subscript *1, 2, 3, ... n* indicates forcing cases. If the equation at low forcing level (equation 12) is subtracted from each of the following ones, a new set of equations will be obtained:

$$\left[\Delta_{HF}\right]_2 - \left[\Delta_f\right]_1 = \left[H^{NL}\right]_2^{-1} - \left[H^{NL}\right]_1^{-1} \tag{17}$$

$$\left[\Delta_{HF}\right]_3 - \left[\Delta_f\right]_1 = \left[H^{NL}\right]_3^{-1} - \left[H^{NL}\right]_1^{-1} \tag{18}$$

$$\left[\Delta_{HF}\right]_4 - \left[\Delta_f\right]_1 = \left[H^{NL}\right]_4^{-1} - \left[H^{NL}\right]_1^{-1} \tag{19}$$

$$\vdots$$

$$\left[\Delta_{HF}\right]_n - \left[\Delta_f\right]_1 = \left[H^{NL}\right]_n^{-1} - \left[H^{NL}\right]_1^{-1} \tag{20}$$

Since the linear FRF matrix is not forcing level dependent, then these terms will be canceled out and they will not appear in the resulting equations as can be seen above. There are both zero and nonzero elements in the nonlinearity matrices at the left hand sides of the equations, and nonzero elements are related to nonlinear coordinates. These nonzero elements which can be written as polynomial functions of response amplitudes with unknown coefficients are the describing functions of the corresponding nonlinearities. Since it is always possible to take data points more than the unknown coefficients, least square fit can be used for obtaining the unknown coefficients. In order to find the unknown coefficients, polynomial fit for (*n-1*) data points is applied in a least square sense and the equation of the corresponding regression curve is obtained. For more complex nonlinearities where polynomial fit may be insufficient, nonlinear fit can also be used. Once the unknown coefficients are obtained, by comparing the terms of the regression equation with the corresponding describing functions, nonlinearities are identified and then linear FRFs can easily be calculated by using one of the equations from (12) to (16), one of which is given below.

$$\left[H^{L}\right]_1 = \left[\left[H^{NL}\right]_1^{-1} - \left[\Delta_f\right]_1\right]^{-1} \tag{21}$$

The equations (17) to (20) will be reduced to very simple algebraic equations for a SDOF system:

$$\Delta_{HF_2} - \Delta_{f_1} = \frac{1}{H^{NL}_2} - \frac{1}{H^{NL}_1} \tag{22}$$

$$\Delta_{HF_3} - \Delta_{f_1} = \frac{1}{H^{NL}_3} - \frac{1}{H^{NL}_1} \tag{23}$$

$$\Delta_{HF_4} - \Delta_{f_1} = \frac{1}{H^{NL}_4} - \frac{1}{H^{NL}_1} \tag{24}$$

$$\vdots$$

$$\Delta_{HF_n} - \Delta_{f_1} = \frac{1}{H^{NL}_n} - \frac{1}{H^{NL}_1} \tag{25}$$

For a SDOF system, since all the matrix inversions simplify to inversions of a scalar, it is much easier to obtain the right hand sides of the above equations by using experimental measurements. Then linear FRFs of the system can be calculated by using the following equation:

$$\frac{1}{H^{L}_1} = \frac{1}{H^{NL}_1} - \Delta_{f_1} \tag{26}$$

Equation (26) is valid for low forcing level at any frequency; therefore it is possible to obtain the linear FRFs over the desired frequency range. It should be noted that, although the above equations are valid for a harmonic excitation and therefore harmonic vibration of the system at any frequency, the difference between linear and nonlinear FRFs at an arbitrary frequency may be negligible, making it very difficult to identify the nonlinearity accurately. Hence, the identification can be made most accurately at frequencies where the nonlinearity has the maximum effect on the system response.

3 CASE STUDIES

In this section, applications of the proposed method to SDOF and MDOF nonlinear systems are presented. The first case study is purely a theoretical one and it illustrates the identification of nonlinearities and calculation of the linear frequency response of a nonlinear system from nonlinear FRF measurements. The second case study is an extension of the first one, in which polluted data is used in the analysis in order to simulate the experimental measurements more realistically. In the third case study, the proposed approach is applied to a MDOF system with multiple nonlinearities including friction. In this case study, again simulated experimental data is used. Finally, in order to study the effect of the excitation frequency at which measurements are made, on the accuracy of the proposed method, the same MDOF system is considered. The nonlinear parameters are identified by using simulated experimental FRF values obtained at different excitation frequency each time and the identified values are compared with each other. In obtaining all simulated experimental results, harmonic balance approach is used.

3.1 Application of the Approach to a SDOF System

In this case study, the proposed method is applied to a SDOF system with cubic stiffness and dry friction nonlinearities. The system and the dry friction model used in the case study are given in Fig. 1.

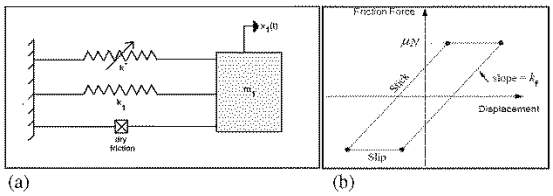

Fig.1 (a) SDOF nonlinear system, (b) Dry friction model

The parameters of these nonlinear elements and the properties of the system are given as follows:

$m_1 = 0.1\,kg,\ \ k_1 = 2x10^6\ N/m\ \ and\ \ \gamma(loss\ factor) = 0.01$

$k^* = 1x10^{10}\ N/m^3$

$\mu = 0.1,\ \ Normal\ Force = 10\ N\ \ \ and\ \ \ k_f = 3x10^5\ N/m$

Firstly, the system is excited harmonically with a low forcing amplitude (F=0.01 N). The harmonic response of the system at this forcing level is compared with the linear frequency response of the system obtained disregarding both friction and cubic stiffness nonlinearity (Fig. 2).

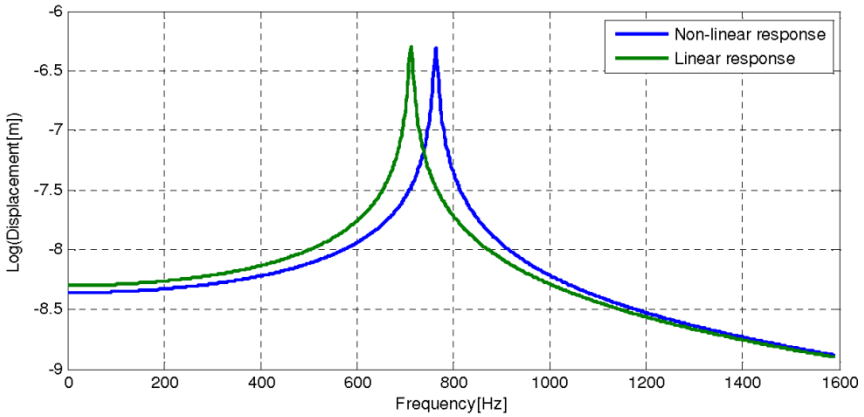

Fig.2 Harmonic response of the system for F=0.01 N

As can be seen in Fig. 2, since at low forcing level nonlinear internal forces due to cubic stiffness are negligible, the only nonlinear effect is due to friction. Frictional internal force causes a shift in the resonance frequency due to its stiffness component. Afterwards, 11 different higher excitation cases are considered by taking the amplitude of the harmonic excitation force between 100 N and 300 N and the responses of the system are obtained. In Fig. 3, nonlinear harmonic responses at only the forcing levels of F=130 N and F=280 N are shown.

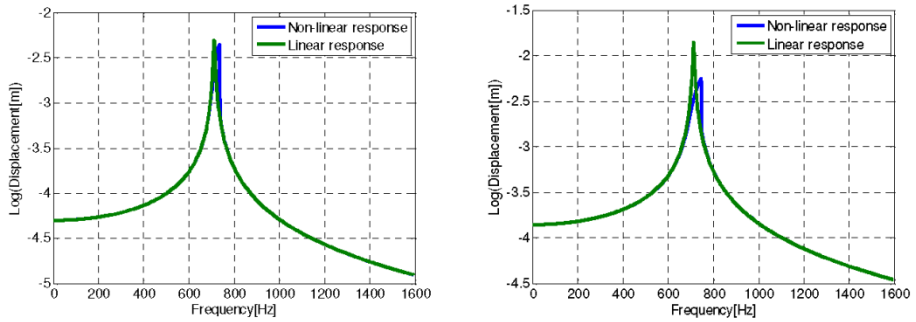

Fig.3 Harmonic response of the system for (a) F = 130 N, (b) F = 280 N

Since frictional nonlinearity is negligible at high forcing levels, as can be seen from the Fig. 3, only the cubic stiffness nonlinearity will be effective, and it will change the frequency response of the system around resonance causing a jump, which is a typical response behavior of cubic stiffness element. All above computations are based on the nonlinear identification made by using 11 different FRFs obtained at the excitation frequency of 710 Hz. By using "polyfit" function of MATLAB, equation of the regression curve is obtained and nonlinear parameters are identified by comparing the terms of the regression equation with the corresponding describing functions. The regression curve obtained can be seen in Fig. 4.

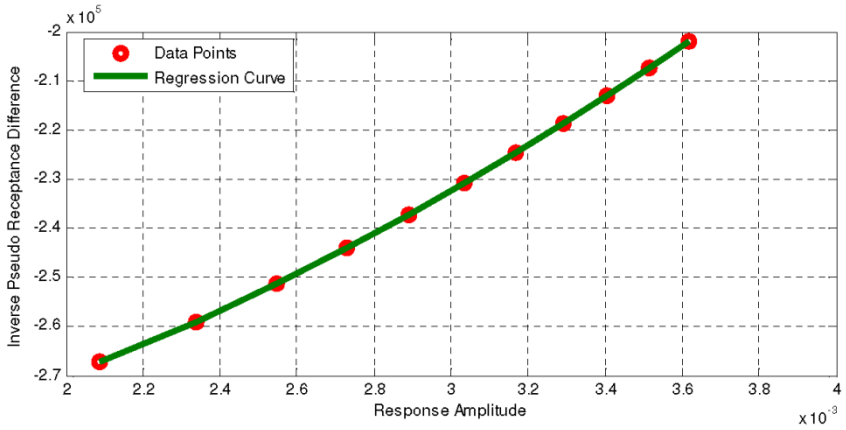

Fig.4 Polynomial regression curve for the available data points

The nonlinear parameters estimated are given below:

$$k^* = 9.9x\,10^9\ N/m^3 \quad and \quad k_f = 3x\,10^5\ N/m$$

It can be seen that the estimated parameters perfectly match with the actual values. The linear FRF of the system now can be calculated by using equation (26). The comparison of the estimated and actual linear frequency response is given in Fig. 5. As expected, there is a perfect match between estimated and actual linear frequency responses of the system.

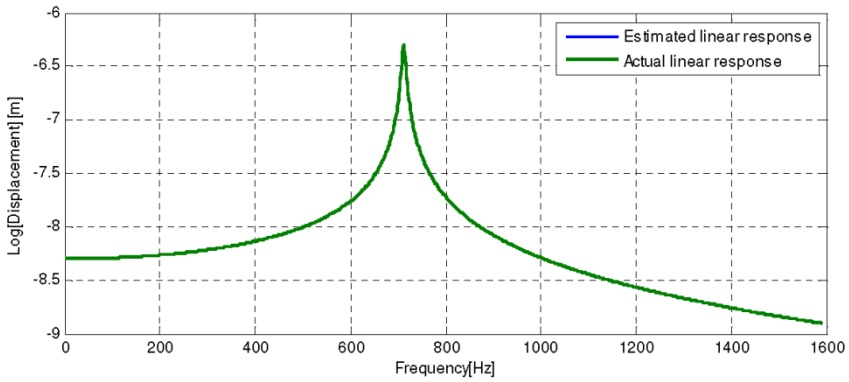

Fig.5 Comparison of the estimated and actual linear frequency responses of the system

3.2 Application of the Approach to a SDOF System with Polluted Data

In the second case study, in order to simulate the experimental data, theoretical data is polluted with 5% noise. The noise has normal distribution and standard deviation of 5% of the amplitude of the original response. In the analysis, SDOF nonlinear system with the same parameters as in the first case study is used. The system is excited with a low forcing amplitude and then with 11 different high forcing amplitudes. In Fig. 6, the FRF of the nonlinear system for F=0.01 N is compared with the linear frequency response of the system obtained disregarding both friction and cubic stiffness nonlinearity. The frequency responses of the system for F=130 N and F=280 N are given in Fig. 7.

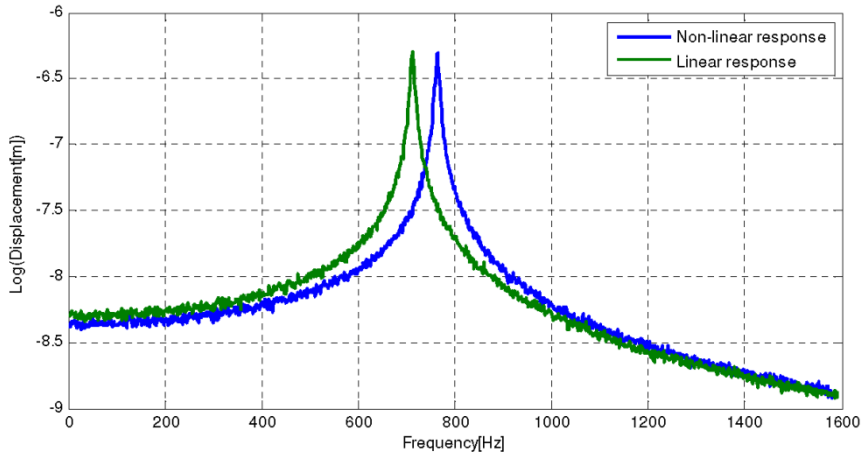

Fig.6 Frequency response of the system at F=0.01 N with 5% noise

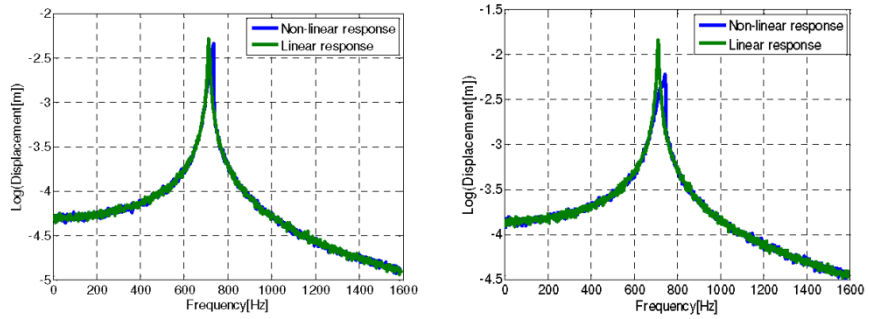

(a) (b)

Fig.7 Frequency response of the system with 5% noise for (a) F = 130 N, (b) F = 280 N

At the excitation frequency of 710 Hz, 11 different data points are generated and the polynomial regression curve given in Fig. 8 is obtained.

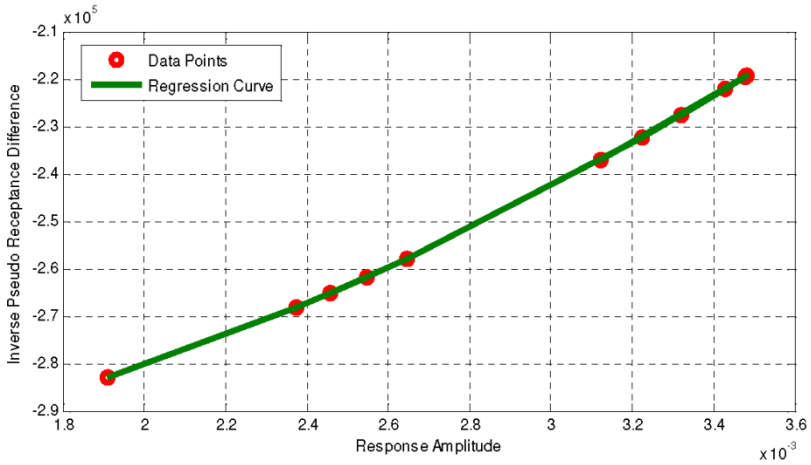

Fig.8 Polynomial regression curve for the available data points

Identified nonlinear parameters and comparison of these values with the actual ones are given in Table 1.

Table 1 Comparison of nonlinear parameters

Nonlinear Parameters	Estimated	Actual	% Error
k^* (N/m^3)	9.9×10^9	1×10^{10}	1
k_f (N/m)	3.1×10^5	3×10^5	3.3

As can be seen in Table 1, there is a slight difference between the estimated and actual nonlinear parameters, mainly due to addition of noise to the theoretical data. Comparison of the estimated and actual linear frequency responses is given in Fig. 9. As expected, estimated linear frequency response matches perfectly with the actual one.

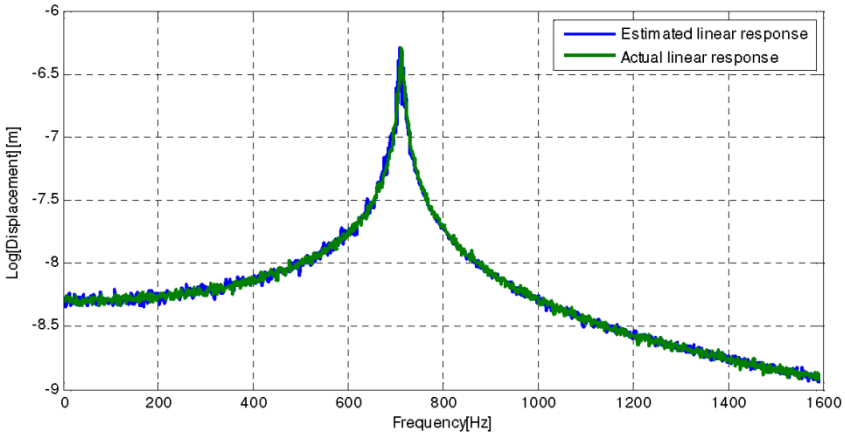

Fig.9 Comparison of the estimated and actual linear frequency response of the system with 5% noise

3.3 Application of the Approach to a MDOF System with Polluted Data

In the third case study, application of the proposed approach to a nonlinear MDOF system with polluted data is illustrated (Fig. 10). The same dry friction model given in previous case study is used here as well.

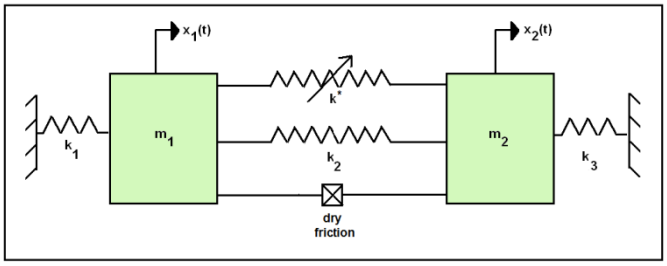

Fig.10 MDOF nonlinear system used in Case Study 3

Parameters of the nonlinear element and the properties of the other system elements are given as follows:

$m_1 = 0.1,\ m_2 = 0.5\,kg,\ \ k_1 = k_2 = k_3 = 1x10^6\ N/m\ \ and\ \ \gamma(loss\ factor) = 0.005$

$\mu = 0.1,\ Normal\ Force = 10\ N\ \ and\ \ k_f = 8x10^4\ N/m$

$k^* = 1x10^{10}\ N/m^3$

In order to simulate the experimental data, theoretical data is polluted with 5% noise. The noise has normal distribution and standard deviation of 5% of the amplitude of the original response. The system is excited with a low forcing level and then with 11 different high forcing levels. The frequency responses of the system at forcing levels of F=0.01 N and F=100 N are given in Fig. 11 and 12, respectively.

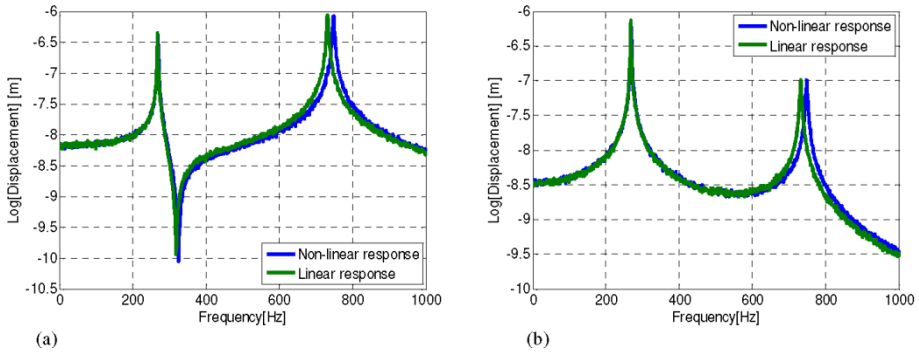

Fig.11 Frequency responses of the system with 5% noise for F=0.01 N
(a) 1st coordinate, (b) 2nd coordinate

As can be seen in Fig. 11, for low forcing amplitudes, the only nonlinear effect is due to friction and frictional internal force causes a shift in the resonance frequency. The frictional nonlinearity is much more effective in the 2nd mode.

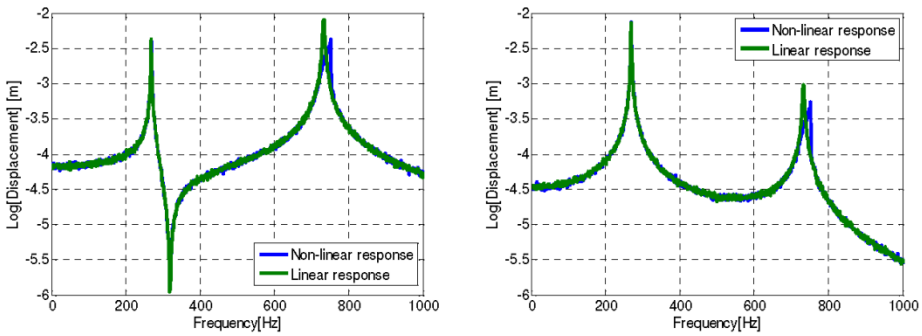

Fig.12 Frequency responses of the system with 5% noise for F=100 N
(a) 1st coordinate, (b) 2nd coordinate

In Fig. 12, it can be seen that, since frictional nonlinear internal forces are negligible for high forcing level, the nonlinearity changes the response of the system around 2nd resonance considerably by causing a jump, which is mainly due to cubic stiffness. As in the low forcing level case, 1st mode is not much affected from the existence of the stiffness nonlinearity in the system. The nonlinear parameters given in Table 2 are estimated as explained in the first case study (Fig. 13).

Table 2 Comparison of nonlinear parameters

Nonlinear Parameters	Estimated	Actual	% Error
k^* (N/m^3)	9.9x 10^9	1x 10^{10}	1
k_f (N/m)	8.03x 10^4	8x 10^4	0.4

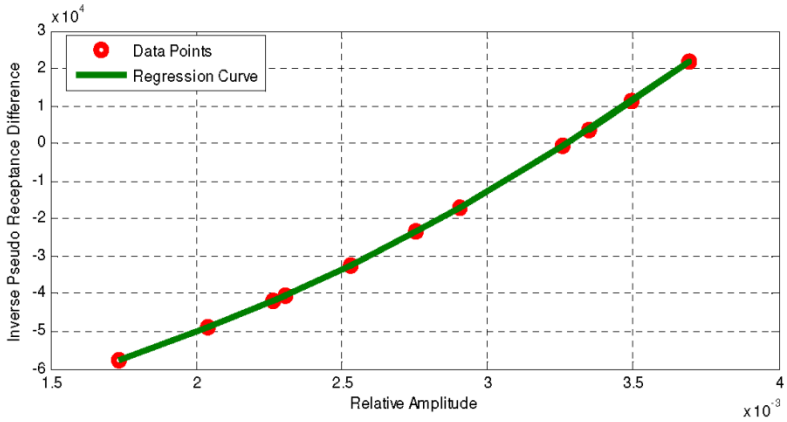

Fig.13 Polynomial regression curve for the available data points

As can be seen from the values in Table 2, estimated and actual nonlinear parameters are in perfect match. However, since in the proposed approach, excitation frequency is a free parameter (i.e., the equations are valid for any forcing level and therefore vibration at any frequency), the effect of the excitation frequency used in the experiments on the performance of the method should be analyzed.

3.4 Performance of the Method at Different Excitation Frequencies

As the last case study, in order to see the effect of excitation frequency on the proposed method, different simulated tests at various frequencies are performed for the MDOF nonlinear system given in the previous case study. For each test case, nonlinearities are identified and they are compared with the actual nonlinear parameters. Comparison of the results is given in Table 3.

Table 3 Comparison of nonlinear parameters identified by using different excitation frequencies

Excitation Frequency (Hz)	Estimated k* (N/m^3)	Actual k* (N/m^3)	% Error for k*	Estimated k_f (N/m)	Actual k_f (N/m)	% Error for k_f
725	9.9×10^9	1×10^{10}	1	8.03×10^4	8×10^4	0.4
730	9.9×10^9		1	7.67×10^4		4.1
745	9.9×10^9		1	16.3×10^4		103.8

Since the nonlinear forces affect the 2nd mode more, excitation frequencies are selected around the 2nd resonance of the system. As can be seen from Table 3, for all the excitation frequencies used, cubic stiffness values are successfully estimated. However, the frictional stiffness value is highly affected from the selection of excitation frequency, even though all frequencies are around the resonance region. It is observed that when the excitation frequency is closer to the 2nd resonance of the linear frequency response, estimated values become more accurate.

4 DISCUSSION AND CONCLUSIONS

When there are multiple nonlinearities including friction in a system, it is not possible to obtain the linear frequency response of the system by using low forcing levels in the experiments. In this paper, an approach for obtaining the linear FRFs of a nonlinear system with multiple nonlinearities including friction is proposed. The basic motivation is to have FRFs of the linear part of a nonlinear structure, so that they can be used in model updating.

In the method proposed, FRF values are measured at all coordinates that we are interested in, but at a constant frequency ω and at different forcing levels. First, the system is excited at a low forcing level, and then several times at different high forcing levels. By using the measured nonlinear FRFs, first the nonlinearities are identified and then linear FRFs are obtained in order to use them in model updating of nonlinear systems.

The method is validated with different case studies using SDOF and MDOF systems and simulated experimental data. In the first and second case studies, application of the approach is demonstrated on a SDOF nonlinear system. It is shown that the approach is very successful in identifying multiple nonlinearities in the system, as well as in determining the linear FRF. In simulated experimental case study it is observed that, the noise added to the data affects the values of the identified nonlinear parameters and linear frequency response. In the third case study, the method is applied to a MDOF nonlinear system by using simulated experimental data again. The results obtained show that nonlinearities can be identified very accurately by using nonlinear FRFs measured at low and high forcing levels. In the last case study, the effect of the excitation frequency used in the experiments on the performance of the method is investigated. From the results obtained it is concluded that excitation frequency should be close to the resonance frequency, otherwise the accuracy of the identified friction nonlinearity can be deteriorated considerably.

Consequently, it can be said that the method can successfully be used for the identification of nonlinearity and calculation of the linear FRFs of a nonlinear structure with multiple nonlinearities including friction. The applicability and accuracy of the approach proposed is demonstrated only on simple SDOF and MDOF systems. The method needs to be tested on real structures, in order to apply it to obtain FRFs of the linear part of a nonlinear structure that can be used in model updating of the nonlinear structure.

5 REFERENCES

[1] Berman A., "Mass Matrix Correction Using an Incomplete Set of Measured Modes", AAIA Journal, 17(1), pp.1147-1148, 1979.

[2] Sidhu J., Ewins D. J., "Correlation of Finite Element and Modal Test Studies of a Practical Structure", Proceedings of the 2nd International Modal Analysis Conference, Orlando, Florida, pp.756-762, 1984.

[3] Caesar B., "Update and Identification of Dynamic Mathematical Models", Proceedings of the 4th International Modal Analysis Conference, Los Angeles, California, pp.394-401, 1986.
[4] Caesar B., "Updating System Matrices Using Modal Test Data", Proceedings of the 5th International Modal Analysis Conference, London, England, pp.453-459, 1987.
[5] Visser W. J., Imregun M., "A Technique to Update Finite Element Models Using Frequency Response Data", Proceedings of the 9th International Modal Analysis Conference, Florence, Italy, pp.462-469, 1991.
[6] Larsson P. O., Sas P., "Model Updating Based on Forced Vibration Testing Using Numerically Stable Formulations", Proceedings of the 10th International Modal Analysis Conference, San Diego, California, pp.966-974, 1992.
[7] Bollinger A. T., "Finite Element Model Updating for FEA/EMA Modal Correlation Via Constrained Optimization Theory", Proceedings of the 12th International Modal Analysis Conference, Honolulu, Hawaii, pp.882-888, 1994.
[8] Lammens S., Brughmans M., Leuridan J., Sas P., "Application of a FRF Based Model Updating Technique for the Validation of the Finite Element Model of an Engine Subframe", Proceedings of the 14th International Modal Analysis Conference, Dearborn, Michigan, pp.1063-1070, 1996.
[9] Girard A., Chatelain J., Bugeat L. P., "Model Updating by Energy Approach for Rotating Shafts", Proceedings of the 15th International Modal Analysis Conference, Orlando, Florida, pp.1419-1425, 1997.
[10] Billet L., Moine P., Lebailly P., "Updating a Finite Element Model of the Hualien Nuclear Reactor Building", Proceedings of the 15th International Modal Analysis Conference, Orlando, Florida, pp.1924-1930, 1997.
[11] Mottershead J. E., Mares C., Friswell M. I., James S., "Model Updating of an Aluminium Space-frame Using Different Parameter Sets", Proceedings of the 18th International Modal Analysis Conference, San Antonio, Texas, pp. 576-583, 2000.
[12] Kozak M. T., Cömert M. D., Özgüven H. N., "Model Updating Routine Based on the Minimization of a New Frequency Response Based Index for Error Localization", Proceedings of the 25th International Modal Analysis Conference, Orlando, Florida USA, pp.84-95, 2007.
[13] Benhafsi Y., Penny J. E. T., Friswell M. I., "A Parameter Identification Method for Discrete Nonlinear Systems Incorporating Cubic Stiffness Elements", International Journal of Analytical and Experimental Modal Analysis, Volume 7, Issue 3, pp.179-196, 1992.
[14] Richard C. M., Singh R., "Feasibility of Identifying Nonlinear Multi-Degree-of-Freedom Systems with Unknown Polynomial Forms", Proceedings of the 18th International Modal Analysis Conference, San Antonio, Texas, pp. 496-502, 2000.
[15] Chong Y. H., İmregün M., "Variable Modal Parameter Identification for Nonlinear MDOF Systems – Parts I: Formulation and Numerical Validation", Journal of Shock and Vibration, pp.217-227, 2000.
[16] Chong Y. H., İmregün M., "Variable Modal Parameter Identification for Nonlinear MDOF Systems – Parts II: Experimental Validation and Advanced Case Study", Journal of Shock and Vibration, pp.229-240, 2000.
[17] Adams D. E., Allemang R. J., "A Frequency Domain Method for Estimating the Parameters of a Non-Linear Structural Dynamic Model Through Feedback", Mechanical Systems and Signal Processing, 14(4), 637-656, 2000.
[18] Kerschen G., Worden K., Vakakis A. F., Golinval J. C., "Past, Present and future of Nonlinear System Identification in Structural Dynamics", Mechanical Systems and Signal Processing, Volume 20, pp 505-592, 2006.
[19] Özer M. B., Özgüven H. N., "A New Method for Localization and Identification of Nonlinearities in Structures", 6th Biennial Conference on Engineering Systems Design and Analysis, İstanbul, Turkey, 2002.
[20] Özer M. B., Özgüven H. N., Royston T.J., "Identification of Structural Non-linearities Using Describing Functions and the Sherman–Morrison Method", Mechanical Systems and Signal Processing, 23, 30–44, 2009.
[21] Jalali H., Bonab B. T., Ahmadian H., "Identification of Weakly Nonlinear Systems Using Describing Function Inversion", Experimental Mechanics, 51:739–747, 2011.
[22] Arslan Ö., Aykan M., Özgüven H. N., "Parametric Identification of Structural Nonlinearities from Measured Frequency Response Data", Mechanical Systems and Signal Processing, 25, 1112–1125, 2011.
[23] Budak E., Özgüven H. N., "A Method for Harmonic Responses of Structures with Symmetrical Nonlinearities", Proceedings of the 15th International Seminar on Modal Analysis and Structural Dynamics, Leuven, Belgium, v.2, pp.901–915, 17-21 September 1990.
[24] Budak E., Özgüven H. N., "Iterative Receptance Method for Determining Harmonic Response of Structures with Symmetrical Non-linearities", Mechanical Systems and Signal Processing, v.7, n.1, pp.75–87, 1993.
[25] Tanrıkulu Ö., Kuran B., Özgüven H. N., İmregün M., "Forced Harmonic Response Analysis of Non-linear Structures Using Describing Functions", AIAA Journal, v.31, n.7, pp.1313-1320, 1993.

Model Updating of Nonlinear Structures*

Güvenç Canbaloğlu[1,2], H. Nevzat Özgüven[1]
[1]Department of Mechanical Engineering, Middle East Technical University, 06800 Ankara, TURKEY
[2]MGEO Division, ASELSAN Inc., 06750 Ankara, TURKEY
e-mail: gcanbal@aselsan.com.tr, ozguven@metu.edu.tr

ABSTRACT

There are always certain discrepancies between modal data of a structure obtained from its mathematical model and experimentally measured ones. Therefore it is a general practice to update the theoretical model by using experimental measurements in order to have a more accurate model. Since in several real life engineering problems there exist structural nonlinearities, model updating of nonlinear structures come into prominence. To be able to apply one of the well-established model updating methods, the linear FRFs of a nonlinear structure are to be measured. Although it may be possible to obtain linear FRFs of a nonlinear structure experimentally with a certain approximation by using low level forcing in FRF measurement, when there is frictional type of nonlinearity, this is not possible. In this study a model updating method for nonlinear structures is proposed. A noble method developed recently by the authors to obtain linear FRFs of nonlinear structures having multiple nonlinearities including friction type of nonlinearity is used in the nonlinear model updating approach proposed. The method is validated by applying the method developed to a nonlinear test system.

KEYWORDS

Nonlinear model updating, model updating, nonlinear structures, nonlinearity, friction nonlinearity.

1 INTRODUCTION

Numerical structural modeling is a common practice to obtain dynamic response of engineering structures, and finite element (FE) method has established itself as the most common numerical method. Since FE methods have certain inaccuracies due to modeling errors, experimental and FE method results do not always match perfectly. In order to correct the mathematical model so that these discrepancies will be eliminated, some of the parameters used in the FE models need to be changed by using model updating techniques.

In literature, various model updating methods were proposed in order to have accurate numerical structural models. However; most of these methods are for linear systems. Sidhu and Ewins [1] used the error matrix equation to correlate FE model and test results of an aerospace structure better. Dascotte and Vanhonacker [2] developed an automatic updating procedure based on natural eigenfrequency sensitivity. Brughmans and Lembregts [3] studied the effect of experimental modal parameter estimation techniques for normal mode shapes on an optimization procedure for FE mass and stiffness matrices. Nalitolela et al. [4] presented a method which is based on exact model reduction and perturbation of both the actual structure and its analytical model by adding mass or stiffness to produce accurate dynamic models. In order to update FE models Roy et al. [5] proposed direct energy approach which uses the expanded set of experimental modes to relate the kinetic and strain energies of each part of a FE model to the experimental data. Visser and Imregun [6] investigated the use of FRFs for model updating, and discussed the requirement for minimum measured data for successful implementation of the technique. Brughmans et al. [7] discussed the application of a FE model updating technique, based on a forward sensitivity formulation, to a twin propeller commuter aircraft. Ibrahim et al. [8] developed direct updating technique for nonconservative FE models by using input and output experimental data. Link and Zhang [9] presented different updating techniques based on the minimization of different residual vectors and applied these techniques to a test structure in order to investigate the sensitivity of updating results in these methods. Jung and Ewins [10] presented the application of the inverse eigensensitivity method for model updating using arbitrarily chosen macro elements to a simple frame. Aiad et al. [11] presented an approach to update both

---

* G. Canbaloglu, H.N. Özgüven, Model Updating of Nonlinear Structures, Nonlinear Dynamics, Volume 2: Proceedings of the 32nd IMAC, A Conference and Exposition on Structural Dynamics, pp.69-182, 2014.

mass and stiffness matrices. Miccoli and Agostoni [12] used the sensitivity analysis in order to localize the areas of potential errors causing the discrepancies between analytical and experimental normal modes. Luber and Sensburg [13] presented an update method which exploits the elastic behavior of a structure. Dascotte et al. [14] combined different parameters in an objective function to use sensitivity based model update method. Hemez [15] presented a sensitivity based updating method for damped FE models using modal parameters, receptance and static data. Lindholm [16] presented an example of updating FE models using nonlinear weighted least squares in a Bayesian statistics context. Lenoir et al. [17] presented a new model updating method based on the modal synthesis of experimental forced responses. Mottershead et al. [18] used different updating parameter sets and compared the effect of the selection of different updating parameters in the model updating of an aluminum space frame. Jung et al. [19] presented a hybrid optimization technique based on the genetic algorithm and Nelder-Mead simplex method for FE model updating of bridge structure. Kozak et al. [20] presented a new error localization method and an updating routine and they used the routine in different case studies. In a more recent work Boulkaibet et al. [21] proposed the use of the Shadow Hybrid Monte Carlo technique for the problem of determining the most probable FE model updating parameters for a given data.

In engineering problems most of the structures show nonlinear behavior, therefore it is important to have model updating techniques for nonlinear structures as well. Hasselman et al [22] proposed Principal Components Analysis for nonlinear model correlation and updating. Principal Components Analysis of nonlinear systems is based on singular value decomposition of a collection of response time history. Anderson et al. [23] used Principal Components Analysis in order to correlate and update a nonlinear FE model using crash test data. In a later work Anderson and Hasselman [24] studied the minimization of the parameter correlation for model updating of nonlinear systems. Burton et al. [25] applied combined model reduction and singular value decomposition approach for nonlinear model updating. Zhang and Guo [26] proposed a model updating and validation procedure to build accurate FE model for a frame structure with nonlinear thin-walled component. Silva et al. [27] conducted a comparative study using different metrics for nonlinear model updating based on vibration test data. Harmonic balance, constitutive relation error, restoring force surface and Karhunen-Loève decomposition methods are compared.

In order to apply model updating techniques developed for linear systems to nonlinear structures the linear dynamic behavior of a nonlinear structure has to be experimentally obtained which may require identification of nonlinearity first. One of the most detailed nonlinear system identification literature surveys was given by Kerschen et al. [28] in which more than 400 papers are cited. After that study, several new nonlinear identification methods are developed. In these studies the general aim is to detect, localize and parametrically identify nonlinearity in a structure. Very recently Canbaloglu and Özgüven [29] developed a method to obtain linear FRFs of a nonlinear structure from FRF measurements, without fully identifying nonlinearities, the ultimate goal being to update linear model parameters of a nonlinear structure having multiple nonlinearities including friction type of nonlinearity. In this study, this method [29] is used in developing a nonlinear model updating approach, and it is applied to a nonlinear test system in order to validate the nonlinear model updating approach.

2 THEORY

The model updating method proposed in this study for nonlinear structures is based on the approach recently developed by Canbaloglu and Özgüven [29]. The response level dependent nonlinear FRF matrix (in the form of receptances) for a nonlinear system can be written as follows:

$$\left[H^{NL}\right]=\left[-\omega^2[M]+i\omega[C]+i[D]+[K]+\Delta\right]^{-1} \tag{1}$$

where $[M]$, $[C]$, $[D]$, $[K]$ represent mass, viscous damping, structural damping and stiffness matrices, respectively. $[\Delta]$ is the "nonlinearity matrix" which was first presented by Budak and Özgüven [30, 31] for certain types of nonlinearities, and later by Tanrıkulu et al. [32] for any type of nonlinearity by using describing functions. The FRF matrix of the linear part of this nonlinear system, in the form of receptances, can be written as follows:

$$\left[H^{L}\right]=\left[-\omega^2[M]+i\omega[C]+i[D]+[K]\right]^{-1} \tag{2}$$

Performing some matrix manipulations the following equation can be obtained:

$$[\Delta]=\left[\Delta_f\right]+[\Delta_{HF}]=\left[H^{NL}\right]^{-1}-\left[H^{L}\right]^{-1} \tag{3}$$

where $[\Delta_f]$ is the nonlinearity matrix due to friction and $[\Delta_{HF}]$ is the nonlinearity matrix due to remaining nonlinearities that are dominant at high forcing levels of excitation. When the structure is excited at low forcing levels, $[\Delta_f]$ will be dominant and $[\Delta_{HF}]$ will have negligible terms. Then, at low forcing levels equation (3) can be approximated as

$$[\Delta_f] \cong [H^{NL}]^{-1} - [H^L]^{-1} \tag{4}$$

On the other hand, for high forcing levels, $[\Delta_{HF}]$ will be more pronounced compared to frictional nonlinear forces, therefore equation (3) can be approximated at high forcing levels as

$$[\Delta_{HF}] \cong [H^{NL}]^{-1} - [H^L]^{-1} \tag{5}$$

Then, by using equations (4) and (5), and measuring FRFs experimentally several times at the same frequency but at different forcing levels, the linear FRFs can be obtained and the nonlinearities can be identified. Firstly, let the system be excited once at a low forcing level, and then (*n-1*) times at different high forcing levels. Using equations (4) and (5), the following set of equations can be written:

$$[\Delta_{HF}]_{i+1} - [\Delta_f]_1 = [H^{NL}]_{i+1}^{-1} - [H^{NL}]_1^{-1} \qquad i = 1,2,...,(n-1) \tag{6}$$

where subscript 1 indicates low forcing case and subscripts 2, 3, … n indicate high forcing cases. The detailed formulation can be found in [29]. In the nonlinearity matrices at the left hand sides of the equations, nonzero elements are related to nonlinear coordinates (coordinates to which nonlinear elements are attached). These nonzero elements which can be written as polynomial functions of response amplitudes with unknown coefficients are the describing functions of the corresponding nonlinearities. In order to find the unknown coefficients, polynomial fit for (*n-1*) data points is applied in a least square sense, and the equation of the corresponding regression curve is obtained. By comparing the terms of the regression equation with the corresponding describing functions, nonlinearities are identified and then linear FRFs can easily be calculated as [29]

$$[H^L]_1 = \left[[H^{NL}]_1^{-1} - [\Delta_f]_1 \right]^{-1} \tag{7}$$

One of the drawbacks of the above equation is that it requires the full matrix inversions. However, for most of the nonlinear structures, nonlinearity is local and it possible to partition the nonlinearity matrix as

$$\Delta = \begin{bmatrix} [\Delta_{aa}] & [0] \\ [0] & [0] \end{bmatrix} \tag{8}$$

where subscript *a* represents coordinates where nonlinear elements are connected ("nonlinear coordinates" in short). Pre-multiplying all the terms in equation (3) by $[H^L]$ and post-multiplying by $[H^{NL}]$, the following equation is obtained:

$$[H^L][\Delta][H^{NL}] = [H^L][H^{NL}]^{-1}[H^{NL}] - [H^L][H^L]^{-1}[H^{NL}] \tag{9}$$

Substituting equation (8) into equation (9), following equation can be written:

$$\begin{bmatrix} [H^L_{aa}] & [H^L_{ab}] \\ [H^L_{ba}] & [H^L_{bb}] \end{bmatrix} \begin{bmatrix} [\Delta_{aa}] & [0] \\ [0] & [0] \end{bmatrix} \begin{bmatrix} [H^{NL}_{aa}] & [H^{NL}_{ab}] \\ [H^{NL}_{ba}] & [H^{NL}_{bb}] \end{bmatrix} = \begin{bmatrix} [H^L_{aa}] & [H^L_{ab}] \\ [H^L_{ba}] & [H^L_{bb}] \end{bmatrix} - \begin{bmatrix} [H^{NL}_{aa}] & [H^{NL}_{ab}] \\ [H^{NL}_{ba}] & [H^{NL}_{bb}] \end{bmatrix} \tag{10}$$

Here subscript *b* corresponds to linear coordinates.

Performing matrix multiplication for the left hand side and considering the first submatrix of the resultant matrix, the following equation is obtained:

$$\left[H^{L}{}_{aa}\right][\Delta_{aa}]\left[H^{NL}{}_{aa}\right]=\left[H^{L}{}_{aa}\right]-\left[H^{NL}{}_{aa}\right] \tag{11}$$

Pre-multiplying all terms in the equation (11) with $\left[H^{L}{}_{aa}\right]^{-1}$ and post-multiplying with $\left[H^{NL}{}_{aa}\right]^{-1}$ equation (11) reduces to

$$[\Delta_{aa}]=\left[H^{NL}{}_{aa}\right]^{-1}-\left[H^{L}{}_{aa}\right]^{-1} \tag{12}$$

from which the linear FRF matrix for the nonlinear coordinates can be obtained as:

$$\left[H^{L}{}_{aa}\right]_{1}=\left[\left[H^{NL}{}_{aa}\right]_{1}^{-1}-\left[\Delta_{f}\right]_{1}\right]^{-1} \tag{13}$$

It is obvious that computational effort will be considerably reduced for locally nonlinear structures. Once the linear FRFs are calculated by using equation (13), then these linear FRFs can be used in the model updating process of a FE model. Note that in several model updating methods having FRFs of limited number of coordinates is sufficient. Therefore, having FRF of even a single coordinate may be enough for model updating. However, depending on the model updating method employed, if FRFs of linear coordinates are also required, then all the remaining submatrix equations given in equation (10) need to be solved. That would also require the measurement of nonlinear responses at required linear coordinates as well.

One of the common methods used for model updating is the sensitivity analysis. In the sensitivity analysis, a response vector $\{r\}$ is corrected by changing the parameter vector $\{p\}$. Sensitivity analysis is based on the following equation given below:

$$\{\Delta r\}=[S]\{\Delta p\} \tag{14}$$

where $\{\Delta r\}$ is the residual vector between the reference and actual response, $\{\Delta p\}$ is the change needs to be done in parameter vector and $[S]$ is the sensitivity matrix. Considering model updating in the modal analysis context, $\{r\}$ vector is composed of mode shapes and natural frequencies, $\{p\}$ vector composed of geometrical parameters or material properties used in the FE model and sensitivity matrix $[S]$ is the modal sensitivity matrix which can be calculated analytically or numerically. Sensitivity matrix $[S]$ can be written as

$$[S]=\begin{bmatrix} S_{r_1}{}^{p_1} & \cdots & S_{r_1}{}^{p_m} \\ \vdots & \ddots & \vdots \\ S_{r_n}{}^{p_1} & \cdots & S_{r_n}{}^{p_m} \end{bmatrix} \tag{15}$$

In equation (15), $S_{r_n}{}^{p_m}$ stands for the sensitivity of the nth response to the mth updating parameter. Mathematically, $S_{r_n}{}^{p_m}$ is the partial differential of the nth response to the mth updating parameter and defined as,

$$S_{r_n}{}^{p_m}=\frac{\partial r_n}{\partial p_m} \tag{16}$$

For simple structures modal parameters can be written as the functions of updating parameters, and the corresponding sensitivities can be calculated by simple differentiation. However for complex structures it is easier to calculate the sensitivities by numerical differentiation. In this study, centered difference approximation with $O(h^4)$ is used to calculate the sensitivities as given in the following equation:

$$r'(p_i) = \frac{-r(p_{i+2}) + 8r(p_{i+1}) - 8r(p_{i-1}) + r(p_{i-2})}{12\Delta p} \tag{17}$$

Obtaining the sensitivity matrix $[S]$ and $\{\Delta r\}$ vector, $\{\Delta p\}$ which is the change needs to be done in parameter vector can be calculated from the following equation:

$$\{\Delta p\} = [S]^{-1}\{\Delta r\} \tag{18}$$

Since the number of equations is usually more than the number of unknowns, least square solution is necessary to solve equation (18). This solution is obtained iteratively.

3 APPLICATION OF THE PROPOSED MODEL UPDATING APPROACH TO SIMULATED TEST SYSTEM

In this section, an application of the proposed model updating approach to a continuous nonlinear simulated experimental test system is presented. Test system is a T-beam with cubic stiffness and dry friction nonlinearities. In order to simulate the nonlinear response of the system, first the linear part of the T-beam used in the simulated experiment is modeled with FE and linear FRFs are calculated, then using linear FRFs and the nonlinear parameters for cubic stiffness and dry friction, nonlinear responses are calculated by using the harmonic balance method. Then the results are polluted and in the analysis the polluted data is used in order to simulate the experimental measurements more realistically. Using the approach proposed, the nonlinearities are identified and estimated experimental linear FRFs of the test system are calculated. On the other hand theoretical linear FE model of the test system is built in ANSYS and in order to reflect the effect of uncertainties on material properties, the material properties in the theoretical linear FE model are taken slightly different from the ones used in the simulated test system. Performing modal analysis for the FE model, the theoretical linear FRFs are obtained and compared with the experimental linear FRFs. Then using sensitivity approach, updating parameters are selected from the candidate parameters used in the theoretical linear FE model and the first three flexural natural frequencies are corrected by updating selected parameters. The nonlinear T-beam test system and the dry friction model used are given in Fig. 1.

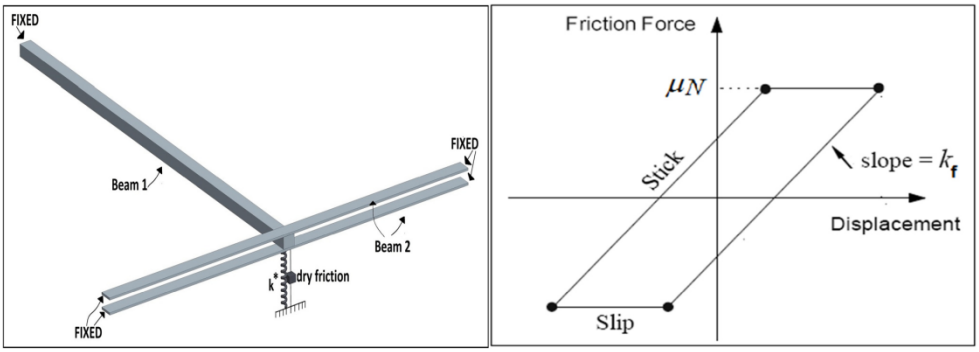

(a) (b)

Fig.1 (a) Nonlinear T-beam test system, (b) Dry friction model

T-beam is composed of two separate beams, geometric and material properties of these beams are given Table 1.

Table 1 Geometric and material properties the T-beam

	Height (mm)	Length (mm)	Width (mm)	Modulus of Elasticity (E) (GPa)	Poisson's Ratio (ν)	Density (ρ) (kg/m^3)
Beam1	8	430	12	210	0.3	7850
Beam2	1.5	400	13	210	0.3	7850

The parameters of the nonlinear elements and loss factor for the system are given as follows

$$\mu = 0.01,\ Normal\ Force = 50\ N,\ k_f = 3x10^4\ N/m \quad and \quad k^* = 3x10^9\ N/m^3$$

$$\gamma(loss\ factor) = 0.02$$

In order to obtain the nonlinear FRFs of the T-beam that will be used as simulated experimental values, ANSYS is used. The mesh used in the FE model is given Fig. 2.

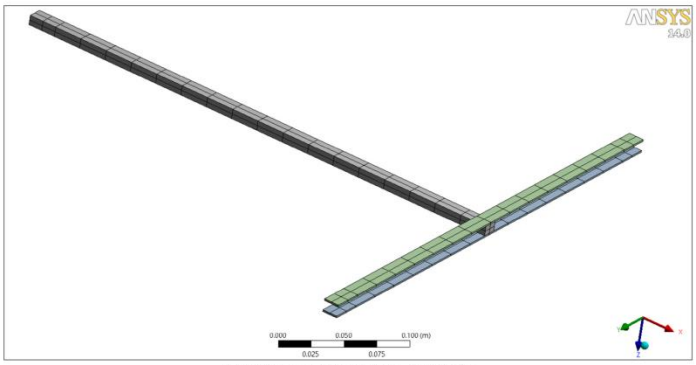

Fig.2 FE mesh used in ANSYS

The linear driving point FRFs of the structure at the tip of the *Beam1* in Z (transverse) direction are calculated by using the ANSYS results and employing the harmonic balance method. The nonlinear driving point FRFs at the tip of *Beam1* are calculated for different forcing levels. In order to simulate experiment, calculated FRF values are polluted with 5% noise. The noise has normal distribution and standard deviation of 5% of the amplitude of the original response. First, the system is excited harmonically with a low forcing amplitude (F_0=0.01 N). The harmonic response of the system at this forcing level is compared with the linear frequency response of the system obtained disregarding both friction and cubic stiffness nonlinearity in Fig. 3.

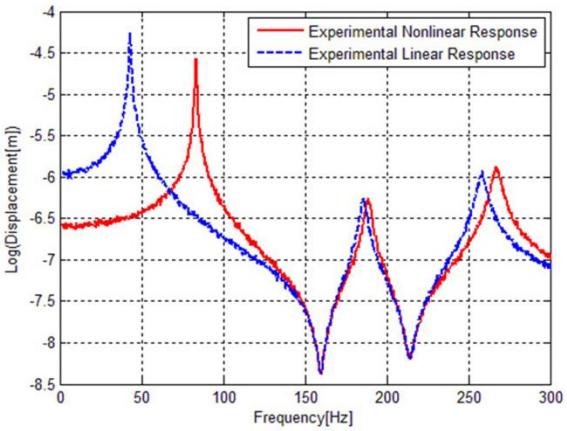

Fig.3 Frequency response of the system at F_0=0.01 N with 5% noise

Since nonlinear internal forces due to cubic stiffness are negligible at low forcing level, as can be seen in Fig. 3, the only nonlinear effect observed is due to friction. The shifts in the resonance frequencies are due to the stiffness component of friction. Similar response curves are obtained for 9 different higher excitation cases by taking the amplitude of the harmonic excitation force between 10 N and 50 N. The nonlinear harmonic responses at only the forcing levels of F_0=25 N and F_0=50 N are shown in Fig. 4.

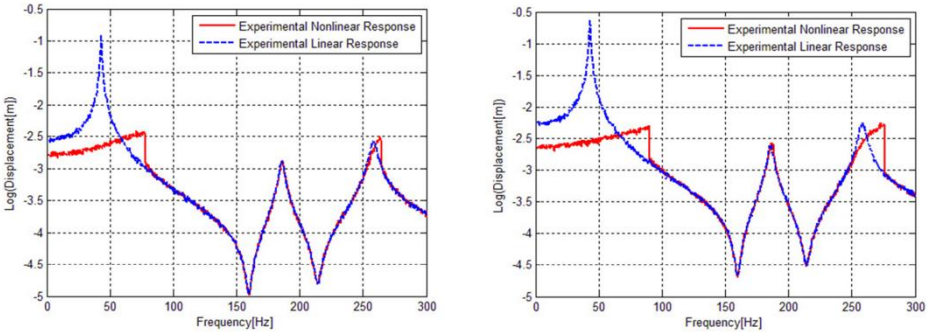

(a) (b)

Fig.4 Frequency responses of the system with 5% noise for (a) F_0 = 25 N, (b) F_0 = 50 N

As can be seen from Fig. 4, since at high forcing levels frictional nonlinearity is negligible, the nonlinearity changes the response of the system around 1st and 3rd resonance considerably by causing a jump, which is mainly due to cubic stiffness. 2nd mode of the system is slightly affected from the existence of the stiffness nonlinearity in the system, since at this mode the deflection of the point where cubic stiffness is attached is relatively small. By using the FRFs obtained for low and several high forcing levels, at the excitation frequency of 42 Hz, the equation of the regression curve is obtained and without fully identifying all the nonlinear parameters, frictional stiffness and cubic stiffness parameters are identified by comparing the terms of the regression equation with the corresponding describing functions. The regression curve obtained is given in Fig. 5.

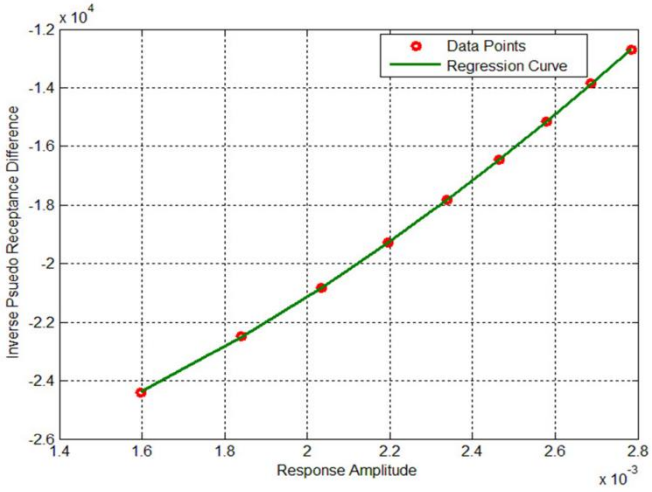

Fig.5 Polynomial regression curve fitted to data points

Identified nonlinear parameters and comparison of these values with the actual ones are given in Table 2.

Table 2 Comparison of nonlinear parameters

Nonlinear Parameters	Estimated	Actual	Error (%)
k^* (N/m^3)	3.04×10^9	3×10^9	1.3
k_f (N/m)	2.99×10^4	3×10^4	0.3

As can be seen in Table 2, there is a very small difference between the estimated and actual nonlinear parameters, Main reason of that discrepancy is having noisy data (used to simulate actual experiments). However, it is shown in the previous study [29] that once the nonlinearities are identified with reasonable accuracy, linear FRF of the nonlinear structure can be calculated quite accurately. From the calculated linear FRF, the first three natural frequencies of the simulated test system are obtained (Table 3).

Table 3 The first three flexural natural frequencies of the simulated test system

Mode Number	Natural Frequency (Simulated Test) (Hz)
1	43.1
2	185.8
3	258.2

On the other hand, the theoretical linear FE model of the system is built by taking the modulus of elasticity and density of the beams slightly different from the ones used in simulated test (Table 4). The effect of these variations on the first 3 natural frequencies of the linear part is given in Table 5.

Table 4 Material properties used in the original FE model

	Modulus of Elasticity (E) (GPa)	Poisson's Ratio (ν)	Density (ρ) (kg/m^3)
Beam1	200	0.3	7950
Beam2	200	0.3	7950

Then, the driving point FRFs at the tip of *Beam1* in Z (transverse) direction are calculated by using the theoretical FE model, and just to see the effect of using slightly different modulus of elasticity and density in the theoretical model, these FRFs are compared with the exact values obtained from the FE model of the simulated test system (Fig. 6). Note that in practical applications the linear FRFs of the actual nonlinear system cannot be directly measured, and it is the intension of this study to calculate these FRFs from measured FRFs of the nonlinear system.

Table 5 Comparison of the natural frequencies obtained from theoretical FE model with the actual values

Mode Number	Actual Natural Frequency (From FE Model of Simulated Test System) (Hz)	Natural Frequency Calculated from Theoretical FE Model (Hz)
1	43.1	41.8
2	185.8	180.3
3	258.2	250.4

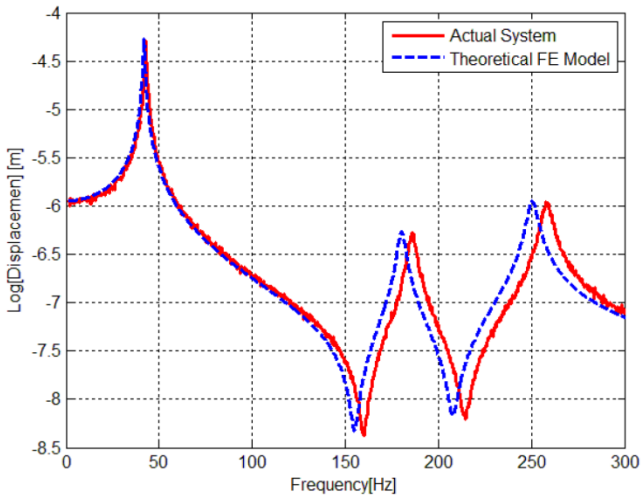

Fig.6 Comparison of the linear responses obtained from theoretical FE model and linear model of the actual system

As can be seen in Table 5 and Fig 6, there are discrepancies between the natural frequencies and linear responses obtained from theoretical FE model and actual values. In order to improve these results, FE model needs to be updated. However, the major problem in practical applications is that when the structure is nonlinear the FRF curve for the linear part cannot be accurately obtained especially when there is friction type of nonlinearity along with other types of nonlinearities.

In the theoretical linear FE model of the system, height of the *Beam1* (h1), height of the *Beam2* (h2), length of the *Beam2* (L2), modulus of elasticity of the *Beam1* and *Beam2* are decided to be the candidates for updating parameters. Selection of the updating parameters is carried out based on the sensitivity of natural frequencies to these parameters. By changing one parameter while keeping all the others constant, several different parameter sets are built. Running several FE analyses for these parameter sets, percentage changes in the natural frequencies with respect to percentage changes in parameters and the average sensitivity values are estimated for the first three flexural natural frequencies. The results are given in Fig.7 to 9.

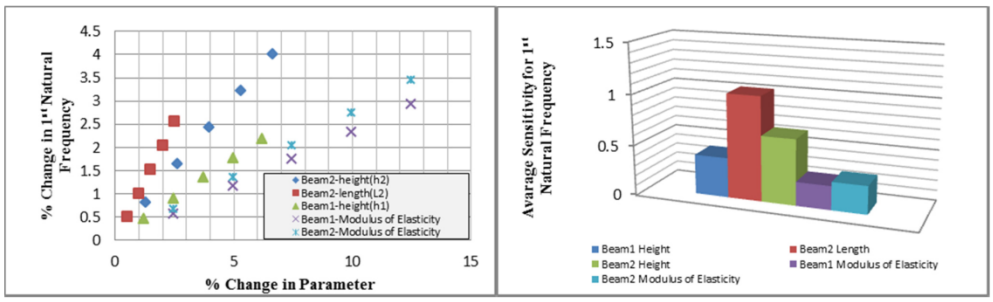

(a) (b)

Fig.7 (a) Change in 1st natural frequency with respect to change in parameters (b) Average sensitivity values

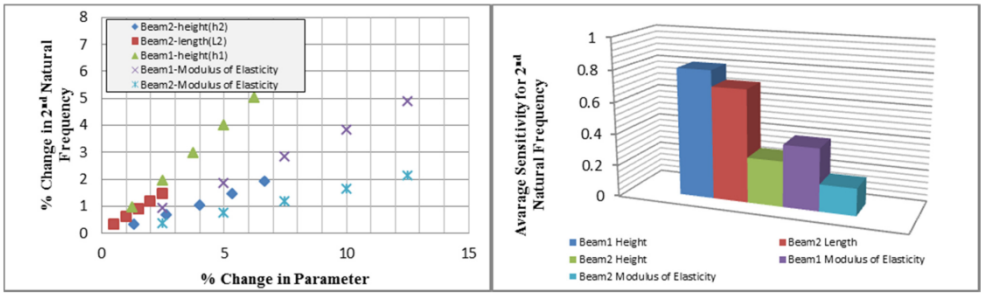

(a) (b)

Fig.8 (a) Change in 2nd natural frequency with respect to change in parameters (b) Average sensitivity values

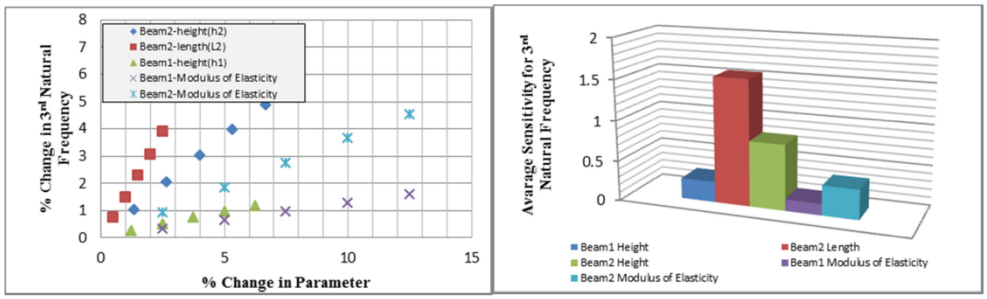

(a) (b)

Fig.9 (a) Change in 3rd natural frequency with respect to change in parameters (b) Average sensitivity values

As can be seen in Fig.7 and and Fig.9, 1st and 3rd flexural natural frequencies have the highest sensitivity values to the height and length of *Beam2*. On the other hand, 2nd flexural natural frequency has the highest sensitivity to the height of *Beam1* and length of *Beam2* as seen in Fig.8. Using these results, height of the *Beam2* (h2), and length of the *Beam2* (L2) are selected as the updating parameters in theoretical linear FE model. For the selected parameters, elements of the sensitivity matrix are calculated using the centered difference approximation with $O(h^4)$ which is given in equation (17) at each iteration step. After 8 iterations, updating parameters are converged and convergence graphs of these parameters are given in Fig. 10.

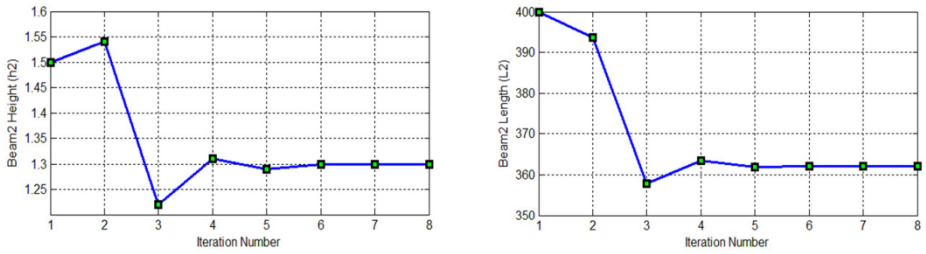

(a) (b)

Fig.10 (a) Convergence of the height of *Beam2* (b) Convergence of the length of *Beam2*

Using the converged parameter values (h2=1.295mm, L2=362.1mm), FE model is updated and modal analysis is performed in order to calculate the natural frequencies of the updated model. These natural frequencies are compared with those of the theoretical FE model and also with the natural frequencies of the actual system in Table 6. Note again that the last set of values cannot be directly measured in practical application; here we make use of the advantage of making simulated experiments.

Table 6 Comparison of natural frequencies obtained from the theoretical FE model (h2=1.5mm, L2=400mm) with those of the updated FE model (h2=1.295mm, L2=362.1mm)

Mode Number	Natural Frequency (Exact Value) (Hz)	Natural Frequency (Theoretical Model) (Hz)	Error (%)	Natural Frequency (Updated Model) (Hz)	Error (%)
1	43.1	41.8	-3.02	42.1	-2.32
2	185.8	180.3	-2.96	185.4	-0.22
3	258.2	250.4	-3.02	258.4	0.08

As can be seen in Table 6, there are considerable improvements for the 2nd and 3rd natural frequencies and a slight improvement in the 1st natural frequency. In Fig.11, the linear responses obtained from theoretical and updated FE models are compared. Exact response is also given in the same figure in order to show the improvement achieved with updating process.

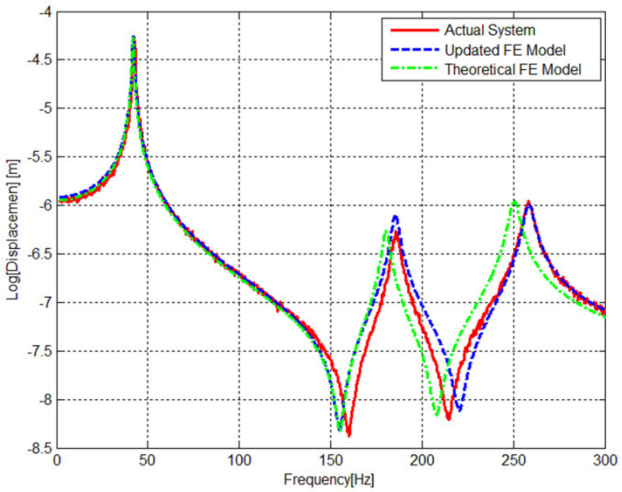

Fig.11 Comparison of linear responses obtained from theoretical and updated FE models with the linear model of the actual system

As can be seen in Fig.11, around 2nd and 3rd resonance regions considerable improvements are obtained in the frequency response when updated FE model is used. Since the ultimate goal is to have accurate nonlinear response predictions from the updated model, experimental nonlinear responses are compared with those obtained from the initial theoretical model and nonlinear responses obtained by using updated model for F_0=0.01 N and F_0=25 N in Fig.12 and Fig.13, respectively.

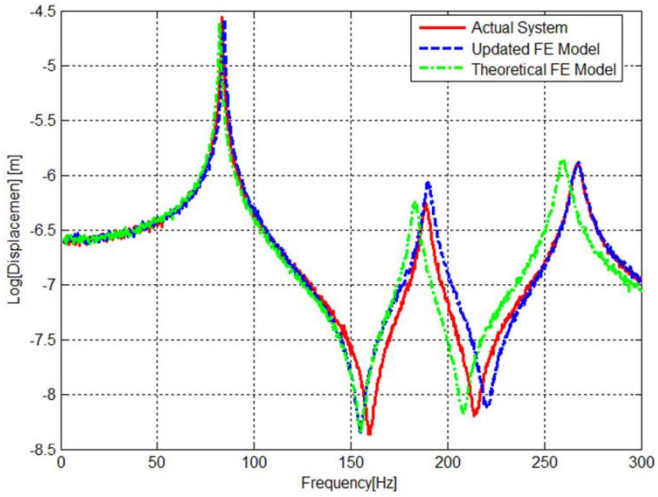

Fig.12 Comparison of nonlinear responses obtained from theoretical and updated models with experimental one for F_0=0.01 N

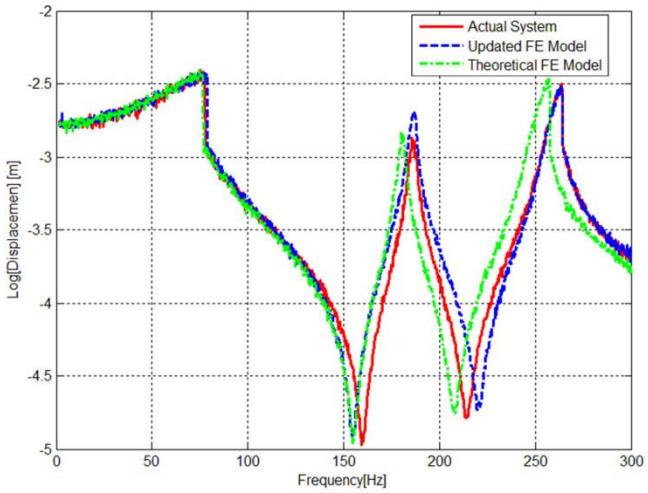

Fig.13 Comparison of nonlinear responses obtained from theoretical and updated models with experimental one for F_0=25 N

As can be observed in Fig.12 and 13 that there are considerable improvements around 2nd and 3rd resonance regions in the updated nonlinear response, and these are the modes which require corrections in this application. The reason for not having similar improvements around anti-resonance frequencies is discussed below.

4 DISCUSSION AND CONCLUSIONS

In this study a model updating method for nonlinear structures is developed. In the nonlinear model updating approach proposed, the method developed recently by the authors to obtain linear FRFs of nonlinear structures having multiple nonlinearities including friction type of nonlinearity is used. Nonlinear model updating method proposed is validated with a nonlinear simulated test system.

The method is based on measuring FRFs of a nonlinear structure at a low forcing level, as well as at several different high forcing levels. Then, by using the FRF values measured at a single frequency the FRF of the corresponding linear part of the structure is calculated, so that any FRF based model updating method can be applied to correct the mathematical model for the linear part of the system. In this approach, the most of the nonlinearities in the system are also identified. Although friction type of nonlinearity cannot be fully identified (normal force and friction coefficient cannot be identified), all nonlinear effects are removed from the measured nonlinear FRF, and thus FRF of the linear part can accurately be calculated.

The nonlinear test system used in this study is a T-beam with cubic stiffness and dry friction nonlinearity. In order to simulate experimental measurements, the nonlinear responses at the tip point of *Beam1* are calculated by using FE model and the nonlinear parameters via harmonic balance method. These responses are first polluted with random noise in order simulate experimental results more realistically. Then, the linear FRF of the system is determined from the simulated experimental measurements of the nonlinear system by using the method suggested. On the other hand, the theoretical FE model of the system is constructed with certain errors in material properties. This mathematical model is used as the theoretical model to be updated.

Since there exists discrepancies between the natural frequencies calculated from the theoretical linear FE model and those obtained from the simulated test results, as expected, the theoretical linear FE model is updated by using Inverse Eigen Sensitivity method. The sensitivity of natural frequencies to the candidate parameters for model updating is obtained by performing several FE analyses. Using the sensitivity values, updating parameters are selected among the candidate parameters. The selected updating parameters are the ones with highest average sensitivity values for the first three natural frequencies. Once the updating parameters are selected, iterations are continued until a convergence is obtained for the solution of values for updating parameters. Note that the selected parameters may not be the actual parameters which are in error, as it is the case in this application. Still the method work with acceptable accuracy as can be seen from the results presented in this study.

Then, the natural frequencies calculated using the updated FE model are compared with the values found from theoretical FE model. As we know the exact values due to using simulated experiments rather than actual test results, it was easy to see the improvements. It is observed that there are improvements in all natural frequencies, and in the 2nd and 3rd natural frequencies where the differences between the responses obtained from the initial theoretical model and experiments are maximum, the improvements are considerably important. Finally, both linear and nonlinear updated responses are compared with the results obtained by using the theoretical model, as well as with simulated experimental results. The nonlinear harmonic responses are calculated for the harmonic forcing amplitudes of F_0=0.01 N and F_0=25 N. It is observed that there is again a considerable improvement around 2nd and 3rd natural frequencies in the updated nonlinear and linear responses. This improvement is less pronounced around the anti-resonance regions which may be due to the model updating method used. Therefore, when our concern in model updating is not limited with resonance regions, then a different method may be employed for linear model updating part of the approach suggested. Therefore, it is concluded that the general approach proposed in this study is very successful in updating linear FE part of a nonlinear system.

5 REFERENCES

[1] Sidhu J., Ewins D. J., "Correlation of Finite Element and Modal Test Studies of a Practical Structure", Proceedings of the 2nd International Modal Analysis Conference, Orlando, Florida, pp.756-762, 1984.

[2] Dascotte E. Vanhonacker P., "Development of an Automatic Mathematical Model Updating Program", Proceedings of the 7th International Modal Analysis Conference, Las Vegas, Nevada, pp.596-602, 1989.

[3] Brughmans M., Lembregts F., "Using Experimental Normal Modes for Analytical Model Updating", Proceedings of the 8th International Modal Analysis Conference, Kissimmee, Florida, pp.389-396, 1990.

[4] Nalitolela N. G., Penny J. E. T., Friswell M. I. "Updating Structural Parameters of a Finite Element Model by Adding Mass or Stiffness to the System", Proceedings of the 8th International Modal Analysis Conference, Kissimmee, Florida, pp.836-842, 1990.

[5] Roy N. A., Girard A., Dupuis P. E., "A Direct Energy Approach for Updating Dynamic Finite Element Models", Proceedings of the 9th International Modal Analysis Conference, Florence, Italy, pp.51-57, 1991.
[6] Visser W. J., Imregun M., "A Technique to Update Finite Element Models Using Frequency Response Data", Proceedings of the 9th International Modal Analysis Conference, Florence, Italy, pp.462-469, 1991.
[7] Brughmans M. Hrycko G., Wyzykowski J., "Application of FEM Model Correlation and Updating Techniques on an Aircraft Using Test Data of a Ground Vibration Survey", Proceedings of the 9th International Modal Analysis Conference, Florence, Italy, pp.517-525, 1991.
[8] Ibrahim S. R., D'Ambrogio W., Salvani P., Sestieri A. J., "Direct Updating of Nonconservative Finite Element Models Measured Input-Output", Proceedings of the 10th International Modal Analysis Conference, San Diego, California, pp.202-210, 1992.
[9] Link M., Zhang L., "Experience with Different Procedures for Updating Structural Parameters of Analytical Models Using Test Data", Proceedings of the 10th International Modal Analysis Conference, San Diego, California, pp.730-738, 1992.
[10] Jung H., Ewins D. J., "Error Sensitivity of the Inverse Eigensensitivity Method for Model Updating", Proceedings of the 10th International Modal Analysis Conference, San Diego, California, pp.1051-1056, 1992.
[11] Aiad A., Level P., Ravalard Y., "A Global Updating Procedure to Improve Finite Elements Models", Proceedings of the 10th International Modal Analysis Conference, San Diego, California, pp.992-998 1992.
[12] Miccoli G., Agostoni F., "Modal Updating Using Sensitivity Analysis", Proceedings of the 11th International Modal Analysis Conference, Kissimmee, Florida, pp.683-689, 1993.
[13] Luber W., Sensburg O. "Identification of Errors and Updating in Analytical Models Using Test Data", Proceedings of the 13th International Modal Analysis Conference, Nashville, Tennessee, pp.407-413, 1995.
[14] Dascotte E., Strobbe J., Hua H., "Sensitivity Based Model Updating Using Multiple Types of Simultaneous State Variables", Proceedings of the 13th International Modal Analysis Conference, Nashville, Tennessee, pp.1035-1040, 1995.
[15] Hemez F., M., "Advanced Tools for Updating Damped Finite Element Models Using Static Modal and Flexibility Data", Proceedings of the 14th International Modal Analysis Conference, Dearborn, Michigan, pp.511-517, 1996.
[16] Lindholm B., E., "A Bayesian Statistics Approach to Updating Finite Element Models with Frequency Response Data (Part II: Application)", Proceedings of the 14th International Modal Analysis Conference, Dearborn, Michigan, pp.1458-1465, 1996.
[17] Lenoir D., Cogan S., Lallement G., Bricout J. N., "Model Updating by Modal Synthesis of Experimental Forced Responses", Proceedings of the 16th International Modal Analysis Conference, Santa Barbara, California, pp.399-405, 1998.
[18] Mottershead J. E., Mares C., Friswell M. I., James S., "Model Updating of an Aluminium Space-frame Using Different Parameter Sets", Proceedings of the 18th International Modal Analysis Conference, San Antonio, Texas, pp. 576-583, 2000.
[19] Jung D. S., Kim C. Y., Kang J. H., "Hybrid Optimization Technique based on GA-NMS for FE Model Updating", Proceedings of the 25th International Modal Analysis Conference, Orlando, Florida USA, 2007.
[20] Kozak M. T., Cömert M. D., Özgüven H. N., "Model Updating Routine Based on the Minimization of a New Frequency Response Based Index for Error Localization", Proceedings of the 25th International Modal Analysis Conference, Orlando, Florida USA, pp.84-95, 2007.
[21] Boulkaibet I., Mthembu L., Marwala T., Friswell M. I., Adhikari S., "Finite Element Model Updating Using the Shadow Hybrid Monte Carlo Technique", Proceedings of the 31th International Modal Analysis Conference, Orange County, California USA, 2013.
[22] Hasselman T. K., Anderson M. C., Gan W., "Principal Components Analysis for Nonlinear Model Correlation, Updating and Uncertainty Evaluation", Proceedings of the 16th International Modal Analysis Conference, Santa Barbara, California, pp.644-651, 1998.
[23] Anderson M. C., Carne T. G., "Model Correlation and Updating of a Nonlinear Finite Element Model Using Crush Test Data", Proceedings of the 17th International Modal Analysis Conference, Kissimmee, Florida, pp.1511-1517, 1999.
[24] Anderson M. C., Hasselman T. K., "Minimizing Parameter Correlation in Nonlinear Model Updating", Proceedings of the 18th International Modal Analysis Conference, San Antonio, Texas, pp.109-115, 2000.
[25] Burton T. D., Hemez F. M., Rhee W., "Combined Model Reduction/SVD Approach to Nonlinear Model Updating", Proceedings of the 18th International Modal Analysis Conference, San Antonio, Texas, pp.116-123, 2000.
[26] Zhang L., Guo Q., "A Case Study of Model Updating and Validation of a Frame Structure with Highly Non-linear Component", Proceedings of the 25th International Modal Analysis Conference, Orlando, Florida USA, 2007
[27] Silva S. D., Cogan S., Foltete E., Buffe F., "Metrics for Non-Linear Model Updating in Mechanical Systems", Proceedings of the 26th International Modal Analysis Conference, Orlando, Florida USA, 2008
[28] Kerschen G., Worden K., Vakakis A. F., Golinval J. C., "Past, Present and future of Nonlinear System Identification in Structural Dynamics", Mechanical Systems and Signal Processing, Volume 20, pp 505-592, 2006.

[29] Canbaloglu G., Özgüven H. N., "Obtaining Linear FRFs for Model Updating in Structures with Multiple Nonlinearities Including Friction", Topics in Nonlinear Dynamics, Volume 1: Proceedings of the 31st IMAC, A Conference on Structural Dynamics, pp.145-157, 2013.
[30] Budak E., Özgüven H. N., "A Method for Harmonic Responses of Structures with Symmetrical Nonlinearities", Proceedings of the 15th International Seminar on Modal Analysis and Structural Dynamics, Leuven, Belgium, v.2, pp.901–915, 17-21 September 1990.
[31] Budak E., Özgüven H. N., "Iterative Receptance Method for Determining Harmonic Response of Structures with Symmetrical Non-linearities", Mechanical Systems and Signal Processing, v.7, n.1, pp.75–87, 1993.
[32] Tanrıkulu Ö., Kuran B., Özgüven H. N., Imregün M., "Forced Harmonic Response Analysis of Non-linear Structures Using Describing Functions", AIAA Journal, v.31, n.7, pp.1313-1320, 1993.

Experimental Validation of Pseudo Receptance Difference (PRD) Method for Nonlinear Model Updating *

Güvenç Canbaloğlu[1,2], H. Nevzat Özgüven[1]
[1]Department of Mechanical Engineering, Middle East Technical University, 06800 Ankara, TURKEY
[2]MGEO Division, ASELSAN Inc., 06750 Ankara, TURKEY
e-mail: gcanbal@aselsan.com.tr, ozguven@metu.edu.tr

ABSTRACT

In real life applications most of the structures have nonlinearities, which restrict us applying model updating techniques available for linear structures. Well-established FRF based model updating methods would easily be extended to a nonlinear system if the FRFs of the underlying linear system (linear FRFs) could be experimentally measured. When frictional type of nonlinearity co-exists with other types of nonlinearities, it is not possible to obtain linear FRFs experimentally by using low level forcing. Pseudo Receptance Difference (PRD) method, recently developed by the authors, calculates linear FRFs of a nonlinear structure by using FRFs measured at various forcing levels, and simultaneously identifies multiple nonlinearities in the system. Then any model updating method can be used to update the linear part of the mathematical model. In this present work, the PRD method is used to predict the linear FRFs from nonlinear FRFs, and the inverse eigensensitivity method is employed to update the linear finite element (FE) model of a nonlinear structure. A real nonlinear T-beam test structure is used to validate the accuracy of the proposed method. First, the linear FRFs are calculated from nonlinear FRFs measured at different forcing levels, and simultaneously, the nonlinearities in the structure are identified. Then the FE model of the linear part of the structure is updated. Finally, the accuracy of the updated nonlinear model of the test structure is demonstrated by comparing the calculated and measured FRFs of the test structure at several different forcing levels.

KEYWORDS

Nonlinear model updating, nonlinearity, nonlinear identification, friction nonlinearity, nonlinear structures

1 INTRODUCTION

Accurate prediction of the dynamic response of a structure is a vital step in the design stage of engineering structures. FE method is the most common numerical method used for obtaining dynamic response of engineering structures. However, usage of FE methods may yield certain inaccuracies arising from modeling errors, Due to these errors experimental and FE method results do not always match perfectly. Therefore FE models need to be updated by using the experimental results and changing some of the parameters used in the FE model.

Various model updating methods were developed in order to correct the mathematical models. However most of the model updating methods available in literature are for linear systems. Nalitolela et al. [1] proposed a method which is based on exact model reduction and perturbation of both the actual structure and its analytical model by adding mass or stiffness in order to produce accurate dynamic models. Roy et al. [2] proposed direct energy approach to relate the kinetic and strain energies of each part of a FE model to the experimental data. Brughmans et al. [3] applied a FE model updating technique, based on a forward sensitivity formulation, to a twin propeller commuter aircraft. Link and Zhang [4] applied different updating techniques to a test structure in order to investigate the sensitivity of updating results in these methods. Jung and Ewins [5] studied the application of the inverse eigensensitivity method for model updating using arbitrarily chosen macro elements to a simple frame. In order to investigate the potential errors causing the discrepancies between analytical and experimental normal modes, Miccoli and Agostoni [6] used the sensitivity analysis. Hemez [7] studied an updating method which is based on sensitivity approach for damped FE models. A new model updating method is proposed by Lenoir et al. [8] which is based

---

*G. Canbaloglu, H.N. Özgüven, Experimental Validation of Pseudo Receptance Difference (PRD) Method for Nonlinear Model Updating , Nonlinear Dynamics, Volume 1: Proceedings of the 33rd IMAC, A Conference and Exposition on Structural Dynamics, 2015

on the modal synthesis of experimental forced responses. Mottershead et al. [9] studied the effect of the selection of different updating parameters in the model updating of an aluminum space frame. In order to update a bridge structure Jung et al. [10] presented a hybrid optimization technique based on the genetic algorithm and Nelder-Mead simplex. Kozak et al. [11] proposed a new error localization method and an updating routine and applied the routine in different case studies. In a more recent work Boulkaibet et al. [12] studied the use of the Shadow Hybrid Monte Carlo technique to determine the selection of updating parameters. Fei and Jiang [13] studied the criteria of evaluating initial models that will be used in the updating procedure. In a very recent work, Boulkaibet et al. [14] proposed the use of Separable Shadow Hybrid Monte Carlo method for the updating of FE models. Hemez [15] briefly overviewed the first 30 years of FE model updating development, from the mid-1960's to the mid-1990's and categorized FE model updating methods into broad categories that each offers their own benefits and limitations.

Since most of the structures have nonlinear behavior, it is vital to have model updating techniques for nonlinear structures as well. Hasselman et al. [16] studied Principal Components Analysis which is based on singular value decomposition of a collection of response time history, for nonlinear model correlation and updating. In a later work Anderson and Hasselman [17] addressed the issue of the minimizing the correlation of parameter estimates in the updating of nonlinear systems. Burton et al. [18] studied the combined model reduction and singular value decomposition approach for model updating of nonlinear structures. Silva et al. [19] studied harmonic balance, constitutive relation error, restoring force surface and Karhunen-Loève decomposition methods for nonlinear model updating, and compared with each other. Canbaloglu and Özgüven, very recently, developed a method to obtain linear FRFs of nonlinear structures having multiple nonlinearities including friction type of nonlinearity, from nonlinear FRF measurements [20] and used this method in the nonlinear model updating approach proposed [21]. The method is validated by applying the method developed to a nonlinear test system.

For nonlinear structures, it is possible to use model updating techniques developed for the linear systems, if the linear dynamic behaviors of the structure are obtained which may require identification of nonlinearity first. Kerschen et al. [22] presented a literature survey which is one of the most detailed nonlinear system identification literature surveys in which more than 400 papers were cited. The method developed by Canbaloglu and Özgüven [20] aims to obtain linear FRFs of a nonlinear structure from FRF measurements, without fully identifying nonlinearities, the ultimate goal being to update linear model parameters of a nonlinear structure having multiple nonlinearities including friction type of nonlinearity. Very recently, Doranga and Wu studied [23] the Nonlinear Resonant Decay method for parameter identification of nonlinear dynamic systems. Grappasonni et al. [24] presented a method for identification of an experimental cantilever beam with a geometrically nonlinear thin beam clamped with prestress. Aykan and Altuntop [25] implemented the method developed for parametrically identifying nonlinearities from measured frequency response functions [26] to a gearbox. Londono and Cooper [27] developed a technique for the experimental identification of structures exhibiting geometric nonlinearities, in particular aircraft with highly flexible wings. In this study, the method [20, 21] developed by the authors for nonlinear model updating, is experimentally validated by applying the approach to a real nonlinear T-beam test structure. First, the linear FRFs are calculated from nonlinear FRFs measured at different forcing levels, and simultaneously the nonlinearities in the structure are identified. Then the FE model of the linear part of the structure is updated. Finally, in order to demonstrate the accuracy of the updated nonlinear model of the test structure, predicted and measured FRFs of the test structure are compared at several different forcing levels.

2 THEORY

The model updating method recently developed by Canbaloglu and Özgüven [20, 21] is used in this study for updating the FE model of a nonlinear structure. Since the theory of the method is given in detail in references 20 and 21, just a very brief summary is presented here.

For a nonlinear system, it is possible to write the following equation.

$$[\Delta]=\left[\Delta_f\right]+[\Delta_{HF}]=\left[H^{NL}\right]^{-1}-\left[H^{L}\right]^{-1} \tag{1}$$

where $[\Delta]$, $\left[\Delta_f\right]$, $[\Delta_{HF}]$, $\left[H^{NL}\right]$, $\left[H^{L}\right]$ are the nonlinearity matrix, nonlinearity matrix due to friction, nonlinearity matrix due to remaining nonlinearities that are dominant at high forcing levels of excitation, response level dependent nonlinear and linear FRF matrices, respectively. Measuring FRFs experimentally several times at the same frequency but at different forcing levels the following set of equations can be written:

$$\left[\Delta_{HF}\right]_{i+1}-\left[\Delta_f\right]_1=\left[H^{NL}\right]_{i+1}^{-1}-\left[H^{NL}\right]_1^{-1} \qquad i=1,2,...,(n-1) \tag{2}$$

In equation (2), subscript 1 indicates low forcing case and subscripts 2, 3, … n indicate high forcing cases. The detailed derivation of the formulation can be found in [20]. The nonzero elements in the nonlinearity matrices at the left hand sides which can be written as polynomial functions of response amplitudes with unknown coefficients are the describing functions of the corresponding nonlinearities. Polynomial fit for (*n-1*) data points is applied in a least square sense and the equation of the corresponding regression curve is obtained in order to find the unknown coefficients. By comparing the terms of the regression equation with the corresponding describing functions, nonlinearities are identified and then linear FRFs can easily be calculated as [20]

$$\left[H^L\right]_1=\left[\left[H^{NL}\right]_1^{-1}-\left[\Delta_f\right]_1\right]^{-1} \tag{3}$$

One of the drawbacks of the above equation is that it requires the full matrix inversions. Therefore the formulation is improved for nonlinear structures where the nonlinearity is local [21]. For local nonlinearities it possible to partition the nonlinearity matrix as

$$[\Delta]=\begin{bmatrix}[\Delta_{aa}] & [0]\\ [0] & [0]\end{bmatrix} \tag{4}$$

where subscript *a* represents coordinates where nonlinear elements are connected ("nonlinear coordinates" in short). Pre-multiplying all the terms in equation (1) by $\left[H^L\right]$, post-multiplying by $\left[H^{NL}\right]$ and using equation (4) for the nonlinearity matrix, the following equation is obtained:

$$\begin{bmatrix}\left[H^L_{aa}\right] & \left[H^L_{ab}\right]\\ \left[H^L_{ba}\right] & \left[H^L_{bb}\right]\end{bmatrix}\begin{bmatrix}[\Delta_{aa}] & [0]\\ [0] & [0]\end{bmatrix}\begin{bmatrix}\left[H^{NL}_{aa}\right] & \left[H^{NL}_{ab}\right]\\ \left[H^{NL}_{ba}\right] & \left[H^{NL}_{bb}\right]\end{bmatrix}=\begin{bmatrix}\left[H^L_{aa}\right] & \left[H^L_{ab}\right]\\ \left[H^L_{ba}\right] & \left[H^L_{bb}\right]\end{bmatrix}-\begin{bmatrix}\left[H^{NL}_{aa}\right] & \left[H^{NL}_{ab}\right]\\ \left[H^{NL}_{ba}\right] & \left[H^{NL}_{bb}\right]\end{bmatrix} \tag{5}$$

Here subscript *b* corresponds to linear coordinates.

Considering the first submatrix of the resultant matrix and performing some matrix manipulations, the linear FRF matrix for the nonlinear coordinates can be obtained as [21]

$$\left[H^L_{aa}\right]_1=\left[\left[H^{NL}_{aa}\right]_1^{-1}-\left[\Delta_f\right]_1\right]^{-1} \tag{6}$$

It is obvious that for locally nonlinear structures computational effort will be considerably reduced by using the above equation compared with equation (3). Once the linear FRFs are calculated by using equation (6), then they can be used in the model updating process of a FE model. Note that in several model updating methods having FRFs of limited number of coordinates is sufficient. Therefore, having FRF of even a single coordinate may be enough for model updating.

One of the common methods used for model updating is the inverse eigensensitivity method [28], which is based on the following equation:

$$\{\Delta r\}=[S]\{\Delta p\} \tag{7}$$

Here, $\{r\}$ is the response vector composed of mode shapes and natural frequencies, $\{p\}$ is the parameter vector composed of geometrical parameters or material properties used in the FE model, and $[S]$ is the modal sensitivity matrix. Modal sensitivity matrix $[S]$ can be written as

$$[S]=\begin{bmatrix} S_{r_1}^{\ p_1} & \cdots & S_{r_1}^{\ p_m} \\ \vdots & \ddots & \vdots \\ S_{r_n}^{\ p_1} & \cdots & S_{r_n}^{\ p_m} \end{bmatrix} \tag{8}$$

In equation (8), $S_{r_n}^{\ p_m}$ stands for the sensitivity of the nth response to the mth updating parameter. For complex structures it is easier to calculate the sensitivities by numerical differentiation. In this study, centered difference approximation with $O(h^4)$ is used to obtain the sensitivities as given in the following equation:

$$\dot{r}(p_i)=\frac{-r(p_{i+2})+8r(p_{i+1})-8r(p_{i-1})+r(p_{i-2})}{12\Delta p} \tag{9}$$

After obtaining the sensitivity matrix $[S]$ and $\{\Delta r\}$ vector, $\{\Delta p\}$ which gives the changes required to be made in parameter vector, can be obtained from the following equation:

$$\{\Delta p\}=[S]^{-1}\{\Delta r\} \tag{10}$$

3 EXPERIMENTAL STUDY

In this section, PRD method developed recently [20] is applied to a nonlinear experimental test system. The test system is a T-beam which is similar to the test rig used by Ferreira [29] and also by Siller [30]. Using the PRD method, both linear FRFs and the nonlinearities in the system are obtained from experimentally measured nonlinear FRFs.

3.1 Experimental setup

The test set-up is a T-beam which consists of a cantilever beam with its free end is maintained between two thin identical beams having fixed-fixed boundary conditions. The thin beams which are attached to the free end of the cantilever beam are the main source of nonlinearity in the test structure. The dimensions of the T-beam are given in Fig.1.

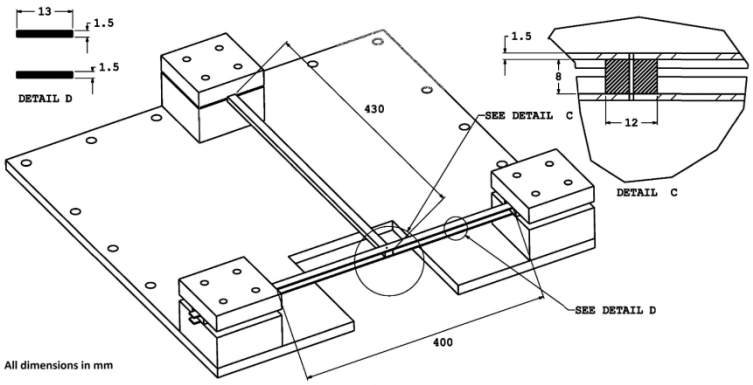

Fig.1 Nonlinear T-beam test system

In order to maintain the fixed boundary conditions, beams are manufactured longer than their original dimensions, so that adequate parts of the beams are fixed between fixture blocks. The material used for the beams is St37. The test rig used in the experiments is shown in Fig.2.

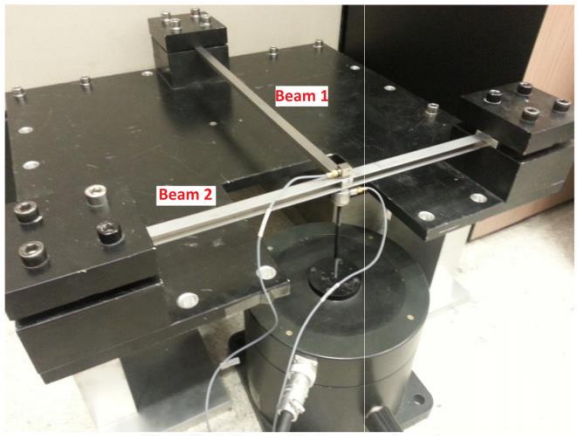

Fig.2 Test rig used in the experiment

In the experiments performed in this study, the structure is excited with B&K Type 4808 modal shaker via a push-rod. In order to increase the excitation level of the shaker, B&K Type 2712 power amplifier is used. Acceleration responses and the forces applied are measured with B&K Type 4507B accelerometer and B&K Type 8230-002 force transducer, respectively. In all the measurements, as a data acquisition system, B&K Type 3560C frontend is used. The equipment used in the experiments is shown in Fig.3.

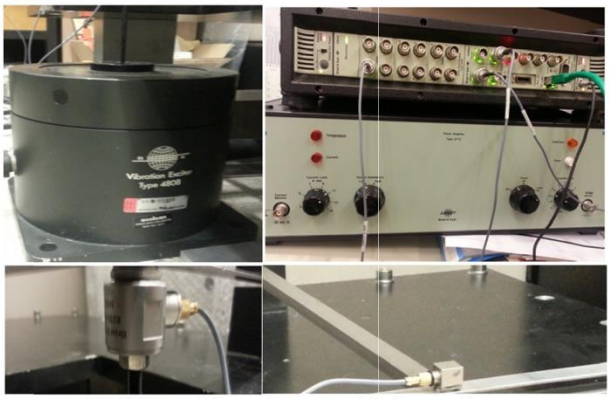

Fig.3 View of the equipment used in the experiments

3.2 First set of experiments

In order to apply the PRD method, a set of experiments is conducted on the test setup. Firstly, the structure is excited with a random excitation. Since the method proposed by Canbaloglu and Özgüven [20, 21] depends on frequency of excitation, and it is shown that method works better around a linear resonance frequency of the structure, a quick test which does not excite nonlinearities considerably is made. In random excitation, low excitation signal level is selected and using this excitation type, driving point FRF at the tip of beam 1 in transverse direction is measured. The frequency range is selected between 0-100 Hz and a frequency resolution of 0.25 Hz is used in the measurements. In order to eliminate the noise in measurements, 130 averages are taken. After the analysis of the measurements, driving point FRF at the tip of beam 1 in transverse direction is obtained as shown in Fig.4.

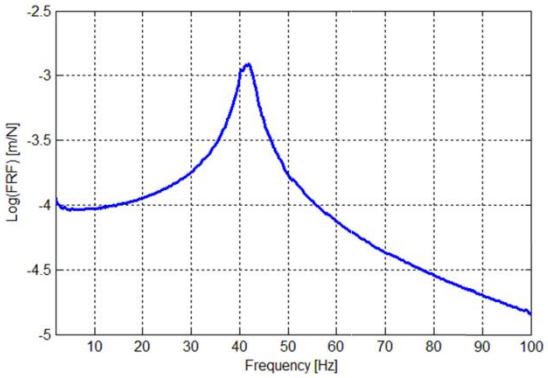

Fig.4 The driving point FRF at the tip of beam 1 in transverse direction

From Fig.4, it is observed that the first resonance of the structure in transverse direction is around 41 Hz. Therefore in order to apply the proposed method, the structure is excited at around that frequency with a pure sine excitation at different forcing levels. The structure is excited at a low forcing level and then at a number of high forcing levels. The advantage of this method is that, there is no need for any vibration controller as in the cases of constant forcing or constant amplitude testing over a certain frequency range.

In order to study the effect of choosing different frequencies of excitation on the performance of the method, two different excitation frequencies (39 Hz, 40 Hz) are used and for each of these excitation frequencies, describing functions of the nonlinearities are obtained by using the method proposed.

3.2.1 Application of the PRD method at excitation frequency 39 Hz

In Fig.5, the calculated real and imaginary parts of the describing function obtained from experimental measurements by using PRD method and the corresponding fitted curves are shown.

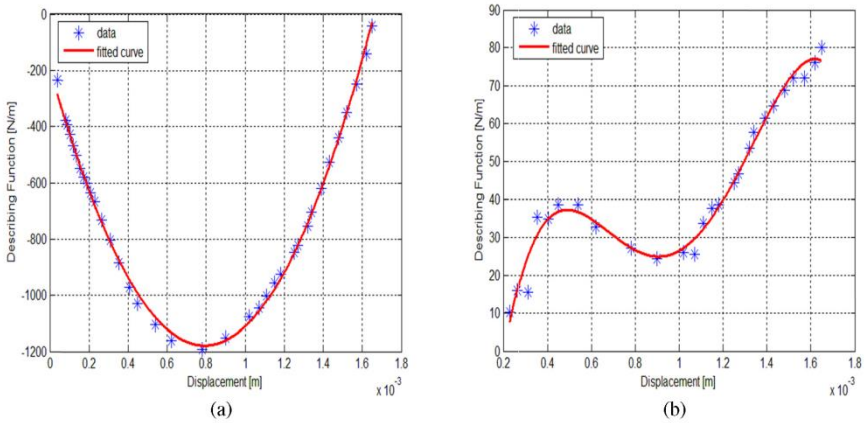

Fig.5 Calculated describing function (a) Real part (b) Imaginary part

For the real part of describing function, 2nd order, for the imaginary part of the describing function 4th order polynomials are fit. The coefficients estimated are given in Table 1.

Table 1 Coefficients of the polynomials fit to the data for real and imaginary parts of the describing function

	p_4	p_3	p_2	p_1	p_0
Real Part of Describing Function $p_2x^2 + p_1x + p_0$	---	---	$1.56\text{x}10^9$	$-2.48\ \text{x}10^6$	-190
Imaginary Part of Describing Function $p_4x^4 + p_3x^3 + p_2x^2 + p_1x + p_0$	$-2.74\text{x}10^{14}$	$1.10\text{x}10^{12}$	$-1.49\text{x}10^9$	$8.0\ \text{x}10^5$	-109

3.2.2 Application of the PRD method at excitation frequency 40 Hz

In Fig.6, calculated real and imaginary parts of the describing function obtained from experimental measurements by using PRD method and the corresponding fitted curves are shown.

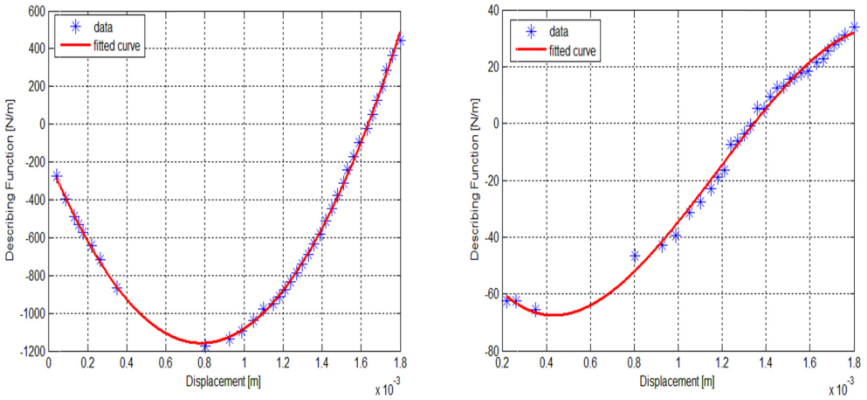

Fig.6 Calculated describing function (a) Real part (b) Imaginary part

For the real part of describing function, 2nd order, for the imaginary part of the describing function 3rd order polynomials are fit. The coefficients estimated are given in Table 2.

Table 2 Coefficients of the polynomials fit to the data for real and imaginary part of the describing function

	p_3	p_2	p_1	p_0
Real Part of Describing Function $p_2x^2 + p_1x + p_0$	---	$1.59\text{x}10^9$	$-2.49\text{x}10^6$	-181
Imaginary Part of Describing Function $p_3x^3 + p_2x^2 + p_1x + p_0$	$-6.0\text{x}10^{10}$	$2.15\text{x}10^8$	$-1.52\text{x}10^5$	-36

If we compare the coefficients for the real part of describing functions obtained using the measurements at 39 Hz and 40 Hz, it can be observed that coefficients are very close to each other. However when coefficients for the imaginary part of describing functions obtained by using the measurements at 39 Hz and 40 Hz are observed, it is seen that there are differences between the coefficients.

As a final test in this set of experiments, a constant low forcing level excitation experiment is performed between 37 Hz and 47 Hz. Stepped sine constant force test is performed for the given test set-up. Frequency resolution of 0.25 Hz is used in the experiment. Pure sine signal is used as the excitation signal. However, in order to make constant force vibration testing over the frequency range, a control strategy is needed in the experiments. This control is maintained manually by checking the forcing level and changing the excitation voltage supplied to the shaker iteratively for each frequency point. In Fig.7, measured FRFs at F=0.05 N are shown.

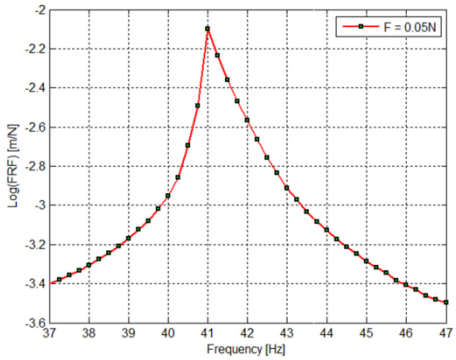

Fig.7 Measured FRF at F=0.05 N

It is observed from the Fig.7 that, the FRFs measured at F=0.05 N seem like a linear FRF, which is an expected result.

3.3 Second set of experiments

In the second set of experiments, the aim is to perform the measurements which will be used to verify the PRD method and the model updating approach proposed. A set of stepped sine constant force tests is performed on the given set-up. Frequency resolution of 0.25 Hz is used in the experiment. Similarly, the constant force excitation is maintained by manually checking the forcing level and changing the excitation voltage supplied to the shaker at each frequency point. The structure is excited with 3 different forcing levels (F=0.6 N, F=0.7 N, F=0.8 N).The measured FRFs are shown in Fig.8.

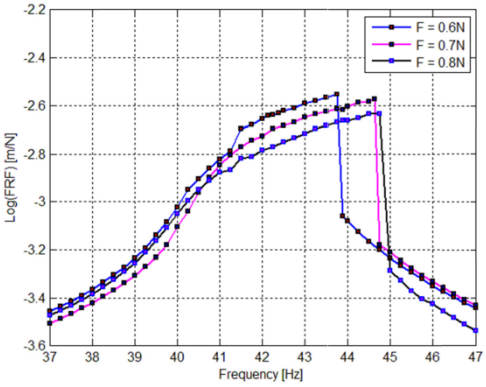

Fig.8 Measured FRF at F=0.6 N, F=0.7 N, F=0.8 N

4 APPLICATION OF THE PRD METHOD

Using the describing function values obtained and the FRF values measured at F=0.05 N in the first set of experiments, linear FRF of the structure is predicted by applying PRD method. Since, describing function values are obtained at two different excitation frequencies, in order to study the effects of test frequency on the performance of the method, two separate linear FRF curves are predicted. The two linear FRF curves predicted by using the describing functions obtained from experiments made at 39 Hz and 40 Hz are compared with the FRFs measured at F=0.05 N in Fig.9, and with each other in Fig.10.

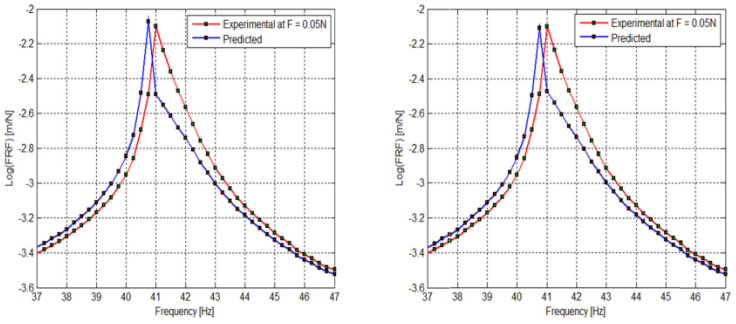

(a) (b)

Fig.9 Comparison of linear FRF at F=0.05 N and predicted linear FRF by using PRD method using experiments conducted at (a) 39 Hz (b) 40 Hz

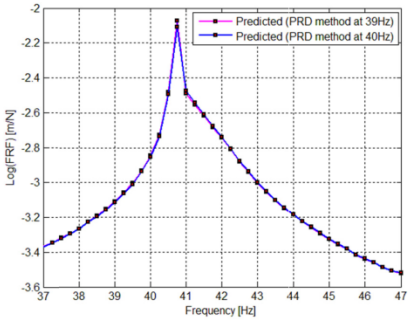

Fig.10 Comparison of predicted linear FRF by using PRD method using experiments conducted at 39 Hz and 40 Hz

As can be observed from Fig.9, FRFs measured at low forcing level (F = 0.05 N) deviate from the linear FRFs obtained by using the proposed PRD method. It was recently shown [21] that PRD method yields the FRFs of the underlying linear system in a nonlinear system accurately; therefore it can be concluded here that FRFs measured even at a very low forcing level may not represent the linear FRF accurately, which is consistent with the observations made in a recent study [26]. Furthermore, it is observed from Fig.10 that linear FRFs obtained using the describing functions identified from the tests made at 39 Hz and 40 Hz are very close to each other, although the imaginary parts of the describing functions identified from these tests are slightly different from each other.

5 MODEL UPDATING OF THE TEST SYSTEM AND VERIFICATION OF THE UPDATED MODEL

In this section, linear FE model of the test system is built in ANSYS and then the linear FE model is updated by employing the approach proposed. The accuracy of the updated nonlinear model of the test structure is also demonstrated. First, the PRD method is applied; thus the describing functions representing the nonlinearity in the system are identified and the linear FRFs are predicted from the measured nonlinear FRFs. Secondly, the linear FE model of the test structure is updated by using the linear FRFs and applying inverse eigensensitivity method. Using the identified nonlinearity and updated linear FE model updated nonlinear model of the test structure is constructed. Finally, predicted and measured FRFs of the test structure are compared at different forcing levels in order to demonstrate the accuracy of the updated nonlinear model of the system.

The FE model of the test structure is shown in Fig.11 and the material properties used in the initial FE model is given Table 3.

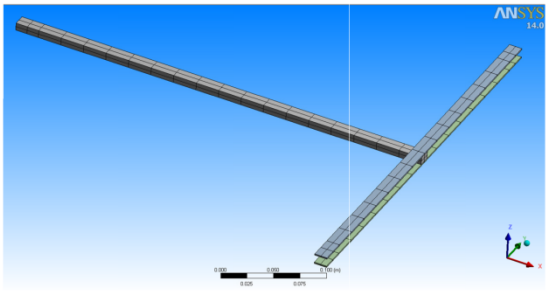

Fig.11 FE model of the test structure

Table 3 Material properties used in the initial FE model

	Modulus of Elasticity (E) (GPa)	**Poisson's Ratio (ν)**	**Density (ρ) (kg/m^3)**
Beam1	210	0.3	7850
Beam2	210	0.3	7850

The first natural frequency and the driving point FRF at the tip of beam 1 in Z (transverse) direction are calculated in ANSYS by using the FE model. Comparisons of the natural frequency and linear FRFs obtained from FE analysis with those obtained from experiments by using PRD method are given in Table 4 and Fig.12, respectively.

Table 4 Comparison of the first natural frequency obtained from initial FE model with the experimental value obtained by using PRD method

Mode Number	**Natural Frequency (PRD method) (Hz)**	**Natural Frequency (Initial FE model) (Hz)**	**Error (%)**
1	40.75	43.1	5.77

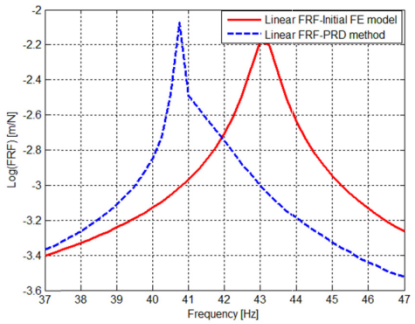

Fig.12 Comparison of the linear FRFs obtained from initial FE model with those obtained by using PRD method

As can be seen in Table 4 and Fig.12, there are discrepancies between the results; therefore the FE model of the test structure needs to be updated. Since most of the uncertainty is generally in modulus of elasticity of the materials, as an updating parameter in FE model, the modulus of elasticity is selected. For the selected parameter, element of the sensitivity matrix is calculated using the centered difference approximation with $O(h^4)$ which is given in equation (9), at each iteration step. After 5 iterations, updating parameter is converged to 188 GPa. The convergence graph of this parameter is given in Fig. 13.

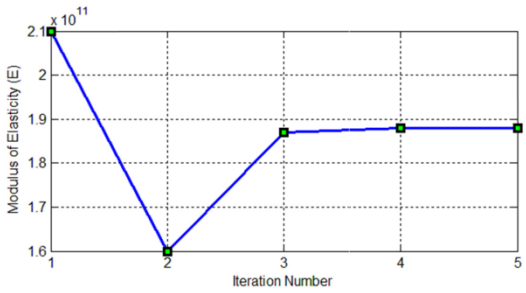

Fig.13 Convergence of the modulus of elasticity of the beams

Using the converged value of E, the FE model is updated. Then the first natural frequency of the updated linear model is calculated and compared with that of initial FE model, as well as with the natural frequency obtained from experiments by using PRD method in Table 5.

Table 5 Comparison of the first natural frequency obtained from initial and updated FE models with experimental value obtained by using PRD method

Mode Number	Natural Frequency (PRD method) (Hz)	Natural Frequency (Initial FE model) (Hz)	Error (%)	Natural Frequency (Updated FE model) (Hz)	Error (%)
1	40.75	43.1	5.77	40.75	0.00

As can be seen in Table 5, the first natural frequency is very accurately estimated by using the updated FE model. In Fig.14, the linear FRFs obtained by using PRD method from experimentally measured nonlinear FRFs are compared with those calculated from, initial and updated FE models. As can be seen in Fig.14, considerable improvement is obtained when updated FE model is used.

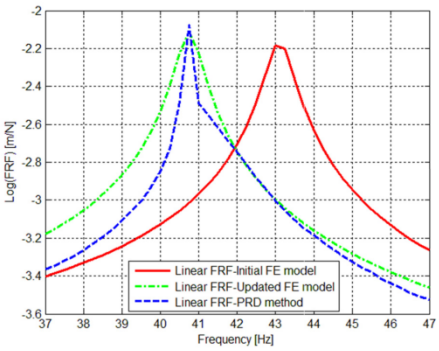

Fig.14 Comparison of the linear FRF obtained by using PRD method from experimentally measured values, with those calculated from, initial and updated FE models.

Since the ultimate goal is to have accurate nonlinear response predictions from the updated model, nonlinear FRFs measured experimentally for F=0.6 N, F=0.7 N and F=0.8 N are compared with those obtained from the initial and updated models (composed of original and updated FE combined with identified nonlinearity). The results are given in Fig.15. As observed in Fig.15 there is a considerable improvement in the FRFs calculated with the updated model for all forcing levels.

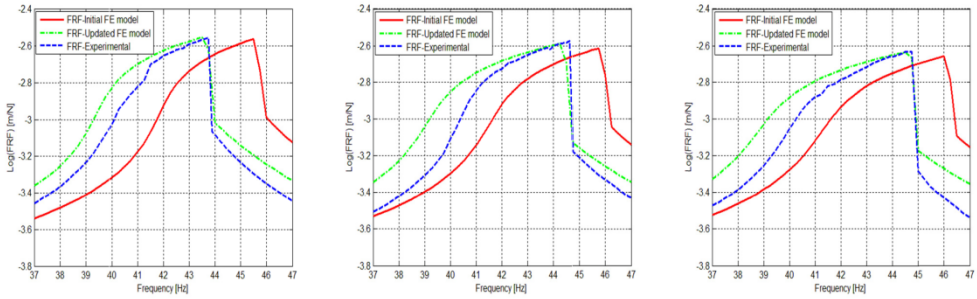

(a) (b) (c)

Fig.15 Comparison of FRFs obtained from initial and updated models with the experimental ones for (a) F=0.6 N (b) F=0.7 N (c) F=0.8 N

6 SUMMARY AND CONCLUSIONS

In this study, a nonlinear T-beam test structure is used to validate the accuracy of the nonlinear model updating approach suggested. Pseudo Receptance Difference (PRD) method, recently developed by the authors [20] calculates the linear FRFs of a nonlinear structure by using nonlinear FRFs experimentally measured at various forcing levels. The method, at the same time, identifies nonlinearities in the system. In the approach suggested, first, the linear FRFs are calculated from experimentally measured nonlinear FRFs, and the nonlinearities in the structure are identified. Then by using the linear FRFs obtained employing PRD method, FE model of the linear part of the structure is updated. In this work the inverse eigensensitivity method is used to update the linear FE model. Finally, the accuracy of the updated nonlinear model of the test structure is demonstrated by comparing calculated and measured FRFs of the nonlinear test structure at several different forcing levels.

In the experiments, firstly the structure is excited with a random excitation in order to find the range of frequencies where the first resonance occurs. Then, in order to apply the PRD method, the structure is excited at a constant frequency (which is close to the resonance frequency of the underlying linear system) with a pure sine excitation at different forcing levels. Finally, a set of stepped sine constant force experiments is performed on the test structure in order to measure nonlinear FRFs at various forcing levels.

Computationally; by applying the PRD method, first the describing functions of the nonlinearities are identified from test results, and then using these describing functions and the FRF values measured at low forcing level, linear FRFs of the structure are predicted. In the model updating of the FE model of the linear part of the structure, the predicted linear FRFs of the test system are used.

In this study it is shown that in a nonlinear structure, FRFs measured at a low forcing level (F=0.05 N, in this experimental work) may deviate from the actual FRFs of the linear part of the system. So it can be concluded that if sufficiently low forcing level cannot be applied in the experiments, or if there is friction type of nonlinearity in the system along with other types of nonlinearity, then the linear FRFs cannot be directly measured accurately. It is furthermore experimentally demonstrated that PRD method is very successful in predicting linear FRFs of a nonlinear structure from measured nonlinear FRFs. It is also observed that the frequency at which the experiments are made for the application of PRD method does not have a considerable effect on the accuracy of the predicted linear FRFs, as long as it is close to the resonance frequency.

Finally, the nonlinear model updating approach proposed is validated in this experimental study by comparing the nonlinear FRFs measured at various forcing levels, with those obtained from the original and updated models (which are defined by the original and updated FE models combined with identified nonlinearity). It is shown that with the updated nonlinear model considerable improvements can be obtained in predicting FRFs of a nonlinear structure at different forcing levels.

7 REFERENCES

[1] Nalitolela N. G., Penny J. E. T., Friswell M. I., "Updating Structural Parameters of a Finite Element Model by Adding Mass or Stiffness to the System", Proceedings of the 8th International Modal Analysis Conference, Kissimmee, Florida, pp.836-842, 1990.

[2] Roy N. A., Girard A., Dupuis P. E., "A Direct Energy Approach for Updating Dynamic Finite Element Models", Proceedings of the 9th International Modal Analysis Conference, Florence, Italy, pp.51-57, 1991.

[3] Brughmans M., Hrycko G., Wyzykowski J., "Application of FEM Model Correlation and Updating Techniques on an Aircraft Using Test Data of a Ground Vibration Survey", Proceedings of the 9th International Modal Analysis Conference, Florence, Italy, pp.517-525, 1991.

[4] Link M., Zhang L., "Experience with Different Procedures for Updating Structural Parameters of Analytical Models Using Test Data", Proceedings of the 10th International Modal Analysis Conference, San Diego, California, pp.730-738, 1992.

[5] Jung H., Ewins D. J., "Error Sensitivity of the Inverse Eigensensitivity Method for Model Updating", Proceedings of the 10th International Modal Analysis Conference, San Diego, California, pp.1051-1056, 1992.

[6] Miccoli G., Agostoni F., "Modal Updating Using Sensitivity Analysis", Proceedings of the 11th International Modal Analysis Conference, Kissimmee, Florida, pp.683-689, 1993.

[7] Hemez F. M., "Advanced Tools for Updating Damped Finite Element Models Using Static Modal and Flexibility Data", Proceedings of the 14th International Modal Analysis Conference, Dearborn, Michigan, pp.511-517, 1996.

[8] Lenoir D., Cogan S., Lallement G., Bricout J. N., "Model Updating by Modal Synthesis of Experimental Forced Responses", Proceedings of the 16th International Modal Analysis Conference, Santa Barbara, California, pp.399-405, 1998.

[9] Mottershead J. E., Mares C., Friswell M. I., James S., "Model Updating of an Aluminium Space-frame Using Different Parameter Sets", Proceedings of the 18th International Modal Analysis Conference, San Antonio, Texas, pp. 576-583, 2000.

[10] Jung D. S., Kim C. Y., Kang J. H., "Hybrid Optimization Technique based on GA-NMS for FE model Updating", Proceedings of the 25th International Modal Analysis Conference, Orlando, Florida USA, 2007.

[11] Kozak M. T., Cömert M. D., Özgüven H. N., "Model Updating Routine Based on the Minimization of a New Frequency Response Based Index for Error Localization", Proceedings of the 25th International Modal Analysis Conference, Orlando, Florida USA, pp.84-95, 2007.

[12] Boulkaibet I., Mthembu L., Marwala T., Friswell M. I., Adhikari S., "Finite Element Model Updating Using the Shadow Hybrid Monte Carlo Technique", Proceedings of the 31st International Modal Analysis Conference, Orange County, California USA, 2013.

[13] Fei Q., Jiang D., "Evaluating Initial Model for Dynamic Model Updating: Criteria and Application", Proceedings of the 32nd International Modal Analysis Conference, Orlando, Florida USA, 2014.

[14] Boulkaibet I., Mthembu L., Marwala T., Friswell M. I., Adhikari S., "Finite Element Model Updating Using the Separable Shadow Hybrid Monte Carlo Technique", Proceedings of the 32nd International Modal Analysis Conference, Orlando, Florida USA, 2014.

[15] Hemez F. M., "A Brief History of 30 Years of Model Updating in Structural Dynamics", Proceedings of the 32nd International Modal Analysis Conference, Orlando, Florida USA, 2014.

[16] Hasselman T. K., Anderson M. C., Gan W., "Principal Components Analysis for Nonlinear Model Correlation, Updating and Uncertainty Evaluation", Proceedings of the 16th International Modal Analysis Conference, Santa Barbara, California, pp.644-651, 1998.

[17] Anderson M. C., Hasselman T. K., "Minimizing Parameter Correlation in Nonlinear Model Updating", Proceedings of the 18th International Modal Analysis Conference, San Antonio, Texas, pp.109-115, 2000.

[18] Burton T. D., Hemez F. M., Rhee W., "Combined Model Reduction/SVD Approach to Nonlinear Model Updating", Proceedings of the 18th International Modal Analysis Conference, San Antonio, Texas, pp.116-123, 2000.

[19] Silva S. D., Cogan S., Foltete E., Buffe F., "Metrics for Non-Linear Model Updating in Mechanical Systems", Proceedings of the 26th International Modal Analysis Conference, Orlando, Florida USA, 2008.

[20] Canbaloglu G., Özgüven H. N., "Obtaining Linear FRFs for Model Updating in Structures with Multiple Nonlinearities Including Friction", Topics in Nonlinear Dynamics, Volume 1: Proceedings of the 31st IMAC, A Conference on Structural Dynamics, pp.145-157, 2013.

[21] Canbaloglu, G., Özgüven, H. N., "Model Updating of Nonlinear Structures", Proceedings of the 32nd International Modal Analysis Conference, Orlando, Florida USA, 2014.

[22] Kerschen G., Worden K., Vakakis A. F., Golinval J. C., "Past, Present and future of Nonlinear System Identification in Structural Dynamics", Mechanical Systems and Signal Processing, Volume 20, pp 505-592, 2006.

[23] Doranga S., Wu C. Q., "Parameter Identification for Nonlinear Dynamic Systems Via Multilinear Least Square Estimation", Proceedings of the 32nd International Modal Analysis Conference, Orlando, Florida USA, 2014.

[24] Grappasonni C., Noel J. P., Kerschen G., "Subspace and nonlinear-normal-modes-based identification of a beam with softening-hardening behaviour", Proceedings of the 32nd International Modal Analysis Conference, Orlando, Florida USA, 2014.
[25] Aykan M., Altuntop E., "Parametric Nonlinearity Identification of a Gearbox from Measured Frequency Response Data", Proceedings of the 32nd International Modal Analysis Conference, Orlando, Florida USA, 2014.
[26] Aykan M., Özgüven, H. N., "Identification of Restoring Force Surfaces in Nonlinear MDOF Systems from FRF Data Using Nonlinearity Matrix", Proceedings of the 31st International Modal Analysis Conference, Garden Grove, California USA, 2013.
[27] Londono J. M., Cooper J. E., "Experimental Identification of a System Containing Geometric Nonlinearities", Proceedings of the 32nd International Modal Analysis Conference, Orlando, Florida USA, 2014.
[28] Collins J. D., Hart G. C., Hasselman T. K. and Kennedy B., "Statistical Identification of Structure", AIAA Journal, Vol.12, No. 2, pp. 185-190, 1974.
[29] Ferreira J. V., "Dynamic response analysis of structures with nonlinear components", Ph.D. Thesis, Department of Mechanical Engineering, Imperial College London, 1998.
[30] Siller H. R. E., "Non-linear modal analysis methods for engineering structures", Ph.D. Thesis, Department of Mechanical Engineering, Imperial College London/University of London, 2004.